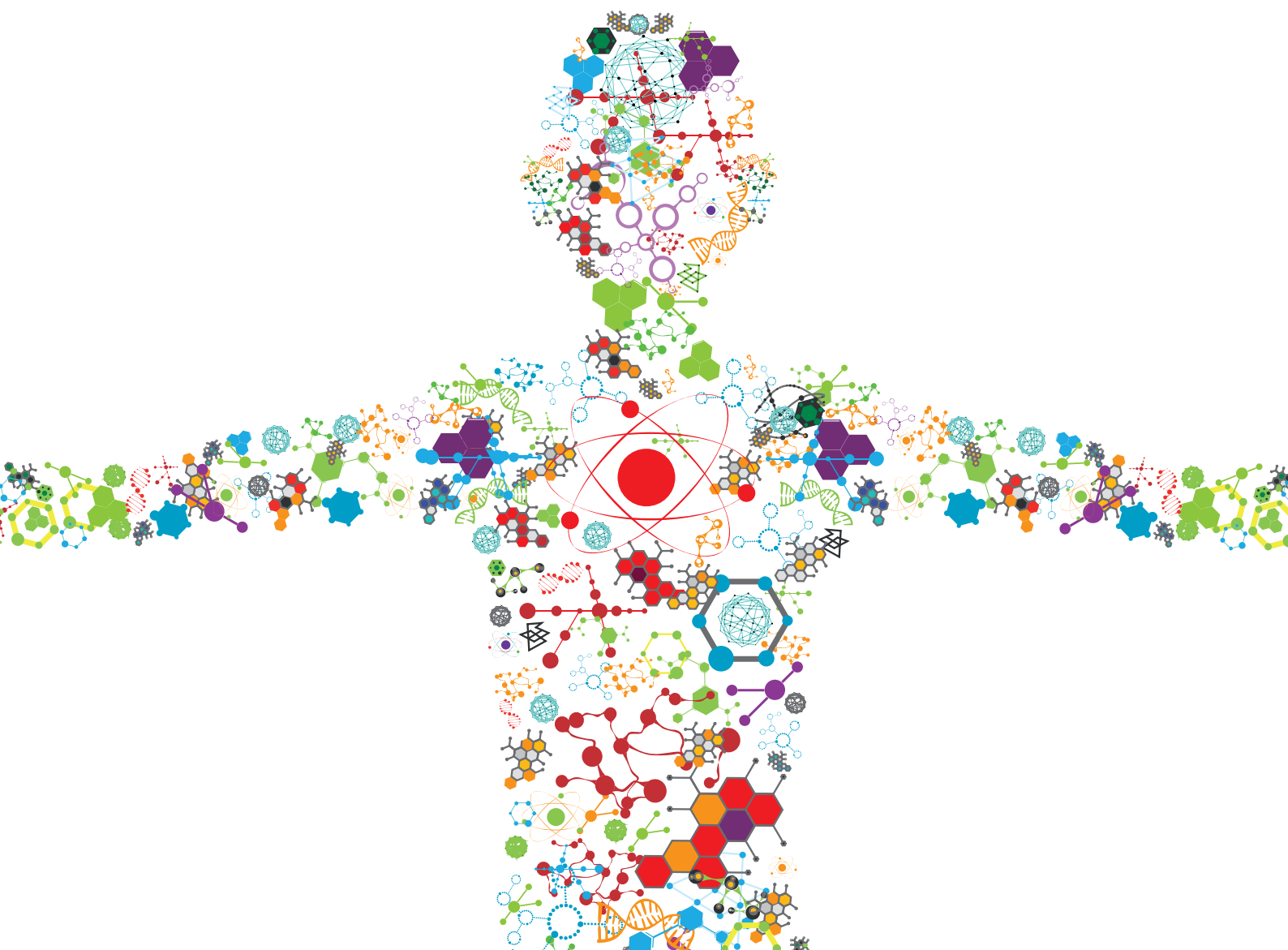


ALGAL BIOMASS AND BIOFUELS

EDITED BY: Kanhaiya Kumar, Namita Khanna, Probir Das,
Wanthanee Khetkorn and Eya Damergi

PUBLISHED IN: Frontiers in Bioengineering and Biotechnology





frontiers

Frontiers eBook Copyright Statement

The copyright in the text of individual articles in this eBook is the property of their respective authors or their respective institutions or funders. The copyright in graphics and images within each article may be subject to copyright of other parties. In both cases this is subject to a license granted to Frontiers.

The compilation of articles constituting this eBook is the property of Frontiers.

Each article within this eBook, and the eBook itself, are published under the most recent version of the Creative Commons CC-BY licence.

The version current at the date of publication of this eBook is CC-BY 4.0. If the CC-BY licence is updated, the licence granted by Frontiers is automatically updated to the new version.

When exercising any right under the CC-BY licence, Frontiers must be attributed as the original publisher of the article or eBook, as applicable.

Authors have the responsibility of ensuring that any graphics or other materials which are the property of others may be included in the CC-BY licence, but this should be checked before relying on the CC-BY licence to reproduce those materials. Any copyright notices relating to those materials must be complied with.

Copyright and source acknowledgement notices may not be removed and must be displayed in any copy, derivative work or partial copy which includes the elements in question.

All copyright, and all rights therein, are protected by national and international copyright laws. The above represents a summary only. For further information please read Frontiers' Conditions for Website Use and Copyright Statement, and the applicable CC-BY licence.

ISSN 1664-8714

ISBN 978-2-83250-804-6

DOI 10.3389/978-2-83250-804-6

About Frontiers

Frontiers is more than just an open-access publisher of scholarly articles: it is a pioneering approach to the world of academia, radically improving the way scholarly research is managed. The grand vision of Frontiers is a world where all people have an equal opportunity to seek, share and generate knowledge. Frontiers provides immediate and permanent online open access to all its publications, but this alone is not enough to realize our grand goals.

Frontiers Journal Series

The Frontiers Journal Series is a multi-tier and interdisciplinary set of open-access, online journals, promising a paradigm shift from the current review, selection and dissemination processes in academic publishing. All Frontiers journals are driven by researchers for researchers; therefore, they constitute a service to the scholarly community. At the same time, the Frontiers Journal Series operates on a revolutionary invention, the tiered publishing system, initially addressing specific communities of scholars, and gradually climbing up to broader public understanding, thus serving the interests of the lay society, too.

Dedication to Quality

Each Frontiers article is a landmark of the highest quality, thanks to genuinely collaborative interactions between authors and review editors, who include some of the world's best academicians. Research must be certified by peers before entering a stream of knowledge that may eventually reach the public - and shape society; therefore, Frontiers only applies the most rigorous and unbiased reviews.

Frontiers revolutionizes research publishing by freely delivering the most outstanding research, evaluated with no bias from both the academic and social point of view. By applying the most advanced information technologies, Frontiers is catapulting scholarly publishing into a new generation.

What are Frontiers Research Topics?

Frontiers Research Topics are very popular trademarks of the Frontiers Journals Series: they are collections of at least ten articles, all centered on a particular subject. With their unique mix of varied contributions from Original Research to Review Articles, Frontiers Research Topics unify the most influential researchers, the latest key findings and historical advances in a hot research area! Find out more on how to host your own Frontiers Research Topic or contribute to one as an author by contacting the Frontiers Editorial Office: frontiersin.org/about/contact

ALGAL BIOMASS AND BIOFUELS

Topic Editors:

Kanhaiya Kumar, Indian Institute of Integrative Medicine (CSIR), India

Namita Khanna, Birla Institute of Technology and Science, India

Probir Das, Qatar University, Qatar

Wanthanee Khetkorn, Rajamangala University of Technology Thanyaburi,
Thailand

Eya Damergi, Swiss Federal Institute of Technology Lausanne, Switzerland

Citation: Kumar, K., Khanna, N., Das, P., Khetkorn, W., Damergi, E., eds. (2023).

Algal Biomass and Biofuels. Lausanne: Frontiers Media SA.

doi: 10.3389/978-2-83250-804-6

Table of Contents

- 04 Editorial: Algal Biomass and Biofuels**
Kanhaiya Kumar, Wanthanee Khetkorn and Namita Khanna
- 07 Metabolic Analysis of Schizochytrium Mutants With High DHA Content Achieved With ARTP Mutagenesis Combined With Iodoacetic Acid and Dehydroepiandrosterone Screening**
Lei Zeng, Yanqi Bi, Pengfei Guo, Yali Bi, Tiantian Wang, Liang Dong, Fangzhong Wang, Lei Chen and Weiwen Zhang
- 19 Maximizing Energy Content and CO₂ Bio-fixation Efficiency of an Indigenous Isolated Microalga Parachlorella kessleri HY-6 Through Nutrient Optimization and Water Recycling During Cultivation**
Wasif Farooq
- 31 Effective Two-Stage Heterotrophic Cultivation of the Unicellular Green Microalga Chromochloris zofingiensis Enabled Ultrahigh Biomass and Astaxanthin Production**
Qiaohong Chen, Yi Chen, Quan Xu, Hu Jin, Qiang Hu and Danxiang Han
- 44 Bioprospecting Indigenous Marine Microalgae for Polyunsaturated Fatty Acids Under Different Media Conditions**
Priyanshu Jain, Amritpreet Kaur Minhas, Sadhana Shukla, Munish Puri, Colin J. Barrow and Shovon Mandal
- 57 Genetic Engineering of Microalgae for Secondary Metabolite Production: Recent Developments, Challenges, and Future Prospects**
Arathi Sreenikethanam, Subhisha Raj, Rajesh Banu J, Poornachandar Gugulothu and Amit K. Bajhaiya
- 71 Evaluation of Euglena gracilis 815 as a New Candidate for Biodiesel Production**
Zixi Chen, Yehua Chen, Hua Zhang, Huan Qin, Jiayi He, Zezhou Zheng, Liqing Zhao, Anping Lei and Jiangxin Wang
- 82 Comparative Proteomics Reveals Evidence of Enhanced EPA Trafficking in a Mutant Strain of Nannochloropsis oculata**
Wan Aizuddin Wan Razali, Caroline A. Evans and Jagroop Pandhal
- 98 Pilot-Scale Cultivation of the Snow Alga Chloromonas typhlos in a Photobioreactor**
Floris Schoeters, Jornt Spit, Rahmasari Nur Azizah and Sabine Van Miert
- 111 Nutrient Management and Medium Reuse for Cultivation of a Cyanobacterial Consortium at High pH and Alkalinity**
Alexandre J. Paquette, Agasteswar Vadlamani, Cigdem Demirkaya, Marc Strous and Hector De la Hoz Siegler
- 126 Assessment of CO₂ Biofixation and Bioenergy Potential of Microalga Gonium pectorale Through Its Biomass Pyrolysis, and Elucidation of Pyrolysis Reaction via Kinetics Modeling and Artificial Neural Network**
Ahmed Altriki, Imtiaz Ali, Shaikh Abdur Razzak, Irshad Ahmad and Wasif Farooq



OPEN ACCESS

EDITED AND REVIEWED BY

Manfred Zinn,
HES-SO Valais-Wallis, Switzerland

*CORRESPONDENCE

Kanhaiya Kumar,
k.kumar222@iiim.res.in

SPECIALTY SECTION

This article was submitted to Bioprocess Engineering, a section of the journal Frontiers in Bioengineering and Biotechnology

RECEIVED 31 August 2022

ACCEPTED 17 October 2022

PUBLISHED 02 November 2022

CITATION

Kumar K, Khetkorn W and Khanna N (2022), Editorial: Algal biomass and biofuels.
Front. Bioeng. Biotechnol. 10:1008760.
doi: 10.3389/fbioe.2022.1008760

COPYRIGHT

© 2022 Kumar, Khetkorn and Khanna. This is an open-access article distributed under the terms of the [Creative Commons Attribution License \(CC BY\)](https://creativecommons.org/licenses/by/4.0/). The use, distribution or reproduction in other forums is permitted, provided the original author(s) and the copyright owner(s) are credited and that the original publication in this journal is cited, in accordance with accepted academic practice. No use, distribution or reproduction is permitted which does not comply with these terms.

Editorial: Algal biomass and biofuels

Kanhaiya Kumar^{1,2*}, Wanthanee Khetkorn³ and Namita Khanna⁴

¹Fermentation and Microbial Biotechnology Division, CSIR–Indian Institute of Integrative Medicine (IIIM), Jammu, India, ²Academy of Scientific and Innovative Research (AcSIR), CSIR–Human Resource Development Centre, Ghaziabad, India, ³Division of Biology, Faculty of Science and Technology, Rajamangala University of Technology Thanyaburi, Thanyaburi, Pathumthani, Thailand, ⁴Department of Biotechnology, Birla Institute of Technology and Science, Pilani, Dubai, United Arab Emirates

KEYWORDS

photobioreactor, cultivation, spent media, fatty acids, secondary metabolites (SMs)

Editorial on the Research Topic

Algal biomass and biofuels

Algal technology is one of the promising areas of research that can alleviate several ongoing global challenges such as global warming, food, and fuel scarcity, and the growing demand for biopharmaceutical products for humans and animals. Algae bio sequester CO₂ from the environment during photosynthesis and produce biomass. Algal biomass is a promising feedstock for extracting biofuels and commercially important biopharmaceutical products. The scope of this Research Topic is to collect high-quality research articles that can address the challenges associated with algal technology spanning over three broad domains: algal cultivation for biomass, biofuels production, and extraction of commercially valuable biomolecules (Figure 1). The process of algal biomass cultivation should be scalable, cost-effective, environment-friendly, and sustainable. The algal cultivation in photobioreactors has advantages over open ponds because of easy control of physio-chemical parameters and preventing contamination. In addition to these attributes, biomass should contain energy-dense or value-added biomolecules. The energy-dense biomolecules should be extracted and converted to biofuels efficiently, and the process should be benign to the environment. Several algal species are known to synthesize high-value secondary metabolites (SMs), such as docosahexaenoic acid (DHA), eicosapentaenoic acid (EPA), and astaxanthin. However, selecting the most promising strain and enhancing their yield is a top priority.

This Research Topic contains ten high-quality articles, which include nine original research articles and one review paper. Fifty two authors belonging to eight countries: India, China, Malaysia, Saudi Arabia, Australia, the United Kingdom, Belgium, and Canada, have participated in this Research Topic. Furthermore, some articles also show inter-country and inter-continental research collaborations.

The isolation of indigenous microalgal species, random mutation of them, and exploring psychrotolerant (low temperature) microalga for cold climate countries are some of the suggested strategies for sustainably improving the algal biomass productivity. Further, the algal cultivation process can be cost-effective and environment-friendly when

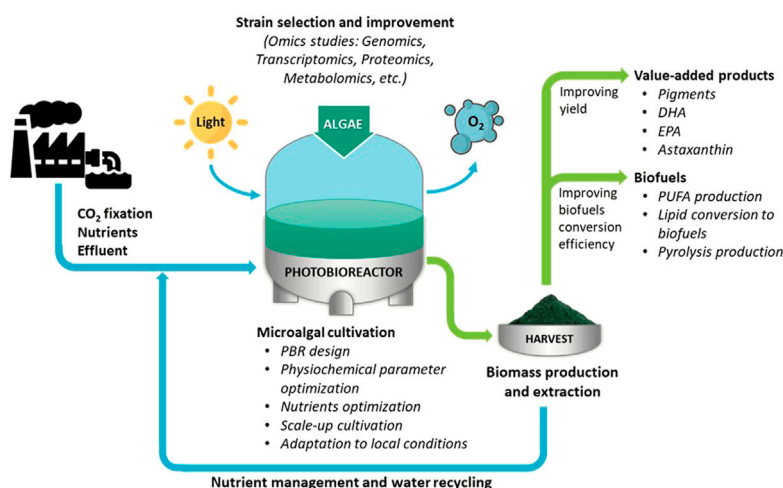


FIGURE 1

The challenges of algal technology for algal cultivation, biofuels production, and utilization of algal biomass to extract value-added products. PBR, photobioreactor; DHA, docosahexaenoic acid; EPA, eicosapentaenoic acid; PUFA, polyunsaturated fatty acids.

applying a better nutrients management strategy and recycling spent water several times. Three original research articles are focused on microalgal cultivation for improving biomass production and CO₂ fixation efficiency in a photobioreactor. Schoeters et al. cultivated the psychrotolerant snow alga *Chloromonas typhlos* at colder ambient temperatures in a 350 L pilot scale photobioreactor. Their primary purpose was to assess its biomass productivity and CO₂ fixation efficiency. The study by Paquette et al. on cyanobacteria consortium at high pH and alkalinity revealed that spent cultivation medium could be reused at least five times by proper nutrient management without significantly inhibiting the biomass productivity. Farooq conducted a similar study of nutrient optimization (nitrogen and carbon dioxide) and water recycling during cultivation but used *Parachlorella kessleri* HY-6 as a model microalga. The author found the inhibitory effect of organics accumulated in the spent media for the subsequent cultivation and therefore applied activated carbon to remove the organics and improve the water recyclability. The water recycling strategy circumvents the water-intensive algal cultivation process, especially in arid countries.

Three original research articles describe the biofuels potential of microalgae. Jain et al. isolated several indigenous marine microalgae such as *Nannochloropsis oculata*, *Chlorella* sp., and *Planophila* sp., from the coast of the Arabian Sea. They explored their potential for polyunsaturated fatty acids (PUFA) synthesis, especially α -Linolenic acid. Similarly, Chen et al. isolated indigenous *Euglena gracilis* 815 and evaluated it as a new candidate for biodiesel production. The microalgal biomass of *Gonium pectoral* was a potential feedstock for pyrolysis. The study also assessed the CO₂ biofixation potential along with pyrolytic kinetics of *G. pectoral* using kinetics modeling and an artificial neural network Altriki et al.

Four manuscripts containing three original research articles and one review article investigate the potential of microalgal biomass for secondary metabolites (SMs) production. The review summarized different genetic engineering studies targeting the improvement of microalgae for secondary metabolite production in microalgae (Sreenikethanam et al.). Three original research articles describe the production of SMs such as DHA, EPA, and astaxanthin from microalgae: *Schizochytrium* sp. (Zeng et al.), *Nannochloropsis oculata* (Razali et al.), and *Chromochloris zofingiensis* (Chen et al.), respectively. The mutagenesis on *Schizochytrium* sp. and *N. oculata* and nutrient optimization on *C. zofingiensis* enhanced the synthesis of SMs. The study on *Schizochytrium* sp., *N. oculata*, and *C. zofingiensis* was supported by metabolome, proteome, and bioprocess-based analysis, respectively. The atmospheric and room-temperature plasma (ARTP) mutagenesis combined with screening by iodoacetic acid and dehydroepiandrosterone enhanced the DHA synthesis in *Schizochytrium* sp. (Zeng et al.). The primary metabolites quantified using LC/MS correlated with the increased growth rate and DHA biosynthesis. The mutant strain produced the highest reported DHA concentration and productivity of 41.4 g L⁻¹ and 430.7 mg L⁻¹ h⁻¹, respectively, at the end of 96 h fermentation. Similarly, the random mutagenesis coupled with the chemical (Ethyl methane sulfonate)-inhibitor-based selection method improved the EPA synthesis in the marine microalga, *N. oculata* (Razali et al.). The study also revealed the presence of alternative pathways for EPA synthesis when analyzed using label-free quantitative proteomics for differential protein expression. Based on Fatty acid methyl ester (FAME) data, the most suitable mutant strain had enhanced EPA content (1.7-fold) and EPA concentration (1.4-fold) compared to the wild type. Further, an effective two-stage

heterotrophic cultivation of the unicellular green microalga, *C. zofingiensis*, enabled the synthesis of ultrahigh biomass and astaxanthin production (Chen et al.). *C. zofingiensis* was cultivated on a laboratory scale (7.5 L) and later scaled up in the 500 L fermenter. The combination of suitable concentrations of phytohormones gibberellic Acid-3 (GA3), C/N ratio, and NaCl enhanced the biomass and the astaxanthin synthesis. The highest biomass and astaxanthin yields were 235.4 g L⁻¹ and 0.318 g L⁻¹ (0.144% of DW), respectively. The astaxanthin yield was 5.4-fold more significant than the highest reported value in popular microalga, *Haematococcus pluvialis*. In this way, articles communicated in this Research Topic show significant improvement in the scientific knowledge base and contribute to the ongoing challenges of the commercialization of algal technology.

Author contributions

KK: writing, review, editing, and conceptualization. WK: figure drawing, and review. NK: writing and review. All authors contributed to the article and approved the submitted version.

Acknowledgments

The author KK would like to thank the CSIR-Director, Indian Institute of Integrative Medicine (IIIM), Jammu for providing the platform to continue this work.

Conflict of interest

The authors declare that the research was conducted in the absence of any commercial or financial relationships that could be construed as a potential conflict of interest.

Publisher's note

All claims expressed in this article are solely those of the authors and do not necessarily represent those of their affiliated organizations, or those of the publisher, the editors and the reviewers. Any product that may be evaluated in this article, or claim that may be made by its manufacturer, is not guaranteed or endorsed by the publisher.



Metabolic Analysis of *Schizochytrium* Mutants With High DHA Content Achieved With ARTP Mutagenesis Combined With Iodoacetic Acid and Dehydroepiandrosterone Screening

Lei Zeng^{1,2,3}, Yanqi Bi^{1,2,3}, Pengfei Guo^{1,2,3}, Yali Bi^{1,2,3}, Tiantian Wang^{1,2,3}, Liang Dong^{1,2,3}, Fangzhong Wang^{1,4*}, Lei Chen^{1,2,3} and Weiwen Zhang^{1,4,2,3*}

¹Laboratory of Synthetic Microbiology, School of Chemical Engineering & Technology, Tianjin University, Tianjin, China, ²Frontier Science Center for Synthetic Biology and Key Laboratory of Systems Bioengineering (MOE), School of Chemical Engineering and Technology, Tianjin University, Tianjin, China, ³SynBio Research Platform, Collaborative Innovation Center of Chemical Science and Engineering, Tianjin, China, ⁴Center for Biosafety Research and Strategy, Tianjin University, Tianjin, China

OPEN ACCESS

Edited by:

Kanhaiya Kumar,
Norwegian University of Science and
Technology, Norway

Reviewed by:

Geetanjali Yadav,
National Renewable Energy
Laboratory (DOE), United States
Maurycy Daroch,
Peking University, China

*Correspondence:

Fangzhong Wang
fangzhong.wang@tju.edu.cn
Weiwen Zhang
wwzhang8@tju.edu.cn

Specialty section:

This article was submitted to
Bioprocess Engineering,
a section of the journal
Frontiers in Bioengineering and
Biotechnology

Received: 08 July 2021

Accepted: 04 October 2021

Published: 18 November 2021

Citation:

Zeng L, Bi Y, Guo P, Bi Y, Wang T,
Dong L, Wang F, Chen L and Zhang W
(2021) Metabolic Analysis of
Schizochytrium Mutants With High
DHA Content Achieved With ARTP
Mutagenesis Combined With
Iodoacetic Acid and
Dehydroepiandrosterone Screening.
Front. Bioeng. Biotechnol. 9:738052.
doi: 10.3389/fbioe.2021.738052

High DHA production cost caused by low DHA titer and productivity of the current *Schizochytrium* strains is a bottleneck for its application in competition with traditional fish-oil based approach. In this study, atmospheric and room-temperature plasma with iodoacetic acid and dehydroepiandrosterone screening led to three mutants, 6–8, 6–16 and 6–23 all with increased growth and DHA accumulations. A LC/MS metabolomic analysis revealed the increased metabolism in PPP and EMP as well as the decreased TCA cycle might be relevant to the increased growth and DHA biosynthesis in the mutants. Finally, the mutant 6–23, which achieved the highest growth and DHA accumulation among all mutants, was evaluated in a 5 L fermentor. The results showed that the DHA concentration and productivity in mutant 6–23 were 41.4 g/L and 430.7 mg/L/h in fermentation for 96 h, respectively, which is the highest reported so far in literature. The study provides a novel strain improvement strategy for DHA-producing *Schizochytrium*.

Keywords: *schizochytrium*, DHA, metabolomic analysis, ARTP mutagenesis, iodoacetic Acid, dehydroepiandrosterone

INTRODUCTION

Docosahexaenoic acid (DHA; C22:6, n-3) has been demonstrated to be beneficial to human health. It was reported that DHA is an essential component of human cerebral cortex and retina, and has roles in the nervous development of infants and children. It also has positive effect in the preventing cardiovascular diseases and anti-inflammatory and anti-tumor effects (Dessi et al., 2013). Marine fish is the traditional source of DHA, however, due to decrease in the number of marine fish and accumulate heavy metals and organic pollutants, many work focus on finding more sustainable and high-quality alternative approach of DHA source (Ganuza et al., 2008). Microalgae is well-known for DHA rich. Compared with other microalgae, thraustochytrid, a heterotrophic algae-like protist, *Schizochytrium* grows faster, accumulates more biomass and has higher DHA ratio in total fatty acid, furthermore, it also contains docosapentaenoic acid (DPA; C22:5, n-6), which is essential fatty acid

of human breast milk, the cortex of the human brain, and the retina of the eye (Makrides et al., 1994). Therefore, *Schizochytrium* has been used for industrial-scale production of DHA worldwide.

Since relatively low titer and productivity of DHA during fermentation process, high cost is a bottleneck for industrial DHA production using *Schizochytrium*. In recent years, several approaches, such as strain improvement, fermentation process optimization and genetic engineering, have been evaluated for increasing DHA titer and productivity in *Schizochytrium*. For example, 1) alleviate oxidative damage of *Schizochytrium* sp. HX-308 under high salinity by adaptive evolution resulted in improving lipid productivity by 1.96-fold (Sun et al., 2018); 2) By optimizing the oxygen supply strategy in the fermentation process, the DHA content and DHA yield of *Schizochytrium* M209059 were increased by 15.1 and 11.2%, respectively. (Ren et al., 2010); 3) overexpression of malonyl-CoA:ACP transacylase led to 81.5% increase of DHA titer after a glucose fed-batch fermentation in *Schizochytrium* sp. MYA1381 (Li et al., 2018). Up to now, the highest report in the literature showed that *Schizochytrium* sp. 31 produced 151.4 g/L of dry cell weight and 28.9 g/L of DHA after 96 h fermentation, when using glycerol as carbon source (Chang et al., 2013). Nevertheless, more efforts are still needed for improving DHA titer and productivity for large-scale industry application.

Compared with other breeding methods, atmospheric and room temperature plasma (ARTP) technology, which is based on radio-frequency atmospheric-pressure glow discharge plasma, has many advantages, such as high positive efficiency and more table mutants (Wang et al., 2014; Ottenheim et al., 2018). Therefore, it has been widely applied to marine microorganisms breeding including *Schizochytrium* sp., resulting in identifying mutants with increasing DHA and biomass accumulation in recent years (Yuan et al., 2015; Zhao et al., 2018; Li et al., 2020). For example, a novel approach of ARTP mutagenesis coupled with malonic acid and zeocin screening was developed to obtain *Schizochytrium* mz-17. After Fe²⁺ supplementation in fed-batch fermentation, DHA titer reached 14.0 g/L, which was two-fold higher than the wild type (Zhao et al., 2018).

It was proposed that *Schizochytrium* might likely utilize polyketide synthase systems for DHA production (Metz et al., 2001). The acetyl-CoA producing pathway, NADPH producing pathway, fatty acid synthase (FAS) are important metabolic modules for achieving efficient DHA accumulation in marine microorganisms (Qiu et al., 2020). Several screening agents targeting these metabolic modules have been evaluated in *Schizochytrium* (Supplementary Table S1), including the iodoacetic acid inhibiting Embden-Meyerhof-Parnas (EMP) pathway (Chance and Park, 1967), and malonic acid weakening tricarboxylic acid (TCA) cycle (Beever, 1952), leading to decreased acetyl-CoA formation and utilization, respectively. An iodoacetic acid-resistant and malonic acid-resistant mutant named *Schizochytrium* sp. HX-308M, which was proved enhancing acetyl-CoA supply, was obtained. The lipid concentration and DHA ratio in total fatty acid of *Schizochytrium* sp. HX-308M were increased 34.8 and 38.9% (Lian et al., 2010). Two *Schizochytrium* mutants named OUC002 and OUC007 were also

achieved based on their resistance to quizalofop-p-ethyl, a FAS inhibitor. The DHA concentrations of *Schizochytrium* OUC002 and OUC007 were elevated by 13.7 and 28.8%, comparing with the wild type (Xu et al., 2012). The 2', 2'-bipyridine can induce ROS pathway, resulting in death of strains with weaker antioxidant capacity. *Schizochytrium* mutant survived in plates containing 2', 2'-bipyridine exhibited 29.8% improvement of DHA titer, in comparison with the wild type (Yuan et al., 2015). In addition, overexpression of malic enzyme coding gene to strengthen NADPH supply could also elevate DHA titer in *Schizochytrium* (Wang et al., 2019). However, so far, few reports have focused on agents targeting NADPH-producing pathway for microalgal breeding. Dehydroepiandrosterone is an adrenal hormone used to inhibit the activity of glucose-6-phosphate dehydrogenase, a key enzyme that catalyzes NADPH supply, in bovine serum red blood cells (Tian et al., 1999). The roles of glucose-6-phosphate dehydrogenase in improving DHA and lipid accumulation were also previously demonstrated in marine microorganisms (Cui et al., 2016; Xue et al., 2017; Xue et al., 2018). For example, enhanced glucose-6-phosphate dehydrogenase expression could lead to more DHA production in *Aurantiochytrium* sp. SD116, closely related species of *Schizochytrium*, but the growth was significantly decreased (Cui et al., 2016). However, there is no report whether dehydroepiandrosterone can be used for screening agents in marine microorganisms.

In this study, an integrated ARTP mutagenesis and dehydroepiandrosterone and iodoacetic acid-based screening method was applied to *Schizochytrium* ATCC 20888, resulting in several mutants with increased growth and DHA content. In addition, a LC-MS based metabolomics was carried out to study mechanisms associated with improved growth and DHA content in the mutants. The new findings could be valuable for the better understanding of *Schizochytrium* metabolism and provide valuable information regarding regulatory targets for engineering *Schizochytrium* for even high DHA titer in the future.

MATERIALS AND METHODS

Strains and Chemicals

Schizochytrium ATCC 20888 was purchased from the American Type Culture Collection (ATCC). Sea salt, fatty acid standard and antifoam SE-15 were purchased from Sigma-Aldrich (St. Louis, MO, United States). Yeast extract was purchased from OXOID (Basingstoke, United Kingdom). All the other chemicals were purchased from Jiang Tian Chemical Technology Co., Ltd., (Tianjin, China).

Cultivation

For shaking-flask cultures, strain grown at basal liquid medium for 2 days was used as seed cultures. Approximately 0.95 OD₆₆₀ or 0.004 g dry cell weight (DCW) of seed cultures were transferred into 20 ml of rich medium and cultivated at 28°C and 180 rpm for 3 days. OD₆₆₀ was determined by a UV-1750 spectrophotometer (Shimadzu, Japan).

Fed-batch culture was carried out in a 5-L bioreactor with an initial volume of 2.2 L fermentation medium equipped with

automatic controls of agitation, temperature, airflow, pH and dissolved oxygen concentration. The seed culture grown in rich medium was transferred into a 5 L fermentor at an inoculum size of 10% (v/v) (Approximately 950 OD₆₆₀ or 4 g DCW). The temperature controlled at 28°C. The dissolved oxygen levels were kept above 30%. The pH was maintained at 6.5 ± 0.1 by automated addition of 0.5 M H₂SO₄. A 60% (w/v) glucose solution was fed into the fermentation medium to maintain glucose concentration at 20–50 g/L (Qu et al., 2013a).

The composition of basal, rich and fermentation medium followed the previous study (Zhao et al., 2017; wang et al., 2019). The composition of 1 L basal liquid includes 5 g glucose, 1 g peptone, 1 g yeast extract and 20 g sea salt. Rich medium containing 40 g/L glucose, 10 g/L yeast extract, 1 g/L (NH₄)₂SO₄, 4 g/L K₂HPO₄·2H₂O, 12 g/L Na₂SO₄, 10 g/L Mg SO₄·7H₂O, 7 g/L K₂SO₄ and 2 g/L KCl. The fermentation medium is the same as the rich medium except that the concentration of glucose and yeast extract is 100 g/L and 25 g/L.

Assay of *Schizochytrium* sp. 31 Sensitivity to Selected Agents

One hundred microliters of exponential phased *Schizochytrium* sp. 31 were spread on solid plates containing 0, 20, 60, 100, 160, 180, 200 mg/L of iodoacetic acid (IAA) or 0, 10, 20, 30, 40, 50, 60, 70 mg/L of dehydroepiandrosterone (DHEA) or 0, 10, 20, 30, 40, 50, 60, 70, 80 mg/L of IAA and DHEA (IAA and DHEA at a ratio of 4:1), respectively, and then cultivated at 28°C until the colony was no longer become larger (3 days) (Zhao et al., 2018). A minimal three replicated plates were conducted for determination of the selective concentration.

Atmospheric and Room Temperature Plasma Mutagenesis of *Schizochytrium*

ARTP mutagenesis of *Schizochytrium* ATCC 20888 was carried out according to the methods with minor modification on the ARTP treated time (Liu et al., 2017). Briefly, approximate 10⁶–10⁷ of exponential phased cells were inoculated to a sterilized sample plate, exposed to an ARTP breeding mutagenesis machine (a Model ARTP-M, Yuan Qing Tian Mu Biotechnol Inc., Wuxi, China) for 0, 20, 40, 60, 80, 100, or 120 s, and then quickly transferred to basal medium. Fifty microliters of diluted cultures were inoculated on basal medium plates and incubated until the colony occurred. The optimized ARTP treated time was measured by the lethal rate. The mutants were screened on basal medium plates supplemented with 40 g/L iodoacetic acid and 10 g/L dehydroepiandrosterone. The lethality rate was determined as follows:

$$\text{Lethality rate (\%)} = \frac{\text{control colonies} - \text{survival colonies}}{\text{control colonies}} \times 100\% \quad (1)$$

The individual colonies with ARTP treatment of 0 s for control colonies and each other ARTP treated colonies were counted, respectively. (Zhao et al., 2018).

Biomass, Glucose, Fatty Acids and Specific Growth Rate Determination

Biomass determination of supernatant followed the previous study (Li et al., 2017). 2 ml of fermentation broth was centrifuged at 8,000 × g for 5 min, washed once with distilled water, and vacuum freeze-dried for 12 h to determine the DCW. Glucose in the supernatant was determined with glucose oxidase method (De Swaaf et al., 1999) using Glucose Oxidase Assay Kit (Biosino Biotechnology and science Co., Ltd., China). Fatty acid contents were measured according the methods described (Wang et al., 2019). Briefly, 20 mg of lyophilized cell powder was added with 2 ml of chloroform, 2 ml of methanol containing 3% (v/v) sulfuric acid and 0.5 mg/L nonadecanoic acid (an internal standard). The reaction was performed at 97°C for 2 h, and added 1 ml of distilled water to separate the water phase from chloroform phase. The extracted chloroform phase was used for fatty acid determination by a GC–MS system-GC 7890 coupled to an MSD 5975 (Agilent Technologies, Inc., Santa Clara, CA) equipped with a HP-5MS capillary column (30 m × 250 mm id). The fatty acids content was calculated using standard curve methods with nonadecanoic acid as an internal standard. The specific growth rate was calculated by the equation, $\mu \text{ (h}^{-1}\text{)} = (\ln X_2 - \ln X_1) / (t_2 - t_1)$, where X_1 and X_2 are the cell dry weight (g/L) at the time t_1 and t_2 , respectively (Sun et al., 2016).

Determination of Glucose-6-Phosphate Dehydrogenase and 3-Phosphoglyceraldehyde Dehydrogenase Enzyme Activities

The preparation of cell homogenates was as follows. Briefly, 1 ml of cells were harvested at 12, 24, 36 or 72 h, added with 1 ml of extract solution, and then disrupted by cell disruptor. The solution was centrifuged 8,000 g for 10 min at 4°C. The supernatant was extracted for protein concentration and enzymatic activities analysis. The protein concentration was measured by Bradford method (Nouroozi et al., 2015) using Bradford Protein Assay Kit (Sangon Biotech. Co., Ltd., Shanghai, China). The glucose-6-phosphate dehydrogenase and 3-phosphoglyceraldehyde dehydrogenase activity followed the previous study (Langdon, 1966; Zwickl et al., 1990). Briefly, the glucose-6-phosphate dehydrogenase or 3-phosphoglyceraldehyde dehydrogenase activity was determined spectrophotometrically in 340 nm by monitoring the rate of NADPH or NADH formation at 30°C. The determination of the activity of glucose-6-phosphate dehydrogenase and 3-phosphoglyceraldehyde dehydrogenase followed the instructions of 6-Phosphate Dehydrogenase Activity Assay Kit (Nanjing Biobox Biotech. Co., Ltd., Nanjing, China) and Glyceraldehyde 3-Phosphate Dehydrogenase Activity Assay Kit (Nanjing Biobox Biotech. Co. Ltd., Nanjing, China). The activity of glucose-6-phosphate dehydrogenase or 3-phosphoglyceraldehyde dehydrogenase was normalized by the protein concentration.

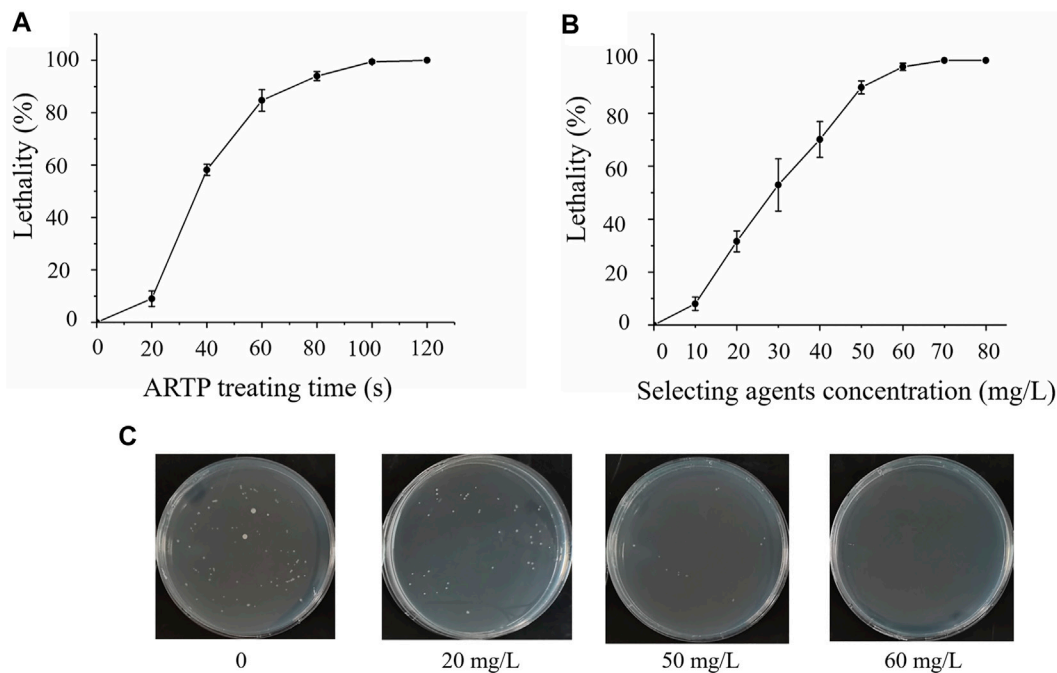


FIGURE 1 | Screening and sensitivity of *Schizochytrium* ATCC20888 to selected agents. **(A)** Atmospheric and room temperature plasma (ARTP) treatment time; **(B)** Sensitivity of *Schizochytrium* ATCC 20888 to selected agents (iodoacetic acid (IAA) and dehydroepiandrosterone (DHEA) at a ratio of 4:1); **(C)** Sensitivity of *Schizochytrium* ATCC 20888 on solid plates supplemented with iodoacetic acid and DHEA at a ratio of 4:1. Error bar represents standard deviation of three biological replicates.

Comparative LC-MS Metabolomics Analysis

Samples preparation for LC-MS metabolomics analysis followed the previous study (Li et al., 2015). Briefly, cells grown at the 24 or 48 h were centrifuged at $8,000 \times g$ for 5 min at 25°C (Eppendorf 5430R, Hamburg, Germany). The supernatant was discarded. The sediment was resuspended in 900 μL of solution 1 (80:20 MeOH/ H_2O , stored at -80°C), quickly frozen in liquid nitrogen, and thawed on dry ice to release metabolites (Park et al., 2011). The cells were frozen-thawed for three times to release the whole metabolites, and the supernatants were collected by centrifugation at $150,00 \times g$ for 5 min at 4°C (Park et al., 2011). The left cell debris were then re-suspended in solution 1 and the above extraction process was repeated. The twice supernatants were mixed and stored at -80°C until LC-MS analysis. An Agilent 1,260 series binary HPLC system (Agilent Technologies, Waldbronn, Germany) using a SYnergi Hydro-RP (C18) 150 mm \times 2.0 mm I.D., 4 μm 80 \AA 549 particles column (Phenomenex, Torrance, CA, United States), coupled to an Agilent 6410 550 triple quadrupole mass analyser equipped with an electrospray ionization source was used for LC-MS analysis. Data processing and statistical analysis were conducted according to the method described previously (Wang et al., 2019).

Statistical Analysis

Two-tailed Student's *t*-tests were carried out for significant difference. A minimal three replicates were carried out, and $p < 0.05$ was considered significant different.

RESULTS

Atmospheric and Room Temperature Plasma Mutagenesis With Iodoacetic Acid- and Dehydroepiandrosterone-Based Screening

Schizochytrium ATCC 20888 cells were mutated with ARTP for varying times with a lethal rate as the selected parameter. As shown in **Figure 1A**, the optimal treatment was 60 s with a lethal rate of 90%. It was previously reported that strengthening pentose phosphate pathway (PPP) results in improving total fatty acid content with sacrificing biomass accumulation in marine microorganisms (Cui et al., 2016; Xue et al., 2018), while enhancing EMP could improve growth of marine microorganisms (Lian et al., 2010; Sun et al., 2020). Therefore, iodoacetic acid or DHEA, an inhibitor of EMP or PPP pathways, was applied to determine the sensitivity of *Schizochytrium* ATCC 20888. The results showed that the lethal rate of *Schizochytrium* ATCC 20888 reached 90% when the concentration of iodoacetic acid and DHEA was over 160 and 40 mg/L, respectively (**Supplementary Figures S1A, S1B**). The iodoacetic acid was combined with dehydroepiandrosterone at the concentration ratio of 4:1 for screening on the plates. It was found that the growth of *Schizochytrium* ATCC 20888 was significantly inhibited over 90% when the concentration of both selected agents together was over 50 mg/L (iodoacetic acid: 40 mg/L; DHEA: 10 mg/L) (**Figures 1B,C**).

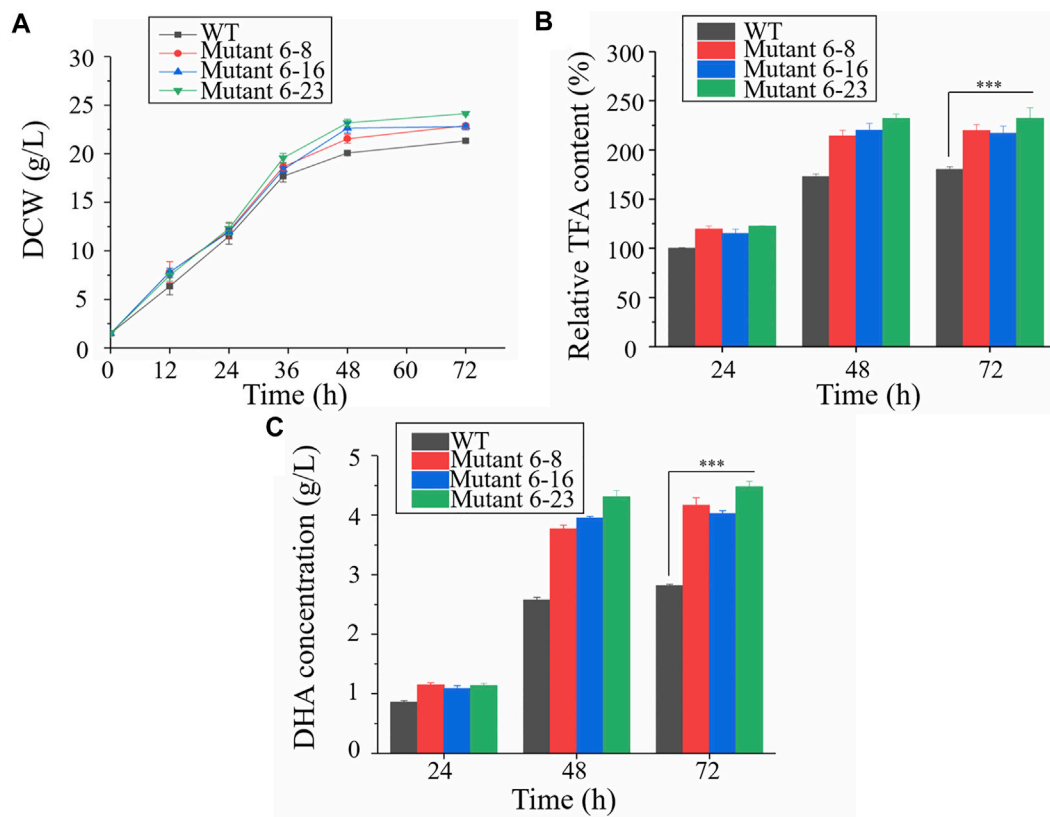


FIGURE 2 | Comparison of biomass accumulation, total fatty acid and DHA concentration in shake-flask cultures. Black represents the wild type; red represents mutant 6-8; blue represents strain 6-16; green represents mutant 6-23, respectively. **(A)** Biomass accumulation; **(B)** Total fatty acid. The total lipid content in the wildtype at 24 h was set as 100%; **(C)** DHA concentration. WT, wild type; DCW, dry cell weight; TFA, total fatty acid. Error bar represents standard deviation of three biological replicates. Asterisks indicate significant difference between the control and stress treatments based on Student's *t*-tests (**p* < 0.05; ***p* < 0.01; ****p* < 0.005).

The mutagenesis was carried out using the above optimal parameters. Mutants were first screened based on colony size, and then confirmed by comparative DHA concentration and growth analysis after cultivating these mutants in flask cultures. The analysis showed that mutant 6 was the highest in terms of the dry cell weight or DHA concentration, which was 1.1- or 1.4-fold higher than that of the wild type ATCC 20888 (Supplementary Figure S2A; Supplementary Table S2). In addition, only mutant 6 could survive on plates supplemented with increased iodoacetic acid and DHEA concentration. The whole process was then repeated with mutant 6 as the starting strain, and the concentration of iodoacetic acid and DHEA was further increased up to 16 mg/L and 64 mg/L, respectively. As shown in Supplementary Figure S2B, we identified that DCW of mutant 6-8, 6-16, or 6-23 from the 25 second-round mutants analysed was significantly higher than that of mutant 6 from the first round. The DCW was elevated by 1.1-, 1.1- or 1.2-fold in mutant 6-8, 6-16 or 6-23, respectively. The DHA concentration of mutant 6-8, 6-16, or 6-23 was improved by 1.5-, 1.4- or 1.6-fold, respectively (Supplementary Table S3). In addition, the DPA concentration of mutant 6-23 was improved by 1.4-fold, while it was decreased by 38.4% or 40.4% in mutant 6-8 or 6-16.

At last, mutant 6-8, 6-16 and 6-23 were sub-cultivated for 20 more times, the DCW and DHA titre of the 20th passages were compatible to these of the first passages, suggesting the stability of mutant 6-8, 6-16 and 6-23 (Supplementary Figure S3).

Characterization of Mutant 6-8, 6-16, and 6-23 in Shake-Flask Culture

Approximately 0.95 OD₆₆₀ or 0.004 g dry cell weight (DCW) of the wild type and mutant 6-8, 6-16, and 6-23 seed cultures were inoculated into shake flasks to compare the growth, enzyme activities and fatty acid concentration. It was shown in Figure 2, mutant 6-8, 6-16, and 6-23 accumulated much more biomass at the stationary growth phase, compared with the wild type. The specific growth rate of wild type, mutant 6-8, 6-16, and 6-23 were $\mu = 0.011, 0.012, 0.012, 0.013 \text{ h}^{-1}$ during logistical growth phase, respectively. Mutant 6-23 performed better than other mutants, as its dry cell weight was 1.2-fold higher than the wild type at the 72 h. The activities of phosphoglycerate dehydrogenase and glucose-6-phosphate dehydrogenase, which were the targets of iodoacetic acid and DHEA, respectively, were determined. As shown in

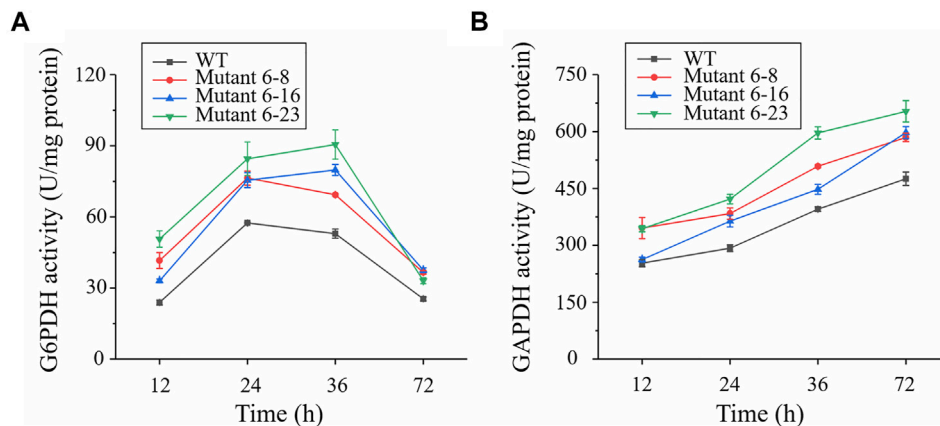


FIGURE 3 | Comparison of glucose-6-phosphate dehydrogenase and phosphoglycerate dehydrogenase in shake-flask cultures. Black represents the wild type; red represents strain 6-8; blue represents mutant 6-16; green represents mutant 6-23, respectively. **(A)** Enzymatic activity of glucose-6-phosphate dehydrogenase (G6PDH); **(B)** Enzymatic activity of phosphoglycerate dehydrogenase (GAPDH). Error bar represents standard deviation of three biological replicates.

Figure 3A, the activity of glucose-6-phosphate dehydrogenase was the highest at the 24 h for wild type and mutant 6-8, and it was at the 36 h for mutant 6-16 or 6-23. The activity of glucose-6-phosphate dehydrogenase in all strains was decreased when it reached the peak. Comparing with glucose-6-phosphate dehydrogenase, the activities of phosphoglycerate dehydrogenase were increased with cultivation time course on in all strains (**Figure 3B**). The phosphoglycerate dehydrogenase and glucose-6-phosphate dehydrogenase activities in the mutants were both increased 1.3-fold over the wild type (**Figures 3A,B**) at all selected time points, which further confirmed the effectiveness of iodoacetic acid and DHEA-based screening. The most significant increase in phosphoglycerate dehydrogenase and glucose-6-phosphate dehydrogenase activities was found in mutant 6-23, which was 71.0 and 37.4% higher than the wild type at 72 h, respectively.

Cells were harvested at the exponential and stationary phases to compare total fatty acid content. The results showed that the total fatty acid contents of mutant 6-8, 6-16 and 6-23 were significantly enhanced than that of the wild type at the 48 and 72 h, respectively, among which mutant 6-23 accumulated the most amount of fatty acids, 1.2-, 1.2-, 1.3-fold higher than mutant 6-8, 6-16 and the wild type at the 72 h, respectively. The fatty acid contents of mutants and the wild type were also comparatively determined. Consistent with the results of phosphoglycerate dehydrogenase and glucose-6-phosphate dehydrogenase activities, DHA concentrations of mutant 6-8, 6-16 and 6-23 were also significantly enhanced compared to the wild type at both 48 and 72 h (**Figure 2C**). The DHA concentration in mutant 6-23 was the highest, reaching a level of 4.6 g/L at 72 h. Therefore, it was likely to suggest the correlation between DHA content and activities of dehydrogenase and glucose-6-phosphate dehydrogenase.

Comparative Metabolomic Analysis Between Mutants and the Wild Type

Metabolomics, which was for identification and quantitation of metabolites in biological reaction, is a powerful technology to compare the metabolic status in different biological samples (Zhou et al., 2012). Among these technologies, the coupling of liquid chromatography to mass spectrometry (LC-MS) has gradually become an important tool to quantitative analysis of central carbon metabolites since its high throughput, good metabolites coverage and soft ionization (Zhou et al., 2012). The LC-MS has been recently applied to many marine microorganisms, including explaining chemodiversity of a rich marine microorganism tropical ecosystem (Reveillon et al., 2019), identifying hub metabolites relevant to resist Fe^{2+} and high light stress condition in *Haematococcus pluvialis* (Su et al., 2014), and exploring possible mechanisms of elevating fatty acid contents after overexpressing *EL O3* gene in *Schizochytrium* sp. 31 (Wang et al., 2019). In all, LC-MS can provide accurate metabolic changes in marine microorganisms.

In this study, cells of mutant 6-8, 6-16, 6-23 and WT were harvested at the exponential (24 h) and stationary phases (48 h) and then subjected to LC-MS based metabolomic analysis (**Supplementary Table S4**). The principal component analysis (PCA) was used to judge the quality of the LC-MS metabolomics (**Supplementary Figure S4**). It was shown that 1) a good reproducibility of each sample as three biological replicates are obviously clustered together; 2) an apparent metabolic change occurred among mutant 6-8, 6-16, 6-23 and the wild type since samples of these mutants were visibly separated in the PCA plots at both points; 3) the most significant metabolic changes occurred between wild type and mutant 6-8 or 6-16, because of samples of mutant 6-8 and 6-16 far away from the wild type at both 24 and 48 h.

Heat maps is a popular tool to display information-rich data in two or three dimensions, and a visualization route to represent

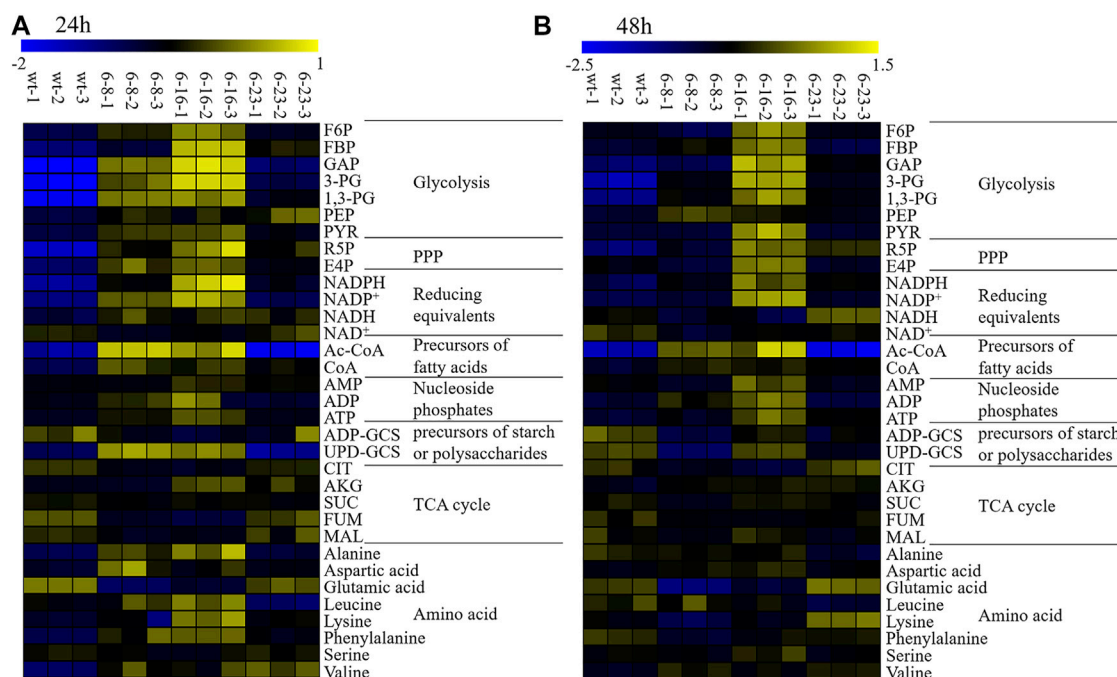


FIGURE 4 | Heatmaps of LC-MS targeted metabolomics of the wild type and mutants. NADPH, nicotinamide adenine dinucleotide phosphate; NADP⁺, oxidized form of nicotinamide adenine dinucleotide phosphate; NAD⁺, nicotinamide adenine dinucleotide; NADH, Nicotinamide adenine dinucleotide; ADP-GCS, adenosine 5'-diphosphoglucose; UDP-GCS, uridine 5'-diphosphoglucose; ATP, adenosine triphosphate; ADP, adenosine diphosphate; CoA, Coenzyme A hydrate; AMP, adenosine monophosphate; FBP, fructose 1,6-bisphosphate; F6P, fructose 6-phosphate; R5P, ribose 5-phosphate; E4P, erythrose 4-phosphate; CIT, citric acid; 3-PG, 3-phosphoglyceric acid; 1,3-PG, 1,3-phosphoglyceric acid; GAP, glyceraldehyde 3-phosphate; PEP, phosphoenolpyruvic acid; GLU, glutamic acid; PYR, pyruvic acid; AKG, 2-oxoglutaric acid; MAL, malate acid; SUC, succinic acid; FUM, fumaric acid; Ac-CoA, Acetoacetyl coenzyme A. **(A)** WT, mutant 6–8, mutant 6–16 and mutant 6–23 at 24 h; **(B)** WT, mutant 6–8, mutant 6–16 and mutant 6–23 at 48 h. Three biological replicates were carried out.

the relative abundance of ions in samples which is described with color intensity (Ivanisevic et al., 2015). It allows for sample classification and the description of features that are driving the classification by adding dimension of data visualization (Babicki et al., 2016). It has been well used for exploring metabolic flux of microalgae previously (Wang et al., 2019; Lv et al., 2020). In this study, heatmaps of targeted metabolite analysis in all samples were generated for better interpreting the qualitative information of these metabolites. The results were shown in **Figure 4**.

The metabolomic analysis showed similar metabolic changes among these mutants, including: 1) EMP seemed strengthened as the up-regulation of 3-PG, 1,3-PG, PYR at both 24 and 48 h was observed. EMP is known to produce ATP, Ac-CoA, NADH and which are necessary substances for biomass accumulation (Chen et al., 2017); 2) PPP seemed enhanced, as it key metabolite R5P were up-regulated at both 24 and 48 h. One of alternative NADPH-producing sources is PPP. It was previously reported that elevation expression of PPP leads to significant increase of total fatty acid content in *Yarrowia lipolytica* or *Aurantiochytrium sp.* SD116 (Cui et al., 2016; Xu et al., 2017; Liu et al., 2019); 3) The lipogenesis pathway seemed up-regulated, as CoA and NADPH, the precursors of lipid biosynthesis, were up-regulated; 4) TCA cycles seemed attenuated, as metabolites involved in TCA cycles, such as CIT, MAL, SUC, FUM at 24 and

48 h in M-6-8; CIT, FUM at 24 and 48 h in M-6-16; CIT, SUC at 24 h or MAL at 48 h in M-23, were down-regulated. Pushing carbon source of TCA cycle into lipogenesis could significantly increase lipid accumulation in oleaginous yeast *Y. lipolytica* or *Saccharomyce cerevisiae* (Silverman et al., 2016; Yu et al., 2018).

Evaluation of Application Potential of Mutant 6–23 in Fermentor

Pulse-feeding glucose fed-batch fermentation was performed in a 5 L fermentor to assess the growth and fatty acid biosynthesis, as well as application potential of mutant 6–23. The glucose concentration was maintained at 20–50 g/L (**Figure 5B**). Both mutant 6–23 and the wild type entered exponential growth phase at 12 h, and the specific growth rate of mutant 6–23 was $\mu = 0.028 \text{ h}^{-1}$, while it was $\mu = 0.023 \text{ h}^{-1}$ for wild type during exponential growth phase. Therefore, mutant 6–23 grew faster than the wild type, and mutant 6–23 approached the stationary phase at 76 h, earlier than the 84 h for the wild type (**Figure 5A**). The final biomass accumulation of mutant 6–23 was $154.8 \pm 1.2 \text{ g/L}$ at 96 h, 10% higher than that of the wild type ($140.4 \pm 0.9 \text{ g/L}$).

As mutant 6–23 achieved the maximal growth approximately 8 h earlier than that of the wild type, cells of mutant 6–23 were harvested at 36, 64, and 76 h, while the cells of the wild type were

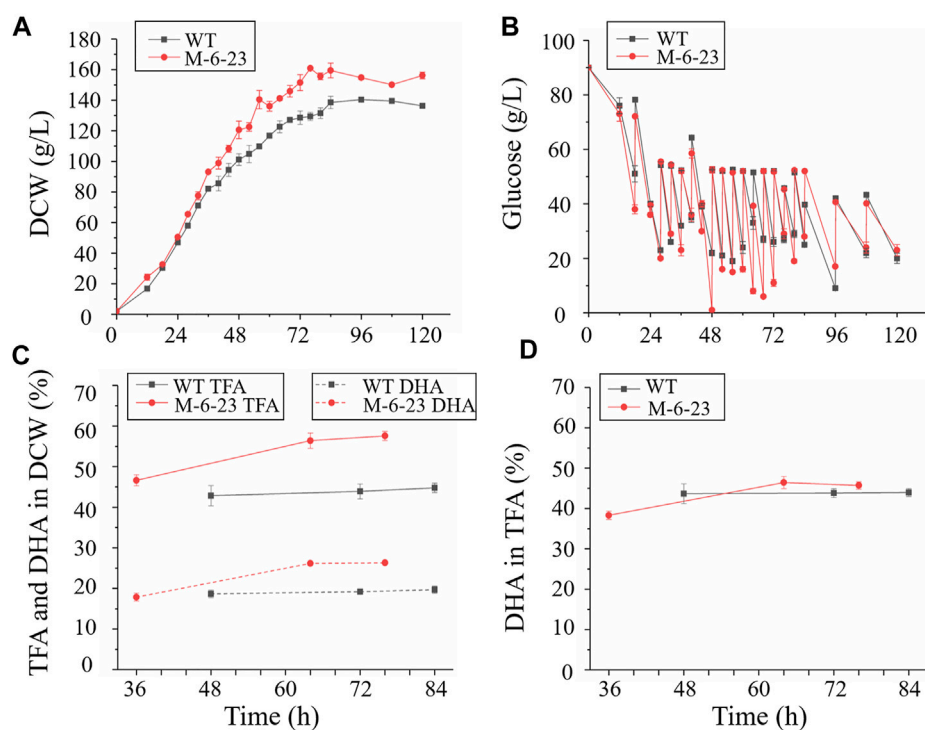


FIGURE 5 | Comparison of biomass accumulation, glucose concentration total fatty acid and DHA content in 5 L fermentors. Black represents wild type (WT); red represents mutant 6–23 (M-6-23), respectively. **(A)** biomass accumulation of wild type and mutant 6–23; **(B)** biomass accumulation of mutant 6–23; **(C)** total fatty acid (TFA) and DHA content in dry cell weight (DCW); **(D)** DHA content in total fatty acid. Error bar represents standard deviation of three biological replicates.

TABLE 1 | Comparison of DHA production by *Schizochytrium* strains in different reports.

<i>Schizochytrium</i> sp.	Experimental conditions	Yield (g DHA per g DCW)	Fermentation time (h)	Dry cell weight (g/L)	DHA titer (g/L)	DHA productivity (mg/L/h)	References
CCTCC M209059	Fed-batch culture using glucose in 10-L fermentor	0.253	120	67.21	17.02	146.7	Qu et al. (2013b)
HX-308-ALE Endpoint strain	Fed-batch culture using glucose in 5 L fermentor	0.313	120	84.34	26.40	220.04	Sun et al. (2016)
HX-308	Fed-batch culture using glucose and cane molasses in 50 L fermentor	0.194	120	78.26	15.22	126.83	Yin et al. (2019)
ATCC 20888 AB-610	Fed-batch culture using glucose in 7.5 L fermentor	0.191	120	59.96	11.44	95.33	Zhao et al. (2017)
LU301	Culture in 1,000 ml baffled flasks with glucose	0.293	120	84.34	24.74	241.5	Ling et al. (2015)
PQ6	Fed-batch culture using glucose in 30 L fermentor	0.056	96	105.25	5.919	61.66	Hoang et al. (2018)
ATCC 20888	Fed-batch culture using glycerol in 7.5 L fermentor	0.192	96	151.4	28.93	301	Chang et al. (2013)
M-6-23	Fed-batch culture using in 5 L fermentor	0.267	96	154.8	41.35	430.73	This study

collected at 48, 72, and 84 h, which were corresponding to middle and late exponential and stationary phases of each of their growth phases, respectively. They were then subjected to total fatty acid and DHA analysis. As shown in **Figure 5C**, the total fatty acid and DHA content of mutant 6–23 were significantly elevated by 28.6 and 33.7% at stationary phase, respectively, while DHA ratio in total fatty acid was not enhanced in mutant 6–23 (**Figure 5D**).

The results showed that DHA concentration and productivity of mutant 6–23 were 42.4 g/L and 557.5 mg/L/h at stationary phase, respectively. The significant enhancement of biomass and DHA content in DCW collectively increased DHA concentration and productivity by 55.3 and 71.6% in mutant 6–23. DHA production by different *Schizochytrium* or *Aurantiochytrium* strains reported so far were summarized in **Table 1**, which showed that mutant

6–23 achieved the highest synthesis based on DHA concentration and productivity among all studies reported so far.

DISCUSSION

ARTP has successfully applied to various marine microorganisms to obtain mutants with better phenotype. For example, enhancing the production capacity of lipid in the oleaginous microalgae *Chlorella pyrenoidosa* (Cao et al., 2017). In addition, improving productivity and the yield of DHA were increased by 1.7- and 1.3-fold in *Cryptocodinium cohnii* (Lv et al., 2020). In this study, *Schizochytrium* ATCC 20888 was treated by ARTP mutagenesis with a new screening approach using EMP and PPP inhibitor, iodoacetic acid and DHEA, as screening agents. This led to identification of three mutants named 6–8, 6–16, and 6–23 with increased biomass and DHA accumulation. LC-MS metabolomic analysis was applied to explore possible mechanisms relevant to enhanced growth and DHA accumulation. The analysis suggested that the upregulated metabolism in PPP and EMP as well as the downregulated TCA cycle might be relevant to the increased growth and DHA biosynthesis in these mutants. At last, mutant 6–23 fermented in 5 L fermentors produced the highest DHA titer and productivity reported in literature.

Metabolic inhibitors have been well studied for screening mutants with improved characterization (Liu et al., 2015). It was reported that EMP, TCA, fatty acid synthase, and ROS are potential metabolic pathways responsible for biomass and DHA production increase in marine microorganisms, and the corresponding targeted inhibitors such as iodoacetic acid, malonic acid, quizalofop-p-ethyl, and 2', 2'-bipyridine were well developed for screening mutants with increased biomass and lipid production (Lian et al., 2010; Xu et al., 2012; Yuan et al., 2015). However, no report focused on inhibitors targeted for PPP, which has demonstrated to increase lipid accumulation by elevating NADPH supply in marine microorganisms (Cui et al., 2016). In this study, it was the first time to prove dehydroepiandrosterone, an effective inhibitor of PPP, can be used as a screening agent for obtaining mutants with increasing DHA production in *Schizochytrium*. Since enhancing PPP could impair growth in *Aurantiochytrium* sp. SD116 and *Chlorella pyrenoidosa* (Cui et al., 2016; Xue et al., 2018), iodoacetic acid, an inhibitor of EMP pathways, was also added into plates and larger colonies were picked up. These efforts led to discover mutants 6–8, 6–16 and 6–23 with better performance in DHA production.

Samples harvesting for the analysis of cellular metabolites is a challenging task since it may affect the final conclusions. Centrifugation is a widely used technique for harvesting microbes, however, centrifugal forces could lead to the uncontrolled reaction of metabolism during centrifugation (Veyel et al., 2014). There are different views on centrifugation temperature for harvesting cells. Some people argue that cold stress led to change TCA intermediates and organic acids, even its related enzymes in the microalgae (Vallador et al., 2013; Willette et al., 2018), while other think NAD⁺, NADH, NADP⁺, and

NADPH show considerable instability at elevated temperature (Gil et al., 2015). Despite the different views mentioned, we argue from the early studies that it will be good to maintain cells at the similar temperature as its cultivation for metabolite, as long as the cells not broken (Li et al., 2015; Diao et al., 2019).

LC/MS revealed that PPP and EMP were both increased in mutants 6–8, 6–16 and 6–23, consistent with increased the activity of phosphoglyceraldehyde dehydrogenase and glucose-6-phosphate dehydrogenase. Although it still needs more evidence that phosphoglyceraldehyde dehydrogenase and glucose-6-phosphate dehydrogenase were likely to play vital roles in biomass and DHA accumulations in *Schizochytrium* sp. Genes encoding phosphoglyceraldehyde dehydrogenase and glucose-6-phosphate dehydrogenase of the wild type and mutant 6–8, 6–16, and 6–23 were PCR amplified and resequencing. However, no mutation site was found inside coding gene, suggesting that other changes, such as mutation of regulatory protein, possibly provoked the up-regulated activity of phosphoglyceraldehyde dehydrogenase and glucose-6-phosphate dehydrogenase, which may worth further investigation in the future. Similar phenomenon was observed in screening *C. cohnii* mutants using ARTP mutagenesis combined with acetyl-CoA carboxylase inhibitor sethoxydim (Liu et al., 2017).

As shown in **Figure 2**, the fatty acid was not enhanced after 48 h cultivation, and while growth was continued until 72 h. Phosphoglyceraldehyde dehydrogenase is involved in EMP pathway, which is provided acetyl-CoA and ATP for fatty acid and biomass accumulation, while glucose-6-phosphate dehydrogenase is a part of PPP pathway, which is for NADPH supply. It was inferred that NADPH needed for fatty acid biosynthesis was decreased since fatty acids content was no longer increased. This led to the decreased the activity of glucose-6-phosphate dehydrogenase. Acetyl-CoA and ATP were continuously needed as biomass was gradually accumulated until 72 h, resulting in increasing the activity of phosphoglyceraldehyde dehydrogenase. The decrease of glucose-6-phosphate dehydrogenase activity is also observed in *Aurantiochytrium* sp. SD116, a closed relationship of *Schizochytrium* (Cui et al., 2016).

Although many similar changes among these strains were observed, there still exist many different metabolic changes among these mutants, notably: 1) The down-regulated ADP-GCS and UDP-GCS suggested that the carbon source flowed from starch or extracellular polysaccharides into lipid or biomass accumulation in mutant 6–23 (Lv et al., 2020); however, UDP-GCS in mutant 6–16 was up-regulated, suggesting different carbon source partition mechanisms from mutant 6–23; 2) It was observed that NADH at 24 and 48 h was up-regulated in mutant 6–23, but not at 48 h in mutant 6–8 and 6–16. The NADH generated by EMP beyond cellular oxidative capacity could lead to overflow metabolism and repress respiratory genes (Vemuri et al., 2007; Bhat et al., 2016). The down-regulated TCA cycles in mutant 6–23 seemed to be consistent with the phenomenon. The possible reasons of down-regulated TCA cycles in mutant 6–8 and 6–16 might obviously different from that of mutant 6–23; 3) It was discovered that acetyl-CoA, the important precursor of

lipogenesis, was obviously decreased in mutant 6–23, but not in mutant 6–8 and 6–16. PUFA ratio (DPA + DHA) in total fatty acid profiles were significantly enhanced in mutant 6–23, but not in mutants 6–8 and 6–16. These results suggested the diversity and complexity of the regulation related to growth and DHA accumulation in *Schizochytrium*.

The results from the comparison of different metabolic changes among these mutants could lead to several possible strategies for further increasing DHA production in mutant 6–23: 1) Overexpressing NADH kinase or replacing NAD⁺-glyceraldehyde-3-phosphate dehydrogenase by NADP⁺-glyceraldehyde-3-phosphate dehydrogenase to convert NADH into NADPH in mutant 6–23. Overexpressing the mitochondrial NADH kinase increased the μ_{max} by 11% in *S. cerevisiae* (Hou et al., 2009). Introducing NADP⁺-glyceraldehyde-3-phosphate dehydrogenase to replace NAD⁺-glyceraldehyde-3-phosphate dehydrogenase could improve 17.8–20.0% lipid yields in *Y. lipolytica* (Qiao et al., 2017); 2) Enhancement of acetyl-CoA production by installing non-oxidative glycolytic pathway (NOG). NOG pathway can produce 3 mol acetyl-CoA from 1 mol glucose, which is efficient than EMP. Introducing NOG results in 16.4% higher lipid content and 41% higher dry cell weight in *Y. lipolytica* (Qiao et al., 2017). The genetic manipulation platforms, such as electrotransformation, *Agrobacterium tumefaciens* mediated transformation and *Cre-loxp* method, have been established in *Schizochytrium* (Cheng et al., 2012; Ren et al., 2015; Sun et al., 2015; Wang et al., 2019). Fully sequencing of mutant 6–23 will provide much more useful information for further investigation, which will be carried out in the near future. Above, these researches make application of above-mentioned strategies feasible in the future.

DHA titer and productivity are important to evaluate the commercial application potential of marine microorganism strains. Before our study, the highest DHA concentration achieved 28.93 g/L, and the highest DHA productivity 301 mg/L/h using *Schizochytrium* ATCC 20888 using glycerol as carbon source (Chang et al., 2013). In this study, DHA titer and productivity were improved to 41.4 g/L and 430.7 mg/L/h respectively by a fermentation of mutant 6–23 with glucose as carbon source. In addition, the maximum yield of glycerol into fatty acid is around 0.10 ± 0.02 g/g, while it is approximately 0.365 g/g of glucose (Chang et al., 2013; Qiao et al., 2017). In all, mutant 6–23 seems a good candidate marine microorganism for industrial production of DHA in the near future.

CONCLUSION

A new mutagenesis strategy based on ARTP and two biochemical inhibitors, iodoacetic acid and dehydroepiandrosterone, was

applied to *Schizochytrium* ATCC20888. After two rounds of screening, mutants 6–8, 6–16 and 6–23 were obtained. Comparing the starting strain, the growth and total fatty acid content of these strains were significantly elevated, resulting in the DHA concentration increases of 51.9, 45.0, 58.5% in mutants 6–8, 6–16 and 6–23 in shaking flask cultivations, respectively. A targeted LC-MS metabolomic analysis showed that the strengthening metabolism in PPP and EMP as well as attenuating TCA cycles might be related to the increased growth and lipid biosynthesis in *Schizochytrium*. At last, mutant 6–23 was evaluated in a 5-L fermentor, and the results showed that the DHA concentration and productivity of mutant 6–23 were 41.4 g/L and 430.7 mg/L/h in fermentation for 96 h, respectively, which represent the highest reported in literature so far.

DATA AVAILABILITY STATEMENT

The original contributions presented in the study are included in the article/Supplementary Material, further inquiries can be directed to the corresponding authors.

AUTHOR CONTRIBUTIONS

FW and WZ conceived the project and designed the experiments. LZ, YB, FW, PG, TW, LD and YB performed the experiments. FW, LZ, LC, WZ analyzed the data and wrote the article. FW, LC and WZ revised the article. All the authors discussed the article and agreed to its publication.

FUNDING

This research was supported by grants from the National Key Research and Development Program of China (Grant Nos. 2020YFA0908703, 2019YFA0904600), the Tianjin Municipal Science Foundation (Nos. 18JCQNJC10000), National Natural Science Foundation of China (Nos. 3210120152, 31770100, 31972931, 31770035, 91751102, 21621004, 31370115 and 31470217), and Zaoneng Biotechnology Inc.

SUPPLEMENTARY MATERIAL

The Supplementary Material for this article can be found online at: <https://www.frontiersin.org/articles/10.3389/fbioe.2021.738052/full#supplementary-material>

REFERENCES

- Babicki, S., Arndt, D., Marcu, A., Liang, Y., Grant, J. R., Maciejewski, A., et al. (2016). Heatmapper: Web-Enabled Heat Mapping for All. *Nucleic Acids Res.* 44 (W1), W147–W153. doi:10.1093/nar/gkw419
- Beevers, H. (1952). Malonic Acid as an Inhibitor of maize Root Respiration. *Plant Physiol.* 27 (4), 725–735. doi:10.1104/pp.27.4.725
- Bhat, S. A., Iqbal, I. K., and Kumar, A. (2016). Imaging the NADH:NAD⁺ Homeostasis for Understanding the Metabolic Response of Mycobacterium to Physiologically Relevant Stresses. *Front. Cel. Infect. Microbiol.* 6, 145. doi:10.3389/fcimb.2016.00145

- Cao, S., Zhou, X., Jin, W., Wang, F., Tu, R., Han, S., et al. (2017). Improving of Lipid Productivity of the Oleaginous Microalgae *Chlorella Pyrenoidosa* via Atmospheric and Room Temperature Plasma (ARTP). *Bioresour. Technol.* 244, 1400–1406. doi:10.1016/j.biortech.2017.05.039
- Chance, B., and Park, J. H. (1967). The Properties and Enzymatic Significance of the Enzyme-Diphosphopyridine Nucleotide Compound of 3-phosphoglyceraldehyde Dehydrogenase. *J. Biol. Chem.* 242 (21), 5093–5105. doi:10.1016/s0021-9258(18)99480-9
- Chang, G., Gao, N., Tian, G., Wu, Q., Chang, M., and Wang, X. (2013). Improvement of Docosahexaenoic Acid Production on Glycerol by *Schizochytrium* Sp. S31 with Constantly High Oxygen Transfer Coefficient. *Bioresour. Technol.* 142, 400–406. doi:10.1016/j.biortech.2013.04.107
- Chen, H., Zheng, Y., Zhan, J., He, C., and Wang, Q. (2017). Comparative Metabolic Profiling of the Lipid-Producing green Microalga *Chlorella* Reveals that Nitrogen and Carbon Metabolic Pathways Contribute to Lipid Metabolism. *Biotechnol. Biofuels* 10 (1), 1–20. doi:10.1186/s13068-017-0839-4
- Cheng, R., Ma, R., Li, K., Rong, H., Lin, X., Wang, Z., et al. (2012). Agrobacterium Tumefaciens Mediated Transformation of marine Microalgae *Schizochytrium*. *Microbiol. Res.* 167 (3), 179–186. doi:10.1016/j.micres.2011.05.003
- Cui, G.-Z., Ma, Z., Liu, Y.-J., Feng, Y., Sun, Z., Cheng, Y., et al. (2016). Overexpression of Glucose-6-Phosphate Dehydrogenase Enhanced the Polyunsaturated Fatty Acid Composition of Aurantiochytrium Sp. SD116. *Algal Res.* 19, 138–145. doi:10.1016/j.algal.2016.08.005
- De Swaaf, M. E., De Rijk, T. C., Eggink, G., and Sijtsma, L. (1999). Optimisation of Docosahexaenoic Acid Production in Batch Cultivations by *Cryptocodinium Cohnii*. *J. Biotechnol.* 70, 185–192. doi:10.1016/s0168-1656(99)00071-1
- Dessi, M., Noce, A., Bertucci, P., Manca di Villahermosa, S., Zenobi, R., Castagnola, V., et al. (2013). Atherosclerosis, Dyslipidemia, and Inflammation: the Significant Role of Polyunsaturated Fatty Acids. *ISRN Inflamm.* 2013, 1–13. doi:10.1155/2013/191823
- Diao, J., Song, X., Cui, J., Liu, L., Shi, M., Wang, F., et al. (2019). Rewiring Metabolic Network by Chemical Modulator Based Laboratory Evolution Doubles Lipid Production in *Cryptocodinium Cohnii*. *Metab. Eng.* 51, 88–98. doi:10.1016/j.jymben.2018.10.004
- Ganuz, E., Anderson, A. J., and Ratledge, C. (2008). High-cell-density Cultivation of *Schizochytrium* Sp. In an ammonium/pH-Auxostat Fed-Batch System. *Biotechnol. Lett.* 30 (9), 1559–1564. doi:10.1007/s10529-008-9723-4
- Gil, A., Siegel, D., Permentier, H., Reijngoud, D.-J., Dekker, F., and Bischoff, R. (2015). Stability of Energy Metabolites—An Often Overlooked Issue in Metabolomics Studies: A Review. *Electrophoresis* 36 (18), 2156–2169. doi:10.1002/elps.201500031
- Hoang, L. A. T., Nguyen, H. C., Le, T. T., Hoang, T. H. Q., Pham, V. N., Hoang, M. H. T., et al. (2018). Different Fermentation Strategies by *Schizochytrium Mangrovei* Strain Pq6 to Produce Feedstock for Exploitation of Squalene and omega-3 Fatty Acids. *J. Phycol.* 54 (4), 550–556. doi:10.1111/jpy.12757
- Hou, J., Lages, N. F., Oldiges, M., and Vemuri, G. N. (2009). Metabolic Impact of Redox Cofactor Perturbations in *Saccharomyces cerevisiae*. *Metab. Eng.* 11 (4–5), 253–261. doi:10.1016/j.jymben.2009.05.001
- Ivanisevic, J., Benton, H. P., Rinehart, D., Epstein, A., Kurczyk, M. E., Boska, M. D., et al. (2015). An Interactive Cluster Heat Map to Visualize and Explore Multidimensional Metabolomic Data. *Metabolomics* 11 (4), 1029–1034. doi:10.1007/s11306-014-0759-2
- Langdon, R. G. (1966). [24] Glucose 6-phosphate Dehydrogenase from Erythrocytes. *Methods Enzymol.* 9, 126–131. doi:10.1016/0076-6879(66)09030-X
- Li, J., Niu, X., Pei, G., Sui, X., Zhang, X., Chen, L., et al. (2015). Identification and Metabolomic Analysis of Chemical Modulators for Lipid Accumulation in *Cryptocodinium Cohnii*. *Bioresour. Technol.* 191, 362–368. doi:10.1016/j.biortech.2015.03.068
- Li, X., Pei, G., Liu, L., Chen, L., and Zhang, W. (2017). Metabolomic Analysis and Lipid Accumulation in a Glucose Tolerant *Cryptocodinium Cohnii* Strain Obtained by Adaptive Laboratory Evolution. *Bioresour. Technol.* 235, 87–95. doi:10.1016/j.biortech.2017.03.049
- Li, Z., Meng, T., Ling, X., Li, J., Zheng, C., Shi, Y., et al. (2018). Overexpression of Malonyl-CoA: ACP Transacylase in *Schizochytrium* Sp. To Improve Polyunsaturated Fatty Acid Production. *J. Agric. Food Chem.* 66 (21), 5382–5391. doi:10.1021/acs.jafc.8b01026
- Li, J. T., Liu, X. H., He, Y. D., and Wang, G. Y. (2020). Mutagenesis Breeding in DHA Production by Oleaginous Microorganisms. *Biotechnol. Bull.* 36 (1), 110–115. doi:10.13560/j.cnki.biotech.bull.1985.2019-0637
- Lian, M., Huang, H., Ren, L., Ji, X., Zhu, J., and Jin, L. (2010). Increase of Docosahexaenoic Acid Production by *Schizochytrium* Sp. Through Mutagenesis and Enzyme Assay. *Appl. Biochem. Biotechnol.* 162 (4), 935–941. doi:10.1007/s12010-009-8865-8
- Ling, X., Guo, J., Liu, X., Zhang, X., Wang, N., Lu, Y., et al. (2015). Impact of Carbon and Nitrogen Feeding Strategy on High Production of Biomass and Docosahexaenoic Acid (DHA) by *Schizochytrium* Sp. LU310. *Bioresour. Technol.* 184, 139–147. doi:10.1016/j.biortech.2014.09.130
- Liu, C., Zhang, X., Rao, Z.-m., Shao, M.-l., Zhang, L.-l., Wu, D., et al. (2015). Mutation Breeding of High 4-Androstene-3,17-Dione-Producing *Mycobacterium Neoaurum* ZADF-4 by Atmospheric and Room Temperature Plasma Treatment. *J. Zhejiang Univ. Sci. B* 16 (4), 286–295. doi:10.1631/jzus.B1400274
- Liu, J., Pei, G., Diao, J., Chen, Z., Liu, L., Chen, L., et al. (2017). Screening and Transcriptomic Analysis of *Cryptocodinium Cohnii* Mutants with High Growth and Lipid Content Using the Acetyl-CoA Carboxylase Inhibitor Sethoxydim. *Appl. Microbiol. Biotechnol.* 101 (15), 6179–6191. doi:10.1007/s00253-017-8397-z
- Liu, H., Marsafari, M., Deng, L., and Xu, P. (2019). Understanding Lipogenesis by Dynamically Profiling Transcriptional Activity of Lipogenic Promoters in *Yarrowia Lipolytica*. *Appl. Microbiol. Biotechnol.* 103 (7), 3167–3179. doi:10.1007/s00253-019-09664-8
- Lv, M., Wang, F., Zeng, L., Bi, Y., Cui, J., Liu, L., et al. (2020). Identification and Metabolomic Analysis of a Starch-Deficient *Cryptocodinium Cohnii* Mutant Reveals Multiple Mechanisms Relevant to Enhanced Growth and Lipid Accumulation. *Algal Res.* 50, 102001. doi:10.1016/j.algal.2020.102001
- Makrides, M., Neumann, M. A., Byard, R. W., Simmer, K., and Gibson, R. A. (1994). Fatty Acid Composition of Brain, Retina, and Erythrocytes in Breast- and Formula-Fed Infants. *Am. J. Clin. Nutr.* 60 (2), 189–194. doi:10.1093/ajcn/60.2.189
- Metz, J. G., Roessler, P., Facciotti, D., Levering, C., Dittrich, F., Lassner, M., et al. (2001). Production of Polyunsaturated Fatty Acids by Polyketide Synthases in Both Prokaryotes and Eukaryotes. *Science* 293 (5528), 290–293. doi:10.1126/science.1059593
- Nouroozi, R. V., Noroozi, M. V., and Ahmadzadeh, M. (2015). Determination of Protein Concentration Using Bradford Microplate Protein Quantification Assay. *Int. Electron. J. Med.* 4 (1), 11–17. doi:10.31661/iejm.158
- Ottenheim, C., Nawrath, M., and Wu, J. C. (2018). Microbial Mutagenesis by Atmospheric and Room-Temperature Plasma (ARTP): the Latest Development. *Bioresour. Bioproc.* 5 (1), 1–14. doi:10.1186/s40643-018-0200-1
- Park, C.-H., Park, C.-H., Lee, Y.-J., Lee, S.-Y., Oh, H.-B., and Lee, J.-W. (2011). Determination of the Intracellular Concentrations of Metabolites in *Escherichia coli* Collected during the Exponential and Stationary Growth Phases Using Liquid Chromatography-Mass Spectrometry. *Bull. Korean Chem. Soc.* 32 (2), 524–530. doi:10.5012/bkcs.2011.32.2.524
- Qiao, K., Wasylenko, T. M., Zhou, K., Xu, P., and Stephanopoulos, G. (2017). Lipid Production in *Yarrowia Lipolytica* Is Maximized by Engineering Cytosolic Redox Metabolism. *Nat. Biotechnol.* 35 (2), 173–177. doi:10.1038/nbt.3763
- Qiu, X., Xie, X., and Meesapyodsuk, D. (2020). Molecular Mechanisms for Biosynthesis and Assembly of Nutritionally Important Very Long Chain Polyunsaturated Fatty Acids in Microorganisms. *Prog. Lipid Res.* 79, 101047. doi:10.1016/j.plipres.2020.101047
- Qu, L., Ren, L.-J., Sun, G.-N., Ji, X.-J., Nie, Z.-K., and Huang, H. (2013a). Batch, Fed-Batch and Repeated Fed-Batch Fermentation Processes of the marine Thraustochytrid *Schizochytrium* Sp. For Producing Docosahexaenoic Acid. *Bioproc. Biosyst. Eng.* 36 (12), 1905–1912. doi:10.1007/s00449-013-0966-7
- Qu, L., Ren, L.-J., Li, J., Sun, G.-N., Sun, L.-N., Ji, X.-J., et al. (2013b). Biomass Composition, Lipid Characterization, and Metabolic Profile Analysis of the Fed-Batch Fermentation Process of Two Different Docosahexaenoic Acid Producing *Schizochytrium* Sp. Strains. *Appl. Biochem. Biotechnol.* 171 (7), 1865–1876. doi:10.1007/s12010-013-0456-z
- Ren, L.-J., Ji, X.-J., Huang, H., Qu, L., Feng, Y., Tong, Q.-Q., et al. (2010). Development of a Stepwise Aeration Control Strategy for Efficient

- Docosahexaenoic Acid Production by *Schizochytrium* Sp. *Appl. Microbiol. Biotechnol.* 87 (5), 1649–1656. doi:10.1007/s00253-010-2639-7
- Ren, L.-j., Zhuang, X.-y., Chen, S.-l., Ji, X.-j., and Huang, H. (2015). Introduction of ω -3 Desaturase Obviously Changed the Fatty Acid Profile and Sterol Content of *Schizochytrium* Sp. *J. Agric. Food Chem.* 63 (44), 9770–9776. doi:10.1021/acs.jafc.5b04238
- Réveillon, D., Tunin-Ley, A., Grondin, I., Othmani, A., Zubia, M., Bunet, R., et al. (2019). Exploring the Chemodiversity of Tropical Microalgae for the Discovery of Natural Antifouling Compounds. *J. Appl. Phycol.* 31 (1), 319–333. doi:10.1007/s10811-018-1594-z
- Silverman, A. M., Qiao, K., Xu, P., and Stephanopoulos, G. (2016). Functional Overexpression and Characterization of Lipogenesis-Related Genes in the Oleaginous Yeast *Yarrowia Lipolytica*. *Appl. Microbiol. Biotechnol.* 100 (8), 3781–3798. doi:10.1007/s00253-016-7376-0
- Su, Y., Wang, J., Shi, M., Niu, X., Yu, X., Gao, L., et al. (2014). Metabolomic and Network Analysis of Astaxanthin-Producing *Haematococcus pluvialis* under Various Stress Conditions. *Bioresour. Technol.* 170, 522–529. doi:10.1016/j.biortech.2014.08.018
- Sun, H., Chen, H., Zang, X., Hou, P., Zhou, B., Liu, Y., et al. (2015). Application of the *Cre/loxP* Site-specific Recombination System for Gene Transformation in *Aurantiochytrium Limacinum*. *Molecules* 20 (6), 10110–10121. doi:10.3390/molecules200610110
- Sun, X.-M., Ren, L.-J., Ji, X.-J., Chen, S.-L., Guo, D.-S., and Huang, H. (2016). Adaptive Evolution of *Schizochytrium* Sp. By Continuous High Oxygen Stimulations to Enhance Docosahexaenoic Acid Synthesis. *Bioresour. Technol.* 211, 374–381. doi:10.1016/j.biortech.2016.03.093
- Sun, X.-M., Ren, L.-J., Bi, Z.-Q., Ji, X.-J., Zhao, Q.-Y., and Huang, H. (2018). Adaptive Evolution of Microalgae *Schizochytrium* Sp. Under High Salinity Stress to Alleviate Oxidative Damage and Improve Lipid Biosynthesis. *Bioresour. Technol.* 267, 438–444. doi:10.1016/j.biortech.2018.07.079
- Sun, H., Li, X., Ren, Y., Zhang, H., Mao, X., Lao, Y., et al. (2020). Boost Carbon Availability and Value in Algal Cell for Economic Deployment of Biomass. *Bioresour. Technol.* 300, 122640. doi:10.1016/j.biortech.2019.122640
- Tian, W.-N., Braunstein, L. D., Apse, K., Pang, J., Rose, M., Tian, X., et al. (1999). Importance of Glucose-6-Phosphate Dehydrogenase Activity in Cell Death. *Am. J. Physiology-Cell Physiol.* 276 (5), C1121–C1131. doi:10.1152/ajpcell.1999.276.5.c1121
- Valledor, L., Furuhashi, T., Hanak, A.-M., and Weckwerth, W. (2013). Systemic Cold Stress Adaptation of *Chlamydomonas Reinhardtii*. *Mol. Cell Proteomics* 12 (8), 2032–2047. doi:10.1074/mcp.m112.026765
- Vemuri, G. N., Eiteman, M. A., McEwen, J. E., Olsson, L., and Nielsen, J. (2007). Increasing NADH Oxidation Reduces Overflow Metabolism in *Saccharomyces cerevisiae*. *Proc. Natl. Acad. Sci.* 104 (7), 2402–2407. doi:10.1073/pnas.0607469104
- Veyel, D., Erban, A., Fehrle, I., Kopka, J., and Schroda, M. (2014). Rationales and Approaches for Studying Metabolism in Eukaryotic Microalgae. *Metabolites* 4 (2), 184–217. doi:10.3390/metabo4020184
- Wang, X., Lu, M., Wang, S., Fang, Y., Wang, D., Ren, W., et al. (2014). The Atmospheric and Room-Temperature Plasma (ARTP) Method on the Dextranase Activity and Structure. *Int. J. Biol. Macromol.* 70, 284–291. doi:10.1016/j.ijbiomac.2014.07.006
- Wang, F., Bi, Y., Diao, J., Lv, M., Cui, J., Chen, L., et al. (2019). Metabolic Engineering to Enhance Biosynthesis of Both Docosahexaenoic Acid and Odd-Chain Fatty Acids in *Schizochytrium* Sp. S31. *Biotechnol. Biofuels* 12, 141. doi:10.1186/s13068-019-1484-x
- Willette, S., Gill, S. S., Dungan, B., Schaub, T. M., Jarvis, J. M., St. Hilaire, R., et al. (2018). Alterations in Lipidome and Metabolome Profiles of *Nannochloropsis salina* in Response to Reduced Culture Temperature during Sinusoidal Temperature and Light. *Algal Res.* 32, 79–92. doi:10.1016/j.algal.2018.03.001
- Xu, Y., Zang, X. N., Xu, D., and Zhnag, X. C. (2012). Mutation of *Schizochytrium Limacinum* and Screening of Elite Mutants. *Periodical Ocean Univ. China* 42 (12), 054–058. doi:10.16441/j.cnki.hdx.2012.12.008
- Xu, P., Qiao, K., and Stephanopoulos, G. (2017). Engineering Oxidative Stress Defense Pathways to Build a Robust Lipid Production Platform in *Yarrowia Lipolytica*. *Biotechnol. Bioeng.* 114 (7), 1521–1530. doi:10.1002/bit.26285
- Xue, J., Balamurugan, S., Li, D.-W., Liu, Y.-H., Zeng, H., Wang, L., et al. (2017). Glucose-6-phosphate Dehydrogenase as a Target for Highly Efficient Fatty Acid Biosynthesis in Microalgae by Enhancing NADPH Supply. *Metab. Eng.* 41, 212–221. doi:10.1016/j.ymben.2017.04.008
- Xue, J., Chen, T.-T., Zheng, J.-W., Balamurugan, S., Cai, J.-X., Liu, Y.-H., et al. (2018). The Role of Diatom Glucose-6-Phosphate Dehydrogenase on Lipogenic NADPH Supply in green Microalgae through Plastidial Oxidative Pentose Phosphate Pathway. *Appl. Microbiol. Biotechnol.* 102 (24), 10803–10815. doi:10.1007/s00253-018-9415-5
- Yin, F.-W., Zhu, S.-Y., Guo, D.-S., Ren, L.-J., Ji, X.-J., Huang, H., et al. (2019). Development of a Strategy for the Production of Docosahexaenoic Acid by *Schizochytrium* Sp. From Cane Molasses and Algae-Residue. *Bioresour. Technol.* 271, 118–124. doi:10.1016/j.biortech.2018.09.114
- Yu, T., Zhou, Y. J., Huang, M., Liu, Q., Pereira, R., David, F., et al. (2018). Reprogramming Yeast Metabolism from Alcoholic Fermentation to Lipogenesis. *Cell* 174 (6), 1549–1558. doi:10.1016/j.cell.2018.07.013
- Yuan, J., Zhao, B., Sun, M., Wang, W., and Yang, H. (2015). Rapid Mutation Breeding *Schizochytrium* Strains Producing High-Yield Docosahexaenoic Acid by Atmospheric and Room Temperature Plasmas (ARTP). *Biotechnol. Bull.* 31 (10), 199–204. doi:10.13560/j.cnki.biotech.bull.1985.2015.10.030
- Zhao, B., Li, Y., Mbifile, M. D., Li, C., Yang, H., and Wang, W. (2017). Improvement of Docosahexaenoic Acid Fermentation from *Schizochytrium* Sp. AB-610 by Staged pH Control Based on Cell Morphological Changes. *Eng. Life Sci.* 17 (9), 981–988. doi:10.1002/elsc.201600249
- Zhao, B., Li, Y., Li, C., Yang, H., and Wang, W. (2018). Enhancement of *Schizochytrium* DHA Synthesis by Plasma Mutagenesis Aided with Malonic Acid and Zeocin Screening. *Appl. Microbiol. Biotechnol.* 102 (5), 2351–2361. doi:10.1007/s00253-018-8756-4
- Zhou, B., Xiao, J. F., Tuli, L., and Ransom, H. W. (2012). LC-MS-based Metabolomics. *Mol. Biosyst.* 8 (2), 470–481. doi:10.1039/c1mb05350g
- Zwickl, P., Fabry, S., Bogedain, C., Haas, A., and Hensel, R. (1990). Glyceraldehyde-3-phosphate Dehydrogenase from the Hyperthermophilic Archaeobacterium *Pyrococcus Woesei*: Characterization of the Enzyme, Cloning and Sequencing of the Gene, and Expression in *Escherichia coli*. *J. Bacteriol.* 172 (8), 4329–4338. doi:10.1128/jb.172.8.4329-4338.1990

Conflict of Interest: The authors declare that the research was conducted in the absence of any commercial or financial relationships that could be construed as a potential conflict of interest.

Publisher's Note: All claims expressed in this article are solely those of the authors and do not necessarily represent those of their affiliated organizations, or those of the publisher, the editors, and the reviewers. Any product that may be evaluated in this article, or claim that may be made by its manufacturer, is not guaranteed or endorsed by the publisher.

Copyright © 2021 Zeng, Bi, Guo, Bi, Wang, Dong, Wang, Chen and Zhang. This is an open-access article distributed under the terms of the Creative Commons Attribution License (CC BY). The use, distribution or reproduction in other forums is permitted, provided the original author(s) and the copyright owner(s) are credited and that the original publication in this journal is cited, in accordance with accepted academic practice. No use, distribution or reproduction is permitted which does not comply with these terms.



Maximizing Energy Content and CO₂ Bio-fixation Efficiency of an Indigenous Isolated Microalga *Parachlorella kessleri* HY-6 Through Nutrient Optimization and Water Recycling During Cultivation

Wasif Farooq^{1,2*}

¹Chemical Engineering Department, King Fahd University of Petroleum and Minerals (KFUPM), Dhahran, Saudi Arabia,

²Integrated Research Centre for Membranes and Water Security (IRC-MWS), King Fahd University of Petroleum and Minerals (KFUPM), Dhahran, Saudi Arabia

OPEN ACCESS

Edited by:

Namita Khanna,
Birla Institute of Technology and
Science, India

Reviewed by:

Ihana Aguiar Severo,
Federal University of Paraná, Brazil
Dillirani Nagarajan,
National Cheng Kung University,
Taiwan
Ramachandran Subramanian,
Birla Institute of Technology and
Science, United Arab Emirates

*Correspondence:

Wasif Farooq
wasif@kfupm.edu.sa

Specialty section:

This article was submitted to
Bioprocess Engineering,
a section of the journal
Frontiers in Bioengineering and
Biotechnology

Received: 29 October 2021

Accepted: 29 December 2021

Published: 10 February 2022

Citation:

Farooq W (2022) Maximizing Energy
Content and CO₂ Bio-fixation
Efficiency of an Indigenous Isolated
Microalga *Parachlorella kessleri* HY-6
Through Nutrient Optimization and
Water Recycling During Cultivation.
Front. Bioeng. Biotechnol. 9:804608.
doi: 10.3389/fbioe.2021.804608

An alternative source of energy and materials with low negative environmental impacts is essential for a sustainable future. Microalgae is a promising candidate in this aspect. The focus of this study is to optimize the supply of nitrogen and carbon dioxide during the cultivation of locally isolated strain *Parachlorella kessleri* HY-6. This study focuses on optimizing nitrogen and CO₂ supply based on total biomass and biomass per unit amount of nitrogen and CO₂. Total biomass increased from 1.23 to 2.30 g/L with an increase in nitrogen concentration from 15.8 to 47.4 mg/L. However, biomass per unit amount of nitrogen supplied was higher at low nitrogen content. Biomass and CO₂ fixation rate increased at higher CO₂ concentrations in bubbling air, but CO₂ fixation efficiency decreased drastically. Finally, the energy content of biomass increased with increases in both nitrogen and CO₂ supply. This work thoroughly analyzed the biomass composition via ultimate, proximate, and biochemical analysis. Water is recycled three times for cultivation at three different nitrogen levels. Microalgae biomass increased during the second recycling and then decreased drastically during the third. Activated carbon helped remove the organics after the third recycling to improve the water recyclability. This study highlights the importance of selecting appropriate variables for optimization by considering net energy investment in terms of nutrients (as nitrogen) and CO₂ fixation efficiency and effective water recycling.

Keywords: microalgae, CO₂ bio-fixation, light intensity, energy content, biofuel production

INTRODUCTION

Greenhouse gas emissions are increasing, and the CO₂ concentration has reached 410 ppm and is expected to reach 450 ppm by 2035 (Bernard 2011). The highest contributors to CO₂ emission are the power generation, industrial, and transportation sectors. Carbon capture and utilization (CCU) is an emerging approach to mitigate the effect of anthropogenic CO₂ emissions. CCU relies on CO₂ capture from a point source emitter and converts it to valuable and innovative new products through

chemical or biological routes (Chen L. et al., 2017). CO₂ is captured and managed *via* pre-combustion, post-combustion, or oxyfuel combustion methods (Coimbra et al., 2019). Several options are proposed for CCU to convert CO₂ to various valuable molecules, such as bio-fixation of CO₂ or direct catalytic conversion. Biological systems are more competent in utilizing CO₂ than chemical conversion techniques. Different natural processes, such as forestation and ocean fertilization, and microbes or microalgae fixed and used CO₂ (Daneshvar et al., 2022).

Microalgae are photosynthetic microorganisms that utilize CO₂ as the primary carbon source, and their rate of fixing CO₂ is 100 times faster than that of terrestrial plants. Most of the eukaryotic algae comprise of pyrenoids, a proteinaceous sub-cellular compartmentalized structure capable of fixing nearly 30–40% of atmospheric CO₂ due to the presence of the Rubisco enzyme. The photosynthetic efficiency of microalgae is 10 times higher than that of terrestrial plants due to their energy-conserving structures and simple cell structure. Moreover, many microalgae did not need fresh water and fertilized land to pre-literate and offer a rapid multiplication rate and arial productivity than higher plants (Singh and Ahluwalia, 2013). Microalgae can utilize CO₂ as inorganic carbon in three modes: passive diffusion of CO₂, active uptake of HCO₃[−], and CO₂ or external carbonic anhydrase enzyme to the plasma membrane to facilitate HCO₃[−] (Colman et al., 2002). Many researchers have investigated microalgae as an alternative approach for CO₂ capture and utilization. A recent detailed review on biobased CCU highlights the advantages and, most notably, the gaps in research and potential future research directions to improve the efficiency of the process, especially by integrating new innovative CO₂ capture technologies with microalgae cultivation (Daneshvar et al., 2022).

Microalgae convert CO₂ into several commercially valuable molecules, such as lipids, carbohydrates, proteins, and pigments, through photosynthesis (Chen L. et al., 2017). Moreover, first- and second-generation biofuel feedstocks are limited and unsustainable for long-term and high yield. Alternatively, third-generation biofuel feedstocks, such as algal biomass, are excellent alternative sources for biofuel production. Microalgae offer higher productivity, faster growth rates, and high photosynthetic efficiency than traditional crops. Microalgae can grow over a wide range of CO₂ concentrations (1–40%) (Li et al., 2013). In addition, algae can be used to remove phosphorus, nitrogen, and heavy metals from wastewater (López Barreiro et al., 2015). Microalgae can grow on wastewater and under extreme environmental conditions (Farooq et al., 2013; Pires et al., 2014). Microalgae are cultivated mainly under three different modes: heterotrophic, photoautotrophic, and mixotrophic (Khalili et al., 2015). Expensive organic substrate and strict operational control are required to avoid undesirable bacterial contamination during mixotrophic and heterotrophic cultivation (Moon et al., 2014). The use of mixotrophic and heterotrophic cultivation modes will lose the advantage of CO₂ fixation. A photoautotrophic method is preferred where natural light is the energy source, and CO₂ is fixed during cultivation. Researchers are studying several

parameters affecting the microalgal growth, biomass, and lipid production linked with CO₂ capture. However, the commercialization of microalgae is still facing many challenges despite its favorable characteristics of CO₂ capture and higher yield of biomass and biofuel (Mustapha et al., 2021).

The phototrophic growth of microalgae needs a substantial amount of nitrogen (and phosphorus-based fertilizer) and water. Various life cycle analysis studies reported very high water demand (Farooq et al., 2015a). Without adequate water reuse during cultivation, microalgae require approximately 3,000 L of water per liter of biodiesel. Therefore, water reuse is essential, and estimates showed that water reuse could reduce the consumption to <1,000 L of water per liter of biodiesel (Farooq et al., 2015b). Higher water demand puts stress on the water resources and will offset the benefits of CO₂ fixation due to the energy required for acquiring water. Therefore, to maximize the CO₂ fixation potential of microalgae, direct and indirect emissions of CO₂ must be reduced. Synthetic fertilizers are produced by fossil fuel sources and result in CO₂ emissions. Estimates showed that, for 1 kg of nitrogenous fertilizer, 49.9–63.2 MJ of fossil fuel energy is required. As a result, 3.39–6.92 kg of CO₂ equivalent is emitted per kilogram of nitrogenous fertilizer (Brentrup et al., 2016). Though CO₂ fixation rate by microalgae is reported widely in literature, limited data is available on factors affecting CO₂ fixation efficiency (Leflay et al., 2021). Therefore, optimizing nutrient requirements and using unused nutrients in water through water recycling is inevitable. Thus, water reuse during cultivation is essential to minimize the energy to acquire water and reduce the stress on water bodies (Hadj-Romdhane et al., 2013). The microalgal photosynthetic mechanism is supported by a light-harvesting system containing various pigments. Variation in pigment content changes when microalgae are under stress. Chlorophyll is essential for effective photosynthesis and CO₂ biological fixation (Chen B. et al., 2017).

Majorities of studies focused on nutrient optimization for biomass production without realizing their net impact on CO₂ fixation efficiency and recyclability of water during cultivation. Notably, this study investigated the effect of four different nutrient regimes of nitrogen and phosphorus on overall energy contents as higher heating value (HHV) of biomass and CO₂ fixation efficiency under six different CO₂ concentrations at three different light intensities along with changes in water chemistry during growth for its potential reuse in the cultivation stage and subsequent CO₂ fixation. More specifically, the impact of nutrients is investigated on variation in photosynthetic pigments, CO₂ fixation rate, CO₂ capture efficiency, and variation in water chemistry after growth under different light intensities.

MATERIALS AND METHODS

Microalgae Growth

Locally isolated microalgae strain identified as *Parachlorella kessleri* HY-6 was cultivated using modified Bold's basal (BBM) medium as described (Wadood et al., 2020). The BBM growth medium contains macronutrients (in mM) such as 3.38

NaNO₃, 0.17 CaCl₂·2H₂O, 0.30 MgSO₄·7H₂O, 0.05 KH₂PO₄, 0.05 K₂HPO₄, 0.43 NaCl, 0.18 H₃BO₃, and EDTA solution (in mM) which contained 0.17 Na₂EDTA·2H₂O, 0.55 KOH, and ferric solution (in μM) which contained 17.9 FeSO₄·7H₂O. Essential micronutrients were supplied as trace metal element solution (in μM) containing 7.28 MnCl₂·4H₂O, 30.70 ZnSO₄·7H₂O, 1.68 Co(NO₃)₂·6H₂O, and 6.29 CuSO₄·5H₂O. Microalgae were grown in 500-ml autoclaved Erlenmeyer flasks with a working volume of 350 ml at 25 ± 1°C under varying light intensities of 30, 60, and 100 μmol m⁻² s⁻¹. The culture was aerated at an average flow rate of 0.5 vvm with different percentages of CO₂ (0–15%). Microalgae biomass was harvested at the end of a 12-day cultivation cycle using a centrifuge at 7,000 rpm for 4 min, followed by rinsing with distilled water to remove any residual salt. Biomass was dried at 105°C. Experiments on the effects of different total nitrogen (TN) concentrations were conducted with four different initial TN concentrations of 15.8, 31.6, 47.4, and 63.2 ppm. Microalgae growth was conducted under different ratios of nitrogen to phosphorus (N/P), such as 1:1, 5:1, 10:1, and 15:1, where total phosphorus (TP) was 47.4, 9.48, 4.74, and 3.16 ppm at a total nitrogen concentration of 47.4 ppm. The growth behavior of the microalgae at various CO₂ amounts was tested by varying concentrations of CO₂ (0, 2, 4, 6, 10, and 15%) diluted with air under initial TN and TP of 47.4 and 3.16 ppm, respectively.

Determination of Biomass and Lipid Productivity

The growth of *P. kessleri* HY-6 was measured by optical density (OD) at 680 nm using a UV-vis spectrophotometer (Thermo Fisher Scientific Evolution 200 Series). The weight of dried biomass collected by centrifugation and dried at 105°C was measured for dry biomass calculation to establish the relationship between biomass and optical density. The relationship between the biomass concentration and OD at A_{680 nm} was found by appropriate standard calibration as shown in the following equation:

$$OD_{680} = 3.426DW (R^2 = 0.983) \quad (1)$$

DW is dry biomass in (g L⁻¹). Lipid productivity was calculated by lipid content (%) multiplied by biomass productivity. Microalgae biomass productivity (mg L⁻¹ day⁻¹) was calculated by dividing the biomass per unit volume with time for cultivation as follows:

$$P = \frac{\Delta X}{\Delta t} \quad (2)$$

where ΔX is the biomass concentration (in mg L⁻¹) within a cultivation period of Δt (in days).

Determination of Nitrogen and Phosphorus Removal Efficiency

TN and TP were analyzed every 48 h with a Hach analysis kit by using a DR3900 spectrophotometer. The culture cells were

centrifuged at 4,500 rpm for 5 min and vacuum-filtered through a membrane filter (Whatman GF/F, 47 mm, nominal pore size: 0.7 μm). The filtered supernatant was used for the determination of TN and TP. The nitrogen and phosphorus removal efficiency was calculated using Eq. 3, where C₀ and C are the nutrient values at t₀ and t, respectively.

$$R_e [\%] = \frac{|C_0 - C|}{C_0} \times 100 \quad (3)$$

Determination of Pigment Content

Pigment content was measured using a UV/vis spectrophotometer (Thermo Fisher Scientific Evolution 200 Series). Pigments were extracted from dry cells using methanol (99.8%) with ultrasonication for 30 min and 45°C followed by centrifugation at 4,500 rpm for 3 min. Absorbance was corrected from turbidity by subtracting absorbencies at 750 nm. The absorption spectrum was collected in the range 400–750 nm where chlorophyll-a, chlorophyll-b, and photoprotective carotenoid concentrations were determined according to the following equations (19):

$$\text{Chlorophyll a} \left[\frac{\mu\text{g}}{\text{mL}} \right] = -8.0962 \times A_{652} + 16.5169 \times A_{665} \quad (4)$$

$$\text{Chlorophyll b} \left[\frac{\mu\text{g}}{\text{mL}} \right] = 27.4405 \times A_{652} - 12.1688 \times A_{665} \quad (5)$$

$$\text{Carotenoids} \left[\frac{\mu\text{g}}{\text{mL}} \right] = 4.0 \times A_{480} \quad (6)$$

Determination of CO₂ Fixation Rate

The carbon content of the biomass was measured using an elemental analyzer (PerkinElmer 2400 Series II CHNS/O Elemental Analyzer, Perkin Elmer Corporation). Dried biomass samples were weighted up to 0.8–2.0 mg in pre-weighted and pre-cleaned tin capsules (5 × 8 mm, Perkin Elmer). The samples were then combusted at 1,000°C using pure helium as the carrier gas and pure oxygen as the combustion gas. The instrument was calibrated with acetanilide standards with delta-calibrated criteria of ±0.15 for carbon, ±3.75 for hydrogen, and ±0.16 for nitrogen. The rate of CO₂ fixation (mg/L/day) and CO₂ fixation efficiency is estimated by the following equation (20):

$$R_{CO_2} = P \times C_{Carbon} \times \frac{M_{CO_2}}{M_C} \quad (7)$$

$$CO_2 \text{ removal efficiency (\%)} = \frac{\text{Total } CO_2 \text{ bio fixed (g)}}{\text{Total } CO_2 \text{ input (g)}} \times 100 \quad (8)$$

where P, C_{carbon}, M_{CO₂}, and M_C are the biomass productivity, carbon content, molar mass of CO₂, and carbon, respectively.

Determination of Total Lipid and FAME Content

The total lipids were extracted from 50 mg of biomass in glass vials and quantified gravimetrically by the Bligh and Dyer method

using 3.0 ml of (2:1, v/v) chloroform–methanol solution in two cycles. Biomass was sonicated in an ultra-sonicator to enhance lipid extraction at 50°C for 30 min. The extracted lipids in glass vials were dried using a vacuum oven at 95°C, and later the glass vials were weighted to calculate the lipid content as follows:

$$\text{Lipid Content} = \frac{(m_{\text{Extracted Lipid}} - m_{\text{Glass Vial}})}{m_{\text{Dry Biomass}}} \quad (9)$$

Fatty acid methyl esters (FAME) were converted to biodiesel by transesterification of dried microalgal biomass with sulfuric acid. Briefly, 26 mg of dry biomass was directly trans-esterified with 0.3 ml of H₂SO₄ with 3.0 ml of 9:1 methanol-dimethyl sulfoxide mixture at 60°C. After that, 1.0 ml of the trans-esterified mixture was filtered with a 0.2-μm syringe filter (Whatman, Springfield Mill, United Kingdom). The samples were centrifuged at 4,500 rpm for 3 min for phase separation. The upper organic layer was collected in a new vial, and then the FAME in the organic phase was analyzed by gas chromatography–mass spectrometry (GC-6890N, MSD-5975B, Agilent Technologies, United States). Each FAME was identified and quantified by comparing the respective peak area and retention time with the standard. The FAME percentage was calculated as per the following equation (Salam et al., 2016):

$$\text{FAME}[\%] = \frac{\text{Area}_{\text{FAME}}}{\text{Area}_{\text{FM}}} \times \frac{C_{\text{FM}} \times V_{\text{FM}}}{m_{\text{Dry Biomass}}} \times 100 \quad (10)$$

where Area_{FAME}, Area_{FM}, C_{FM}, V_{FM}, and m_{Dry biomass} are the total peak area, peak area corresponding to the pure FAME mix solution, concentration of the pure FAME mix solution (in mg/ml), volume of the pure FAME mix solution (in ml), and the mass of the dried microalgal sample (in mg), respectively.

Total Protein Analysis

Protein content was estimated using the recommended Kjeldahl conversion factor of 5.95 for elemental nitrogen to protein estimation (López et al., 2010). Total nitrogen of biomass was measured by an elemental analyzer (PerkinElmer 2400 Series II CHNS/O Elemental Analyzer, Perkin Elmer Corporation).

Proximate and Ultimate Analysis of Biomass

Thermogravimetric analysis using TA Instruments SDT 600 measured the fixed carbon, moisture, ash content, and volatile matter of biomass. Moisture content and volatile matter were based on when the weight change was almost zero at 100 and 850°C, respectively. Post-pyrolysis combustion proceeded under air to 800°C, followed by a stepwise function to 850°C to estimate the fixed carbon and ash content. The elemental analyzer determined total carbon, hydrogen, and nitrogen (PerkinElmer 2400 Series II CHNS/O Elemental Analyzer, Perkin Elmer Corporation).

Analysis of Water for Its Recycling for Growth and Its Pretreatment

Extracellular algal organic (EOM) matter released by the microalgae during its growth was analyzed for its total organic

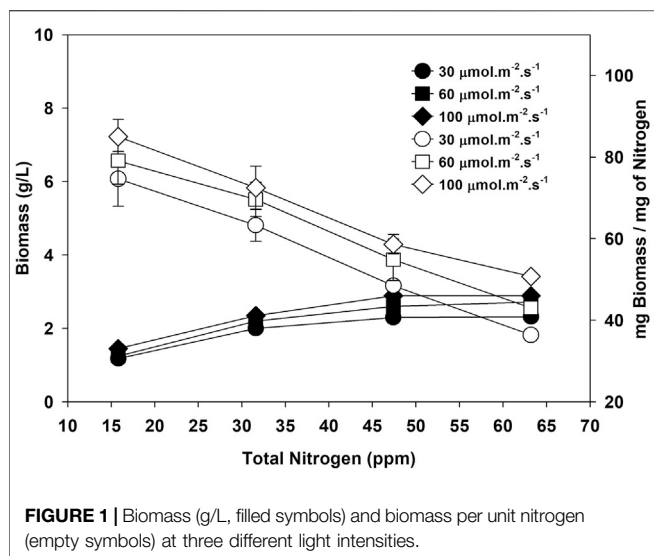
carbon (TOC), humic acid, and pigment contents. Analysis was conducted using a TOC analyzer (TOC-V_{CSN}, Shimadzu) and UV–vis spectrophotometer (UV-2600i, Shimadzu). The growth medium was recycled three times without any pretreatment. After the third cycle, water was treated with commercial granular activated carbon (Sigma Aldrich) to remove the EOM and pigments by measuring the absorbance at 254 and 440 nm, respectively (Mejia-da-Silva et al., 2018). All the macro- and micronutrients were added before each recycle.

RESULTS AND DISCUSSION

Effect of Initial Nitrogen Concentration on Cell Growth and Metabolite Profile

Economical biofuel production and other valuable biochemicals from microalgae cannot be achieved without optimizing the supply of essential inputs such as nutrients, light, and CO₂. The nutrients are expensive and have inherent greenhouse gas emissions (Li et al., 2019). Microalgae store excess nutrients, such as nitrate and phosphate, to utilize during their unavailability in the media (Bernard, 2011). This study investigates the impact of four initial nitrate concentrations as nitrogen (15.8, 31.6, 47.4, and 63.2 ppm) in modified BBM during the growth of microalgae *P. kessleri* HY-6 at a light intensity of 30, 60, and 100 μmol m⁻² s⁻¹. **Supplementary Figures S1A,B** show the cell growth at different nitrogen concentrations for two different light intensities. The data showed that additional nitrogen did not improve the biomass content (Zarrinmehr et al., 2020).

In contrast, the specific growth rate reached a maximum of 0.36 day⁻¹ at 47.4 ppm at 30 μmol m⁻² s⁻¹. Specific growth rate, doubling time, and biomass productivity was not affected much at higher nitrogen concentrations, and their values at two different nitrogen concentrations (47.4 and 63.2 ppm) are 0.3 day⁻¹, 2.3 days, and 167 mg/L/day, respectively. The lipid content decreased from 46.7 to 26.5%, with an increase in nitrogen from 15.8 to 63.2 ppm at 60 μmol m⁻² s⁻¹, respectively. However, the microalgae attained the maximum lipid productivity of 56.2 mg L⁻¹ day⁻¹ at a nitrogen concentration of 47.4 ppm at 60 μmol m⁻² s⁻¹. These preliminary findings imply that the optimal compromise between maximizing the cell biomass and lipid productivity occurs at 47.4 ppm of nitrogen concentration under experimental conditions. Nutrient uptake depends on light intensity during growth, as shown in **Supplementary Figures S2A,B**. A higher light intensity (below light inhibition limit) increases photosynthesis, produces more biomass, and consumes more nitrogen (Khalili et al., 2015). Similar to this study, most studies used algal biomass and lipid productivity as the objective functions to maximize against nitrogen and other nutrients in the microalgae culture (Khalili et al., 2015; Zarrinmehr et al., 2020). However, optimizing biomass and CO₂ fixation per unit amount of nitrogen will be a more realistic parameter. Maximizing biomass and CO₂ fixation with the lowest input of nutrients is necessary to reduce the cost associated with nutrient supply (Selvaratnam et al., 2016). The data in **Figure 1** shows that the total biomass (g/L) and the biomass per unit amount of



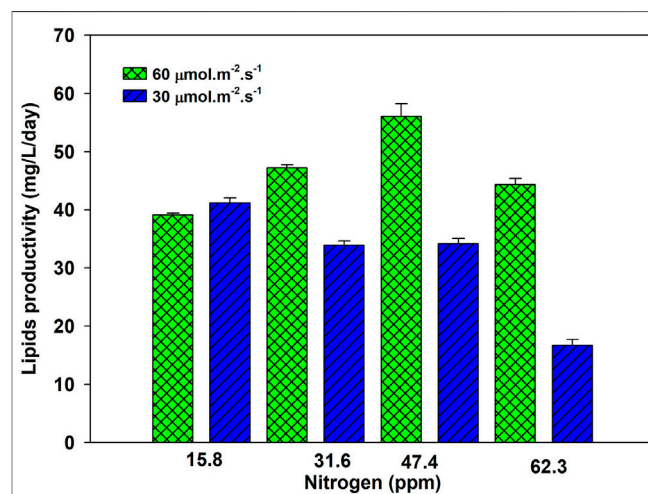
nitrogen are functions of nitrogen concentration and depend on light intensity. Therefore, finding the light inhibition limit for the algae before doing any other optimization is recommended because light is the energy source to derive the photosynthesis process.

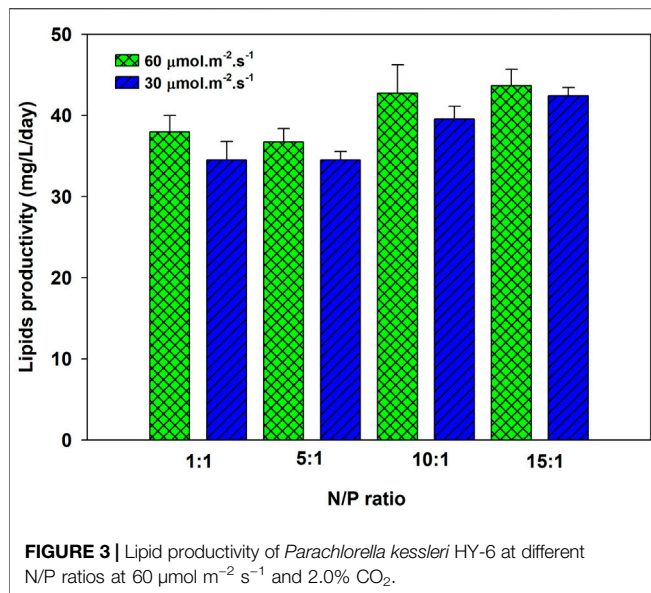
Figure 1 shows that biomass per unit nitrogen is higher at lower nitrogen and decreases as the nitrogen input increases. Total biomass increased with nitrogen, and based on biomass, the optimum nitrogen in the media should be around 47.4 ppm. However, the biomass productivity per unit amount of nitrogen is higher at low nitrogen content, i.e., 15.8 ppm for all three light intensities. Maximizing the biomass productivity at the lowest nitrogen consumption is desirable to decrease the cost of synthetic fertilizer and its associated greenhouse gas emissions. Total CO₂ emission during synthetic fertilizer manufacturing varies according to the type of fertilizer. Ammonium nitrate and urea release 1.1–3.6 and 0.88–1.3 kg of CO₂ equivalent per kilogram of product, respectively (Hoxha and Christensen, 2018). Nitrogen is the second most abundant element in algae biomass after carbon. So, an initial low nitrogen input will decrease fertilizer use and limit the unassimilated counter-ion concentration in media (Na⁺ in case of NaNO₃), which is desired for water recycling for microalgae cultivation (Kumar and Bera, 2020). Nitrogen and phosphorus produced using fossil fuel energy required approximately 56.8 and 33.3 MJ/kg, respectively (Tredici et al., 2015). Biomass and energy content increased to 64, 112, and 125% when nitrogen was increased from 15.8 to 31.6, 47.4, and 63.2 ppm. The nitrogen concentration of 47.4 ppm seemed optimal as the net energy in biomass is 27.8, 45.5, 60.11, and 62.18 MJ/kg at 15.8, 31.6, 47.4, and 63.2 ppm of nitrogen, respectively, after accounting for the energy required for nitrogen production.

Moreover, pretreatment of algal bio-oil will be desired if biomass with high nitrogen is processed via hydrothermal liquefaction (Das et al., 2021; Farooq, 2021). Biomass per unit nitrogen is high at the lowest nitrogen content, but low total biomass per liter (in the case of 15.8 ppm nitrogen) will increase

the harvesting cost. Harvesting is one of the expensive stages in the microalgae process, and culture density significantly affects the cost of harvesting. The cost of harvesting using centrifuge varies from 1.3 to 8 kWh/m³, depending on the culture concentration and harvesting efficiency. A low-density culture will consume more energy to recover a unit mass of microalgae (Dassey and Theegala, 2013). Though the biomass per unit nitrogen is high at low nitrogen (15.8 ppm), the overall biomass per liter of culture is low at this concentration, leading to higher harvesting costs. The energy required for harvesting biomass to produce 1 L of oil decreased with an increase in biomass per liter and its lipid content of biomass. The HHV of microalgae biomass is around 22 MJ/kg (Coimbra et al., 2019). The energy embedded in microalgae biomass produced at 15.8, 31.6, 47.4, and 63.2 ppm at 100 μmol m⁻² s⁻¹ is 9.2, 13.4, 17.11, and 17.72 kWh/m³, respectively. Approximately 14% of the energy in biomass grown at 15.8 ppm will be used if the centrifugal harvesting option with minimum energy (~1.3 kWh/m³) is explored. The energy utilized for harvesting biomass will further increase to 86% of total energy in biomass if harvesting needs 8 kWh/m³ of energy using centrifugation. So, a nitrogen concentration of 47.4 ppm was selected for the next experiment.

Lipid productivity first increased and then decreased at the same light intensity at varying nitrogen concentrations. A higher nitrogen concentration gives lower lipid productivity. Lipid productivity differed at two tested light intensities, as shown in **Figure 2**. This observation highlights the importance of supplying optimal light and nutrients. Lipid productivity is the product of biomass and lipid contents, an increase of both or any one will increase the lipid productivity (Sharma et al., 2012). An increase in lipid productivity with an increase in nitrogen concentration remains almost the same over the tested nitrogen concentrations. An increase in nitrogen from 15.8 to 31.6 ppm increased the lipid productivity from 39 to 48 mg/L/day. A further increase in nitrogen from 31.6 to 47.8 ppm





increased the lipid productivity to 55 mg/L/day. These results showed that increasing the nitrogen beyond 47.4 ppm was not practical to enhance lipid productivity. **Supplementary Figure S2** shows that 99% of nitrogen at all initial concentrations, except 63.4 ppm, was assimilated within 6 days. Light intensity drives the photosynthesis process, which promotes cell growth. At low light intensity, growth is low, and the rate of nitrogen uptake from media is low, as shown in **Supplementary Figure S2**.

Effect of NP Ratio on the Cell Growth and Lipid Profile of *P. kessleri* HY-6

The microalgae biomass contains approximately 1% of phosphorus, depending on the species. Due to limited reserves, optimizing phosphorus as macronutrients is essential without compromising biomass productivity. The nitrogen to phosphorus (N/P) ratio affects the cell growth and lipid accumulation of microalgae (Rasdi and Qin, 2015). *P. kessleri* HY-6 was cultivated in modified BBM media at four different TP concentrations (47.4, 9.5, 4.86, and 3.17 ppm) at 60 $\mu\text{mol.m}^{-2}.\text{s}^{-1}$, which corresponds to NP ratios of 1:1, 5:1, 10:1, and 15:1 while keeping the nitrogen content at 47.4 ppm. The growth at different NP ratios is shown in **Supplementary Figure S3**, which is similar at different N/P ratios. The specific growth rate increased with the increase in the N/P ratio and reached the maximum at 0.45 day⁻¹ at 10:1 NP ratio. Nitrogen is fully consumed at all N/P ratios. However, phosphorus uptake was slower at a lower N/P ratio, such as 1:1, as shown in **Supplementary Figure S4**. Overall, nitrogen and phosphorus were almost entirely consumed by microalgae at an NP ratio between 5:1 and 15:1. The nitrogen removal efficiency decreased due to phosphorus limitation (Xin et al., 2010). The total lipid of *P. kessleri* HY-6 under different NP ratios varies with the N/P ratio (Rasdi and Qin, 2015). The lipid productivity reached as high as 46.0 mg L⁻¹ day⁻¹ at 10:1 and 15:1 N/P ratios. Nutrient limitation has a significant effect on improving the lipid content of algal biomass (Rodolfi et al., 2009). Goldberg

and Cohen stated that the total lipids, such as triacylglyceride, increased substantially from 6.5 to 39.3% under limited phosphorus (Khozin-Goldberg and Cohen, 2006). The lipid content of 45.0% was estimated during the study, leading to the lipid productivity rate of 46.0 mg/L/day at N/P ratio 10:1, under aeration with 2.0% CO₂, as shown in **Figure 3**.

Effect of Light and CO₂ Concentration on the Cell Growth, Heating Value, and Biochemical Composition of *P. kessleri* HY-6

The microalgae *P. kessleri* HY-6 was cultivated at 25 ± 2°C at various light intensities (30, 60, and 100 $\mu\text{mol.m}^{-2}.\text{s}^{-1}$) at different CO₂ concentrations in a modified media with an N/P ratio of 10:1. Optimal light intensity and wavelength are desired for the growth of microalgae. Too low and too high light intensity negatively affect the microalgae growth (Jiang and Zheng, 2018). Earlier studies showed species-dependent growth inhibition at higher CO₂ concentrations (Lim et al., 2021). The microalgae *P. kessleri* HY-6 can grow at a relatively high (6–15%) CO₂ concentration, as shown in **Supplementary Figure S5**. Algal biomass increased with CO₂ concentration at all three light intensities. However, the maximum biomass obtained at an optimal CO₂ concentration varies with light intensity. At 2% CO₂ and 30 $\mu\text{mol.m}^{-2}.\text{s}^{-1}$, the maximum biomass was 1.66 g/L. The maximum biomass at 6.0 and 10.0% CO₂ was 1.88 and 2.0 g/L at a light intensity of 60 and 100 $\mu\text{mol.m}^{-2}.\text{s}^{-1}$. Both light and CO₂ concentration enhanced the specific growth rate of microalgae, as shown in **Supplementary Figure S6**.

Supplementary Figure S7 shows the variation in the productivity of metabolites (lipid, carbohydrate, and protein) at different CO₂ concentrations. The relative amounts of lipids, carbohydrate, protein, and pigment content of biomass are given in **Table 1**. The lipid content increased under the higher light intensity of 100 $\mu\text{mol.m}^{-2}.\text{s}^{-1}$. At the same time, the pigment amount decreased, which could be due to stress conditions at a high light intensity and nitrogen-depleted conditions at the end of the growth stage (Liang et al., 2020). Variation in metabolites content is a complex function of various biotic and abiotic growth factors, such as light intensity, CO₂ availability, pH, and nutrient level in the growth media (Gonçalves et al., 2014; Thawechai et al., 2016). The microalgae convert CO₂ to biomass via a carbon capture mechanism in the presence of light. At high light intensity, growth will be fast, and nutrients will deplete quickly compared at low light intensity for the same cultivation time. Under the nutrient-replete condition, the protein and carbohydrate contents increased in biomass, while the lipid content increased during nutrient-depleted growth. However, this metabolite modulation is species specific as well. The lipid compositions at various CO₂ concentrations and light intensity are provided in **Supplementary Table S1**. The data clearly showed that the total FAME content increased with CO₂ and light intensity. The increasing light intensity increased the amount of saturated fatty acids, such as pentadecanoic acid (C15:0), palmitic acid (C16:0), and stearic acid (C18:0), with a significant variation in C16:0 and C18:0. However, the major

TABLE 1 | Biochemical composition of microalgae biomass under different light and CO₂ conditions.

CO ₂ level	Light intensity (μmol/m ² s)	Biomass content (%)				
		Lipid	Protein	Carbohydrate ^a	Pigment	Ash
Air	30	37.9 ± 3.0	21.5 ± 0.6	33.4 ± 3.4	0.019 ± 0.005	7.2 ± 0.4
	60	24.9 ± 0.7	20.4 ± 0.1	47.2 ± 0.8	0.012 ± 0.002	7.6 ± 1.1
	100	32.0 ± 2.6	16.2 ± 0.4	50.0 ± 2.6	0.005 ± 0.003	1.7 ± 0.9
2%	30	41.5 ± 1.3	18.3 ± 0.7	32.1 ± 1.6	0.015 ± 0.006	8.1 ± 0.6
	60	26.9 ± 0.8	16.3 ± 0.1	51.6 ± 1.1	0.013 ± 0.006	5.2 ± 2.1
	100	45.1 ± 0.8	9.2 ± 0.1	40.4 ± 1.4	0.003 ± 0.001	5.3 ± 0.7
4%	30	32.4 ± 2.7	21.3 ± 0.2	45.6 ± 3.7	0.024 ± 0.002	0.6 ± 0.4
	60	33.0 ± 3.5	16.3 ± 0.4	49.6 ± 3.1	0.024 ± 0.004	1.1 ± 2.5
	100	47.6 ± 2.7	12.2 ± 0.4	39.4 ± 4.2	0.005 ± 0.001	0.9 ± 0.7
6%	30	29.5 ± 2.7	20.0 ± 0.7	49.8 ± 3.6	0.020 ± 0.001	0.6 ± 0.1
	60	34.0 ± 1.3	18.5 ± 0.4	46.0 ± 2.1	0.018 ± 0.003	1.5 ± 0.9
	100	47.7 ± 0.5	12.9 ± 0.6	37.5 ± 0.8	0.011 ± 0.005	1.9 ± 1.6
10%	30	25.9 ± 1.4	21.4 ± 1.8	52.0 ± 1.8	0.022 ± 0.003	0.8 ± 0.6
	60	37.8 ± 0.4	18.3 ± 0.0	43.3 ± 0.6	0.019 ± 0.001	0.6 ± 2.3
	100	59.9 ± 1.2	11.0 ± 0.6	28.3 ± 2.0	0.006 ± 0.004	0.7 ± 1.1
15%	30	32.9 ± 0.2	21.3 ± 1.4	45.2 ± 0.3	0.022 ± 0.007	0.5 ± 0.3
	60	33.9 ± 0.3	19.9 ± 1.7	45.7 ± 0.4	0.019 ± 0.002	0.5 ± 1.2
	100	55.7 ± 0.7	12.7 ± 0.1	29.6 ± 1.0	0.004 ± 0.005	1.9 ± 1.4

^aCarbohydrate = 100 – lipids – protein – pigments – ash.

TABLE 2 | Ultimate and proximate analysis of microalgae biomass obtained at different light intensities and CO₂ concentrations.

CO ₂ level	Light intensity	Ultimate analysis			Proximate analysis			—	—	—
		C	H	N	HHV (MJ/kg)	MC	VM	FC	Ash	HHV (MJ/kg)
Air	30	42.7	6.5	3.6	15.5	9.0	71.0	12.9	7.2	16.8
	60	50.0	8.7	3.4	18.9	7.1	72.3	13.0	7.6	17.1
	100	48.7	8.6	2.7	18.4	7.1	72.3	18.9	1.7	18.5
2%	30	47.7	7.6	3.1	17.6	6.8	72.2	12.9	8.1	17.0
	60	52.1	9.7	2.7	20.0	2.6	73.8	18.5	5.2	18.7
	100	52.6	10.4	1.6	20.5	4.1	80.8	9.8	5.3	17.9
4%	30	52.6	9.2	3.4	19.9	6.9	75.4	17.1	0.6	18.7
	60	53.4	9.4	3.1	20.3	6.0	76.1	16.8	1.1	18.7
	100	55.2	12.0	2.2	22.2	3.7	82.7	12.7	0.9	19.0
6%	30	54.7	9.7	3.6	20.8	5.7	77.4	16.2	0.6	18.8
	60	54.1	9.7	2.7	20.6	5.1	77.9	15.5	1.5	18.8
	100	57.2	11.4	2.0	22.4	3.9	82.6	11.5	1.9	18.6
10%	30	53.5	7.3	3.6	19.2	5.7	77.1	16.4	0.8	18.8
	60	55.0	9.4	3.1	20.7	5.9	76.8	16.8	0.6	18.9
	100	60.3	11.2	1.9	23.3	2.7	86.0	10.6	0.7	19.0
15%	30	53.6	9.4	3.6	20.3	6.3	75.0	18.1	0.5	18.9
	60	55.5	9.2	3.4	20.8	5.5	79.6	14.4	0.5	18.8
	100	61.3	10.8	2.1	23.4	3.0	83.7	11.4	1.9	18.8

portion of fatty acids are palmitic acid and oleic acid (C18:1) (Thawechai et al., 2016). The relative amount of unsaturated fatty acids (C18:1, C18:2, and C18:3) is higher than that of saturated fatty acids. However, the fatty acid composition variation depends on species, light intensity, and light exposure duration for cells (Nzayisenga et al., 2020).

The CO₂ fixation rate is calculated at a different light intensity and CO₂ concentration using the carbon contents of biomass (given in Table 2) and Eq. 7. The CO₂ fixation rate increased with the availability of CO₂ in the media and the availability of light. However, the maximum CO₂ fixation rate depends on light intensity. Under light-limited conditions, the photosynthesis

process becomes less efficient, and the majority of CO₂ will leave the system. The results in Figure 4 show that a CO₂ concentration beyond 6% is not helpful as the fixation rate at 30 and 60 μmol m⁻² s⁻¹ decreased. However, the CO₂ fixation rate increased at 10% CO₂ concentration at 100 μmol m⁻² s⁻¹.

The energy content of biomass as HHV increased with light intensity and CO₂ concentration. The maximum HHV of 20, 20.5, and 22.50 MJ/kg was obtained at 6.0% CO₂ for 30 and 60 μmol m⁻² s⁻¹ and at 10% for 100 μmol m⁻² s⁻¹, respectively, as shown in Figure 5. Growth under higher light intensity and CO₂ concentration increased the CO₂ fixation rate and enhanced the HHV value of the biomass, as given in Table 2.

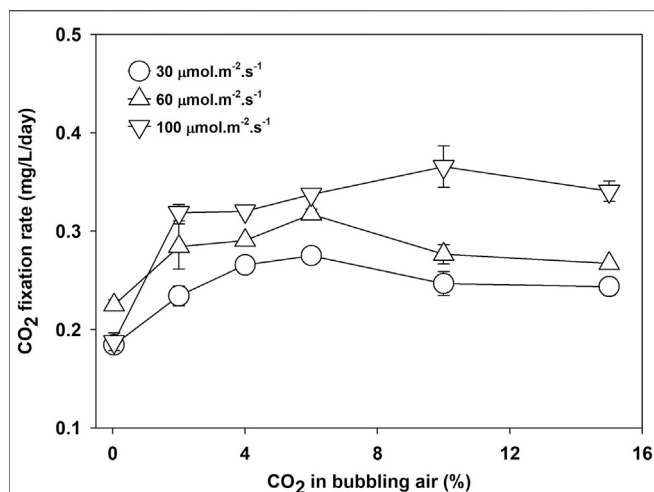


FIGURE 4 | CO₂ fixation rate of *Parachlorella kessleri* HY-6 at different light intensities and CO₂ concentrations.

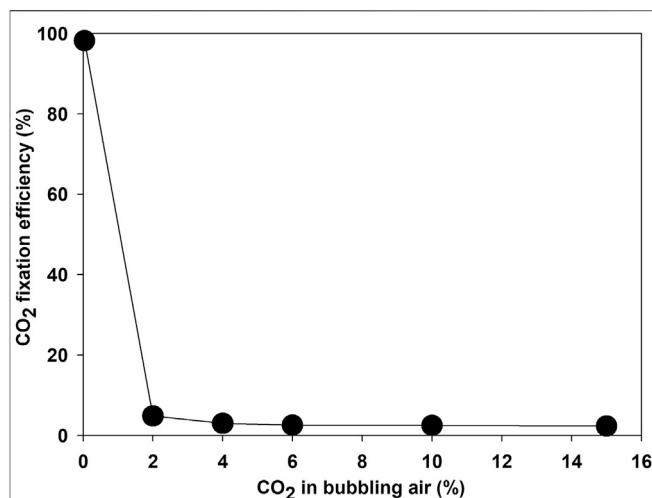


FIGURE 6 | CO₂ fixing efficiency by microalgae *Parachlorella kessleri* HY-6 at a different CO₂ concentration.

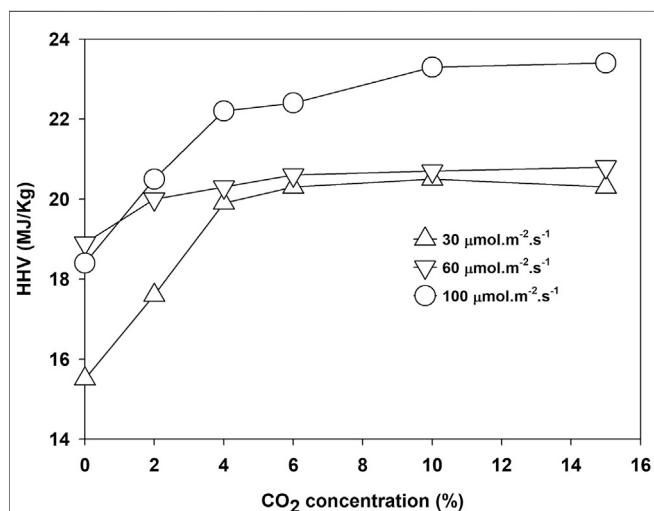


FIGURE 5 | The higher heating value of *Parachlorella kessleri* HY-6 at different light intensities and CO₂ concentrations.

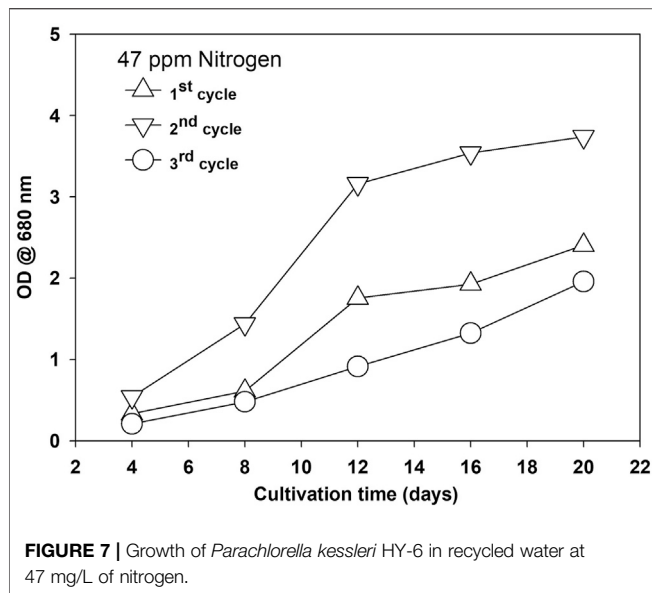
A higher CO₂ concentration enhanced the growth rate of microalgae compared to atmospheric air—for example, the growth rate increased from 0.301 to 0.527 day⁻¹ when bubbling of atmospheric air switched with air containing 15% CO₂. Though the biomass yield, CO₂ consumption, and energy content of the microalgae increased at higher concentrations of CO₂, the CO₂ fixation efficiency declined sharply with an increase in CO₂ concentration in the bubbling air (Lim et al., 2021). The CO₂ removal efficiency was 96% when atmospheric air was supplied as a source of CO₂. The removal efficiency decreased sharply to 2.5, 1.2, and 0.85% at a CO₂ concentration of 2, 4, and 6%, respectively, as shown in Figure 6. The CO₂ removal efficiency depends on microalgae strain, culture pH, bubble size, and hydraulic retention time in the photobioreactor,

along with effective light availability (Thawechai et al., 2016). Most studies reported CO₂ fixation by using the carbon content of microalgae rather than the direct measurement of CO₂ at the outlet, which ignores the release of fixed carbon as EOM and dissolved CO₂ in the water (Leflay et al., 2021). Estimation of EOM during the algae growth as an organic form of CO₂ is necessary for finding the true potential of CO₂ bio-fixation.

Most CO₂ is released back to the atmosphere under low fixation efficiency (Lam and Lee, 2013). These results showed that the potential of microalgae to fix CO₂ is debatable. Low CO₂ fixation efficiency would be counterproductive at high CO₂ concentrations if the energy was spent on acquiring CO₂ from emission sources such as power plants and industrial flue gases. CO₂ capture cost varies between 292 and 425 kJ/kg. Low CO₂ fixation efficiency means loss of almost. One of the main reasons for low bio-fixation efficiency is the lower solubility of CO₂ in water (~ 1.45 g/L) at normal conditions (Daneshvar et al., 2022). The CO₂ solubility and uptake efficiency can be enhanced by controlling the bubble size, design of the photobioreactor, proper selection of microalgae strain, and selecting appropriate operating conditions, such as flow rate, the concentration of CO₂, and pH (Li et al., 2013). Therefore, future research should focus on improving the CO₂ fixation efficiency at higher CO₂ concentrations.

Reuse of Water During Cultivation of Microalgae *P. kessleri* HY-6

Water reuse during microalgae cultivation is essential to reduce the high-water footprint of the cultivation stage (Farooq et al., 2015b; Farooq, 2021; Lu et al., 2020). Many researchers investigated the potential benefits and challenges associated with water reuse during microalgae cultivation. The studies on water recycling are essential for various reasons, such as cost of water itself, cost of water acquiring, loss of nutrients, pretreatment of water if not recycled, and presence of growth-



promoting and growth-inhibiting organics released during the former stage (Chen L. et al., 2017; Mejia-da-Silva et al., 2018).

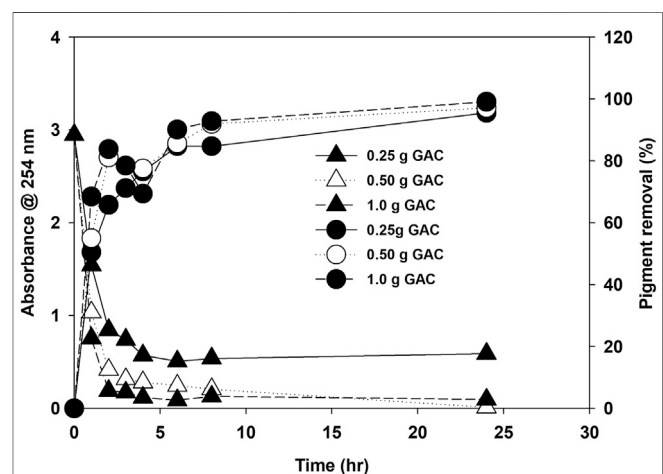
Microalgae growth was enhanced during the first recycle and then decreased in the second recycle, as shown in **Figure 7** and **Supplementary Figure S8A** for two different nitrogen concentrations at 2% CO₂.

The possible reason for growth enhancement during the second recycle could be the growth-promoting organic released by microalgae in the first growth cycle. EOM released during growth are reported for their species-specific growth-promoting and growth-inhibiting role during microalgae cultivation (Liu et al., 2016). Microalgae release various types of extracellular organics during their growth, and their composition and amount depend on the growth conditions and are affected by many biotic and abiotic factors (Loftus and Johnson, 2019; Villacorte et al., 2015). The nature of EOM varies with the growth stage and is also affected by nitrogen availability in the media. Under nitrogen-replete conditions, most EOM is composed of protein, while under nitrogen-deplete conditions, adopted for lipid induction, EOM is mainly composed of polysaccharides (Baroni et al., 2020). Growth was severely inhibited during the third cycle, and bacteria were observed. Extracellular organics act as a source of bacterial growth. The microalgae growth rate was less during the third stage and showed the stress conditions at the early growth stage. The presence of unused salt ions accumulated during water recycling and increased organic load could be the potential growth-inhibiting factors (Sha et al., 2019). TOC was measured as the indicator of the accumulation of organic matter. TOC increased with each cycle at three different nitrogen concentrations, as shown in **Supplementary Figures S8B**. A decrease in TOC in the fourth cycle was observed, and during this stage, severe bacterial contamination was noticed, and the color of the media turned yellow. Various organics, including humic acids, protein, carbohydrates, and free fatty acids, contribute to TOC (Lu et al., 2019; Sha et al., 2019). Water

after the third cycle was treated with a different amount of commercially available granular activated carbon (GAC) to remove the organics and pigment from the recycled water by measuring the absorbance at 254 and 440 nm, respectively. The GAC effectively removed the organic matter composed of various organics and pigments from the culture, as shown in **Figure 8**. Activated carbon is found effective for polishing the recycled water as reported, and a similar growth was observed as in the first cycle (Mejia-da-Silva et al., 2018), but the use of GAC will add to another cost factor as, for >95% removal, 1.0 g of GAC is required for 50 ml of water besides the cost of mixing in our study. Though regeneration of GAC is an option, the amount of GAC will be pretty significant considering the amount of water required to produce 1 L of biodiesel from microalgae biomass (Rocha et al., 2015). This finding suggests that limiting the release of organics and accumulation of unused ions are the first steps toward water recycling in microalgae besides the effective and economical treatment of recycled water. Moreover, the presence of a higher amount of EOM limits the performance of the harvesting system, especially membrane-based system (Zhang et al., 2018).

Limitations and Recommendations for Future Work

This study investigates the impact of initial nitrogen and nitrogen-to-phosphorus ratio on microalgae growth, CO₂ fixation efficiency, and water recycling during cultivation. Despite this initial investigation and valuable results, this study has not considered the impact of optimal light intensity based on the light saturation intensity of the algae under investigation. Light is a source of energy for photosynthesis, and finding the light saturation limit of microalgae is important before optimizing other growth parameters like nutrients and CO₂ supply. Therefore, firstly, the value of light saturation is essential. Secondly, CO₂ fixation efficiency must be tested under an optimal bubble size and flow rate according to



culture depth. Thirdly, activated carbon was tested to remove the organic compounds as total organic carbon. Some organic molecules like carbohydrates and peptides support microalgae growth compared to secreted free-fatty acids and humic substances. Therefore, further studies should focus on the removal rate of different organics in the reused water. Adsorbents like activated carbon can remove the nutrients essential for growth as well. In this study, nutrients like nitrogen and phosphorus were consumed entirely by the microalgae. However, the role of activated carbon for removing unutilized cations (Na⁺, K⁺, Ca⁺², and Mg⁺²) and anions (NO₃⁻¹, PO₄⁻³, SO₄⁻², etc.) must be explored. Loss of CO₂ as secreted organic matter during growth must also be accounted for toward the bio-fixation of CO₂ by the microalgae.

CONCLUSION

The growth and nutrient optimization for *P. kessleri* HY-6 are investigated as algal biomass, lipid productivity, CO₂ fixation efficiency, and water recycling potential under different nutrients and CO₂ concentrations during photoautotrophic cultivation mode. The optimum total nitrogen concentration is 47.4 ppm at fixed environmental conditions of CO₂ and light intensity. *P. kessleri* HY-6 efficiently utilized the nutrients and produced higher lipid productivity at an N/P ratio of 10:1. The CO₂ fixation rate increased with an increase in CO₂ concentration in aerated air, but the efficiency of CO₂ fixation decreased drastically at 2% CO₂ in the air. The CO₂ fixation rate increased with light intensity from 30 to 100 μmol m⁻² s⁻¹. The HHV increased from 15.5 to 21 MJ/kg when the CO₂ concentration was increased from 0.04% (ambient air) to 10% CO₂. HHV also increased from 15.5 to 23.5 MJ/kg when the light intensity was increased from 30 to 100 μmol m⁻² s⁻¹. Water reuse was effective in improving the microalgae growth until second

recycling. Further reuse inhibited the algae and enhanced the bacterial growth, resulting in poor CO₂ utilization and nutrient uptake. Granular activated carbon (1.0 g/L) was effective for removing 95% of organic matter and pigments in 6 h, which is desired for growth in recycled water.

DATA AVAILABILITY STATEMENT

The original contributions presented in the study are included in the article/**Supplementary Material**, further inquiries can be directed to the corresponding author.

AUTHOR CONTRIBUTIONS

All the work was conducted by WF himself, along with paid analysis services for the elemental analysis of biomass and total organic carbon analysis of water.

FUNDING

This work is supported by funding from the Deanship of Research (DSR), KFUPM, via grant number DF191033.

SUPPLEMENTARY MATERIAL

The supplementary material for this article can be found online at: <https://www.frontiersin.org/articles/10.3389/fbioe.2021.804608/full#supplementary-material>

Supplementary Table S1 | FAME composition of *Parachlorella kessleri* HY-6 under different CO₂ levels and light intensities.

REFERENCES

- Baroni, É., Cao, B., Webley, P. A., Scales, P. J., and Martin, G. J. O. (2020). Nitrogen Availability and the Nature of Extracellular Organic Matter of Microalgae. *Ind. Eng. Chem.* 59 (15), 6795–6805. doi:10.1021/acs.iecr.9b05426
- Bernard, O. (2011). Hurdles and Challenges for Modelling and Control of Microalgae for CO₂ Mitigation and Biofuel Production. *J. Process Control.* 21 (10), 1378–1389. doi:10.1016/j.jprocont.2011.07.012
- Brentrup, F., Antoine, H., and Christensen, B. (2016). "Carbon Footprint Analysis of Mineral Fertilizer Production in Europe and Other World Regions," in 11th International Conference on Life Cycle Assessment of Food 2018, Bangkok, Thailand, 17–19 October, 2018.
- Chen, L., Zhu, T., Fernandez, J. S. M., Chen, S., and Li, D. (2017). Recycling Nutrients from a Sequential Hydrothermal Liquefaction Process for Microalgae Culture. *Algal Res.* 27, 311–317. doi:10.1016/j.algal.2017.09.023
- Chen, B., Wan, C., Mehmood, M. A., Chang, J.-S., Bai, F., and Zhao, X. (2017). Manipulating Environmental Stresses and Stress Tolerance of Microalgae for Enhanced Production of Lipids and Value-Added Products-A Review. *Bioresour. Tech.* 244, 1198–1206. doi:10.1016/j.biortech.2017.05.170
- Coimbra, R. N., Escapa, C., and Otero, M. (2019). Comparative Thermogravimetric Assessment on the Combustion of Coal, Microalgae Biomass and Their Blend. *Energies* 12 (15), 2962. doi:10.3390/en12152962
- Colman, B., Huertas, I. E., Bhatti, S., and Dason, J. S. (2002). The Diversity of Inorganic Carbon Acquisition Mechanisms in Eukaryotic Microalgae. *Funct. Plant Biol.* 29 (3), 261–270. doi:10.1071/pp01184
- Daneshvar, E., Wicker, R. J., Show, P.-L., and Bhatnagar, A. (2022). Biologically-Mediated Carbon Capture and Utilization by Microalgae towards Sustainable CO₂ Biofixation and Biomass Valorization – A Review. *Chem. Eng. J.* 427, 130884. doi:10.1016/j.cej.2021.130884
- Das, P., V.P., C., Mathimani, T., and Pugazhendhi, A. (2021). A Comprehensive Review on the Factors Affecting Thermochemical Conversion Efficiency of Algal Biomass to Energy. *Sci. Total Environ.* 766, 144213. doi:10.1016/j.scitotenv.2020.144213
- Dassey, A. J., and Theegala, C. S. (2013). Harvesting Economics and Strategies Using Centrifugation for Cost Effective Separation of Microalgae Cells for Biodiesel Applications. *Bioresour. Tech.* 128, 241–245. doi:10.1016/j.biortech.2012.10.061
- Farooq, W. (2021). Sustainable Production of Microalgae Biomass for Biofuel and Chemicals through Recycling of Water and Nutrient within the Biorefinery Context: A Review. *GCB Bioenergy* 13 (6), 914–940. doi:10.1111/gcbb.12822
- Farooq, W., Lee, Y.-C., Ryu, B.-G., Kim, B.-H., Kim, H.-S., Kim, H.-S., et al. (2013). Two-stage Cultivation of Two *Chlorella* Sp. Strains by Simultaneous Treatment of Brewery Wastewater and Maximizing Lipid Productivity. *Bioresour. Tech.* 132, 230–238. doi:10.1016/j.biortech.2013.01.034
- Farooq, W., Moon, M., Ryu, B.-g., Suh, W. I., Shrivastav, A., Park, M. S., et al. (2015a). Effect of Harvesting Methods on the Reusability of Water for

- Cultivation of *Chlorella Vulgaris*, its Lipid Productivity and Biodiesel Quality. *Algal Res.* 8, 1–7. doi:10.1016/j.algal.2014.12.007
- Farooq, W., Suh, W. I., Park, M. S., and Yang, J.-W. (2015b). Water Use and its Recycling in Microalgae Cultivation for Biofuel Application. *Bioresour. Tech.* 184, 73–81. doi:10.1016/j.biortech.2014.10.140
- Gonçalves, A. L., Simões, M., and Pires, J. C. M. (2014). The Effect of Light Supply on Microalgal Growth, CO₂ Uptake and Nutrient Removal from Wastewater. *Energ. Convers. Manag.* 85, 530–536. doi:10.1016/j.enconman.2014.05.085
- Hadj-Romdhane, F., Jaouen, P., Pruvost, J., Grizeau, D., van Vooren, G., and Bourseau, P. (2012). Development and Validation of a Minimal Growth Medium for Recycling *Chlorella Vulgaris* Culture. *Bioresour. Tech.* 123, 366–374. doi:10.1016/j.biortech.2012.07.085
- Hadj-Romdhane, F., Zheng, X., Jaouen, P., Pruvost, J., Grizeau, D., Croué, J. P., et al. (2013). The Culture of *Chlorella Vulgaris* in a Recycled Supernatant: Effects on Biomass Production and Medium Quality. *Bioresour. Tech.* 132, 285–292. doi:10.1016/j.biortech.2013.01.025
- Hoxha, A., and Christensen, B. (2018). "The Carbon Footprint of Fertiliser Production: Regional Reference Values," in Proceedings 805, International Fertiliser Society Conference in Prague (Czech Republic: International Fertiliser Society), 21. Available at: https://www.fertilizerseurope.com/wp-content/uploads/2020/01/The-carbon-footprint-of-fertilizer-production_Regional-reference-values.pdf. (Accessed May 8, 2018).
- Jiang, M., and Zheng, Z. (2018). Effects of Multiple Environmental Factors on the Growth and Extracellular Organic Matter Production of *Microcystis Aeruginosa*: A Central Composite Design Response Surface Model. *Environ. Sci. Pollut. Res.* 25 (23), 23276–23285. doi:10.1007/s11356-018-2009-z
- Khalili, A., Najafpour, G. D., Amini, G., and Samkhaniyani, F. (2015). Influence of Nutrients and LED Light Intensities on Biomass Production of Microalgae *Chlorella Vulgaris*. *Biotechnol. Bioproc. E* 20 (2), 284–290. doi:10.1007/s12257-013-0845-8
- Khozingoldberg, I., and Cohen, Z. (2006). The Effect of Phosphate Starvation on the Lipid and Fatty Acid Composition of the Fresh Water Eustigmatophyte *Monodus Subterraneus*. *Phytochemistry* 67 (7), 696–701. doi:10.1016/j.phytochem.2006.01.010
- Kumar, A., and Bera, S. (2020). Revisiting Nitrogen Utilization in Algae: A Review on the Process of Regulation and Assimilation. *Bioresour. Tech. Rep.* 12, 100584. doi:10.1016/j.biteb.2020.100584
- Lam, M. K., and Lee, K. T. (2013). Effect of Carbon Source towards the Growth of *Chlorella Vulgaris* for CO₂ Bio-Mitigation and Biodiesel Production. *Int. J. Greenhouse Gas Control.* 14, 169–176. doi:10.1016/j.ijggc.2013.01.016
- Leflay, H., Pandhal, J., and Brown, S. (2021). Direct Measurements of CO₂ Capture Are Essential to Assess the Technical and Economic Potential of Algal-CCUS. *J. CO₂ Utilization* 52, 101657. doi:10.1016/j.jcou.2021.101657
- Li, C.-T., Yelsky, J., Chen, Y., Zuñiga, C., Eng, R., Jiang, L., et al. (2019). Utilizing Genome-Scale Models to Optimize Nutrient Supply for Sustained Algal Growth and Lipid Productivity. *Npj Syst. Biol. Appl.* 5 (1), 33. doi:10.1038/s41540-019-0110-7
- Li, S., Luo, S., and Guo, R. (2013). Efficiency of CO₂ Fixation by Microalgae in a Closed Raceway Pond. *Bioresour. Tech.* 136, 267–272. doi:10.1016/j.biortech.2013.03.025
- Liang, C., Lu, W., Yufei, Z., Jian, Z., Xiaowen, Z., and Naihao, Y. (2020) The Effects of Elevated CO₂ Concentrations on Changes in Fatty Acids and Amino Acids of Three Species of Microalgae. *Phycologia* 59 (3), 208–217. doi:10.1080/00318884.2020.1732714
- Lim, Y. A., Chong, M. N., Foo, S. C., and Ilankoon, I. M. S. K. (2021). Analysis of Direct and Indirect Quantification Methods of CO₂ Fixation via Microalgae Cultivation in Photobioreactors: A Critical Review. *Renew. Sust. Energ. Rev.* 137, 110579. doi:10.1016/j.rser.2020.110579
- Liu, L., Pohnert, G., and Wei, D. (2016). Extracellular Metabolites from Industrial Microalgae and Their Biotechnological Potential. *Mar. Drugs* 14 (10), 191. doi:10.3390/md14100191
- Loftus, S. E., and Johnson, Z. I. (2019). Reused Cultivation Water Accumulates Dissolved Organic Carbon and Uniquely Influences Different Marine Microalgae. *Front. Bioeng. Biotechnol.* 7, 101. doi:10.3389/fbioe.2019.00101
- López Barreiro, D., Bauer, M., Hornung, U., Posten, C., Kruse, A., and Prins, W. (2015). Cultivation of Microalgae with Recovered Nutrients after Hydrothermal Liquefaction. *Algal Res.* 9, 99–106. doi:10.1016/j.algal.2015.03.007
- López, C. V. G., García, M. d. C. C., Fernández, F. G. A., Bustos, C. S., Chisti, Y., and Sevilla, J. M. F. (2010). Protein Measurements of Microalgal and Cyanobacterial Biomass. *Bioresour. Tech.* 101 (19), 7587–7591. doi:10.1016/j.biortech.2010.04.077
- Lu, Z., Loftus, S., Sha, J., Wang, W., Park, M. S., Zhang, X., et al. (2020). Water Reuse for Sustainable Microalgae Cultivation: Current Knowledge and Future Directions. *Resour. Conservation Recycling* 161, 104975. doi:10.1016/j.resconrec.2020.104975
- Lu, Z., Sha, J., Wang, W., Li, Y., Wang, G., Chen, Y., et al. (2019). Identification of Auto-Inhibitors in the Reused Culture Media of the Chlorophyta *Scenedesmus Acuminatus*. *Algal Res.* 44, 101665. doi:10.1016/j.algal.2019.101665
- Moon, M., Chul, W. K., Wasif, F., William, I. S., Anupama, S., Min, S. P., Sanjiv, K. M., and Ji-Won, Y. (2014). Utilization of Lipid Extracted Algal Biomass and Sugar Factory Wastewater for Algal Growth and Lipid Enhancement of *Ettlia* sp. *Biores. Technol.* 163, 180–185. doi:10.1016/j.biortech.2014.04.033
- Mejia-da-Silva, L. d. C., Matsudo, M. C., Morocho-Jacome, A. L., and de Carvalho, J. C. M. (2018). Application of Physicochemical Treatment Allows Reutilization of *Arthrospira Platensis* Exhausted Medium. *Appl. Biochem. Biotechnol.* 186 (1), 40–53. doi:10.1007/s12010-018-2712-8
- Mustapha, S. I., Bux, F., and Isa, Y. M. (2021). Techno-Economic Analysis of Biodiesel Production over Lipid Extracted Algae Derived Catalyst. *Biofuels*, 1–12. doi:10.1080/17597269.2021.1878577
- Nzayisenga, J. C., Farge, X., Groll, S. L., et al. (2020). Effects of Light Intensity on Growth and Lipid Production in Microalgae Grown in Wastewater. *Biotechnol. Biofuels* 13, 4. doi:10.1186/s13068-019-1646-x
- Pires, J. C. M., Gonçalves, A. L., and Simões, M. (2014). The Effect of Light Supply on Microalgal Growth, CO₂ Uptake and Nutrient Removal From Wastewater. *Energ. Convers. Manag.* 85, 530–536. doi:10.1016/j.enconman.2014.05.085
- Rasdi, N. W., and Qin, J. G. (2015). Effect of N:P Ratio on Growth and Chemical Composition of *Nannochloropsis Oculata* and *Tisochrysis Lutea*. *J. Appl. Phycol* 27 (6), 2221–2230. doi:10.1007/s10811-014-0495-z
- Rocha, G. S., Pinto, F. H. V., Melão, M. G. G., and Lombardi, A. T. (2015). Growing *Scenedesmus Quadricauda* in Used Culture Media: Is it Viable? *J. Appl. Phycol* 27 (1), 171–178. doi:10.1007/s10811-014-0320-8
- Rodolfi, L., Zittelli, G. C., Bassi, N., Padovani, G., Biondi, N., Bonini, G., et al. (2009). Microalgae for Oil: Strain Selection, Induction of Lipid Synthesis and Outdoor Mass Cultivation in a Low-Cost Photobioreactor. *Biotechnol. Bioeng.* 102 (1), 100–112. doi:10.1002/bit.22033
- Salam, K. A., Sharon, B. V., and Adam, P. H. (2016). A Sustainable Integrated *In Situ* Transesterification of Microalgae for Biodiesel Production and Associated Co-Product-A Review. *Renew. Sustain. Energy Rev.* 65, 1179–1198. doi:10.1016/j.rser.2016.07.068
- Selvaratnam, T., Henkanatte-Gedera, S. M., Muppaneni, T., Nirmalakhandan, N., Deng, S., and Lammers, P. J. (2016). Maximizing Recovery of Energy and Nutrients from Urban Wastewaters. *Energy* 104, 16–23. doi:10.1016/j.energy.2016.03.102
- Sha, J., Lu, Z., Ye, J., Wang, G., Hu, Q., Chen, Y., and Zhang, X. (2019). The Inhibition Effect of Recycled *Scenedesmus Acuminatus* Culture Media: Influence of Growth Phase, Inhibitor Identification and Removal. *Algal Res.* 42, 101612. doi:10.1016/j.algal.2019.101612
- Sharma, K. K., Schuhmann, H., and Schenk, P. M. (2012). High Lipid Induction in Microalgae for Biodiesel Production. *Energies* 5 (5), 1532–1553. doi:10.3390/en5051532
- Singh, U. B., and Ahluwalia, A. S. (2013). Microalgae: A Promising Tool for Carbon Sequestration. *Mitig Adapt Strateg. Glob. Change* 18 (1), 73–95. doi:10.1007/s11027-012-9393-3
- Tredici, M. R., Bassi, N., Prussi, M., Biondi, N., Rodolfi, L., Zittelli, G. C., et al. (2015). Energy Balance of Algal Biomass Production in a 1-ha "Green Wall Panel" Plant: How to Produce Algal Biomass in a Closed Reactor Achieving a High Net Energy Ratio. *Appl. Energy* 154, 1103–1111. doi:10.1016/j.apenergy.2015.01.086
- Thawechai, T., Benjamas, C., Yasmi, L., Piyaat, B., and Poonsuk, P. (2014). Mitigation of Carbon Dioxide by Oleaginous Microalgae for Lipids and Pigments Production: Effect of Light Illumination and Carbon Dioxide Feeding Strategies. *Biores. Technol.* 219, 13–9149. doi:10.1016/j.biortech.2016.07.109
- Villacorte, L. O., Ekowati, Y., Neu, T. R., Kleijn, J. M., Winters, H., Amy, G., et al. (2015). Characterisation of Algal Organic Matter Produced by Bloom-Forming Marine and Freshwater Algae. *Water Res.* 73, 216–230. doi:10.1016/j.watres.2015.01.028

- Wadood, A., Rana, A., Basheer, C., Razzaq, S. A., and Farooq, W. (2020). *In Situ* Transesterification of Microalgae *Parachlorella Kessleri* Biomass Using Sulfonated Rice Husk Solid Catalyst at Room Temperature. *Bioenerg. Res.* 13 (2), 530–541. doi:10.1007/s12155-019-10060-3
- Xin, L., Hong-ying, H., Ke, G., and Ying-xue, S. (2010). Effects of Different Nitrogen and Phosphorus Concentrations on the Growth, Nutrient Uptake, and Lipid Accumulation of a Freshwater Microalga *Scenedesmus* Sp. *Bioresour. Tech.* 101 (14), 5494–5500. doi:10.1016/j.biortech.2010.02.016
- Zarrinmehr, M. J., Farhadian, O., Heyrati, F. P., Keramat, J., Koutra, E., Kornaros, M., et al. (2020). Effect of Nitrogen Concentration on the Growth Rate and Biochemical Composition of the Microalga, *Isochrysis Galbana*. *Egypt. J. Aquat. Res.* 46 (2), 153–158. doi:10.1016/j.ejar.2019.11.003
- Zhang, W., Cao, Q., Xu, G., and Wang, D. (2018). Flocculation–Dewatering Behavior of Microalgae at Different Growth Stages under Inorganic Polymeric Flocculant Treatment: The Relationships between Algal Organic Matter and Floc Dewaterability. *ACS Sustain Chem. Eng.* 6 (8), 11087–11096. doi:10.1021/acssuschemeng.8b02551

Conflict of Interest: The author declares that the research was conducted in the absence of any commercial or financial relationships that could be construed as a potential conflict of interest.

Publisher's Note: All claims expressed in this article are solely those of the authors and do not necessarily represent those of their affiliated organizations or those of the publisher, the editors, and the reviewers. Any product that may be evaluated in this article or claim that may be made by its manufacturer is not guaranteed or endorsed by the publisher.

Copyright © 2022 Farooq. This is an open-access article distributed under the terms of the Creative Commons Attribution License (CC BY). The use, distribution or reproduction in other forums is permitted, provided the original author(s) and the copyright owner(s) are credited and that the original publication in this journal is cited, in accordance with accepted academic practice. No use, distribution or reproduction is permitted which does not comply with these terms.



Effective Two-Stage Heterotrophic Cultivation of the Unicellular Green Microalga *Chromochloris zofingiensis* Enabled Ultrahigh Biomass and Astaxanthin Production

Qiaohong Chen^{1,2†}, Yi Chen^{1,2†}, Quan Xu¹, Hu Jin¹, Qiang Hu³ and Danxiang Han^{1,4*}

¹Center for Microalgal Biotechnology and Biofuels, Institute of Hydrobiology, Chinese Academy of Sciences, Wuhan, China, ²College of Life Sciences, University of Chinese Academy of Sciences, Beijing, China, ³Institute for Advanced Study, Shenzhen University, Shenzhen, China, ⁴Key Laboratory for Algal Biology, Institute of Hydrobiology, Chinese Academy of Sciences, Wuhan, China

OPEN ACCESS

Edited by:

Wanthanee Khetkorn,
Rajamangala University of Technology
Thanyaburi, Thailand

Reviewed by:

Yongteng Zhao,
Kunming University of Science and
Technology, China
Zhengquan Gao,
Shandong University of Technology,
China

*Correspondence:

Danxiang Han
danxianghan@ihb.ac.cn

[†]These authors share first authorship

Specialty section:

This article was submitted to
Bioprocess Engineering,
a section of the journal
Frontiers in Bioengineering and
Biotechnology

Received: 13 December 2021

Accepted: 09 February 2022

Published: 24 February 2022

Citation:

Chen Q, Chen Y, Xu Q, Jin H, Hu Q and
Han D (2022) Effective Two-Stage
Heterotrophic Cultivation of the
Unicellular Green Microalga
Chromochloris zofingiensis Enabled
Ultrahigh Biomass and
Astaxanthin Production.
Front. Bioeng. Biotechnol. 10:834230.
doi: 10.3389/fbioe.2022.834230

Chromochloris zofingiensis has obtained particular interest as a promising candidate for natural astaxanthin production. In this study, we established a two-stage heterotrophic cultivation process, by using which both the growth of *C. zofingiensis* and astaxanthin accumulation are substantially enhanced. Specifically, the ultrahigh biomass concentration of 221.3 g L⁻¹ was achieved under the optimum culture conditions in 7.5 L fermenter during 12 days. When scaled-up in the 500 L fermentor, the biomass yield reached 182.3 g L⁻¹ in 9 days, while the astaxanthin content was 0.068% of DW. To further promote astaxanthin accumulation, gibberellic Acid-3 (GA3) was screened from a variety of phytohormones and was combined with increased C/N ratio and NaCl concentration for induction. When *C. zofingiensis* was grown with the two-stage cultivation strategy, the astaxanthin yield reached 0.318 g L⁻¹, of which the biomass yield was 235.4 g L⁻¹ and astaxanthin content was 0.144% of DW. The content of the total fatty acids increased from 23 to 42% of DW simultaneously. Such an astaxanthin yield was 5.4-fold higher than the reported highest record and surpassed the level of *Haematococcus pluvialis*. This study demonstrated that heterotrophic cultivation of *C. zofingiensis* is competitive for industrial astaxanthin production.

Keywords: *Chromochloris zofingiensis*, heterotrophic cultivation, biomass, astaxanthin, total fatty acids

INTRODUCTION

Astaxanthin (3, 3'-dihydroxy- β , β -carotene-4, 4'-dione) is a high-value red ketocarotenoid and possesses a wide range of commercial applications in food, feed, cosmetics, pharmaceuticals, and nutraceuticals due to its powerful antioxidative activity, pigmentation function, and many other bioactivities (Ambati et al., 2014; Liu et al., 2014). Astaxanthin can be synthesized artificially or produced by organisms such as green microalgae. The (3S, 3'S) isoform is the most abundant stereoisomer of the natural astaxanthin produced by green microalgae, whereas the artificially synthesized astaxanthin contains a mixture of isomers (3S, 3'S), (3R, 3S), and (3R, 3'R) at the ratio of 1:2:1 (Li et al., 2020). In addition, the natural astaxanthin produced by microalgae are acylated with one or two fatty acids, whereas the synthesized astaxanthin is free type (Katsumata et al., 2014).

Notably, the antioxidant activity of artificially synthesized astaxanthin is 20 times lower than its natural counterpart and is not allowed to apply in human foods in many countries (Rodríguez-Sáiz et al., 2010; Shah et al., 2016). Thus, demands for the natural astaxanthin are increasing and its price reached 7000 US dollars per kg in the global market (Koller et al., 2014). Currently, *H. pluvialis* is the major resource of natural astaxanthin production strain in the industry, as they can accumulate up to 5–6% of astaxanthin on dry weight (Yang et al., 2016). However, astaxanthin production by using *H. pluvialis* is faced with technical bottlenecks such as high cost, low production efficiency, and inevitable contamination by the pathogenic fungus in outdoor mass cultivation (Liu et al., 2013).

One promising way to overcome the techno-economic challenges in natural astaxanthin production is to invent innovative biomanufacturing systems based on discovery and development of novel microalgal species/strains with high growth rates and superior astaxanthin-producing abilities. The green microalga *Chromochloris zofingiensis* is emerging as a promising bioresource for astaxanthin and lipids production (Liu et al., 2014). *C. zofingiensis* can not only utilize light energy and CO₂ for photoautotrophic growth but also use organic carbon sources so can be cultivated under heterotrophic conditions. The dry cell weight of *C. zofingiensis* can reach up to 98.4 g L⁻¹ in fermentation, which is much higher than that under photoautotrophic conditions (Zhang et al., 2017). However, the astaxanthin content in *C. zofingiensis* heterotrophic cells is about 10-fold lower than that of the photoautotrophic cells, of which the former is 0.06% of DW and the latter is 0.5% of DW (Zhang et al., 2016).

Numerous studies have demonstrated the biotechnical significance of heterotrophic cultivation for microalgal biomass and chemicals production (Lee Chang et al., 2015; Morales-Sánchez et al., 2015; Hu et al., 2018). Through optimizing the components of growth media and substrate feeding strategy, ultra-high biomass yield (>200 g L⁻¹) can be achieved for several production strains such as *Chlorella sorokiniana* (Jin et al., 2021), *Chlorella sorokiniana* strain CMBB276 (Xu et al., 2021) and *Scenedesmus acuminatus* (Jin et al., 2020). The capabilities of these species in achieving such high biomass yield have been attributable to the highly active starch biosynthesis under heterotrophic conditions, considering the carbon substrate (i.e. glucose) can be directly utilized as the building blocks of starch, which eliminates the loss of carbon atoms in central carbon metabolism (e.g. from pyruvate to acetyl-CoA) and for reducing equivalents production. Thus, it remains disputed whether microalgae with either high protein or lipid contents possess the potential to reach biomass and products yield as high as that of those starch-producing strains.

For *C. zofingiensis*, challenges in establishing ultra-high cell density heterotrophic cultivation technology are more complicated than that for the other oleaginous microalgae, since biosynthesis astaxanthin needs to consume large amounts of oxygen as indicated by previous study in *H. pluvialis* (Li et al., 2008). Moreover, understanding about astaxanthin accumulation under heterotrophic conditions is limited. Accumulation of astaxanthin has been considered as a

protective response triggered by photo-oxidative stresses, which is linked to over-reduction of photosynthetic electron transport chain and production of reactive oxygen species in microalgal cells. Thus, astaxanthin can be induced by high-light, nutrient depletion and high-salinity stresses in *H. pluvialis* and many other microalgae under photoautotrophic conditions. In contrast, it is unlikely to impose the photo-oxidative stresses on *C. zofingiensis* cells grown under heterotrophic conditions. Thus, it remains to be explored how to trigger the biosynthesis of the secondary carotenoid-astaxanthin. It was found that the high C/N ratio can enhance the astaxanthin production in *C. zofingiensis* in dark (Ip and Chen, 2005). On the other hand, phytohormones as chemical messengers can regulate plant and microalgae growth, development, metabolism, as well as environmental stress responses (Voß et al., 2014; Lu and Xu, 2015). Several previous studies suggested that various phytohormones, such as cytokinins, ethylene precursor, gibberellic acid, and auxins can enhance the accumulation of biomass and metabolites, such as pigments, proteins, carbohydrates, and lipids in microalgae (Hunt et al., 2010; Gao et al., 2013; Bajguz and Piotrowska-Niczyporuk, 2014; Jiang et al., 2015).

This present work aimed to establish a two-stage cultivation strategy to enhance astaxanthin production of *C. zofingiensis* under heterotrophic conditions. Firstly, the growth conditions including nitrogen source, temperature, pH, and substrate concentration were optimized in the bench-top fermentor, and the optimal conditions were scaled-up at the pilot scale. To induce the astaxanthin biosynthesis, the effects of various of phytohormones were compared, from which the most effective phytohormone combined with high C/N and salinity stresses were introduced to the high-cell density heterotrophic conditions. The results of this study suggested heterotrophic cultivation of *C. zofingiensis* is a competitive technical route for producing astaxanthin.

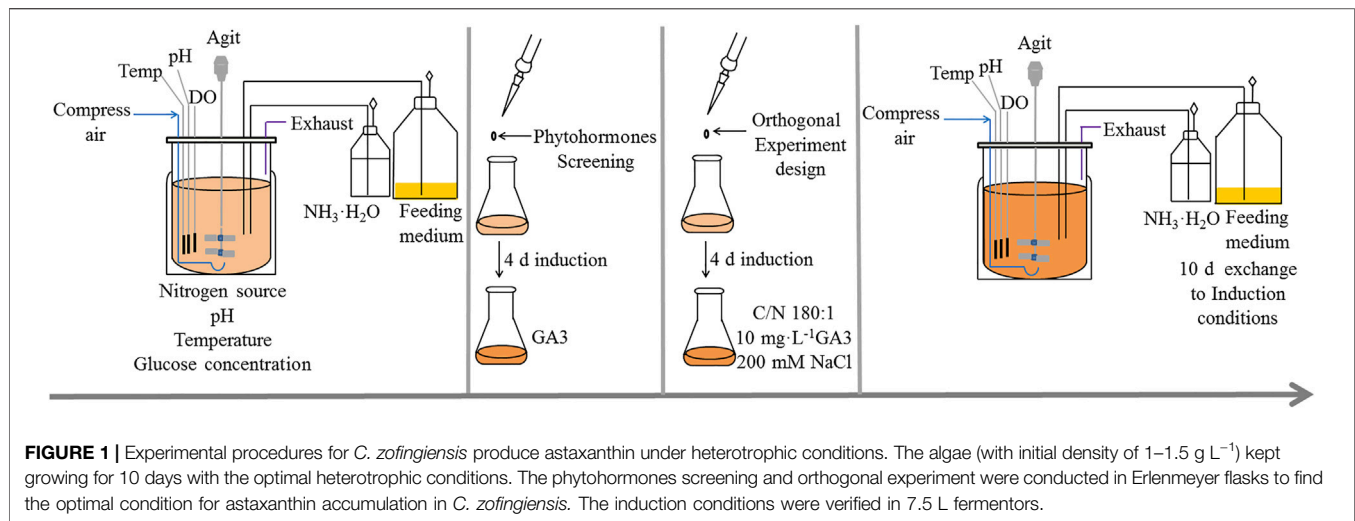
MATERIALS AND METHODS

Microalgal Strain and Growth Media

Chromochloris zofingiensis (ATCC 30412) was obtained from the American Type Culture Collection (ATCC, Rockville, United States) and was maintained in the modified Endo growth medium consisting of 3 g L⁻¹ KNO₃, with the addition of 15 g L⁻¹ agar for plates. The modified Endo growth medium was adjusted to pH 6.5 with 3M NaOH before autoclaving at 121 °C for 15 min.

Culture Conditions

A single colony of *C. zofingiensis* was transferred in 250 ml Erlenmeyer flasks containing 100 ml sterilized modified Endo growth medium and cultivated for 7 days at 26°C with orbital shaking at 180 rpm. Microalgal cells in the exponential phase were used as the inoculum at 10% (v/v) for fermentation experiments. Bench fermentation experiments were carried out in the 7.5 L BIOFLO and CELLIGEN 310 (New Brunswick Scientific Co., Edison, NJ) fermenters with an initial working volume of 3 L. The fermentor was continuously aerated through a



0.2 μm membrane filter at a flow rate of 2.0 L min⁻¹. To minimize evaporation, the vent gas passed through a modified condenser mounted on the head plate of the fermentor. Dissolved oxygen (DO) was controlled automatically at about 20% by coupling with the stirring speed. The changes of DO and stirring speeding during the heterotrophic cultivation period are shown in **Supplementary Figure S1**. The pH was maintained at 6.5 ± 0.5 by the automatic addition of $\text{NH}_3 \cdot \text{H}_2\text{O}$. For the heterotrophic cultivation of *C. zofingiensis*, 20 g L⁻¹ glucose was initially added to the fermentation medium. When the glucose concentration decreased to 5 g L⁻¹, fed-batch fermentation was carried out by continuously feeding the cell cultures with a 25-fold concentrated batch medium containing 750 g L⁻¹ glucose at a predetermined flow rate using a peristaltic pump (Cole Parmer, Vernon Hills, IL, United States) and maintained the range of glucose at a stable level (e.g., 0–30 g L⁻¹). The maximum culture volume was 5 L, from which 500 ml of the culture was discharged when the culture volume almost reached the maximum. The morphology of microalgal cells was observed with an Olympus BX-53 microscope (Olympus Optical Co. Ltd., Tokyo, Japan).

For the heterotrophic cultivation in the 7.5 L fermentors, the initial nitrogen source in the modified Endo growth medium was replaced by sodium nitrate (NaNO_3), urea ($(\text{NH}_2)_2\text{CO}$), and ammonium chloride (NH_4Cl), respectively. For these heterotrophic culturing media, the molar ratio of the nitrogen to carbon source was maintained at 32:1, respectively. The pH values were controlled by feeding with $\text{NH}_3 \cdot \text{H}_2\text{O}$ or 3M H_3PO_4 solutions.

The experimental procedures are schematically illustrated in **Figure 1**.

To mitigate the chance of bacterial contamination, the sterile operation procedure was strictly followed, which included using the ultraviolet lamp frequently to sterilize the air in the culture room, autoclaving the culture media and fermentors at 121°C for 30 min, and conducting sterility test before inoculation. In addition, air filters were installed at the air inlet of the fermentors and were frequently changed to keep the air flowing into the fermentors clean.

Measurement of Biomass dry Weight and Glucose Consumption

The microalgal biomass dry weight was determined as previously reported (Mao et al., 2020). In brief, samples at each time point were harvested and washed twice with 0.5M NH_4HCO_3 and filtered through a pre-dried and pre-weighed dry GF/C filter paper of 1.2 μm pore size (Whatman, Life Sciences, United Kingdom), which was then dried at 105°C in a vacuum oven overnight. The Whatman GF/C filter papers were placed in a desiccator for 20 min to allow the temperature cooling down before dry weight measurement. The glucose concentration was monitored by using a Gold-Accu Glucose Monitoring System (Model BGMS-1; Sinocare Inc., Changsha, China).

Phytohormones Screening

Two-stage cultivation lasting for 14 days was performed to screen among phytohormones including GA3, Indole-3-acetic acid (IAA), Indole-3-propionic (IPA), Indole-3-butyric acid (IBA), 1-Naphthylacetic acid (NAA), and 1-aminocyclopropane-1-carboxylic acid (ACC) that can enhance astaxanthin accumulation (Aladdin Chemical Reagent Co., Ltd, Shanghai). Their physic-chemical properties are presented in **Supplementary Table S1**. In the first stage, algal cells were grown in 7.5 L fermentors to reach the biomass yield of 180 g L⁻¹ during 10 days. Then the collected algal cells were inoculated into the Erlenmeyer flasks to maintain the initial cell density of algae suspension at 2–3 g L⁻¹. Stock solutions of phytohormones were prepared in sterile water or ethanol and then directly added into the heterotrophic culture condition in the Erlenmeyer flasks at the designated concentration.

Orthogonal Experiment Design

The induction conditions were optimized by using an L_{16} orthogonal array. The C/N ratio, GA3 concentration, and NaCl concentration were chosen as the conditional factors of the orthogonal experiments. Each factor was set at four levels as

shown in **Supplementary Table S2**. The pH in each treatment group was successfully controlled in the range of 6.5–7. The inoculum concentrations and heterotrophic culture condition were performed using the same as aforementioned conditions in the Erlenmeyer flasks. The optimal induction condition obtained through orthogonal experiments was verified during the induction period in the 7.5 L fermenters.

Pigments Analysis

The microalgal cells were harvested by centrifugation at 3,000 g for 5 min and washed twice in PBS buffer solution. The cell pellets were freeze-dried to completely remove water. Pigments were extracted by using methanol/dichloromethane (3:1, v/v) till the residues became colorless. The extracts were centrifuged at 12,000 × g for 5 min to remove the debris, and the supernatants were dried, recovered in 0.5 ml of extraction solution, and filtrated through 0.22 µm membrane filters (Pall Life Science, United States) before High-Performance Liquid Chromatography (HPLC) analysis. The pigments were separated on a Waters Symmetry C₁₈ (150 × 4.6 mm, 5 µm) column at 35°C. Ten µL aliquot of the sample was injected into the waters e2695 HPLC (Waters Associates, Milford, MA, United States) system equipped with a 2998 photodiode array detector (Waters, Milford, MA, United States). The mobile phase consisted of eluent A (dichloromethane/methanol/acetonitrile/water, 5.0:85.0:5.5:4.5, v/v) and eluent B (dichloromethane/methanol/acetonitrile/water, 25.0:28.0:42.5:4.5, v/v). Pigments were separated by using the following gradient procedure: 0% B for 8 min, then increasing the gradient to 100% of B within 6 min and holding for 40 min. The flow rate was 1.0 ml min⁻¹. Astaxanthin standard (Sigma-Aldrich, St. Louis, MO, United States) was used as a calibrant for quantification.

Total Fatty Acid Content Quantification

Approximately 10 mg of lyophilized microalgal powder was weighed into a 1.5 ml GC vial, which was used for total fatty acid analysis. Two hundreds microliters of chloroform: methanol (2:1, v/v), 25 µL of ¹³C:0 (200 µg mL⁻¹), and 300 µL of 5% HCl: methanol were added, respectively. The mixture samples were heated at 85 °C for 1 h. After cooling down to room temperature, 1 ml hexane was mixed with the in the room temperature for 1–4 h. Nine hundreds microliters of hexane and 1-µL of hexane top layer were transferred into GC vials and then mixed with 25 µL pentadecane standard (200 µg mL⁻¹) for fatty acid methyl esters (FAME) analysis, which was performed by using an Agilent 7890B gas chromatography equipped with 5977A mass spectrometry (GC-MS). The chromatographic separation was using the same conditions as previously described (Wu et al., 2019).

Statistical Analysis

All the experiments were conducted in at least triplicate. Experimental results shown in the figures are expressed as the mean value ±SD. The data were analyzed by one-way analysis of variance using Dunnett multiple comparison tests and

GraphPad Prism (v. 7.0 for Windows; GraphPad Software, Inc., CA, United States). A value of $p < 0.05$ was considered statistically significant.

RESULTS

Optimization of Heterotrophic Culturing Conditions for *C. zofingiensis*

The effects of various nitrogen sources including NaNO₃, (NH₂)₂CO, and NH₄Cl on the growth of *C. zofingiensis* were investigated in 7.5 L fermenters by using fed-batch culture mode. As shown in **Figure 2A**, *C. zofingiensis* cell can utilize NaNO₃, (NH₂)₂CO, and NH₄Cl as nitrogen source, among which NH₄Cl and urea sustained rapid microalgal growth. Notably, an ultrahigh biomass concentration of 153 g L⁻¹ was achieved in the modified Endo culture medium containing NH₄Cl as the nitrogen source. Therefore, NH₄Cl was selected as the nitrogen source suitable for *C. zofingiensis* growth and was used in the other optimization experiments.

Within the temperature range of 24–28°C, *C. zofingiensis* showed a rapid growth trend, and the highest biomass concentration of 149.5 g L⁻¹ was achieved at 26°C after 9 days of cultivation (**Figure 2B**). However, further increases in the cultivation temperature can inhibit the growth of microalgal cells (**Figure 2B**). Thus, 26°C was chosen as the optimal culture temperature.

The growth parameters of *C. zofingiensis* at different culture pH values are shown in **Figure 2C**. The culture pH was controlled at 4.0–8.0 via utilizing the pH-stat mode. At pH 6.5, the highest biomass concentration of 127.7 g L⁻¹ was achieved at the end of the 8-day fermentation.

Glucose is a common organic carbon for the heterotrophic cultivation of microalgae. The effects of glucose concentration on *C. zofingiensis* growth under heterotrophic conditions are shown in **Figure 2D,E**. The glucose concentration in the fermentation medium was continuously measured to control the glucose in the medium maintained at a stable level (**Figure 2E**). When the glucose in the fermentation medium was consumed to the concentration of approximately 5 g L⁻¹, additional media with glucose were fed to the cultures to reach the initial glucose concentration. The results exhibited that the biomass concentrations were very close among all the microalgal cell cultures with different glucose concentrations. The highest biomass concentration reached 157.3 g L⁻¹ after 8 days of cultivation when the glucose concentrations were maintained at 10 g L⁻¹.

Pilot-Scale Heterotrophic Culture of *C. zofingiensis* Under the Optimal Culture Conditions

Glucose was the best carbon and energy source for heterotrophic growth of *C. zofingiensis* which showed ultrahigh biomass concentrations. Heterotrophic cultures with glucose not only enhanced biomass concentration but also stimulated astaxanthin accumulation (Zhang et al., 2019).

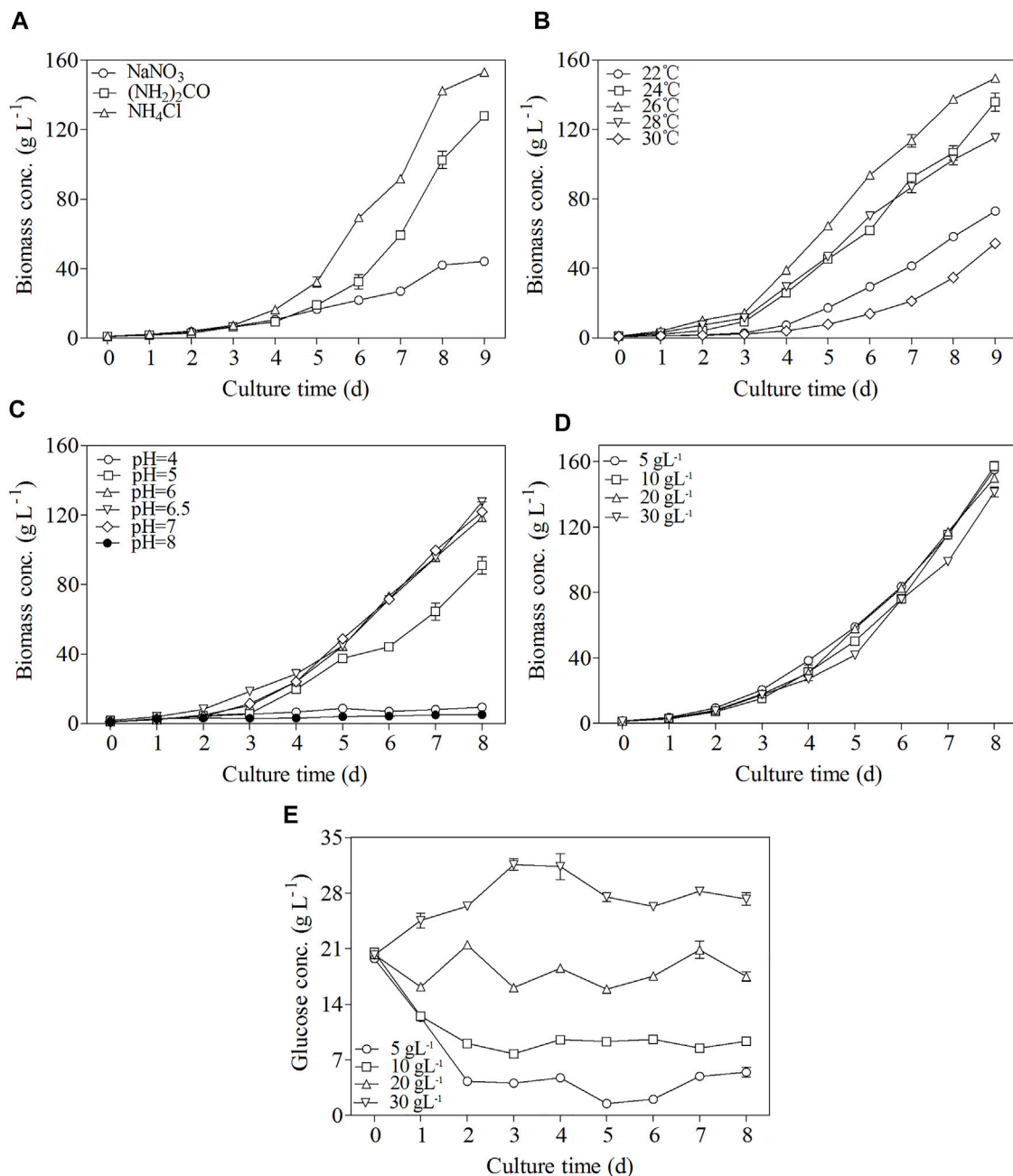


FIGURE 2 | Effects of different nitrogen sources (A), temperature (B), pH (C), glucose concentration (D), and change of glucose concentration (E) on *C. zofingiensis* cellular growth under heterotrophic conditions in 7.5 L fermentors. Data are mean values \pm SD from triplicate measurements ($n = 3$). All cultures were performed in 7.5 L fermentors using NH₄Cl as the nitrogen source.

The astaxanthin content in *C. zofingiensis* increased considerably with increasing biomass concentration in the heterotrophic fed-batch cultures (Figure 3). When the optimal conditions were adopted for the scaling-up experiment conducted in a 500 L fermentor, the highest biomass concentration reached 182.3 g L⁻¹ on Day 9, which was 14% higher than the highest cell density (160 g L⁻¹)

achieved in the 7.5 L fermentor. As compared with the 7.5 L fermentor, the significant enhancement of *C. zofingiensis* biomass in the 500 L fermentor revealed that *C. zofingiensis* has the potential for large-scale industrial production. Meanwhile, the maximum astaxanthin content in 500 L reached 0.068% of DW, slightly higher than the highest astaxanthin content (0.063%) attained in 7.5 L fermentor.

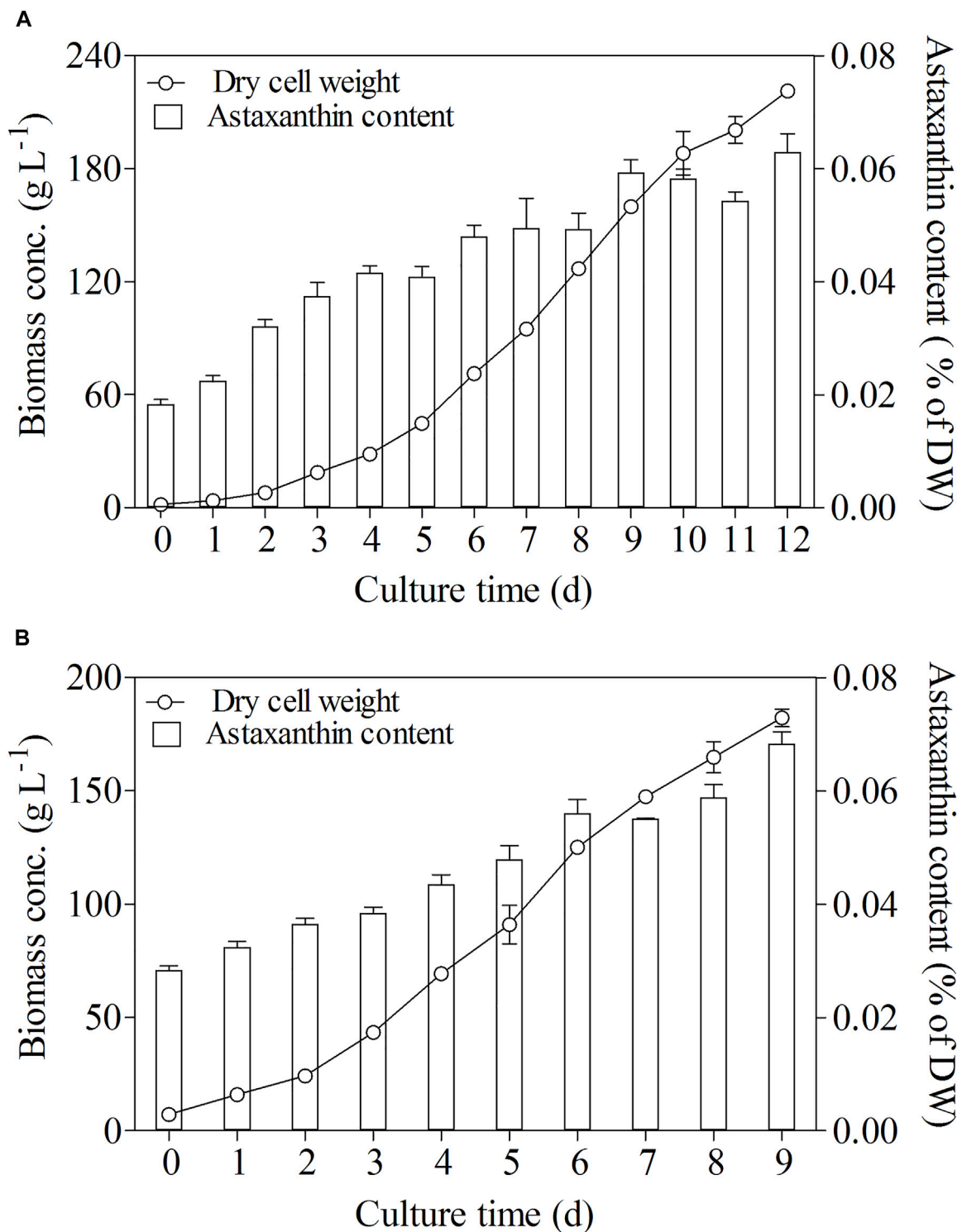


FIGURE 3 | Biomass and astaxanthin content in fed-batch fermentation of *C. zofingiensis* in 7.5 L fermentors (A) and 500 L fermentors (B) with optimal cultural conditions. Data are mean values \pm SD from triplicate measurements ($n = 3$).

TABLE 1 | *C. zofingiensis* biomass concentration (g·L⁻¹), pH, glucose concentration (g·L⁻¹), and astaxanthin content (% of DW) at the termination of each experiment.

Phytohormones concentration	Biomass concentration (g·L ⁻¹)	pH	Glucose concentration (g·L ⁻¹)	Astaxanthin content (% of DW)
Control	6.73 ± 0.247	6.02 ± 0.057	9.40 ± 0.085	0.062 ± 0.002
GA				
5 mg L ⁻¹	4.70 ± 0.144	5.60 ± 0.028	25.29 ± 0.127	0.080 ± 0.002
10 mg L ⁻¹	5.25 ± 0.212	5.54 ± 0.007	27.07 ± 0.099	0.080 ± 0.002
25 mg L ⁻¹	4.35 ± 0.071	5.44 ± 0.049	27.75 ± 0.212	0.081 ± 0.003
50 mg L ⁻¹	3.75 ± 0.212	5.59 ± 0.014	27.99 ± 0.381	0.101 ± 0.003
IAA				
15 mg L ⁻¹	6.25 ± 0.354	5.55 ± 0.071	20.90 ± 1.273	0.089 ± 0.001
70 mg L ⁻¹	4.80 ± 0.141	5.40 ± 0.141	23.89 ± 0.156	0.096 ± 0.002
150 mg L ⁻¹	4.75 ± 0.071	5.42 ± 0.049	25.90 ± 0.141	0.094 ± 0.005
250 mg L ⁻¹	4.55 ± 0.072	5.24 ± 0.085	26.97 ± 0.764	0.076 ± 0.005
IPA				
10 mg L ⁻¹	5.85 ± 0.071	5.70 ± 0.091	20.93 ± 1.315	0.083 ± 0.001
60 mg L ⁻¹	5.10 ± 0.283	5.66 ± 0.042	23.45 ± 0.700	0.089 ± 0.005
120 mg L ⁻¹	4.70 ± 0.141	5.60 ± 0.007	25.38 ± 0.509	0.097 ± 0.002
240 mg L ⁻¹	3.85 ± 0.071	5.51 ± 0.014	27.22 ± 0.311	0.086 ± 0.002
IBA				
10 mg L ⁻¹	5.31 ± 0.233	5.80 ± 0.064	23.80 ± 0.304	0.075 ± 0.003
50 mg L ⁻¹	4.61 ± 0.234	5.71 ± 0.071	24.45 ± 0.212	0.060 ± 0.002
90 mg L ⁻¹	3.93 ± 0.035	5.72 ± 0.028	25.53 ± 0.177	0.059 ± 0.004
130 mg L ⁻¹	3.87 ± 0.099	5.68 ± 0.035	25.27 ± 0.191	0.057 ± 0.003
NAA				
10 mg L ⁻¹	3.65 ± 0.071	5.66 ± 0.021	25.81 ± 0.155	0.082 ± 0.005
20 mg L ⁻¹	3.35 ± 0.071	5.55 ± 0.063	27.00 ± 0.156	0.078 ± 0.002
40 mg L ⁻¹	3.18 ± 0.035	5.35 ± 0.070	27.92 ± 0.106	0.039 ± 0.001
60 mg L ⁻¹	3.05 ± 0.070	5.69 ± 0.014	28.10 ± 0.212	0.036 ± 0.003
ACC				
5 mg L ⁻¹	5.66 ± 0.198	5.77 ± 0.021	27.11 ± 0.127	0.064 ± 0.002
10 mg L ⁻¹	5.81 ± 0.106	5.54 ± 0.020	26.68 ± 0.057	0.068 ± 0.003
20 mg L ⁻¹	4.76 ± 0.148	5.43 ± 0.042	24.63 ± 0.240	0.066 ± 0.002
40 mg L ⁻¹	4.31 ± 0.240	5.34 ± 0.021	25.70 ± 0.141	0.068 ± 0.001

Screening Phytohormones That can Efficiently Enhance Astaxanthin Production in *C. zofingiensis*

The effects of a variety of phytohormones on the astaxanthin production of *C. zofingiensis* were investigated. As shown in **Table 1**, GA3, IAA, IPA, IBA, NAA, and ACC all demonstrated significant effects on *C. zofingiensis* growth characteristics, as compared to the control ($p < 0.01$). Specifically, GA3, IAA, IPA, NAA, and ACC enhanced astaxanthin content, whereas inhibited *C. zofingiensis* biomass accumulation and glucose assimilation (**Table 1**).

Table 1 demonstrated that GA3 was the most effective phytohormone to enhance astaxanthin content, which was 50.7% higher than that of the control ($p < 0.001$). Similarly, IAA and IPA significantly increased astaxanthin content to 0.096 and 0.097% of DW, respectively, significantly higher than that of the control ($p < 0.001$). In addition, low concentration of IBA and NAA could stimulate astaxanthin accumulation, whereas these phytohormones might inhibit astaxanthin accumulation at high concentrations. The addition of ACC showed no significant effect on astaxanthin accumulation as compared to the control.

The inhibition effect of phytohormone on biomass accumulation and glucose assimilation was enhanced with increasing phytohormone concentrations (**Table 1**). With the

use of phytohormone, the pH value of culture decreased constantly from the initial value of 6.1 ($p < 0.01$). However, the enhanced astaxanthin production was accompanied by the reduced biomass yield. The consumption of glucose by *C. zofingiensis* was significantly inhibited when the phytohormones were added as compared to the control ($p < 0.05$).

Optimization of the Induction Conditions

To further enhance the astaxanthin production in *C. zofingiensis*, algal cells were induced with the addition of GA3 combined with simultaneously increasing C/N and salinity. The conditions were optimized with orthogonal experiments. The astaxanthin contents in all treatment groups were greatly enhanced as compared to the control ($p < 0.001$, **Figure 4C**). According to the results, the C/N 180:1, 10 mg L⁻¹ GA3, and 200 mM NaCl turned out to be the most effective treatment group to promote astaxanthin production, in which the astaxanthin content reached 0.115% of DW. The inducing effect of the C/N 220:1, 10 mg L⁻¹ GA3, and 400 mM NaCl on the astaxanthin production is very close to that of the previous one, which was higher than the other treatment groups.

The growth trends of *C. zofingiensis* in terms of biomass accumulation were similar among different treatments during the 4-day induction period and were inhibited as compared to the

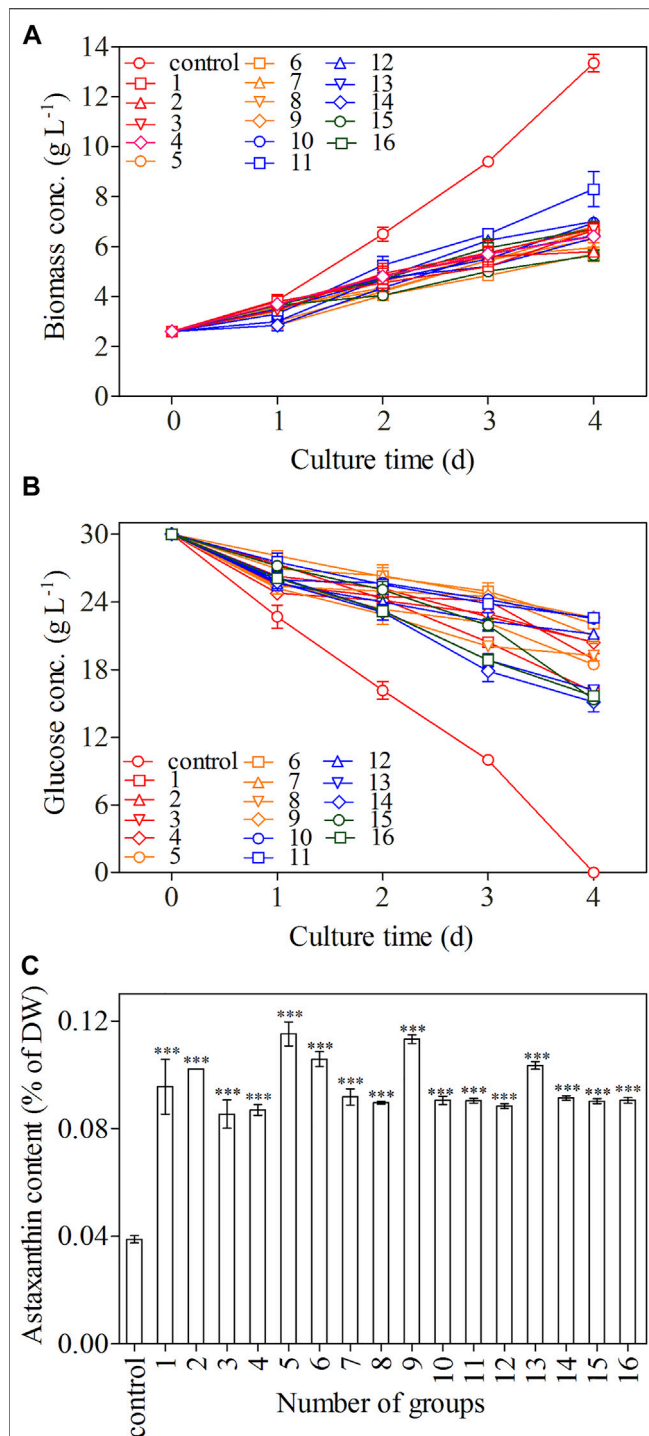


FIGURE 4 | Biomass concentration (A), glucose concentration (B), and astaxanthin content (C) of *C. zofingiensis* in different treatment groups. The biomass concentration, glucose concentration, and astaxanthin content were monitored daily during 4-day induction; astaxanthin content was measured on day 4. All cultures were conducted in Erlenmeyer flasks with modified Endo culture medium containing NH₄Cl as the nitrogen source. Data are mean values \pm SD from triplicate measurements ($n = 3$) (See Table 2 for detailed information on treatment groups 1–16).

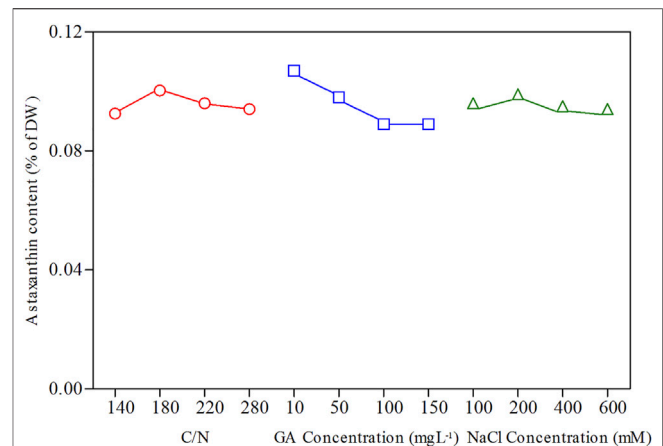


FIGURE 5 | Orthogonal experimental effect curves for astaxanthin content of *C. zofingiensis*. All treatment groups were performed in Erlenmeyer flasks.

control ($p < 0.01$, Figure 4A). *C. zofingiensis* exhibited a short adaptation period in each treatment group (Figure 4A). The biomass concentration obtained under the conditions of C/N 220:1, 100 mg L⁻¹ GA3, and 100 mM NaCl was the highest, whereas that obtained under the conditions of the C/N 280:1, 100 mg L⁻¹ GA3, and 200 mM NaCl was the lowest. The consumption of glucose was similar among different treatments and was slower than that of the control (Figure 4B). Among the 16 treatment groups, the C/N 280:1, 50 mg L⁻¹ GA3, and 400 mM NaCl showed the fastest consumption of glucose during the induction period, whereas C/N 220:1, 100 mg L⁻¹ GA3, and 100 mM NaCl showed the slowest glucose assimilation.

According to Figure 5, the optimal conditions for astaxanthin accumulation were C/N 180:1, 10 mg L⁻¹ GA3, and 200 mM NaCl concentration. The orthogonal test ANOVA results are presented in Table 2. In addition, based on the orthogonal experiment results, it can be concluded that GA3 concentration exerts the most stimulatory effects on the accumulation of astaxanthin among the three factors.

Two-Stage Heterotrophic Cultivation of *C. zofingiensis* for Astaxanthin Production in 7.5L Fermenters

A two-stage process with the combination of the optimal induction conditions (i.e. C/N 180:1, 10 mg L⁻¹ GA3 and 200 mM NaCl) with the high cell-density cultivation conditions was employed for the heterotrophic cultivation of *C. zofingiensis* in the 7.5L fermentor. The changes in the appearance of *C. zofingiensis* cell culture and the cell morphology were shown in Figure 6. The color of the algal cell culture gradually turn to reddish from green over 16 days (Figure 6A). Once the algal cells were subjected to the induction conditions (stage II), the changes in the color are more obvious and rapid than that of the control. Significant decreases in the size

TABLE 2 | Orthogonal range analysis and variance analysis.

No	A: C/N ratio	B: GA3 (mg·L ⁻¹)	C: NaCl (mM)	Astaxanthin content (% of DW)
1	140:1	10	100	0.096
2	140:1	50	200	0.102
3	140:1	100	400	0.085
4	140:1	150	600	0.087
5	180:1	10	200	0.115
6	180:1	50	100	0.106
7	180:1	100	600	0.092
8	180:1	150	400	0.090
9	220:1	10	400	0.113
10	220:1	50	600	0.091
11	220:1	100	100	0.090
12	220:1	150	200	0.088
13	280:1	10	600	0.104
14	280:1	50	400	0.091
15	280:1	100	200	0.090
16	280:1	150	100	0.091
K1	0.370	0.428	0.383	Σ1.531
K2	0.403	0.390	0.395	—
K3	0.382	0.357	0.379	—
K4	0.376	0.356	0.374	—
k1	0.093	0.107	0.096	—
k2	0.100	0.098	0.099	—
k3	0.096	0.089	0.095	—
k4	0.094	0.089	0.094	—
R	0.007	0.018	0.003	—
F*	1.151	7.045	0.523	—
Significant	—	*	—	—
Optimal case	—	A ₂ B ₁ C ₂	—	—

K1, K2, and K3 are the sum of each level value of each factor.

k1, k2, and k3 are the average of each level value of each factor.

R is the range of each factor.

of *C. zofingiensis* cells were observed during the induction period, as compared with that of the control (**Figure 6B**).

In the first phase, the dry cell weight of *C. zofingiensis* increased dramatically and reached 160 g L⁻¹ after 10 days of cultivation. After Day 10, when the C/N ratio of the feeding medium changed to 180:1, and GA3 and NaCl were added at concentrations of 10 mg L⁻¹ and 200 mM, respectively, the microalgal cells exhibited a short adaption during the first 2 days of the induction stage, and then the dry cell weight of *C. zofingiensis* remained at a stable level. Afterwards, the dry cell weight of *C. zofingiensis* increased rapidly and reached the highest cell density at 235.4 g L⁻¹ on Day 16 (**Figure 7A**). **Figure 7B** demonstrated that *C. zofingiensis* could adapt to a wide range of glucose concentrations.

The changes in astaxanthin content and yield during the whole cultivation period of *C. zofingiensis* were shown in **Figure 7C,D**. In the first stage, astaxanthin content and yield increased with cultivation time. Notably, the astaxanthin content and yield reached 0.066% of DW and 0.107 g L⁻¹, respectively, after 10 days of cultivation. From the beginning of the second stage, the astaxanthin content and yield increased more dramatically as compared to that of the control ($p < 0.05$). The highest astaxanthin content and yield were achieved at 0.144% of DW and 0.318 g L⁻¹, respectively, after 5 days of induction.

C. zofingiensis cells not only possess the ability to produce astaxanthin but also accumulate lipids under induction conditions. Thus, the TFA contents were analyzed in this study as well. As shown in **Figure 7E**, the TFA content increased from 23 to 42% of DW during 5-day induction, and then slightly declined to 38.6% of DW on Day 16, which was still 56% higher than that of the control. Under the two-stage cultivation conditions, the maximum TFA yield of 92.7 g L⁻¹ was achieved on Day 15 (the fifth day after induction) and then leveled off, which was significantly higher than that of the control (66.5 g L⁻¹, **Figure 7F**). These results indicate the optimized induction conditions can simultaneously stimulate lipid and astaxanthin production.

DISCUSSION

In this study, a two-stage heterotrophic cultivation process was developed for *C. zofingiensis*, which enabled achieving the highest biomass yield and astaxanthin content to date. In the first stage when the *C. zofingiensis* cells were grown under the optimal conditions, the maximum biomass yield of 221.3 g L⁻¹ and 182.3 g L⁻¹ was attained in 7.5-L (on Day 12) and 500-L fed-batch fermenters (on Day 9), respectively. During the second stage, the astaxanthin was substantially accumulated through

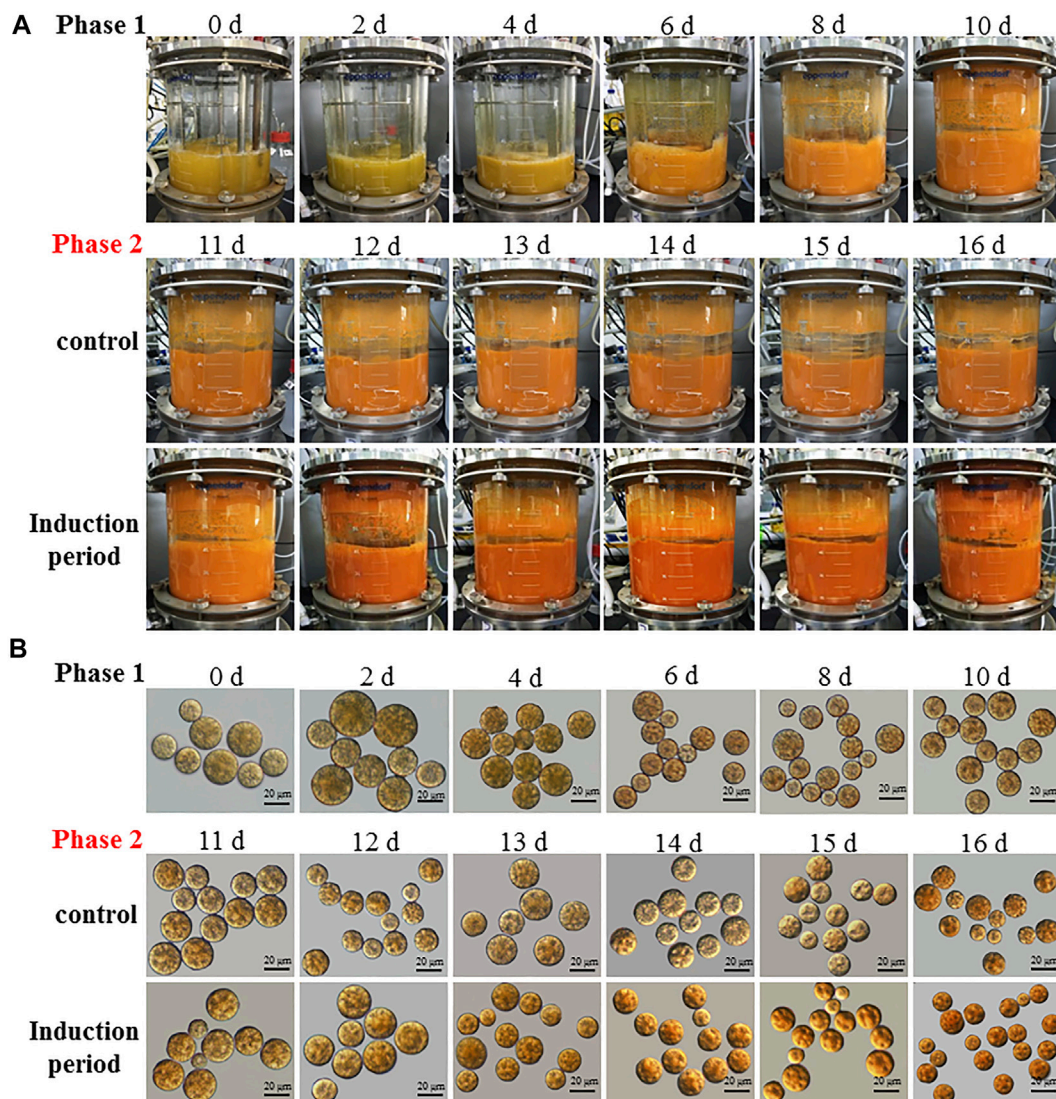


FIGURE 6 | The culture appearance **(A)** and morphological **(B)** changes of *C. zofingiensis* cells during the induction period in the 7.5 L fermentors. Induction conditions, the C/N ratio of the feeding medium change to 180:1 with the addition of 10 mg L^{-1} GA3 and 200 mM NaCl at the end of 10 days.

employing the inductive conditions that combined the phytochrome GA3, high C/N, and salinity. At the endpoint of fermentation (Day 16), the astaxanthin yield reached 0.318 g L^{-1} when biomass yield was 235.4 g L^{-1} and astaxanthin content was 0.144% of DW, which was 5.4-fold higher than the highest record that had been reported (Sun et al., 2008). Such high astaxanthin yield surpassed the level of *H. pluvialis*, of which the astaxanthin yield is about 0.077 g L^{-1} (López et al., 2006).

The optimal growth conditions attained in this study distinguished *C. zofingiensis* from *C. sorokiniana* and *S. acuminatus*, the two green algae that can be grown under heterotrophic conditions to ultrahigh cell densities as well. Firstly, *C. zofingiensis* favored relatively lower temperature (i.e. 26°C) as compared to *C. sorokiniana* and *S. acuminatus*, for which the optimal temperatures were both above 30°C .

Secondly, little difference in the cell growth was observed among the groups with different glucose concentrations, suggesting *C. zofingiensis* can adapt to a wide range of glucose concentrations (**Figure 2D**). In contrast, glucose concentration exerted significant impacts on the growth of *C. sorokiniana* and *S. acuminatus*. In addition, when *C. zofingiensis* was grown under neutral condition ($\text{pH} = 7$), it grew as fast as that under weak acidic conditions, though it is usually believed that heterotrophic microalgae prefer to the weak acidic conditions since microalgal cells transport one molecule of proton in stoichiometry for uptake of one molecule of sugar from the growth media (Perez-Garcia et al., 2011). It is noteworthy the conversion efficiency of the glucose to biomass is 50% for *C. zofingiensis* grown under favorable conditions, which is lower than that of *C. sorokiniana* and *S. acuminatus* (i.e. 60%). The relative low glucose conversion efficiency for *C. zofingiensis* is attributable

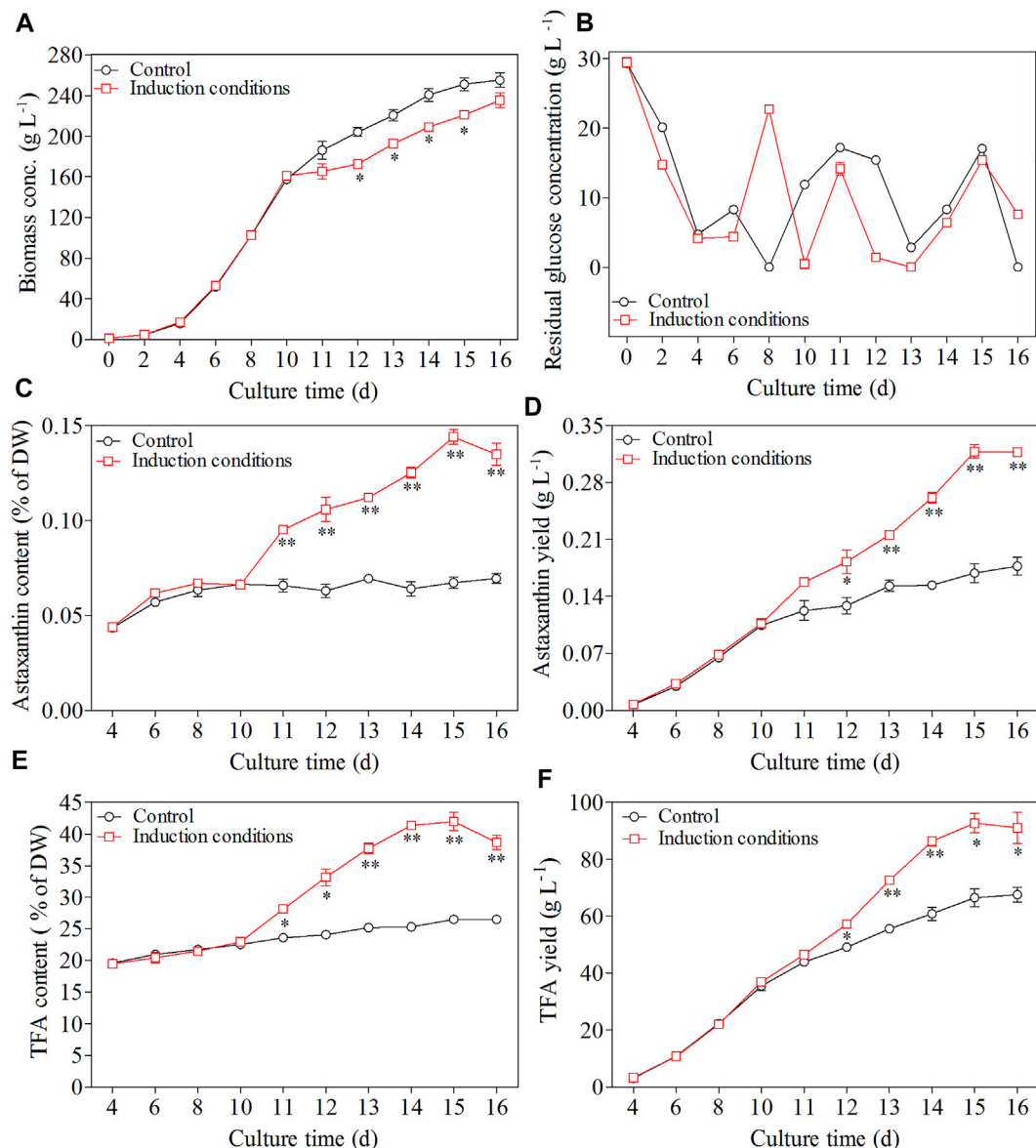


FIGURE 7 | Effect of induction conditions on the growth of *C. zofingiensis* and astaxanthin production during the heterotrophic cultivation in 7.5 L fermentors. **(A)** Time course of dry cell weight. **(B)** Residual glucose concentration. **(C)** Astaxanthin content. **(D)** Astaxanthin yield. **(E)** TFA content **(F)** TFA yield. Induction conditions, the C/N ratio of the feeding medium change to 180:1 with the addition of 10 mg L⁻¹ GA3 and 200 mM NaCl at the end of 10 days. Data are mean values \pm SD from triplicate measurements ($n = 3$). * and ** were statistically significant at $p < 0.05$ and $p < 0.01$, respectively.

to its higher lipid contents than that of *C. sorokiniana* and *S. acuminatus*.

Although heterotrophic cultivation of *C. zofingiensis* is regarded as a potential technical route for natural astaxanthin production, the content of astaxanthin obtained under such mode is generally lower than that obtained under photoautotrophic modes. In this study, GA3 is proved to be the most effective factor to promote astaxanthin biosynthesis in heterotrophically-grown *C. zofingiensis*. GA3 was found to induce astaxanthin biosynthesis in *H. pluvialis* through up-regulating the transcription of β -carotene ketolase genes, which is involved in converting β -

carotene to the canxathathin-the precursor of astaxanthin (Lu et al., 2010; Yu et al., 2015). GA is a diterpene phytochrome that control the growth and development of plants, including seed germination, hypocotyl elongation, flower initiation, stem elongation via enhanced cell division and elongation. Thus, GA3 may promote the cell deviation of *C. zofingiensis* under heterotrophic conditions. GA can cause rewiring of central carbon metabolism during fruit setting in tomatoes, including increasing the supply of hexoses, hexose phosphates, the intermediates and derivatives of glycolysis, and tricarboxylic acid, and these responses are suggested to be predominantly under

transcriptional control (Shinozaki et al., 2020). These findings can explain why GA3 can promote astaxanthin biosynthesis under both photoautotrophy and heterotrophy conditions in a photooxidative signals-independent manner. However, increasing C/N might not be specific enough, since large amounts of carbon were rechanneled into the fatty acid biosynthesis (Figure 7E). As a result, the glucose conversion efficiency during the second stage was 36%, much lower than that under favorable conditions. In future studies, it is necessary to design strategies that can specifically increase the supply of precursors for astaxanthin biosynthesis.

CONCLUSION

In this study, a two-stage heterotrophic cultivation process that enabled achievement of both high biomass and astaxanthin yield was developed for *C. zofingiensis*. The fed-batch heterotrophic cultivation was optimized in 7.5 L fermentor and scaled-up in 500 L fermentor. The phytochrome GA3 was selected as one of the most effective phytohormones to induce astaxanthin accumulation, and it was combined with high C/N ratio and NaCl concentration to enhance astaxanthin production in fed-batch fermentation. By employing the novel two-stage heterotrophic cultivation strategy, the astaxanthin yield from *C. zofingiensis* surpassed that of *H. pluvialis*, indicating it is a promising technical route to sustainably produce astaxanthin under the well-controlled conditions.

REFERENCES

- Ambati, R., Phang, S.-M., Ravi, S., and Aswathanarayana, R. (2014). Astaxanthin: Sources, Extraction, Stability, Biological Activities and its Commercial Applications-A Review. *Mar. Drugs* 12, 128–152. doi:10.3390/md12010128
- Bajguz, A., and Piotrowska-Niczyporuk, A. (2014). Interactive Effect of Brassinosteroids and Cytokinins on Growth, Chlorophyll, Monosaccharide and Protein Content in the green Alga *Chlorella Vulgaris* (Trebouxiphyceae). *Plant Physiol. Biochem.* 80, 176–183. doi:10.1016/j.plaphy.2014.04.009
- Gao, Z., Meng, C., Gao, H., Li, Y., Zhang, X., Xu, D., et al. (2013). Carotenoid Genes Transcriptional Regulation for Astaxanthin Accumulation in Fresh Water Unicellular Alga *Haematococcus pluvialis* by Gibberellin A3 (GA3). *Indian J. Biochem. Biophys.* 50, 548–553.
- Hu, J., Nagarajan, D., Zhang, Q., Chang, J.-S., and Lee, D.-J. (2018). Heterotrophic Cultivation of Microalgae for Pigment Production: A Review. *Biotechnol. Adv.* 36, 54–67. doi:10.1016/j.biotechadv.2017.09.009
- Hunt, R. W., Chinnasamy, S., Bhatnagar, A., and Das, K. C. (2010). Effect of Biochemical Stimulants on Biomass Productivity and Metabolite Content of the Microalga, *Chlorella Sorokiniana*. *Appl. Biochem. Biotechnol.* 162, 2400–2414. doi:10.1007/s12010-010-9012-2
- Ip, P.-F., and Chen, F. (2005). Production of Astaxanthin by the green Microalga *Chlorella Zofingiensis* in the Dark. *Process Biochem.* 40, 733–738. doi:10.1016/j.procbio.2004.01.039
- Jiang, L., Pei, H., Hu, W., Han, F., Zhang, L., and Hou, Q. (2015). Effect of Diethyl Aminoethyl Hexanoate on the Accumulation of High-Value Biocompounds Produced by Two Novel Isolated Microalgae. *Bioresour. Technology* 197, 178–184. doi:10.1016/j.biortech.2015.08.068
- Jin, H., Chuai, W., Li, K., Hou, G., Wu, M., Chen, J., et al. (2021). Ultrahigh-cell-density Heterotrophic Cultivation of the Unicellular green Alga *Chlorella Sorokiniana* for Biomass Production. *Biotechnol. Bioeng.* 118, 4138–4151. doi:10.1002/bit.27890
- Jin, H., Zhang, H., Zhou, Z., Li, K., Hou, G., Xu, Q., et al. (2020). Ultrahigh-cell-density Heterotrophic Cultivation of the Unicellular green Microalga *Scenedesmus Acuminatus* and Application of the Cells to Photoautotrophic Culture Enhance Biomass and Lipid Production. *Biotechnol. Bioeng.* 117, 96–108. doi:10.1002/bit.27190
- Katsumata, T., Ishibashi, T., and Kyle, D. (2014). A Sub-chronic Toxicity Evaluation of a Natural Astaxanthin-Rich Carotenoid Extract of *Paracoccus Carotinifaciens* in Rats. *Toxicol. Rep.* 1, 582–588. doi:10.1016/j.toxrep.2014.08.008
- Koller, M., Muhr, A., and Braunnegg, G. (2014). Microalgae as Versatile Cellular Factories for Valued Products. *Algal Res.* 6, 52–63. doi:10.1016/j.algal.2014.09.002
- Lee Chang, K. J., Rye, L., Dunstan, G. A., Grant, T., Koutoulis, A., Nichols, P. D., et al. (2015). Life Cycle Assessment: Heterotrophic Cultivation of *Thraustochytrids* for Biodiesel Production. *J. Appl. Phycol.* 27, 639–647. doi:10.1007/s10811-014-0364-9
- Li, X., Wang, X., Duan, C., Yi, S., Gao, Z., Xiao, C., et al. (2020). Biotechnological Production of Astaxanthin from the Microalga *Haematococcus pluvialis*. *Biotechnol. Adv.* 43, 107602. doi:10.1016/j.biotechadv.2020.107602
- Li, Y., Sommerfeld, M., Chen, F., and Hu, Q. (2008). Consumption of Oxygen by Astaxanthin Biosynthesis: A Protective Mechanism against Oxidative Stress in *Haematococcus pluvialis* (Chlorophyceae). *J. Plant Physiol.* 165, 1783–1797. doi:10.1016/j.jplph.2007.12.007
- Liu, J., Sun, Z., Gerken, H., Liu, Z., Jiang, Y., and Chen, F. (2014). *Chlorella Zofingiensis* as an Alternative Microalgal Producer of Astaxanthin: Biology and Industrial Potential. *Mar. Drugs* 12, 3487–3515. doi:10.3390/md12063487

DATA AVAILABILITY STATEMENT

The original contributions presented in the study are included in the article/Supplementary Material, further inquiries can be directed to the corresponding author.

AUTHOR CONTRIBUTIONS

QC, contributed to the conception and design of the study, the acquisition, analysis, and interpretation of data, drafting and revising the manuscript. YC contributed to the conception and design of the study, the acquisition, analysis, and interpretation of data. QX and HJ participated in heterotrophic cultivation. QH participated in design of experiment. Dan Xiang Han, contributed to the design of the study and revising the manuscript critically. All authors contributed to the final approval of the article.

FUNDING

This work was supported by The National Key R&D Program of China (2018YFA0902500).

SUPPLEMENTARY MATERIAL

The Supplementary Material for this article can be found online at: <https://www.frontiersin.org/articles/10.3389/fbioe.2022.834230/full#supplementary-material>

- Liu, J., Sun, Z., Zhong, Y., Gerken, H., Huang, J., and Chen, F. (2013). Utilization of Cane Molasses towards Cost-Saving Astaxanthin Production by a *Chlorella Zofingensis* Mutant. *J. Appl. Phycol.* 25, 1447–1456. doi:10.1007/s10811-013-9974-x
- López, M. C. G.-M., Sánchez, E. D. R., López, J. L. C., Fernández, F. G. A., Sevilla, J. M. F., Rivas, J., et al. (2006). Comparative Analysis of the Outdoor Culture of *Haematococcus pluvialis* in Tubular and Bubble Column Photobioreactors. *J. Biotechnol.* 123, 329–342. doi:10.1016/j.biotech.2005.11.010
- Lu, Y., Jiang, P., Liu, S., Gan, Q., Cui, H., and Qin, S. (2010). Methyl Jasmonate- or Gibberellins A3-Induced Astaxanthin Accumulation Is Associated with Up-Regulation of Transcription of β -carotene Ketolase Genes (Bkts) in Microalga *Haematococcus pluvialis*. *Bioresour. Technology* 101, 6468–6474. doi:10.1016/j.biortech.2010.03.072
- Lu, Y., and Xu, J. (2015). Phytohormones in Microalgae: A New Opportunity for Microalgal Biotechnology? *Trends Plant Sci.* 20, 273–282. doi:10.1016/j.tplants.2015.01.006
- Mao, X., Lao, Y., Sun, H., Li, X., Yu, J., and Chen, F. (2020). Time-resolved T-ranscriptome A-nalysis during T-ransitions of S-ulfur N-utritional S-tatus P-rovides I-n-sight into T-riacylglycerol (TAG) and A-staxanthin A-ccumulation in the green A-lga Chromochloris Z-ofingensis. *Biotechnol. Biofuels* 13, 1–18. doi:10.1186/s13068-020-01768-y
- Morales-Sánchez, D., Martínez-Rodríguez, O. A., Kyndt, J., and Martínez, A. (2015). Heterotrophic Growth of Microalgae: Metabolic Aspects. *World J. Microbiol. Biotechnol.* 31, 1–9. doi:10.1007/s11274-014-1773-2
- Perez-García, O., Escalante, F. M. E., de-Bashan, L. E., and Bashan, Y. (2011). Heterotrophic Cultures of Microalgae: Metabolism and Potential Products. *Water Res.* 45, 11–36. doi:10.1016/j.watres.2010.08.037
- Rodríguez-Sáiz, M., De La Fuente, J. L., and Barredo, J. L. (2010). *Xanthophyllomyces Dendrorhous* for the Industrial Production of Astaxanthin. *Appl. Microbiol. Biotechnol.* 88, 645–658. doi:10.1007/s00253-010-2814-x
- Shah, M. M. R., Liang, Y., Cheng, J. J., and Daroch, M. (2016). Astaxanthin-producing green Microalga *Haematococcus pluvialis*: From Single Cell to High Value Commercial Products. *Front. Plant Sci.* 7. doi:10.3389/fpls.2016.00531
- Shinozaki, Y., Beauvoit, B. P., Takahara, M., Hao, S., Ezura, K., Andrieu, M.-H., et al. (2020). Fruit Setting Rewires central Metabolism via Gibberellin Cascades. *Proc. Natl. Acad. Sci. USA* 117, 23970–23981. doi:10.1073/pnas.2011859117
- Sun, N., Wang, Y., Li, Y.-T., Huang, J.-C., and Chen, F. (2008). Sugar-based Growth, Astaxanthin Accumulation and Carotenogenic Transcription of Heterotrophic *Chlorella Zofingensis* (Chlorophyta). *Process Biochem.* 43, 1288–1292. doi:10.1016/j.procbio.2008.07.014
- Voß, U., Bishopp, A., Farcot, E., and Bennett, M. J. (2014). Modelling Hormonal Response and Development. *Trends Plant Sci.* 19, 311–319. doi:10.1016/j.tplants.2014.02.004
- Wu, M., Zhang, H., Sun, W., Li, Y., Hu, Q., Zhou, H., et al. (2019). Metabolic Plasticity of the Starchless Mutant of *Chlorella Sorokiniana* and Mechanisms Underlying its Enhanced Lipid Production Revealed by Comparative Metabolomics Analysis. *Algal Res.* 42, 101587. doi:10.1016/j.algal.2019.101587
- Xu, Q., Hou, G., Chen, J., Wang, H., Yuan, L., Han, D., et al. (2021). Heterotrophically Ultrahigh-Cell-Density Cultivation of a High Protein-Yielding Unicellular Alga *Chlorella* with a Novel Nitrogen-Supply Strategy. *Front. Bioeng. Biotechnol.* 9, 1–9. doi:10.3389/fbioe.2021.774854
- Yang, Z., Cheng, J., Li, K., Zhou, J., and Cen, K. (2016). Optimizing Gas Transfer to Improve Growth Rate of *Haematococcus pluvialis* in a Raceway Pond with Chute and Oscillating Baffles. *Bioresour. Technology* 214, 276–283. doi:10.1016/j.biortech.2016.04.107
- Yu, X., Niu, X., Zhang, X., Pei, G., Liu, J., Chen, L., et al. (2015). Identification and Mechanism Analysis of Chemical Modulators Enhancing Astaxanthin Accumulation in *Haematococcus pluvialis*. *Algal Res.* 11, 284–293. doi:10.1016/j.algal.2015.07.006
- Zhang, Z., Huang, J. J., Sun, D., Lee, Y., and Chen, F. (2017). Two-step Cultivation for Production of Astaxanthin in *Chlorella Zofingensis* Using a Patented Energy-free Rotating Floating Photobioreactor (RFP). *Bioresour. Technology* 224, 515–522. doi:10.1016/j.biortech.2016.10.081
- Zhang, Z., Sun, D., Mao, X., Liu, J., and Chen, F. (2016). The Crosstalk between Astaxanthin, Fatty Acids and Reactive Oxygen Species in Heterotrophic *Chlorella Zofingensis*. *Algal Res.* 19, 178–183. doi:10.1016/j.algal.2016.08.015
- Zhang, Z., Sun, D., Zhang, Y., and Chen, F. (2019). Glucose Triggers Cell Structure Changes and Regulates Astaxanthin Biosynthesis in *Chromochloris Zofingensis*. *Algal Res.* 39, 101455. doi:10.1016/j.algal.2019.101455

Conflict of Interest: The authors declare that the research was conducted in the absence of any commercial or financial relationships that could be construed as a potential conflict of interest.

Publisher's Note: All claims expressed in this article are solely those of the authors and do not necessarily represent those of their affiliated organizations, or those of the publisher, the editors and the reviewers. Any product that may be evaluated in this article, or claim that may be made by its manufacturer, is not guaranteed or endorsed by the publisher.

Copyright © 2022 Chen, Chen, Xu, Jin, Hu and Han. This is an open-access article distributed under the terms of the Creative Commons Attribution License (CC BY). The use, distribution or reproduction in other forums is permitted, provided the original author(s) and the copyright owner(s) are credited and that the original publication in this journal is cited, in accordance with accepted academic practice. No use, distribution or reproduction is permitted which does not comply with these terms.



Bioprospecting Indigenous Marine Microalgae for Polyunsaturated Fatty Acids Under Different Media Conditions

Priyanshu Jain^{1,2}, Amritpreet Kaur Minhas¹, Sadhana Shukla¹, Munish Puri³, Colin J. Barrow² and Shovon Mandal^{1*}

¹TERI Deakin Nanobiotechnology Centre, Sustainable Agriculture Division, The Energy and Resources Institute, New Delhi, India, ²School of Life and Environmental Sciences, Deakin University, Geelong, VIC, Australia, ³Medical Biotechnology, College of Medicine and Public Health, Flinders University, Adelaide, SA, Australia

OPEN ACCESS

Edited by:

Namita Khanna,
Birla Institute of Technology and
Science, India

Reviewed by:

Changhong Yao,
Sichuan University, China
Pau Loke Show,
University of Nottingham Malaysia
Campus, Malaysia

*Correspondence:

Shovon Mandal
shovon.mandal_c@teri.res.in

Specialty section:

This article was submitted to
Bioprocess Engineering,
a section of the journal
Frontiers in Bioengineering and
Biotechnology

Received: 24 December 2021

Accepted: 07 February 2022

Published: 17 March 2022

Citation:

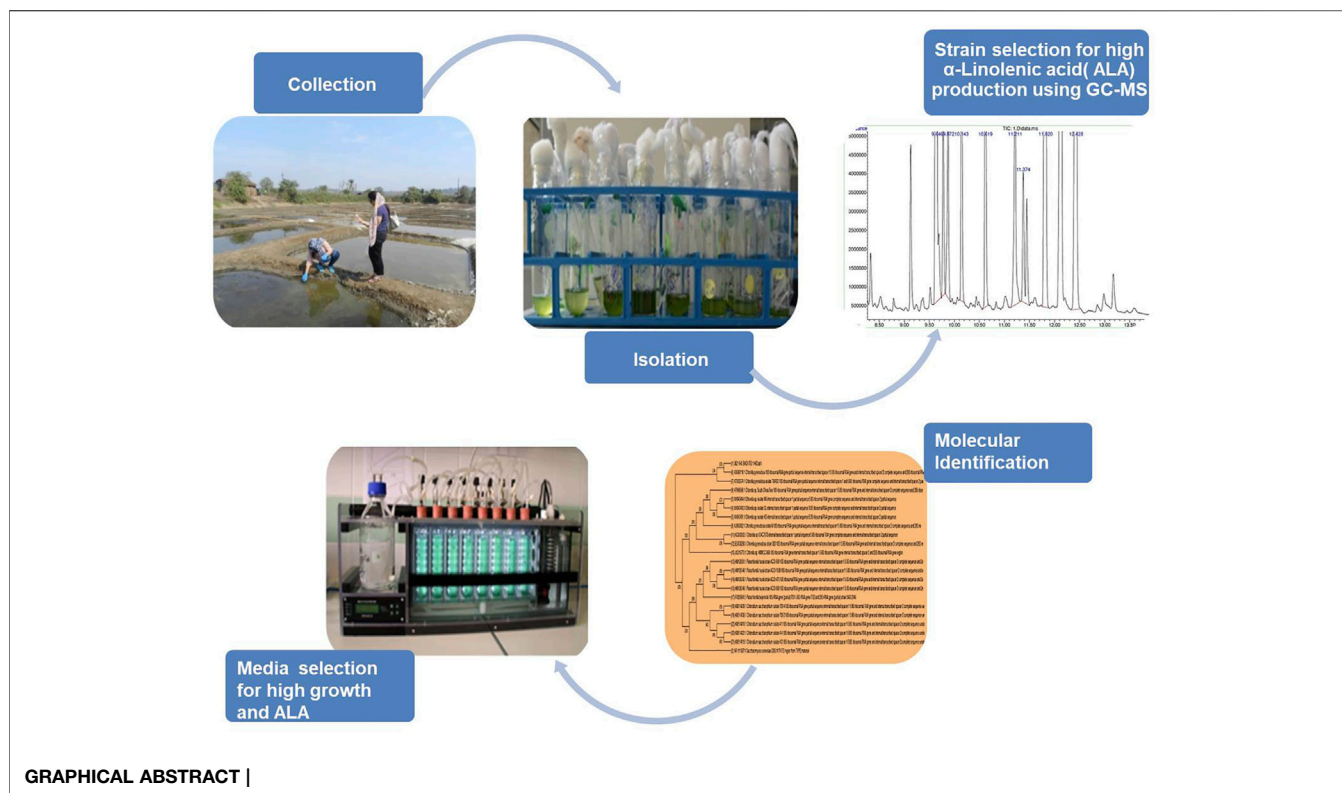
Jain P, Minhas AK, Shukla S, Puri M,
Barrow CJ and Mandal S (2022)
Bioprospecting Indigenous Marine
Microalgae for Polyunsaturated Fatty
Acids Under Different
Media Conditions.
Front. Bioeng. Biotechnol. 10:842797.
doi: 10.3389/fbioe.2022.842797

Marine microalgae produce a number of valuable compounds that have significant roles in the pharmaceutical, biomedical, nutraceutical, and food industries. Although there are numerous microalgal germplasms available in the marine ecosystem, only a small number of strains have been recognized for their commercial potential. In this study, several indigenous microalgal strains were isolated from the coast of the Arabian Sea for exploring the presence and production of high-value compounds such as polyunsaturated fatty acids (PUFAs). PUFAs are essential fatty acids with multiple health benefits. Based on their high PUFA content, two isolated strains were identified by ITS sequencing and selected for further studies to enhance PUFAs. From molecular analysis, it was found both the strains were green microalgae: one of them was a *Chlorella* sp., while the other was a *Planophila* sp. The two isolated strains, together with a control strain known for yielding high levels of PUFAs, *Nannochloropsis oculata*, were grown in three different nutrient media for PUFA augmentation. The relative content of α -linolenic acid (ALA) as a percentage of total fatty acids reached a maximum of 50, 36, and 50%, respectively, in *Chlorella* sp., *Planophila* sp., and *N. oculata*. To the best of our knowledge, this is the first study in exploring fatty acids in *Planophila* sp. The obtained results showed a higher PUFA content, particularly α -linolenic acid at low nutrients in media.

Keywords: α -linolenic acid, indigenous microalgae, media stress, polyunsaturated fatty acids, growth kinetic

HIGHLIGHTS

- Microalgae feedstock is the key to eco-friendly and sustainable PUFA production.
- Indigenous microalgal strains rich in ALA were isolated and identified from the Arabian Sea coast.
- Media with a low level of nutrients and salinity favors ALA enrichment.



INTRODUCTION

Poly unsaturated fatty acids (PUFAs) and monounsaturated fatty acids (MUFAs) are essential bioactive compounds with multiple health benefits (Rincón-Cervera et al., 2022). PUFAs, particularly eicosapentaenoic acid (EPA) and docosahexaenoic acid (DHA), have tremendous applications in a variety of inflammatory conditions, such as arthritis, Alzheimer's disease, and lupus (Yates et al., 2014). The common sources of these FAs are nuts, fishes, seeds (Ferreira-Dias et al., 2022), and organisms from the deep-sea ecosystem (Svetashev, 2021). Traditionally, marine fish are the most conventional source of PUFAs (Bagul and Annapure, 2021). However, due to declining fish stocks and the presence of contamination such as methyl mercury, dioxins, and polychlorinated biphenols (PCBs), alternative sources are required (Ruiz-Rodriguez et al., 2010). In addition, vegetarian consumers prefer algal oil to fish oil. Microalgal oils often exhibit simpler fatty acid profiles and possess a varying ratio of PUFAs with inherent antioxidant properties to protect the oils against oxidation. Marine organisms such as *Schizochytrium*, *Ulkenia*, and *Cryptocodinium* are grown heterotrophically for commercial production of DHA, particularly for uses such as infant formula where low levels of EPA are desired (Barclay et al., 1994; Ren et al., 2010; Klok et al., 2014). On the other hand, common EPA-producing algae are *Nannochloropsis*, *Nitzschia*, and *Phaeodactylum tricornutum* (Spolaore et al., 2006).

Algae are of vital importance in the primary establishment and maintenance of aquatic and marine ecosystems (Beetul et al., 2016; Barkia et al., 2019). The marine environment comprises

diversity of organisms which are potential sources of bioactive, secondary metabolites, with application in pharmaceuticals, nutraceuticals, and functional foods (Barkia et al., 2019). Indigenous microalgal isolates collected from water bodies at diverse geographical locations are potential contenders for high-value compounds, such as PUFAs, and as biofuel feedstock (Maneechote et al., 2021). Moreover, accumulation of high-value compounds can be enhanced using different growth conditions, such as under stress, providing efficient cost-effective production of some metabolites (Chua et al., 2020). Enhancement of lipid and pigment productivity from the same biomass under numerous rate limiting conditions is commonly practiced (Minhas et al., 2016a). For instance, factors such as light intensity, altered photoperiod, and concentration of nutrients highly affect the microalgal growth (Parmar et al., 2011; Minhas et al., 2020). Significant diversity of microalgal isolates occurs at different geographical locations because of different nutrient variability and diverse climatic conditions (Bernal et al., 2008). Depending on the habitat and climatic conditions, microalgal isolates are known to be rich in different types of lipids, hydrocarbons, proteins, and other components (Chisti, 2007).

Microalgae are rich reservoirs of PUFAs, proteins, lipids, polyphenols, minerals, vitamins, etc. (Brown et al., 2014). Fatty acids, protein, and pigments are the most commonly available products from microalgae in market (Nagi et al., 2021). Fatty acids obtained from microalgae are applied as sustainable synthetic dietary alternatives to fish oil and possess potential in the treatment, prevention, and management of some physiological anomalies (Beetul et al., 2016). Advantages of fatty

acids from microalgae over those from fish oil are primarily related to renewable and economical production (Ray et al., 2022), but they can also have tailored levels of different PUFAs that show benefit against inflammation and cardiac-related diseases such as hypertension and thrombosis (Nauroth et al., 2010; Adarme-Vega et al., 2014).

In this study, a bioprospecting pipeline, targeting microalgae along the west coast of India, was developed, and their potential for the production of PUFAs was investigated. The coast was targeted due to suitable climatic and environmental conditions, ideal for spawning and nurturing the marine life (Kamat et al., 2020). The coast has, thus, been explored extensively by numerous researchers for studying microorganisms, especially microalgae, for a wide range of potential uses (Damare et al., 2021). The objective of this work was to isolate and identify indigenous microalgal strains with high PUFA contents and to characterize the isolates by ITS sequencing. The primary selection criterion was an ability to produce high amounts of ALA. Based on high ALA levels, isolates of interest were cultivated in three different media for the assessment of PUFA productivity and fatty acid profiles. ALA productivity was optimized for the media that produced the highest ALA levels, and so this study provides useful strain, media, and growth condition information useful for enhancing PUFA levels in these microalgae.

MATERIAL AND METHODS

Collection and Isolation of Microalgae

Water samples were collected from diverse habitats ranging from the marine, backwater, and salt pans of western India, Goa (15° 32' 0.2904" N 73° 45' 53.8344" E) which possesses a coastline of 101 km (**Supplementary Figure S1**). The samples were collected in April 2018 from various sites during the daytime, when the Sun was overhead; the samples were put in a plastic container marked with their collection site names. Next day, samples were brought to the laboratory, centrifuged, and immediately transferred to artificial seawater media (ASW) (Andersen, 2005) at 25°C with 150 rpm orbital shaking with a photoperiod of 16 h of light (100 $\mu\text{mol}/\text{m}^2/\text{s}$) alternating with 8 h of darkness, up to the late exponential phase (Minhas et al., 2016b).

To segregate large population and to obtain maximum isolates from the collected water samples, the standard dilution plating method was followed. After 2 weeks, serial dilution up to 10^5 and 10^6 was performed on sterile ASW agar plates (1.6% w/v), and samples were incubated until colonies appeared. Individual colonies were transferred axenically in liquid ASW medium and were observed under the microscope (Carl Zeiss, Germany). Morphologically non-identical strains were selected for further study.

Microalgal Strains

Isolated strains were grown in a media broth in 100-ml Erlenmeyer flask containing 50 ml of ASW medium (Lee et al., 2014) at pH 8. The experiments were conducted in a temperature-controlled growth chamber at 25°C under a photoperiod of 16:8 (light:dark) at a light intensity of

120 $\mu\text{mol}/\text{m}^2/\text{sec}$. In order to attain high PUFA-containing isolates, the freeze dried biomass from the stationary phase cultures was processed through lipid extraction and fatty acid analysis, as described in the following analytical methods. All the salts and chemicals used in this study were of analytical grade and procured from Sigma-Aldrich and Merck Chemicals.

Identification of Microalgal Strains

The potential candidate displaying maximum levels of PUFAs was selected further for yield enhancement studies and was subjected to ITS sequencing by implying ITS1 and ITS4 primer sets. ITS sequencing was performed at Eurofins, Bangalore, India, for species identification.

DNA Extraction

The total genomic DNA of the algal isolate was isolated and purified using the DNA extraction kit (NucleoSpin®). About 1.5 ml of the exponentially grown algal culture was centrifuged at 7,500 g for 8 min at 4°C. The resulting cell pellet was lysed using liquid nitrogen and was further dissolved and mixed in 140 μL buffer T1 and 8 μL proteinase K solution. The mixture was left at 56°C for 1 h incubation in a thermomixer (Thermomixer comfort, Eppendorf, New Delhi, India) for complete cell lysis. Thereafter, B3 buffer amounting to 140 μL was added to the same vial and left at 70°C for 5 min incubation in a thermomixer. Samples after attaining room temperature were centrifuged for 5 min at 9,000 \times g, and the obtained supernatant was transferred to a new microcentrifuge tube. Absolute ethanol of 140 μL was added to the samples; immediately after the addition of ethanol, a thread-like precipitate appeared. The vials were then left at -20°C for 15 min for complete precipitation. The obtained precipitate was transferred to a NucleoSpin® tissue column, and a collection tube was placed below it. Centrifugation was performed for all samples for 2 min at 10,000 \times g; all algal samples were eluted separately. The column was placed again in the same collection tube, and 100 μL of washing buffer W1 was added to the same vial; samples were centrifuged for 1 min at 10,000 \times g, and the process was repeated again for proper washing. Finally, a NucleoSpin® tissue column was placed in a new 1.5 ml microcentrifuge vial, and 30 μL elution buffer (BE) was added directly onto the center of the column for eluting DNA, which was centrifuged for 2 min. Extracted DNA was kept at -20°C for further analysis.

PCR Amplification

DNA fragments of selected strains were observed on the gel *via* gel electrophoresis with respect to the 1 kb DNA ladder (GeneDireX, Taiwan, China). The DNA concentration obtained from microalgae was between 70 and 92 ng/ μL . The obtained DNA was subjected to PCR amplification; PCR was carried out using 0.1 mM dNTPs, 10 pmol of each primer, 1 U of Taq DNA polymerase, and the supplied reaction buffer (Biotools, Madrid, Spain) in the total volume of 25 μL . Each reaction was performed in duplicates in a T-100 thermal cycler (Bio Rad Laboratories Inc., California, United States) under the following conditions: initial denaturation at 95°C for 5 min, followed by 35 cycles at 94°C for 35 s, 60°C for 1 min, 72°C for

TABLE 1 | The relative percentage of different fatty acid chains present in the isolated microalgal isolates.

S. No	Collection site and their habitat type	Strain code	Palmitoleic acid (C16:1)	Oleic acid (C18:1)	Transvaccenic acid (C18:1)n-7	Linoleic acid (C18:2)	α -Linolenic acid (C18:3)	Eicosatetraenoic acid (C20:4)	cis-11,14-Eicosadienoic acid (C20:6)	Eicosatrienoic acid (C20:3)	Tetracosanoic acid (C24:0)
1	Bagha (Marine)	BAG1	12.48	3.73	1.40	13.025	69.12	—	—	—	0.22
2	Bagha (Marine)	BAG2	—	12.13	—	40.21	45.14	—	—	—	2.48
3	Sirdao (Backwater)	SIR	—	12.20	10.27	26.95	50.52	—	—	—	0
4	Salim Ali (Backwater)	SA	5.16	13.06	6.25	34.41	36.76	5.65	—	4.28	1.51
5	Dona Paula (Marine)	NIO	3.35	14.50	—	36.33	45.62	—	0.49	—	0

1 min, followed by a final extension period at 72°C for 10 min, and rest at 4°C. Agarose gel electrophoresis was performed which depicted sharp bands of algal PCR products at 600 bp. Sanger sequencing was performed for both the samples at the commercial facility service of Eurofins Private Limited (Bangalore, India). The sequences were subjected to BLAST (BLASTN, NCBI) analysis, and their homology was established.

Study on the Effect of Different Media on Growth and Fatty Acid Profiling

Isolates from different sites were selected (one isolate per site) based on the highest PUFA content. The selected isolates were then grown in three different media (Andersen, 2005), viz., modified F/2 (Guillard et al., 1975), MASM (https://www.ccap.ac.uk/wp-content/uploads/MR_MASM.pdf), and MKM Watanabe, A. (1960) in a multicultivator (MC 1000-OD, Photon Instrument Systems, Drasov, Czech Republic). The isolates with an initial cell count of 3×10^6 cells/mL calculated using a Neubauer hemocytometer (Rohem Instruments, Nashik, Maharashtra, India) were inoculated in the 70 ml of media in multicultivator tubes having a volume of 120 ml under photoautotrophic conditions with a light intensity of 120 $\mu\text{mol}/\text{m}^2/\text{sec}$ and a temperature of $25 \pm 1^\circ\text{C}$, with a 16:8 h (L:D) photoperiod (Minhas et al., 2020). The aeration rate was maintained at 0.12 ml/min. Growth of microalgae was examined by measuring the daily changes in the optical density (OD) at 680 nm by OD viewer software attached to the cultivator. The microalgal growth rate of isolates was determined by fitting the OD at the exponential phase of each isolates to the late stage exponential growth phase (Wang et al., 2010). Once the isolates achieved their optimum growth, at the late stationary phase on an average, they were harvested by centrifuging them at 7,000 rpm for 10 min at 4°C followed by lyophilization. The samples were further subjected to GC-MS for fatty acid profiling. Studies were performed in sets of triplicates.

Analytical Methods

Lipid Extraction and Fatty Acid Analysis

Total lipids were extracted from the freeze dried biomass by adopting the method developed by Lewis et al. (2000) with some modifications. In brief, 3 ml solution of chloroform:methanol (2:1, v/v) was added to 10 mg of the dried algal biomass and was homogenized by using a vortex shaker (Spinix, Maharashtra, India) for 2 min followed by centrifuging for 15 min at $10,000 \times g$. The process is repeated three times for complete extraction until a colorless biomass is achieved. The obtained fractions were pooled, and water was added; the upper layer containing methanol and water was discarded. The chloroform fraction was passed through syringe filters and was transferred in a pre-weighed glass vial. The vials containing lipids were incubated in a hot air oven for 6–7 h at 50°C. Finally, the total lipids were measured gravimetrically.

Preparation of Fatty Acid Methyl Esters

FAME profiles were determined using the method described by Christie (1987) (Christie, 1982). For preparation of FAMES, dried lipid samples were obtained after incubation and oven drying; 500 μL of toluene was added to the sample, followed by the

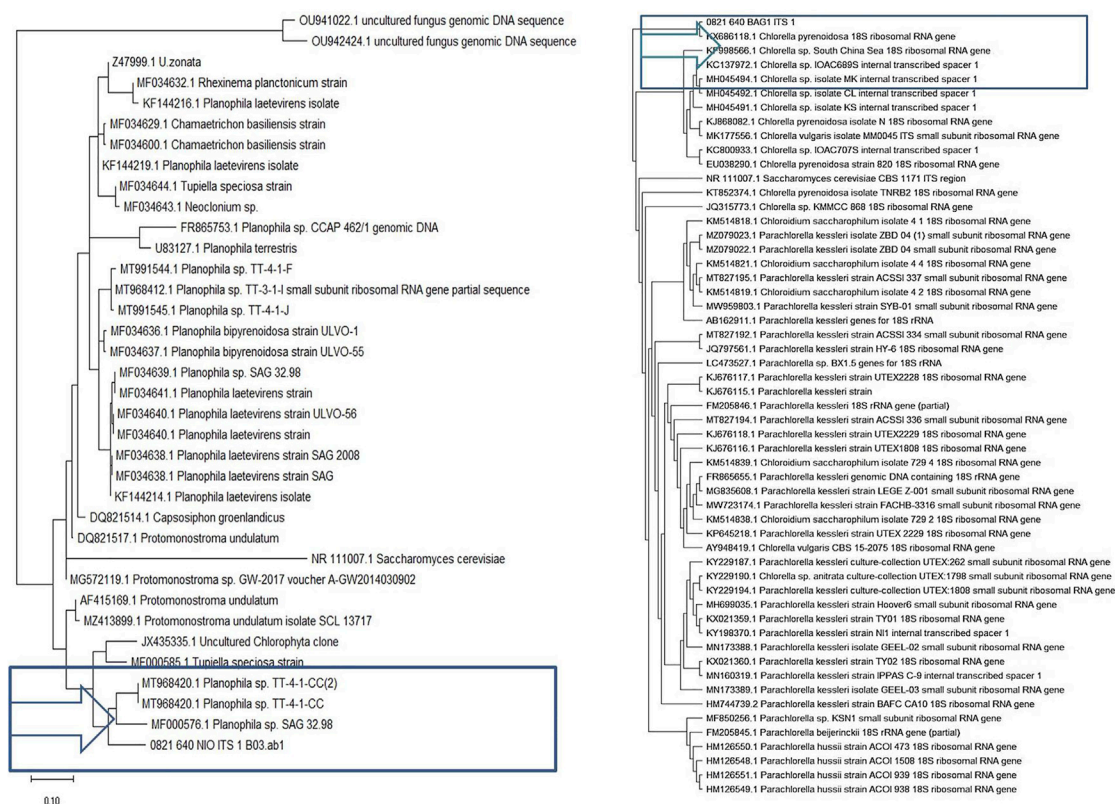


FIGURE 1 | Phylogenetic tree of microalgal isolates revealing cluster grouping of (A) NIO ITS sequences are closely related to *Planophila*. (B) BAG1 ITS sequences are related to *Chlorella*; *Saccharomyces cerevisiae* was used as out-group.

addition of 10 μ L of the internal standard (50 mg of C19:0-methyl non-adeanoate), acetyl chloride 400 μ L (prepared by adding 1 ml acetyl chloride dropwise to 10 ml of methanol on ice), and butylated hydroxytoluene 200 μ L, and the samples were incubated at 50°C overnight. The following day, 1 ml of 5% NaCl and 1 ml of hexane were added to the dried samples. Finally, the solvent layer containing hexane was analyzed by GC (Agilent 122–2,332 column, Santa Clara, California, United States) equipped with mass spectrometry (MS) with capillary columns (DB-23; 30 \times 0.25 mm; film thickness, 0.25 μ m). Retention time of the known fatty acid standard mix (37 FAME mix, Supelco, Sigma-Aldrich) was identified, and the peaks of fatty acid chains were analyzed and quantified. ChemStation chromatography software (Agilent Technologies, Santa Clara, California, United States) was utilized further for integrating the peaks of targeted fatty acids. 1 μ L volume of the sample was injected in the instrument maintained at 250°C with helium as a carrier gas. The chemicals and standard for FAMES (C19:0) used in this study were of analytical grade and were procured from Sigma-Aldrich (St. Louis, United States).

Statistical Analysis

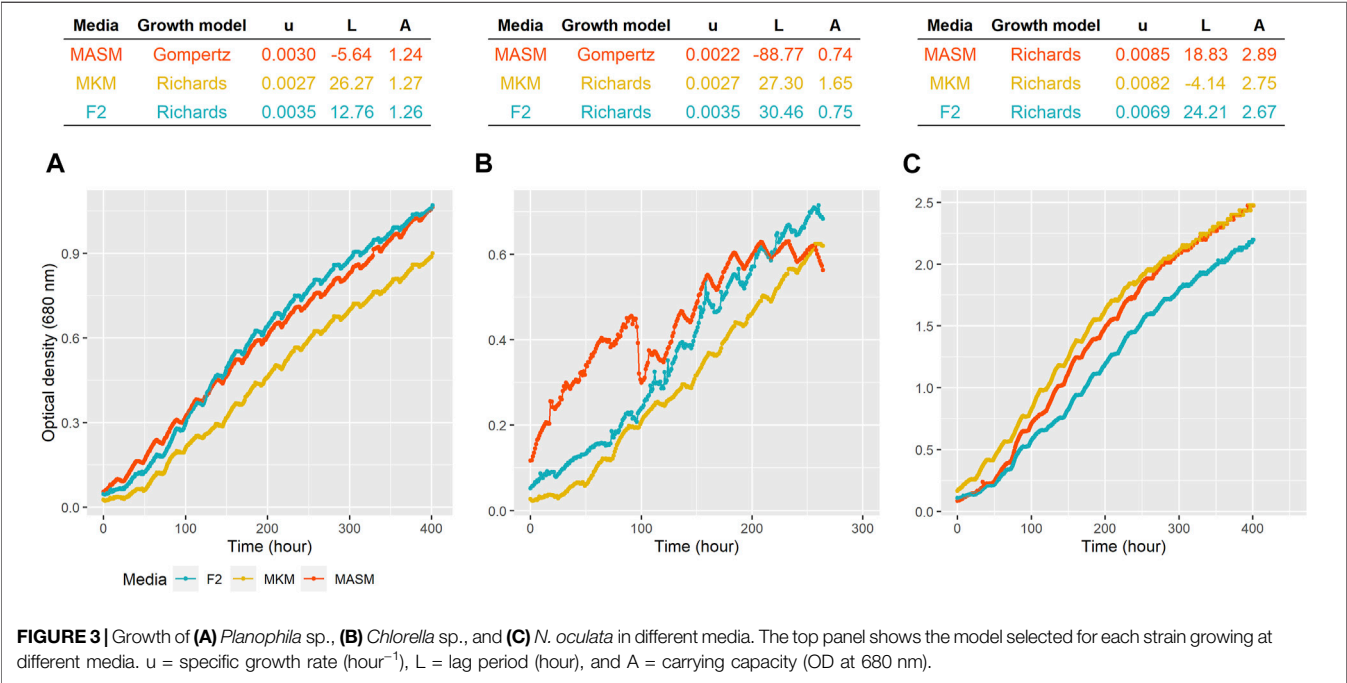
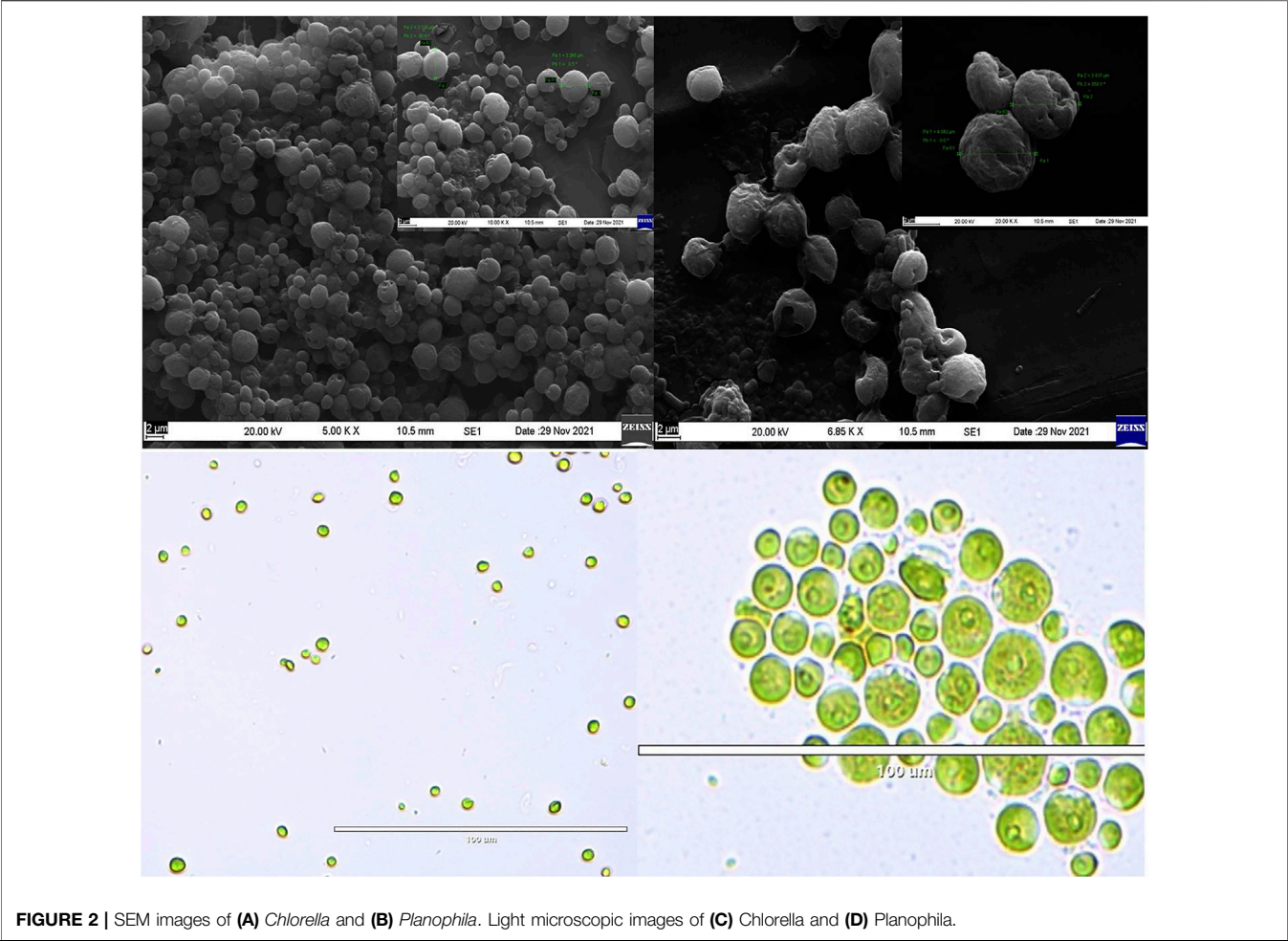
All statistical analyses and graphics were performed using R (version 4.1.2). To measure the growth rate, optical density was fitted against four different growth models (Richard,

logistic, Gompertz, and modified Gompertz) using the gcFitModel function of the “grofit” package. The best fit model was selected based on Akaike information criterion (AIC) values. Instead of using the popularly used logistic growth curve, different growth models were applied because of the variation of growth curves. For principal component analysis (PCA), the “factextra” package was applied. The function “glht” in the package “multcomp” was used for Tukey’s *post hoc* test.

RESULTS AND DISCUSSIONS

GC-MS Analysis of Isolated Microalgae for the Presence of Omega-3 Fatty Acid

The unialgal cultures established from the samples collected from diverse water bodies of Goa were subjected for GC-MS profiling and are tabularized in **Table 1**. Goa is identified as a suitable area for microalgae cultivation, as per reports of the National Renewable Energy Laboratory, United States (Milbrandt and Jarvis, 2010). Several species of zooplanktons (Sai Elangovan and Gauns, 2021) and phytoplanktons (Untawale et al., 1980; Raghukumar et al., 1991; Bhandari et al., 2012) are identified from their water bodies on a regular basis (Damare et al., 2021). Therefore, different water bodies, namely, Bagha (marine), Salim Ali (mangrove), NIO (marine), and Sirdao (brackish)



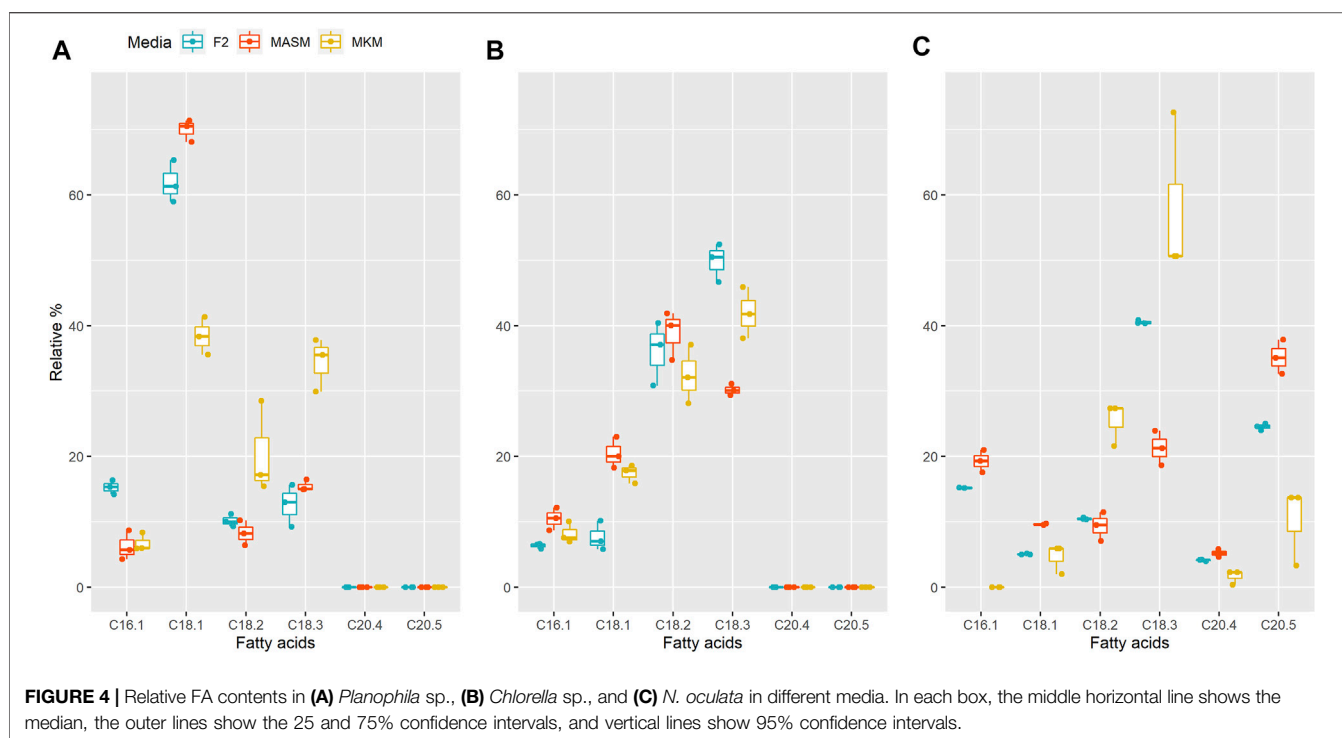


TABLE 2 | ALA content (%Total fatty acids) present in different microalgal species.

S. No	Microalgal species	ALA (% total fatty acids)	References
1	<i>Dunaliella primolecta</i>	41.1	Viso and Marty, (1993)
2	<i>Nannochloris</i> sp	28.2	Lang et al. (2011)
3	<i>Parietochloris incisa</i>	14.3	Lang et al. (2011)
4	<i>Nostoc commune</i>	38.1	Lang et al. (2011)
5	<i>Skeletonema costatum</i>	25.31	Widianingsih et al. (2013)
6	<i>Thalassiosira</i> sp.	7.93	Widianingsih et al. (2013)
7	<i>Isochrysis</i> sp.	11.57	Widianingsih et al. (2013)
8	<i>Acutodesmus obliquus</i> CN01	38	Othman et al. (2019)
9	<i>Chlorella vulgaris</i> NIES-1269	35	Othman et al. (2019)
10	<i>Chlorella</i> sp. Carolina-15-2069	17.9	Othman et al. (2019)
13	<i>Planophila</i> sp	35.5	This study
14	<i>Nannochloropsis oculata</i>	50	This study
15	<i>Chlorella</i> sp.	50	This study

were targeted for sample collection. The unialgal established cultures were screened for their FA profiling for estimating the contents of PUFAs present in the established strains. GC-MS profiling established the major fatty acids in all the strains including oleic acid (C18:1), linoleic acid (C18:2), and ALA (18:3). ALA (18:3) accumulated in the highest amounts in all the strains compared with the other two fatty acids, followed by linoleic acid (C18:2) and oleic acid (C18:1). Similar to this study, researchers isolated the four algal strains belonging to the family Chlorophyceae from the coastal zone of Goa. FA profiling revealed the presence of both saturated FAs and unsaturated FAs, including oleic, linoleic, and linolenic acids (Bhandari et al., 2012).

The highest amount of ALA was accumulated in one of the species (BAG1) collected from the site Bagha at 69%, followed by

51% for SIR and ~46% for NIO (Table 1). The second most abundant fatty acid for all three strains was linoleic acid (C18:2) with ~40.2% for the isolate BAG2, followed by NIO, SA, and SIR (Table 1). The relative FA percentage of palmitoleic acid (C16:1) was the highest in BAG1 at ~12%, followed by 5% in SA and 3% in NIO. In a study conducted by Nagappan et al., they identified a *Desmodesmus* sp. strain with the potential for production of biodiesel and omega-3 FAs (Nagappan and Kumar Verma, 2018). BAG1, having the highest amount of C18:3 and C16:1, may also find application in both biodiesel and nutraceutical production.

NIO depicted traces of eicosadienoic acid ~0.49%, whereas eicosatrienoic acid and eicosatetraenoic acid were accumulated by SA at 6% and 4%, respectively. Isolates BAG1 and NIO were selected

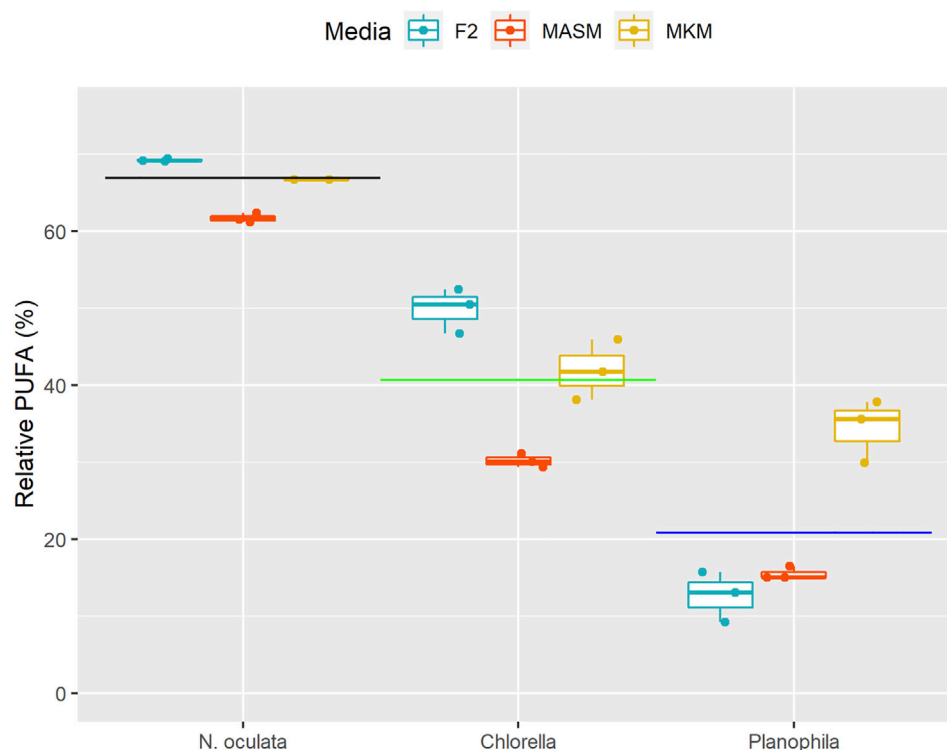


FIGURE 5 | PUFA percentages of three different algal isolates grown in three diverse media. In each box, the middle horizontal line shows the median, the outer lines show the 25 and 75% confidence intervals, and vertical lines show 95% confidence intervals. The black line indicates the mean PUFA content of *N. oculata*, green for *Chlorella* sp., and blue for *Planophila* sp.

TABLE 3 | ANOVA table showing the effect of strain and media on the PUFA content.

	Degree of freedom	Sum square	Mean sum square	F Value	Probability (>F)
Strain	2	9,621	4,810	515	01 < 2e-16 ***
Media	2	771	386	41.29	1.88e-07 ***
Strain: Media	4	781	195	20.91	1.44e-06 ***
Residuals	18	168	9	—	—

for further study due to their highest percentage of C18:3, at 70% and 45%, respectively. SIR was not selected, partly because of its slower growth rate (data not shown). The two selected isolates, namely, NIO and BAG1 were further evaluated for their efficiency in producing biomass and lipid yields. At the stationary phase, after 15 days of cultivation in ASW media, biomass of NIO and BAG1 reached up to 620.6 and 498.8 mg/L, respectively, whereas the lipid content of the NIO and BAG1 reached 14.5 and 14.9% of the dry weight of biomass, respectively. The two selected strains were subjected to molecular identification followed by media studies.

Molecular Identification and Phylogenetic Analyses

The high molecular weight DNA of BAG1 and NIO strains was extracted by the NucleoSpin kit. ITS1 (TCCGTAGGTGAACCT

GCGC) and ITS4 (TCCTCCGCTTATTGATATGC) were employed as the universal primers for the amplification of aforementioned strains. ITS sequencing was conducted for the molecular identification of two algal isolates (Eurofins, Bangalore, India). The obtained sequences of both the strains were subjected to BLAST (BLASTN, NCBI) analysis, and their homology was established. Results revealed NIO was identical to *Planophila* (MT991544.1), with 91.53% similarity, and the other strain BAG1 showed 98.81% similarity with *Chlorella* (MH045494.1) in the homology analysis.

Phylogenetic analysis was conducted on the BLASTN results of both samples using maximum likelihood algorithms. Sequences were aligned with the MUSCLE (MEGAX), and a phylogenetic tree was constructed for NIO and BAG1 strains with other 50 different species of algae and with one out-group species *Saccharomyces cerevisiae*, respectively. Phylogenetic analysis

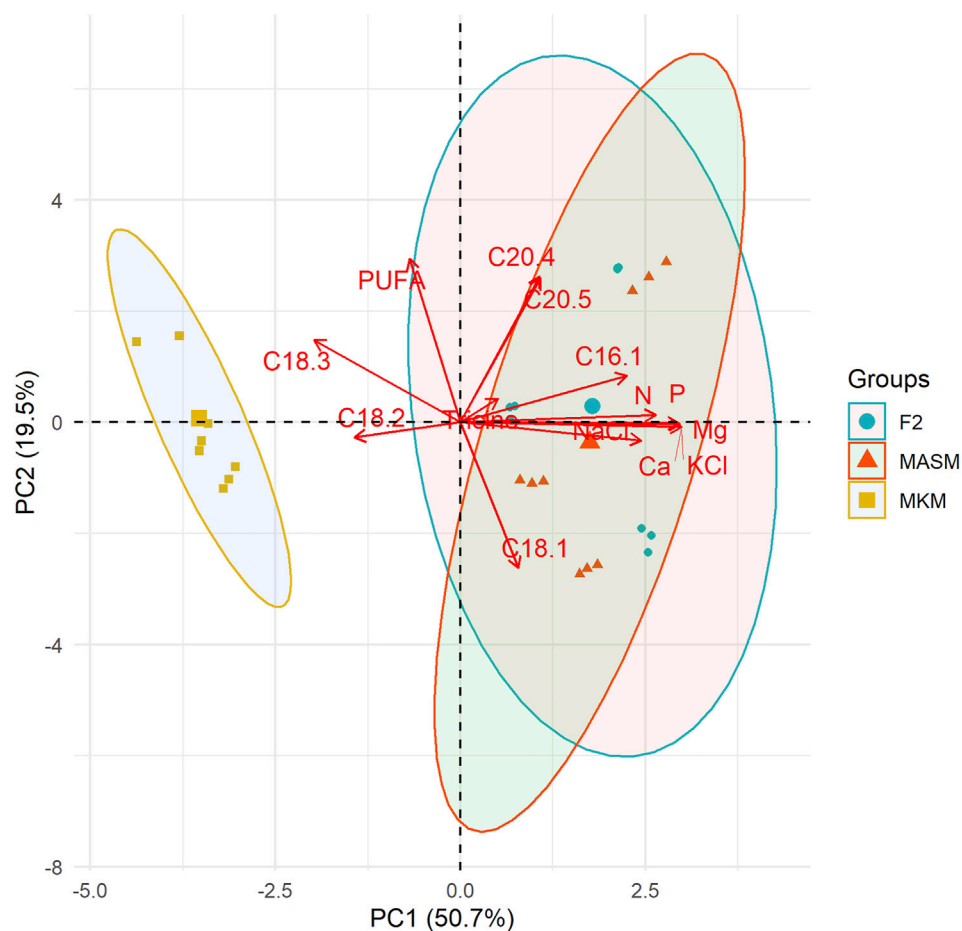


FIGURE 6 | Principal component analysis (PCA) shows the correlation among nutrients contents and fatty acids of the three different strains. Each point indicates the position of the strain along PC1 and the color for media.

showed that NIO clustered together with *Planophila* sp. (MT991544.1) **Figure 1A** and BAG1 with *Chlorella* (MH045494.1) **Figure 1B**. Thus, the results confirmed that NIO is highly identical with *Planophila* and BAG1 with *Chlorella*, respectively.

To the best of our knowledge, this is the first time the strain *Planophila* sp. was isolated from the region of Goa and is studied for fatty acid profiling in different media. However, *Planophila* sp. was previously reported to be isolated from Asian regions (Watanabe, 1983). The species were reported to be found in fresh water and soil (Szymańska and Werblan-Jakubiec, 1999; Friedl et al., 2012). The morphology of these strains is presented in **Figure 2**.

Effect of Different Media on Growth and Fatty Acid Profiling

Nutrients are the key driver for microalgal growth and metabolite synthesis (Mandal and Mallick, 2009). A trade-off between growth and lipid levels has been reported in some microalgal studies (Shurin et al., 2014; Pandey et al., 2020). In this study, instead of applying the direct stress-based approach by

eliminating or reducing nutrients from a particular medium, isolated *Planophila* sp. and *Chlorella* sp. were subjected to three different nutrient media, a method to elevate PUFAs. The commercial strain *N. oculata*, known for a higher PUFA content (Zanella and Vianello, 2020), was selected as a control for comparison.

Four different growth kinetic models logistic, Gompertz, Richards, and modified Gompertz were applied to understand the growth dynamics attained under the different media conditions (**Supplementary Figure S2**). As shown in **Figure 3**, kinetic model Richards and Gompertz were selected as the best model based on the lowest Akaike information criterion (AIC) values. For *Planophila* sp., the highest growth is observed for F/2 and MASM media in which salinity was 30 practical salinity units (PSU), as opposed to 15 PSU in MKM. The highest growth of *Planophila* sp. in the media with higher salinity conditions indicated their selective preference towards a marine-like environment, mimicking their natural marine habitat (Pandit et al., 2017). The salinity stress affects the microalgal cells and their physiological mechanism. Parameters such as precursors, influx, and uptake of ions in and outside the cell membrane (Srivastava et al., 2014) and sodium ions and their role in

photosynthesis (Salama et al., 2013) are the key factors for the changes and enhanced specific fatty acid composition (Srivastava et al., 2014). The presence of excess sodium chloride causes reactive oxygen species (ROS) formation, leading to oxidative stress and breakdown of cellular macromolecules (Chokshi et al., 2015). Another possible explanation of the lower growth rate in the MKM medium is the lower nutrient concentration which is limited in the media (Pandit et al., 2017). *Chlorella* sp. depicted highest growth in F2 media followed by MKM media. The lower growth rate in MASM in *Chlorella* sp. is due to the sudden growth depression between 80 and 90 h (Figure 4B). The control strain *N. oculata* exhibited a maximum growth in MASM media, followed by MKM and F/2. The growth of *N. oculata* is much higher and reached the carrying capacity at 2.89 (OD) which is 3–4 times than the isolated strain. These results suggest further optimization in growth parameters such as light intensity (Metsoviti et al., 2020) and temperature (Chokshi et al., 2020) may be required.

In order to combat diverse environments, specifically higher salinity conditions and low nitrogen availability, microalgae alters or enhances the PUFA production (Dhanya et al., 2020). Enhancement in the TAG content (Kan et al., 2012) and intracellular lipids in microalgae (Zhila et al., 2011) are also reported for salinity stress. For instance, Annamalai et al., reported the enhanced lipid production in one of his selected strain under lower salinity conditions (Annamalai et al., 2016). Interestingly, the results revealed that the percentage of ALA (C18:3) was the highest in media with the lowest salinity (9 g/L), amounting to 35.5% in *Planophila* sp. and 41% in *Chlorella* sp. in MKM media. A similar finding was obtained for the control strain *N. oculata* with 50% of the ALA content in the same media. Differences in the fatty acid composition among different media for a particular strain indicated that the salt type and concentrations in media impacts the fatty acid content, consistent with optimizing media, for salt can be useful for targeting levels of specific fatty acids (Minhas et al., 2016a; Haris et al., 2022).

In *Planophila* sp., the highest percentage of oleic acid at 71% occurred in MASM media, with lower levels in F/2 and MKM media, whereas linoleic (17%) and linolenic acid (35%) were maximal in MKM media (Figure 4A). Similar to *Planophila* sp., *N. oculata* showed highest linoleic acid and linolenic acid contents in MKM media (Figure 4C). However, in *Chlorella* sp. maximum accumulation of linolenic acid (50%) and linoleic acid (37%) was observed in F/2 media, followed by MKM and MASM media. The differences in types of fatty acid accumulation in different media support earlier findings in which nutrients were found to regulate FA biosynthesis (Ren et al., 2010; Dhanya et al., 2020). Thus, selection of optimum media should be carried out before attenuation of specific stress factors for enhancing targeted fatty acids. The findings of the present study in terms of highest ALA content of the two well characterized isolates are tabulated together with the other microalgae in Table 2. The ALA content found in two different strains of *Chlorella*, i.e., *Chlorella vulgaris* NIES-1269 and *Chlorella* sp. Carolina-15–2069 was 35 and 17.9%, respectively (Othman et al., 2019), whereas the same isolate in the present study was producing an ALA content about

50% in F/2 media. Therefore, explaining the variations in the ALA/PUFA productivity in similar microalgal species collected from different habitats is possibly due to their growth, media, and nutrient conditions.

Fatty acid data was further analyzed by considering only PUFAs (Figure 5) in which only FA molecules (unsaturation >2) with a chain length of 18 or more carbon atoms were counted (Park et al., 2002). The PUFA content was significantly different in three different strains ($F_{2,18} = 515.01$, $p < 0.0001$, Table 3). The high PUFA content was found in *N. oculata* followed by *Chlorella* sp. and *Planophila* sp. (Tukey's *post hoc* test, $p < 0.05$, Supplementary Table S1). Although the media have a significant effect on the PUFA content ($F_{2,18} = 41.29$, $p < 0.0001$, Table 3), PUFA contents were not different between MKM and F2 media (Tukey's *post hoc* test, $p = 0.282$, Supplementary Table S2).

The principal component analysis (PCA) in Figure 6 summarizes the correlations among media components and fatty acids of the three strains. Principal component 1 (PC1) and principal component 2 (PC2) axes explained 47.4% and 24.4% of variation among strains. The overlapping between F2 and MASM indicates their similarities in media composition and FA profiling as compared to the MKM medium. The accumulation of linoleic (C18:2) and linolenic acids (C18:3) was closely associated and negatively related to the nutrient content of the media. Linolenic acid (C18:3) accumulated more in MKM media in which the nutrient concentration is comparatively low. Similar to our observation, Trommer et al. (2019) reported a decline in ALA in phytoplanktons under higher nutrient concentrations in the natural lake community. Our results agree with others that salinity had a negative correlation with ALA (Trommer et al., 2019). Overall PUFA accumulation in this study is independent of the nutrient concentration. In contrast to our study, several studies reported higher nutrient level results in increasing galactolipids which are rich in PUFAs (Guschina and Harwood, 2006; Guo et al., 2016). The close association among the nutrient components in the PCA plot is the major limitation in our study to describe the variation FA unsaturation based on each component of the media. Thus, further experiment with larger variation in nutrients of the media is recommended to establish the relation between the media component and FA unsaturation. Although, this study showed that MKM with comparatively lower nutrients could be a suitable growth media for improved FAs without compromising growth.

CONCLUSION

In the present study, authors reported the isolation and identification of two microalgal isolates, *Planophila* sp. and *Chlorella* sp. collected from the west coast of India, Goa. The work demonstrated the initial screening and selection of these microalgae based on their PUFA contents, followed by their molecular characterization. Additionally, media studies employing three different media were performed to compare

and analyze variations in the FA content, including levels of ALA, within the same isolates in diverse media. Furthermore, growth kinetics studies of the isolates were performed to compare the growth patterns in three different media. The results showed that media with lower nutrient levels increased the ALA content, as found in MKM media, amounting to 35.5% in *Planophila* sp. and 41% in *Chlorella* sp., respectively. The study shows that media optimization is important before attenuation of stress factors for optimizing targeted FA levels. The media studies are simple, economical, and act as a preliminary selection tool for defining the optimum physiological conditions for each indigenous algal strain. Each indigenous strain from a particular environment requires experimentation to determine optimum growth conditions since growth does not correlate directly with that of standard algal strains. Thus, targeted growth studies of indigenous strains are required to determine the potential of local organisms for the optimization of bioresource production from algae.

DATA AVAILABILITY STATEMENT

The original contributions presented in the study are publicly available. This data can be found here: NCBI gen bank, accession numbers SUB10895695, SUB10888826.

REFERENCES

- Adarme-Vega, T., Thomas-Hall, S., Lim, D., and Schenk, P. (2014). Effects of Long Chain Fatty Acid Synthesis and Associated Gene Expression in Microalga *Tetraselmis* Sp. *Mar. Drugs* 12 (6), 3381–3398. doi:10.3390/md12063381
- Andersen, R. A. (2005). "Recipes for Freshwater and Seawater media," in *Algal Culturing Techniques* (London: Elsevier Academic Press), 429–538.
- Annamalai, J., Shanmugam, J., and Nallamuthu, T. (2016). Salt Stress Enhancing the Production of Phytochemicals in *Chlorella Vulgaris* and *Chlamydomonas Reinhardtii*. *J. Algal Biomass Utilization* 7 (1), 37–44.
- Bagul, V. P., and Annapure, U. S. (2021). Isolation and Characterization of Docosahexaenoic Acid-Producing Novel Strain *Aurantiochytrium* Sp. ICTFD5: A Sterol with Vitamin D-Cholecalciferol, and Cellulase and Lipase Producing *Thraustochytrid*. *Bioresour. Techn. Rep.* 14, 100688. doi:10.1016/j.biteb.2021.100688
- Barclay, W. R., Meager, K. M., and Abril, J. R. (1994). Heterotrophic Production of Long Chain omega-3 Fatty Acids Utilizing Algae and Algae-like Microorganisms. *J. Appl. Phycol* 6 (2), 123–129. doi:10.1007/bf02186066
- Barkia, I., Saari, N., and Manning, S. R. (2019). Microalgae for High-Value Products towards Human Health and Nutrition. *Mar. Drugs* 17 (5), 304. doi:10.3390/md17050304
- Beetel, K., Gopechund, A., Kaulysing, D., Mattan-Moorgawa, S., Puchooa, D., and Bhagooli, R. (2016). *Challenges and Opportunities in the Present Era of marine Algal Applications*, 237–276. London: IntechOpen. doi:10.5772/63272
- Bernal, C. B., Vázquez, G., Quintal, I. B., and Bussy, A. L. (2008). Microalgal Dynamics in Batch Reactors for Municipal Wastewater Treatment Containing Dairy Sewage Water. *Water Air Soil Pollut.* 190 (1–4), 259–270. doi:10.1007/s11270-007-9598-3
- Bhandari, R., Talwar, S., Sandya, S., and Sharma, P. K. (2012). Photosynthetic Pigments and Fatty Acid Composition of Four marine green Algae from the Coastal Zone of Goa. *Indian Hydrobiology* 14 (2), 181–191.
- Brown, E. M., Allsopp, P. J., Magee, P. J., Gill, C. I., Nitecki, S., Strain, C. R., et al. (2014). Seaweed and Human Health. *Nutr. Rev.* 72 (3), 205–216. doi:10.1111/nure.12091

AUTHOR CONTRIBUTIONS

PJ: conducted the experiments, analyzed the results, and wrote the original draft. AM: conceptualization and editing the draft. SS: assisted in the molecular identification experiments. MP and CB: conceptualization and editing the draft. SM: data analysis, visualization, editing the draft, and supervision.

ACKNOWLEDGMENTS

The authors acknowledge Alok Adholeya for his suggestions and support. PJ duly acknowledges the financial support provided through the TERI- Deakin collaborative project in the form of a doctoral fellowship. SM is thankful to the Department of Biotechnology, India for the Ramaligaswami Fellowship.

SUPPLEMENTARY MATERIAL

The Supplementary Material for this article can be found online at: <https://www.frontiersin.org/articles/10.3389/fbioe.2022.842797/full#supplementary-material>

- Chisti, Y. (2007). Biodiesel from Microalgae. *Biotechnol. Adv.* 25 (3), 294–306. doi:10.1016/j.biotechadv.2007.02.001
- Chokshi, K., Pancha, I., Trivedi, K., George, B., Maurya, R., Ghosh, A., et al. (2015). Biofuel Potential of the Newly Isolated Microalgae *Acutodesmus Dimorphus* under Temperature Induced Oxidative Stress Conditions. *Bioresour. Techn.* 180, 162–171. doi:10.1016/j.biortech.2014.12.102
- Chokshi, K., Pancha, I., Trivedi, K., Maurya, R., Ghosh, A., and Mishra, S. (2020). Physiological Responses of the green Microalga *Acutodesmus Dimorphus* to Temperature Induced Oxidative Stress Conditions. *Physiol. Plantarum* 170 (4), 462–473. doi:10.1111/ppl.13193
- Christie, W. W. (1982). *Lipid Analysis*, 207. Lincoln, United Kingdom: Pergamon press Oxford.
- Chua, E. T., Dal'Molin, C., Thomas-Hall, S., Netzel, M. E., Netzel, G., and Schenk, P. M. (2020). Cold and Dark Treatments Induce omega-3 Fatty Acid and Carotenoid Production in *Nannochloropsis Oceanica*. *Algal Res.* 51, 102059. doi:10.1016/j.algal.2020.102059
- Damare, V. S., Fernandes, E. T., Naik, A. A., Cardozo, S., Borges, V., and Phuge, P. (2021). Occurrence of *Thraustochytrids*: the Fungoid Protists Vis-A-Vis marine Macroalgae (Seaweeds) along the Coast of Goa, India. *Botanica Marina* 64 (6), 461–475. doi:10.1515/bot-2021-0052
- Dhanya, B. S., Sowmiya, G., Jeslin, J., Chamundeswari, M., and Verma, M. L. (2020). "Algal Biotechnology: A Sustainable Route for Omega-3 Fatty Acid Production," in *Microalgae Biotechnology for Food, Health and High Value Products*. Editors M. A. Alam, J.-L. Xu, and Z. Wang (Singapore: Springer), 125–145. doi:10.1007/978-981-15-0169-2_4
- Ferreira-Dias, S., Osório, N., and Tecelão, C. (2022). "Bioprocess Technologies for Production of Structured Lipids as Nutraceuticals," in *Current Developments in Biotechnology and Bioengineering*. Editors A. K. Rai, S. P. Singh, A. Pandey, C. Larroche, and C. R. Soccol (Amsterdam, Netherlands: Elsevier), 209–237. doi:10.1016/b978-0-12-823506-5.00007-2
- Friedl, T., and Rybalka, N. (2012). "Systematics of the Green Algae: A Brief Introduction to the Current Status," in *Progress in Botany*. U. Lüttge, W. Beyschlag, B. Büdel, et al. Editors (Berlin, Heidelberg: Springer), 73, 259–280. doi:10.1007/978-3-642-22746-2_10
- Guillard, R. R. L. (1975). "Culture of Phytoplankton for Feeding Marine Invertebrates," in *Culture of Marine Invertebrate Animals: Proceedings — 1st*

- Conference on Culture of Marine Invertebrate Animals Greenport. Editors W. L. Smith and M. H. Chanley (Boston, MA: Springer US), 29–60. doi:10.1007/978-1-4615-8714-9_3
- Guo, F., Kainz, M. J., Sheldon, F., and Bunn, S. E. (2016). The Importance of High-Quality Algal Food Sources in Stream Food Webs - Current Status and Future Perspectives. *Freshw. Biol.* 61 (6), 815–831. doi:10.1111/fwb.12755
- Guschina, I. A., and Harwood, J. L. (2006). Lipids and Lipid Metabolism in Eukaryotic Algae. *Prog. Lipid Res.* 45 (2), 160–186. doi:10.1016/j.plipres.2006.01.001
- Haris, N., Manan, H., Jusoh, M., Khatoon, H., Katayama, T., and Kasan, N. A. (2022). Effect of Different Salinity on the Growth Performance and Proximate Composition of Isolated Indigenous Microalgae Species. *Aquacult. Rep.* 22, 100925. doi:10.1016/j.aqrep.2021.100925
- Kamat, S., Kumari, M., Taritla, S., and Jayabaskaran, C. (2020). Endophytic Fungi of Marine Alga from Konkan Coast, India—A Rich Source of Bioactive Material [Original Research]. *Front. Mar. Sci.* 7 (31). doi:10.3389/fmars.2020.00031
- Kan, G., Shi, C., Wang, X., Xie, Q., Wang, M., Wang, X., et al. (2012). Acclimatory Responses to High-Salt Stress in *Chlamydomonas* (Chlorophyta, Chlorophyceae) from Antarctica. *Acta Oceanol. Sin.* 31 (1), 116–124. doi:10.1007/s13131-012-0183-2
- Klok, A. J., Lamers, P. P., Martens, D. E., Draaisma, R. B., and Wijffels, R. H. (2014). Edible Oils from Microalgae: Insights in TAG Accumulation. *Trends Biotechnology* 32 (10), 521–528. doi:10.1016/j.tibtech.2014.07.004
- Lang, I., Hodac, L., Friedl, T., and Feussner, I. (2011). Fatty Acid Profiles and Their Distribution Patterns in Microalgae: a Comprehensive Analysis of More Than 2000 Strains from the SAG Culture Collection. *BMC Plant Biol.* 11 (1), 124. doi:10.1186/1471-2229-11-124
- Lee, K., Eisterhold, M., Rindi, F., Palanisami, S., and Nam, P. (2014). Isolation and Screening of Microalgae from Natural Habitats in the Midwestern United States of America for Biomass and Biodiesel Sources. *J. Nat. Sc Biol. Med.* 5 (2), 333. doi:10.4103/0976-9668.136178
- Lewis, T., Nichols, P. D., and McMeekin, T. A. (2000). Evaluation of Extraction Methods for Recovery of Fatty Acids from Lipid-Producing Microheterotrophs. *J. Microbiol. Methods* 43 (2), 107–116. doi:10.1016/s0167-7012(00)00217-7
- Mandal, S., and Mallick, N. (2009). Microalga *Scenedesmus Obliquus* as a Potential Source for Biodiesel Production. *Appl. Microbiol. Biotechnol.* 84 (2), 281–291. doi:10.1007/s00253-009-1935-6
- Maneechote, W., Cheirsilp, B., Srinuanpan, S., and Pathom-aree, W. (2021). Optimizing Physicochemical Factors for Two-Stage Cultivation of Newly Isolated Oleaginous Microalgae from Local lake as Promising Sources of Pigments, PUFAs and Biodiesel Feedstocks. *Bioresour. Technol. Rep.* 15, 100738. doi:10.1016/j.biteb.2021.100738
- Metsoviti, M. N., Papapolymerou, G., Karapanagiotidis, I. T., and Katsoulas, N. (2020). Effect of Light Intensity and Quality on Growth Rate and Composition of *Chlorella Vulgaris*. *Plants (Basel)* 9 (1), 31. doi:10.3390/plants9010031
- Milbrandt, A., and Jarvis, E. (2010). *Resource Evaluation and Site Selection for Microalgae Production in India*. Golden, Colorado, United States: National Renewable Energy Lab. NREL.
- Minhas, A. K., Hodgson, P., Barrow, C. J., and Adholeya, A. (2016a). A Review on the Assessment of Stress Conditions for Simultaneous Production of Microalgal Lipids and Carotenoids. *Front. Microbiol.* 7, 546. doi:10.3389/fmicb.2016.00546
- Minhas, A. K., Hodgson, P., Barrow, C. J., and Adholeya, A. (2020). Two-phase Method of Cultivating *Coelastrella* Species for Increased Production of Lipids and Carotenoids. *Bioresour. Technol. Rep.* 9, 100366. doi:10.1016/j.biteb.2019.100366
- Minhas, A. K., Hodgson, P., Barrow, C. J., Sashidhar, B., and Adholeya, A. (2016b). The Isolation and Identification of New Microalgal Strains Producing Oil and Carotenoid Simultaneously with Biofuel Potential. *Bioresour. Technol.* 211, 556–565. doi:10.1016/j.biortech.2016.03.121
- Nagappan, S., and Kumar Verma, S. (2018). Co-production of Biodiesel and Alpha-Linolenic Acid (omega-3 Fatty Acid) from Microalgae, *Desmodesmus* Sp. MCC34. *Energy Sourc. A: Recovery, Utilization, Environ. Effects and Environ. Effects* 40 (24), 2933–2940. doi:10.1080/15567036.2018.1514434
- Nagi, G. K., Minhas, A. K., Gaur, S., Jain, P., and Mandal, S. (2021). Integration of Algal Biofuels with Bioremediation Coupled Industrial Commodities towards Cost-Effectiveness [Review]. *Front. Energy Res.* 9 (489). doi:10.3389/fenrg.2021.735141
- Nauroth, J. M., Liu, Y. C., Van Elswyk, M., Bell, R., Hall, E. B., Chung, G., et al. (2010). Docosahexaenoic Acid (DHA) and Docosapentaenoic Acid (DPAn-6) Algal Oils Reduce Inflammatory Mediators in Human Peripheral Mononuclear Cells *In Vitro* and Paw Edema *In Vivo*. *Lipids* 45 (5), 375–384. doi:10.1007/s11745-010-3406-3
- Othman, F. S., Jamaluddin, H., Ibrahim, Z., Hara, H., Yahya, N. A., Iwamoto, K., et al. (2019). Production of α -linolenic Acid by an Oleaginous Green Algae *Acutodesmus Obliquus* Isolated from Malaysia. *J. Pure Appl. Microbiol.* 13 (3), 1297–1306. doi:10.22207/jpam.13.3.01
- Pandey, A., Gupta, A., Sunny, A., Kumar, S., and Srivastava, S. (2020). Multi-objective Optimization of media Components for Improved Algae Biomass, Fatty Acid and Starch Biosynthesis from *Scenedesmus* Sp. ASK22 Using Desirability Function Approach. *Renew. Energ.* 150, 476–486. doi:10.1016/j.renene.2019.12.095
- Pandit, P. R., Fulekar, M. H., and Karuna, M. S. L. (2017). Effect of Salinity Stress on Growth, Lipid Productivity, Fatty Acid Composition, and Biodiesel Properties in *Acutodesmus Obliquus* and *Chlorella Vulgaris*. *Environ. Sci. Pollut. Res.* 24 (15), 13437–13451. doi:10.1007/s11356-017-8875-y
- Park, S., Brett, M. T., Müller-navarra, D. C., and Goldman, C. R. (2002). Essential Fatty Acid Content and the Phosphorus to Carbon Ratio in Cultured Algae as Indicators of Food Quality for *Daphnia*. *Freshwat. Biol.* 47 (8), 1377–1390. doi:10.1046/j.1365-2427.2002.00870.x
- Parmar, A., Singh, N. K., Pandey, A., Gnansounou, E., and Madamwar, D. (2011). Cyanobacteria and Microalgae: a Positive prospect for Biofuels. *Bioresour. Technol.* 102 (22), 10163–10172. doi:10.1016/j.biortech.2011.08.030
- Raghukumar, C., Sharma, S., and Lande, V. (1991). Distribution and Biomass Estimation of Shell-boring Algae in the Intertidal at Goa, India. *Phycologia* 30 (3), 303–309. doi:10.2216/i0031-8884-30-3-303.1
- Ray, A., Nayak, M., and Ghosh, A. (2022). A Review on Co-culturing of Microalgae: A Greener Strategy towards Sustainable Biofuels Production. *Sci. Total Environ.* 802, 149765. doi:10.1016/j.scitotenv.2021.149765
- Ren, L.-J., Ji, X.-J., Huang, H., Qu, L., Feng, Y., Tong, Q.-Q., et al. (2010). Development of a Stepwise Aeration Control Strategy for Efficient Docosahexaenoic Acid Production by *Schizochytrium* Sp. *Appl. Microbiol. Biotechnol.* 87 (5), 1649–1656. doi:10.1007/s00253-010-2639-7
- Rincón-Cervera, M. Á., Bravo-Sagua, R., Manólio Soares Freitas, R. A., López-Arana, S., and de Camargo, A. C. (2022). “Chapter 8 - Monounsaturated and Polyunsaturated Fatty Acids: Structure, Food Sources, Biological Functions, and Their Preventive Role against Noncommunicable Diseases,” in *Bioactive Food Components Activity in Mechanistic Approach*. Editors C. B. B. Cazarin, J. L. Bicas, G. M. Pastore, and M. R. Maróstica Júnior (London: Academic Press), 185–210.
- Ruiz-Rodriguez, A., Reglero, G., and Ibañez, E. (2010). Recent Trends in the Advanced Analysis of Bioactive Fatty Acids. *J. Pharm. Biomed. Anal.* 51 (2), 305–326. doi:10.1016/j.jpba.2009.05.012
- Sai Elangovan, S., and Gauns, M. U. (2021). A Comparative Study on Microzooplankton Communities in Two Tropical Monsoonal Estuaries. *J. Sea Res.* 171, 102034. doi:10.1016/j.seares.2021.102034
- Salama, E.-S., Kim, H.-C., Abou-Shanab, R. A. I., Ji, M.-K., Oh, Y.-K., Kim, S.-H., et al. (2013). Biomass, Lipid Content, and Fatty Acid Composition of Freshwater *Chlamydomonas Mexicana* and *Scenedesmus Obliquus* Grown under Salt Stress. *Bioproc. Biosyst. Eng.* 36 (6), 827–833. doi:10.1007/s00449-013-0919-1
- Shurin, J. B., Mandal, S., and Abbott, R. L. (2014). Trait Diversity Enhances Yield in Algal Biofuel Assemblages. *J. Appl. Ecol.* 51 (3), 603–611. doi:10.1111/1365-2664.12242
- Spolaore, P., Joannis-Cassan, C., Duran, E., and Isambert, A. (2006). Commercial Applications of Microalgae. *J. Biosci. Bioeng.* 101 (2), 87–96. doi:10.1263/jbb.101.87
- Srivastava, A., Singh, S. S., and Mishra, A. K. (2014). Modulation in Fatty Acid Composition Influences Salinity Stress Tolerance in *Frankia* Strains. *Ann. Microbiol.* 64 (3), 1315–1323. doi:10.1007/s13213-013-0775-x
- Svetashev, V. I. (2021). Investigation of Deep-Sea Ecosystems Using Marker Fatty Acids: Sources of Essential Polyunsaturated Fatty Acids in Abyssal Megafauna. *Mar. Drugs* 20 (1), 17. doi:10.3390/md20010017
- Szymańska, H., and Werblan-Jakubiec, H. (1999). Some Rare Species of Algae from the Biebrza Fens, Poland. *Algological Studies/Archiv für Hydrobiologie* 93, 103–118. doi:10.1127/algol_stud/93/1999/103
- Trommer, G., Lorenz, P., Lentz, A., Fink, P., and Stibor, H. (2019). Nitrogen Enrichment Leads to Changing Fatty Acid Composition of Phytoplankton and

- Negatively Affects Zooplankton in a Natural lake Community. *Sci. Rep.* 9 (1), 16805. doi:10.1038/s41598-019-53250-x
- Untawale, A., Jagtap, T., and Dhargalkar, V. (1980). Dichotomosiphon salina Sp. Nov.-A New marine Algal Form from Goa Estuary, India. *Mahasagar* 13 (1), 73–76.
- Viso, A.-C., and Marty, J.-C. (1993). Fatty Acids from 28 marine Microalgae. *Phytochemistry* 34 (6), 1521–1533. doi:10.1016/s0031-9422(00)90839-2
- Wang, L., Min, M., Li, Y., Chen, P., Chen, Y., Liu, Y., et al. (2010). Cultivation of green Algae Chlorella Sp. In Different Wastewaters from Municipal Wastewater Treatment Plant. *Appl. Biochem. Biotechnol.* 162 (4), 1174–1186. doi:10.1007/s12010-009-8866-7
- Watanabe, A. (1960). List of algal strains in collection at the Institute of Applied Microbiology, University of Tokyo. *J. Gen. Appl. Microbiol.* 6 (4), 283–292. doi:10.2323/jgam.6.283
- Watanabe, S. (1983). New and Interesting Green Algae from Soils of Some Asian and Oceanian Regions. *Archiv für Protistenkunde* 127 (3), 223–270. doi:10.1016/s0003-9365(83)80021-9
- Widianingsih, W., Hartati, R., Endrawati, H., and Mamuaja, J. (2013). Fatty Acid Composition of Marine Microalgae in Indonesia. *Res. J. Soil Biol.* 10, 75–82.
- Yates, C. M., Calder, P. C., and Ed Rainger, G. (2014). Pharmacology and Therapeutics of omega-3 Polyunsaturated Fatty Acids in Chronic Inflammatory Disease. *Pharmacol. Ther.* 141 (3), 272–282. doi:10.1016/j.pharmthera.2013.10.010
- Zanella, L., and Vianello, F. (2020). Microalgae of the Genus Nannochloropsis: Chemical Composition and Functional Implications for Human Nutrition. *J. Funct. Foods* 68, 103919. doi:10.1016/j.jff.2020.103919
- Zhila, N. O., Kalacheva, G. S., and Volova, T. G. (2011). Effect of Salinity on the Biochemical Composition of the Alga Botryococcus Braunii Kütz IPPAS H-252. *J. Appl. Phycol* 23 (1), 47–52. doi:10.1007/s10811-010-9532-8

Conflict of Interest: The authors declare that the research was conducted in the absence of any commercial or financial relationships that could be construed as a potential conflict of interest.

Publisher's Note: All claims expressed in this article are solely those of the authors and do not necessarily represent those of their affiliated organizations, or those of the publisher, the editors, and the reviewers. Any product that may be evaluated in this article, or claim that may be made by its manufacturer, is not guaranteed or endorsed by the publisher.

Copyright © 2022 Jain, Minhas, Shukla, Puri, Barrow and Mandal. This is an open-access article distributed under the terms of the Creative Commons Attribution License (CC BY). The use, distribution or reproduction in other forums is permitted, provided the original author(s) and the copyright owner(s) are credited and that the original publication in this journal is cited, in accordance with accepted academic practice. No use, distribution or reproduction is permitted which does not comply with these terms.



Genetic Engineering of Microalgae for Secondary Metabolite Production: Recent Developments, Challenges, and Future Prospects

Arathi Sreenikethanam¹, Subhisha Raj¹, Rajesh Banu J², Poornachandar Gugulothu² and Amit K. Bajhaiya^{1*}

¹Algal Biotechnology Lab, Department of Microbiology, School of Life Sciences, Central University of Tamil Nadu, Thirvarur, India,

²Department of Biotechnology, Central University of Tamil Nadu, Thirvarur, India

OPEN ACCESS

Edited by:

Wanthanee Khetkorn,
Rajamangala University of Technology
Thanyaburi, Thailand

Reviewed by:

Jiangxin Wang,
Shenzhen University, China
Archana Tiwari,
Amity University, India
Pau Loke Show,
University of Nottingham Malaysia
Campus, Malaysia

*Correspondence:

Amit K. Bajhaiya
amitkumar@cutn.ac.in

Specialty section:

This article was submitted to
Bioprocess Engineering,
a section of the journal
Frontiers in Bioengineering and
Biotechnology

Received: 15 December 2021

Accepted: 03 March 2022

Published: 23 March 2022

Citation:

Sreenikethanam A, Raj S, J RB,
Gugulothu P and Bajhaiya AK (2022)
Genetic Engineering of Microalgae for
Secondary Metabolite Production:
Recent Developments, Challenges,
and Future Prospects.
Front. Bioeng. Biotechnol. 10:836056.
doi: 10.3389/fbioe.2022.836056

Microalgae are highly diverse photosynthetic organisms with higher growth rate and simple nutritional requirements. They are evolved with an efficiency to adapt to a wide range of environmental conditions, resulting in a variety of genetic diversity. Algae accounts for nearly half of global photosynthesis, which makes them a crucial player for CO₂ sequestration. In addition, they have metabolic capacities to produce novel secondary metabolites of pharmaceutical, nutraceutical and industrial applications. Studies have explored the inherent metabolic capacities of microalgae with altered growth conditions for the production of primary and secondary metabolites. However, the production of the targeted metabolites at higher rates is not guaranteed just with the inherent genetic potentials. The strain improvement using genetic engineering is possible hope to overcome the conventional methods of culture condition improvements for metabolite synthesis. Although the advanced gene editing tools are available, the gene manipulation of microalgae remains relatively unexplored. Among the performed gene manipulations studies, most of them focus on primary metabolites with limited focus on secondary metabolite production. The targeted genes can be overexpressed to enhance the production of the desired metabolite or redesigning them using the synthetic biology. A mutant (KOR1) rich in carotenoid and lipid content was developed in a recent study employing mutational breeding in microalgae (Kato, Commun. Biol, 2021, 4, 450). There are lot of challenges in genetic engineering associated with large algal diversity but the numerous applications of secondary metabolites make this field of research very vital for the biotech industries. This review, summarise all the genetic engineering studies and their significance with respect to secondary metabolite production from microalgae. Further, current genetic engineering strategies, their limitations and future strategies are also discussed.

Keywords: microalgae, high value products, secondary metabolites, genetic engineering, transformation, synthetic biology

INTRODUCTION

Microalgae are eukaryotic organisms that have evolved through a series of primary and secondary endosymbiosis (Fu et al., 2019). They are ubiquitous in nature and are adapted to cope with a wide range of environmental conditions. Microalgae are regarded as most promising feed-stocks for metabolite production due to its higher growth rate, biomass production and ease of cultivation. However, improved productivity is dependent on a number of parameters including light intensity and nutrient requirements, which varies with species and the target metabolite (Gimpel et al., 2015). Microalgae are taxonomically diverse and have complex metabolic pathways that provide a source for a variety of value-added molecules which can be used in commercial production of antimicrobials, photo protectants, bioplastics (Bajhaiya, 2021), antivirals etc. (Fu et al., 2019). These molecules are lipids, carbohydrates, or secondary metabolites that can be applied in a bio-refinery approach to produce commercially viable pharmaceutical, nutraceutical, or cosmeceutical products. However, under natural conditions, the rate of metabolite production inside the cell is insufficient for large-scale production. Moreover, metabolite composition changes with the growth stages to meet the needs of the cell. Although, microalgae have a simple organisation and genetic makeup compared to plants, but their enormous diversity and genetic stability make it difficult to develop advanced molecular tools for biotechnological applications. Once advanced techniques have been developed, the next challenge is the delivery of foreign genetic material into algal cells. Various gene delivery systems are used to accomplish this. However, because most genome editing research is done in simple species like bacteria and yeasts, microalgae do not have exposure to all of the existing gene delivery mechanisms (Gutiérrez and Lauersen, 2021).

Just like plants, carbohydrates and other primary metabolites are required for cell development and division in microalgae. This is especially more important in the early phases of the growth, when the algal cells are actively growing. Secondary metabolites are usually produced near the end of the growth cycle, when the organism is approaching the end of life cycle. This is because cells will be encountered with stress due to environmental factors such as nutrient availability and toxin exposure at this stage. These secondary metabolites have features that assist cells in coping with stress and initiate certain signalling pathways involved in the defence responses (Jeong et al., 2020). Up till now the intrinsic ability of microalgae to produce and accumulate significant amounts of secondary metabolites under stress conditions is used. Therefore, as of now there are not many secondary metabolites of algal origin, which are commercialized. Due to various benefits of algal metabolites, the focus has recently shifted to algal genome editing, and several algal strains are thoroughly investigated for their possible biotechnological applications (Gutiérrez and Lauersen, 2021). Currently, stress responses are mostly studied through “omic” analysis to identify the major regulators of metabolite production pathways, and the genetic manipulations are carried out to increase the yields (Guihéneuf et al., 2016). Usually the genetic

alterations are performed with an objective of increasing target metabolite production. But, sometime foreign genes, either nuclear or plastid genomes, can also be acquired naturally from other species via horizontal gene transfer (Gutiérrez and Lauersen, 2021). Similarly the metabolic drifts are also reported in evolution studies (Koch et al., 2017; Belcour et al., 2020). Bioinformatic tools are efficiently used to identify these types of transfers by comparing homologues in the relevant genome sequences. Further, combining algal engineering with advanced technologies like Artificial Intelligence (AI) will help in prediction of molecular interactions and their products (Yong et al., 2020). In addition, active metabolic profiling and comparison can also help in discovering the novel secondary metabolites of commercial importance.

Microalgae can serve as a sustainable feedstock for production of several secondary metabolites to meet the requirements of growing population. These metabolites can be of pharmaceuticals, cosmeceuticals or nutraceuticals applications. In particular, the wide spectrum of applications are due to their key features such as antioxidant, anti-inflammatory, antimicrobial, hepatoprotective, neuroprotective and anticancer properties (Jeong et al., 2020). Here we have discussed in detail the microalgal secondary metabolites and their industrial applications. Furthermore, the significance of algal genetic engineering, various gene delivery systems, current approaches, challenges, possible future strategies, along with key findings is critically analysed and discussed.

MICROALGAL SECONDARY METABOLITES

Microalgae are considered as unique phototrophic cell factories, which can convert CO₂ and carbon containing organic substance into primary and secondary metabolites. The primary metabolites (Carbohydrates, proteins and lipids) are key compounds, which are essential for the survival of the organism (Vuppaladadiyam et al., 2018). The secondary metabolites are compounds (pigments, alkaloids, isoprenoids, mycosporine-like amino acids (MAAs), sterols), which are required for the auxiliary purpose, such as defence mechanism, stress responses, signalling, etc. and are produced in the idiophase of the growth cycle (Jeong et al., 2020). It is important to understand the structure and properties of these secondary metabolites to utilize them at industrial level. Below different classes of secondary metabolites produced by microalgae are discussed with their known applications and further summarized in Table 1.

Bio-Pigments

Microalgae consist of three major classes of bio-pigments *viz.*, chlorophylls, carotenoids and accessory pigments like phycobilins. These bio-pigments are light-absorbing substances that absorb light in a variety of visible spectrum wavelengths (Chakdar and Pabbi, 2017). The backbone of these bio-pigments consists of tetrapyrrole rings primarily

TABLE 1 | Microalgal secondary metabolites and its applications.

Class	Secondary metabolite	Organism	Percentage (dry weight)	Applications	References
Carotenoids	β-carotene	<i>Dunaliella salina</i> , <i>Spirulina maxima</i> , <i>Dunaliella bardawil</i>	0.2–1%	Anti-inflammatory, Anti-oxidant, food colorant, Vitamin A precursor, Reduces macular degeneration and colorectal cancer risk	(Bule et al., 2018)
	—	—	—	—	—
	Lutein	<i>Dunaliella salina</i> , <i>Chlorella pyrenoidosa</i> , <i>Chlorella protothecoids</i> , <i>Chlorella sorokiniana</i> , <i>Chlorella vulgaris</i>	0.5–1.2%	Prevents age-related cataract and maculopathy, anti-tumor, food coloring agent (egg-yolk coloring agent), feed additive, anti-oxidant	(Bule et al., 2018)
	—	—	—	—	—
	Astaxanthin	<i>Haematococcus pluvialis</i> , <i>Chlorella zofigiensis</i> , <i>Chlorella vulgaris</i> , <i>Chlorococcum</i> sp	1–8%	Anti-inflammatory, Anti-oxidant, anti-tumour, food coloring agent, poultry and aquaculture feed additive, anti-ageing, sun protection, anti-diabetic	—
	—	—	—	—	—
	—	—	—	—	—
	Violaxanthin	<i>Dunaliella tertiolecta</i> , <i>Chlorella ellipsoidea</i>	—	Anti-inflammatory, Anti-tumor	Bule et al. (2018) (Bule et al., 2018)
	—	—	—	—	—
Polyunsaturated Fatty Acids (PUFAs)	Zeaxanthin	<i>Dunaliella salina</i> , <i>P. cruentum</i> , <i>Chlorella saccharophila</i> , <i>Synechocystis</i> sp., <i>Microcystis aeruginosa</i> , <i>Nannochloropsis oculata</i>	1–2%	Anti-inflammatory, Anti-oxidant, prevents age related cataract, reduces macular degeneration	—
	—	—	—	—	—
	—	—	—	—	—
	Fucoxanthin	<i>Phaeodactylum tricornutum</i> , <i>Isochrysis</i> sp	>1.5%	Anti-inflammatory, Anti-oxidant, anti-cancer, anti-obesity, prevents cerebrovascular diseases	Bule et al. (2018) (Bule et al., 2018)
	—	—	—	—	—
Tocopherols	—	<i>Chlorella vulgaris</i> , <i>Tetraselmis</i> sp., <i>Nannochloropsis oculata</i> , <i>Cryptocodinium conhi</i> , <i>Nannochloropsis gaditana</i> , <i>Schizochytrium</i> sp., <i>Ulkenia</i> sp	—	Role in neurogenesis and neurotransmission, treatment of various diseases (cancer, atherosclerosis, rheumatoid arthritis, Alzheimer's, and psoriasis), anti-inflammatory, nutrition supplements	(Bule et al., 2018)
	—	—	—	—	—
	—	—	—	—	—
phenolic compounds	—	<i>Porphyridium</i> sp., <i>Spirulina platensis</i> , <i>Desmodesmus</i> sp.	—	Vitamin-E antioxidant activity, anti-inflammatory, anti-tumoural	—
	hydroxycinnamic acids	<i>Chlorella vulgaris</i> , <i>Haematococcus pluvialis</i> , <i>Diatronema lutheri</i> , <i>Phaeodactylum</i> sp., <i>Tetraselmis suecica</i> , <i>Porphyridium purpureum</i>	—	Anti-oxidant, anti-inflammatory	—
	4-hydroxybenzaldehyde	<i>Spongiocloris spongiosa</i> , <i>Spirulina platensis</i> , <i>Anabaena doliolum</i> , <i>Nostoc</i> sp., <i>Cylindrospermum</i> sp.	—	—	—
	3,4-dihydroxybenzaldehyde	<i>Spongiocloris spongiosa</i> , <i>Spirulina platensis</i> , <i>Anabaena doliolum</i> , <i>Nostoc</i> sp., <i>Cylindrospermum</i> sp.	—	—	—
Phycobiliproteins	Vanillic/syringic/cafeic/chlorogenic acid	<i>Spirulina</i> sp.	—	—	—
	phycocyanin	<i>Oscillatoria agardhii</i> , <i>Nostoc UAM 206</i> , <i>Spirulina platensis</i> , <i>Galdiera sulphuraria</i>	About 20%	food and cosmetics coloring agent, fluorescence immunoassays reagent, anti-oxidant	—
	phycoerythrin	<i>Nostoc UAM 206</i> , <i>Spirulina platensis</i> , <i>Porphyridium aeruginum</i> , <i>Porphyridium cruentum</i>	—	fluorescence immunoassays reagent, label for biological molecules	—
Mycosporine like Amino acids	—	<i>Nostoc commune</i> , <i>Alexandrium</i> sp.	—	Sunscreen, anti-inflammatory, anti-tumour, anti-oxidative, wound healing	(Llewellyn, n.d) Raj et al., 2021)
	—	<i>(Alexandrium tamarense, A.</i>	—	—	(Continued on following page)

TABLE 1 | (Continued) Microalgal secondary metabolites and its applications.

Class	Secondary metabolite	Organism	Percentage (dry weight)	Applications	References
		<i>catenella</i> and <i>A. minutum</i>), <i>Lyngbya</i> sp., <i>Synechocystis</i> sp., <i>Chlorella sorokiniana</i> , <i>Calothrix</i> sp	—		
scytonemin	—	<i>Fischerella muscicola</i> , <i>Nostoc commune</i> , <i>Chlorogloeopsis</i> sp., <i>Scytonema</i> sp., <i>Nostoc punctiforme</i>	—	Anti-inflammatory, Anti-proliferation, sun protection	(Llewellyn, n.d.)
	—	—	—	—	

in chlorophyll and phycobilins and isoprene units in carotenoids (Saini et al., 2020). Chlorophyll is the major light-harvesting pigment in microalgae (Gan and Bryant, 2015). The chlorophyll structure has four pyrrole rings arranged in a tetrapyrrole ring, which referred as porphyrin, a tetrapyrrole ring structure (Saini et al., 2020).

Carotenoids are light harvesting pigments predominately found with chlorophylls. They primarily absorb electromagnetic radiation in the region of the visible spectrum, which is not absorbed by the chlorophyll (Cerezo et al., 2012). The structure of carotenoids is formed by 40 carbon isoprene unit and are divided into different groups by the presence or absence of oxygen at the terminal end (Vuppaladadiyam et al., 2018). The derivatives, which is non-oxygenated are called carotene, and their oxygenated derivatives are xanthophylls (Sabarinathan and Gomathy, 2011). Carotenoids are well-known for its antioxidant and anticancer properties. The different types of carotenoids produced by microalgae contains β -carotene, astaxanthin, lutein, lycopene, canthaxanthin and Fucoxanthin, etc (Chakdar and Pabbi, 2017). *Chlorella zofingiensis*, *Chlorella vulgaris*, *Dunaliella salina* and *Haematococcus pluvialis* are some of the common species employed in commercial production of carotenoids (Vuppaladadiyam et al., 2018). Although, secondary carotenoids like β -carotene are produced at high levels at stress conditions, primary carotenoids like lutein, when exposed to high stress conditions can undergo degradation. Astaxanthin synthesis is dependent on several factors such as nutrient availability, salt concentration, heavy metal content, nitrogen source, light quality and intensity of light. Factors like nutrient starvations, heavy metal content and high light intensities can enhance astaxanthin synthesis. But, high salt concentrations can affect the cell and promote mortality at higher rate (Markou and Nerantzis, 2013). Phycobilins are coloured different proteins in microalgae, which absorbs solar radiation in the region of the visible spectrum in which chlorophyll have low absorption (Kannaujiya et al., 2018). Unlike other secondary metabolites, these protein-binded pigments show decrease in cellular levels in response to stress conditions like nutrient starvations and heavy metal exposure. But, increase in salt concentration to certain extent can elevate their production rates (Markou and Nerantzis, 2013). Thus, it is important to optimise the culture conditions to make it suitable for enhanced production of the target metabolite along with higher growth rate of the selected organism.

Mycosporine-like Amino Acids

MAAs are water soluble photoprotective compounds with absorption maxima ranging between 309 and 360 nm (Hartmann et al., 2015). The *de novo* synthesis of MAAs can be done by microalgae, macroalgae, cyanobacteria and fungi. MAAs are recognised as the strongest UV-A absorbing molecules and in addition to it, these do not generate any Reactive Oxygen Species. Mycosporine-2- Glycine (M2G) is recently discovered MAA and is sole MAA present in *Aphanothece halophytica* (Tarasuntisuk et al., 2018). MAAs are primarily isolated and purified from fungi and the comparative higher expressions of these compounds in microalgae were identified later. They are extremely stable and have a chromophore ring with amino alcohol and glycine at the C1 and C2 positions, respectively. The shikimate and pentose phosphate pathways are the two metabolic pathways involved in MAA synthesis, with the former being the most common. The amount of MAA expressed inside the cells is associated with the amount of light and UV radiations (Raj et al., 2021). They prevent thymine dimer formation and protect the cells from DNA damage. Due to their potent photoprotectant properties, MAAs are generally referred as microbial sunscreens and MAA like shinorine are widely used in industrial level sunscreen productions (Nowruzzi et al., 2020). Although, MAA are known for their photoprotective properties, only few of them are commercially produced. It is well known that UV stress can enhance MAA production, but optimization of the wavelength and exposure time is necessary in large-scale productions for best product recovery. Abiotic stress related responses and its associated genes responsible for enhanced MAA production are yet to be studied.

Alkaloids

Alkaloids are nitrogen-containing compounds produced by cyanobacteria, microalgae, plate fungus, and other organisms. These compounds are difficult to differentiate from other naturally occurring nitrogen compounds. The majority of the metabolites are commercially valuable, but some of them may have poisonous properties, such as anatoxin, a neurotoxin that can cause paralysis and death in some fish and animals. Similarly, Spirolides are macrocyclic imines which constitute spiroacetal groups in their chemical structure. These compounds exhibit toxic properties and target acetyl-choline receptors and calcium channels (Sasso et al., 2011). Chemical derivative of alkaloid with indole ring in its structure is classified as indole alkaloids. These

compounds often exhibit antimicrobial and anticancer properties (Jeong et al., 2020). In addition, drugs like morphine, quinine, papaverine and several other pharmaceutically important compounds have an alkaloid structure. Microalgae like *Scenedesmus* sps, *Arthrospira platensis* and *Isochrysis galbana* are some of the species which have potential in Alkaloid production and accumulation (Hadizadeh et al., 2019; Kaliwal, 2019; Fabiola et al., 2020). There are different subclasses of alkaloids and the biosynthesis pathways of molecules in each class may vary. Zooxanthellamine, an alkaloid present in dinoflagellates have structural similarity with the nitrogen compounds present in the soft corals which indicate symbiotic relationship between these organisms, where the soft corals might have acquired these compounds through food chain (Sasso et al., 2011).

Terpenoids

Terpenoids are other diverse class of secondary metabolites, which are expressed in almost all domains of life. But, the diversity is high in plants with complex metabolic pathways and interaction with the surrounding environment. It has wide range of applications at industrial level such as in pharmaceutical, medical and food industries. For example, Betulin is a triterpenoid known for its anticancer and antiviral properties. The biosynthesis of terpenoids involve three major steps viz., synthesis of C₅ Precursors, Polyprenyl pyrophosphate synthesis and their processing to form isoprenoids end products. The well-known compounds like sesquiterpene, diterpenes and monoterpenes belong to this class of metabolites (Sasso et al., 2011). Metabolic routes of terpenoid synthesis involve mevalonate (MVA) and the methyl-D-erythritol (MEP) pathways, which produce the precursors of terpenoid synthesis, 5-carbon prenyl phosphate. Metabolites like terpenoids and several others are expressed in plants with complex metabolic pathways. However, the expressions in such natural hosts will be in very low amounts and can be incorporated into photosynthetic microalgae for higher production rates. *Chlamydomonas reinhardtii* and *Phaeodactylum tricornutum* are the common model organisms used in the genetic engineering studies including the foreign gene insertions. (Vavitsas et al., 2018; D'Adamo et al., 2019). As the biosynthesis pathway, enzymes involved and precursors are known, each of them can be a targeted using genetic engineering to enhance the terpenoid production in microalgae.

Lipids and nucleosides are often thought of as primary metabolites, yet due to certain features of these compounds, they are sometimes classified as secondary metabolites. For example, *Tolythrix tenuis* produces nucleosides such as toyocamycin and tubercidin, which have antifungal properties (Jeong et al., 2020). PUFAs (polyunsaturated fatty acids) are fatty acids which can be consumed as nutritional supplements and can help to prevent certain diseases. PUFAs like eicosapentaenoic acid (EPA), docosahexaenoic acid (DHA), linolenic acid and arachidonic acid are some of the widely studied compounds in combination with industrial productions. PUFAs also serve as

substrates for enzymatic oxidations and result in compounds like oxylipins (Sasso et al., 2011). Fish oil is the widely used source of PUFAs but, the primary producers are microalgae. The primary PUFAs can be changed biochemically by undergoing conversions when they pass through the food chain and this process is called as trophic upgrading (Bule et al., 2018). Similarly, sterols are lipid containing molecules and are characteristic feature of eukaryotic cells. They play a role in maintaining the physiochemical properties of the cell and constitutes about 20–30% of the membranes (Vuppaladadiyam et al., 2018). To enhance the production of these secondary metabolites for commercial applications, apart from standardizing the culture conditions, genetic engineering can play an important role. However, there are several limitations with respect to availability of genomic sequencing data for several non-model algal species as well as the standard transformation methods.

ALGAL TRANSFORMATION METHODS

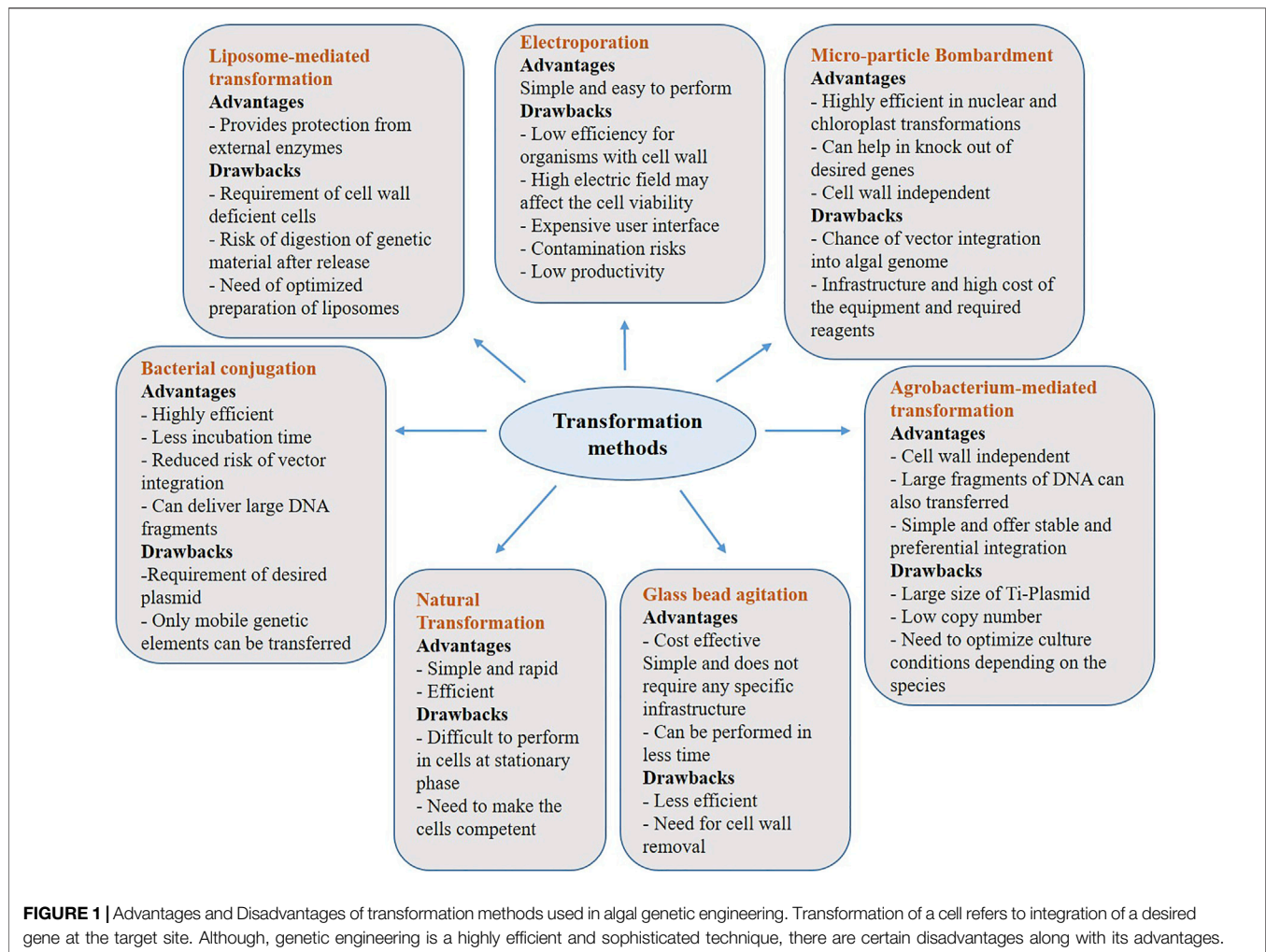
Microalgae can be transformed using various recombinant DNA techniques to ensure higher yields of the targeted metabolite. To alter the genetic makeup of microalgae by inserting foreign genes, different transformation techniques have been employed. Below we have described some of the key transformation methods, which proven to useful in transforming various algal strains and **Figure 1** depicts advantages and disadvantages of each of the below discussed methods.

Electroporation

One of the efficient transformation methods, where algal cells are made competent by applying electric shock for a short period of time using electrodes. This generates a voltage difference across the algal membrane that creates a temporary disturbance in the phospholipid bilayer, creating pores, which in turn allows our desired molecules (foreign DNA) to pass across the membrane (Boni et al., 2015). *Synechococcus* sp. was the first cyanobacterium transformed by electroporation, followed by the cell wall less mutants of *Chlamydomonas reinhardtii*, in which the transformation efficiency was several folds higher than glass-bead transformation (Banerjee et al., 2016). The voltage applied may affect the cell viability and to mitigate such limitations, microfluidic electroporation systems can be used to control the voltage applied. Stable gene transfers in microalgal species like *Scenedesmus obliquus*, *Nannochloropsis* sp. and *Chlorella vulgaris* have been achieved using electroporation. (Im et al., 2015).

Microparticle Bombardment (Biolistics)

This method works on accelerated or high-speed gold/tungsten microparticles, which are coated with DNA and shot using high pressure to transform the target cells (Gutiérrez and Lauersen, 2021). This method can be easily used for the Cas9-gRNA ribonucleoprotein delivery into cells, which helps in the knockout of genes. However, the biggest



concern is transgenic integration of vector DNA into the algal genome because, removing this integrated vector is quite challenging (Sharma et al., 2018). Transformation efficiency depends on cell density, DNA concentration, kinetic energy of the particles, temperature and regeneration efficiency of the cell. (Vazquez-Villegas et al., 2018).

Agrobacterium-Mediated Transformation

Bacterium, *Agrobacterium tumefaciens* is used in this method to transfer DNA segment into the target cells by natural infection process. The T-DNA sequence (part of Ti plasmid) of the bacterium, which allows insertion of the desired DNA construct is utilized for the transformation (Pazhukunnel et al., 2015; Banerjee et al., 2016). This method has been utilized in transformation of microalgal species like *Chlamydomonas reinhardtii*, *Haematococcus lacustris*, *Chlorella* sp., *Dunaliella bardawil*, *Dunaliella salina*, *Symbiodinium* sp., *Nannochloropsis* sp. and *Parachlorella kessleri*. (Vazquez-Villegas et al., 2018). The efficiency depends on pH, temperature, culturing time, bacterial density and their virulence gene induction pattern (San et al., 2011; Gutiérrez and Lauersen, 2021). Pratheesh

et al., in 2014, reported an efficient agrobacterium mediated transformation in *C. reinhardtii*, in which glycine bethaine and pH stress was utilized to induce their virulence gene (*vir* gene), which in turn increased their transformation frequency (Pratheesh et al., 2014).

Glass Bead Agitation

In this method, microalgal cells are mixed with foreign DNA, polyethylene glycol (PEG) and glass beads of about 0.5 mm in size, followed by agitating the mixture. PEG acts as a membrane fusion agent (Fajardo et al., 2014; Vazquez-Villegas et al., 2018). Microalgae with less rigid cell wall or thin cell walls, like *Dunaliella salina* and cell wall deficient strains of *C. reinhardtii* can be efficiently transformed. Presence of cell wall, velocity and duration of the vortexing, cell size, concentration of the non-ionic surfactant used (PEG) are some of the main factors, which can affect the transformation efficiency. Agitation of the cells using silicon-carbide whiskers is also a popular method used in which the cells are vortexed using ceramic microparticles composed of silicon and carbon. Cell walled, *Amphidinium* sp., *Symbiodinium microadriaticum* and *C. reinhardtii* are also transformed using this technique. Although the transformation

efficiency is much better but the health hazard caused by inhaling silicon while handling is one of the major drawback (Rathod et al., 2017).

Natural Transformation

Microalgae and cyanobacteria are capable of DNA uptake from its surrounding environment naturally without using any surfactants (Stucken et al., 2013). Double crossover homologous recombination is the process in which the gene replacement takes place in cyanobacteria and microalgae, after natural transformation. The foreign DNA used for this procedure can be either linear or can be carried on replicative or integrative plasmids. Pili type IV and secretion system type II are two main components of these organisms, which play an important role in natural transformation. *Synechocystis* PCC 7942, *Synechococcus* PCC 7002, *Synechocystis* sp. PCC 6803 and *Thermosynechococcus elongatus* BP-1 are naturally transformable cyanobacterial species (Gutiérrez and Lauenstein, 2021).

Bacterial Conjugation

This method of transformation works on the basis of bacteria's ability to exchange plasmids through their pili via direct contact between the donor and the recipient. This is a natural type of transformation in which combinations of shuttle, helper and conjugative plasmids are used. The main role of helper plasmid is to prevent the degradation of vector by the restriction enzymes. Helper plasmid along with shuttle plasmid mediate the conjugative plasmid transfer from the bacterium to the target cell. The main factors, which affect the transformation efficiency are the ability of the strain to maintain and integrate the vector after transformation and the growth stage of both the recipient and donor organisms, etc. (Karas et al., 2015). *Synechococcus*, *Prochlorococcus*, *N. punctiforme*, *Anabaena variabilis*, *Nostoc* PCC 7120, *S. elongatus* and *Synechocystis* sp. are some of the cyanobacterial species in which this method has been used. *Phaeodactylum tricornutum*, *Thalassiosira pseudonana*, *Acutodesmus obliquus*, and *Neochloris oleoabundans* are some of the microalgal strains transformed using this method. It was found that bacterial conjugation based CRISPR-Cas9 editing has higher efficiency than biolistic-based CRISPR-Cas9 gene editing in microalgae (Banerjee et al., 2016). An efficient and stable transformation of foreign DNA for the first time was performed in oleaginous green microalgae - *Acutodesmus obliquus* and *Neochloris oleoabundans*, via bacterial conjugation using *Escherichia coli* as the donor. In this study, the constructed conjugative plasmids for transformation consisted an origin of transfer (*oriT*), *mob* genes, which are required for the DNA mobilization from the bacterial donor to the microalgal cells, an antibiotic resistance gene, which acts as a selectable marker and the Clover gene as a green fluorescent reporter (Muñoz et al., 2019).

Liposome-Mediated Transformation

Liposomes can be defined as neutrally charged or cationic microscopic, phospholipid vehicles, which are made of single lipid bilayers, in which the foreign DNA to be transformed is loaded in their aqueous compartment. The cationic structure of

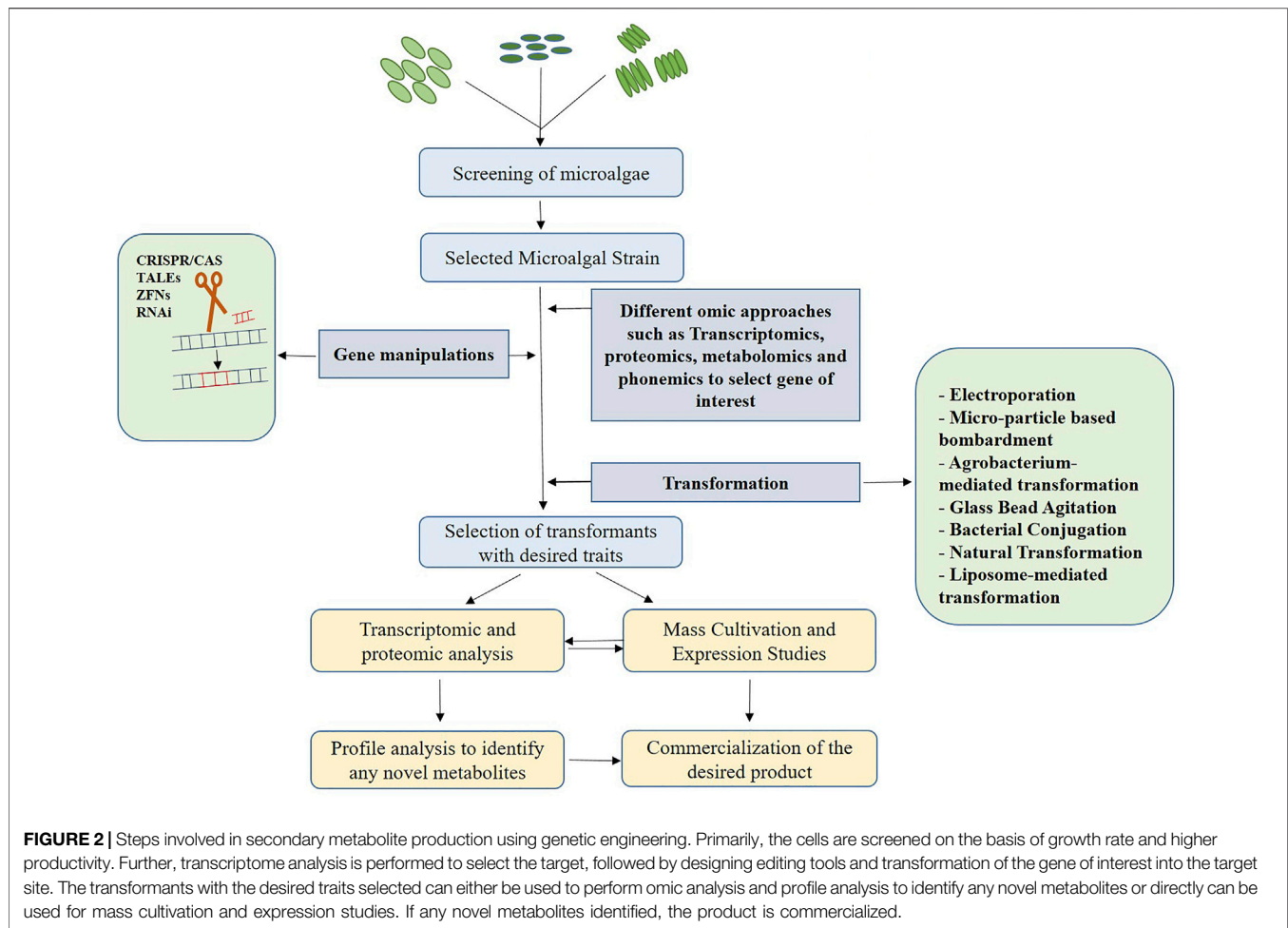
the liposomes enables encapsulation of the foreign genetic material, which helps in transformation. This helps in producing a stable complex that prevents the degradation of the genetic material (Rabinovich and Peng, 1997). Liposome mediated transformation works in such a way in which the cationic liposome complex fuses with the negatively charged membrane to deliver the foreign genetic material into them (Muñoz et al., 2019; Ohta and Ichihashi, 2019). Certain cell wall less mutants of *Chlamydomonas reinhardtii* and *Dunaliella salina* can be studied using this method.

The majority of the transformation strategies discussed above are commonly used in algal genetic engineering. However, each method has its own set of advantages and disadvantages. As a result, selecting a transformation method is an important factor in ensuring a successful transformation. Condition optimization, cell wall rigidity, and the type of genetic material to be transferred are a few of the critical aspects to be considered before deciding on a method to obtain higher transformation efficiency.

Current Approaches in Algal Genetic Engineering

Despite the fact that microalgae are recognized for synthesizing metabolites and value-added products, the majority of them are produced in relatively small quantities. However, in order to commercialize any of the products for industrial use, the production rate must be high to meet economic demands. Random mutagenesis using a variety of physical and chemical mutagens is usually followed by screening techniques in the commercial production process (Fu et al., 2019). But, this is however unpredictable and time-consuming. The ideal strategy involves genetic and metabolic engineering involving omic technologies to identify target sequences for the study and to manipulate the respective gene sequences to yield larger quantities of the desired product. Transcriptome analysis can be used to compare sequences in order to find transcription factors and its expression levels (Bajhaiya et al., 2017), while proteomics can be used to examine post-translational responses using advanced techniques like GC-MS (Arias et al., 2020; Jeong et al., 2020). Liquid chromatography Mass Spectroscopy (LC-MS) can be employed in metabolic profiling to accurately isolate and distinguish the secondary metabolites MAAs (Hartmann et al., 2015). **Figure 2** represents various steps involved in the commercial production process using genetic engineering. Up-regulation and down-regulation of transcriptional and translational genes, as well as knock-out and knock-in of the desired genes, are all part of this process. In the case of secondary metabolites, the target genes will be involved in metabolic pathway regulation, either to produce an enzyme or a product of the pathway (Saini et al., 2020).

Several industrially important secondary metabolites are naturally present in some of the plants. However, the cultivation and purification of these products from natural hosts is not cost-effective. Furthermore, they are produced in extremely small quantities and are found in complicated combinations with related molecules, making isolation difficult. As a result, research is being done to introduce



product-specific genes into suitable hosts such as microalgae due to their photosynthetic properties and most importantly they do not pose any threat to environment (D'Adamo et al., 2019). Lauersen et al. (2018) expressed the plant diterpene synthases (diTPSS) into algal chloroplast and the results show over production of both the enzyme diTPSS and the diterpenoid products like casbene and taxadiene (Lauersen et al., 2018). Extra chromosomal (Episome-based transformation) genetic engineering studies for metabolic pathway engineering by Fabris et al. (2020) on *Phaeodactylum tricornutum* for expression of plant monoterpenoid Geraniol was successful in demonstration and the profiling analysis shows the maximum Geraniol titre as 0.309 mg/L (Fabris et al., 2020).

Several studies have also been performed to identify the target gene to be modified to over-produce the desired metabolite. Kato et al. (2021) performed mutational breeding and resulted in a lipid and carotenoid rich mutant, KOR1. Profile analysis of cell components and metabolome analysis were performed to study the underlying mechanism for lipid and carotenoid accumulation. Insertion/Deletion mutations in *ISA1* gene encoding a Starch debranching enzyme was observed and the disruption of this enzyme enhanced carbohydrate degradation and repartitioning the carbon to lipid and carotenoid

productions. These results suggest the debranching enzyme as a target for metabolic engineering studies (Kato et al., 2021). Similar studies can be performed targeting other key enzymes and regulators to obtain higher rates of secondary metabolite accumulations. Phytoene synthase (PSY) is a rate-limiting enzyme in carotenoid biosynthesis pathway. There are several studies supporting this, such as PSY overexpression showed increased carotenoid production and suppression resulted in reduced production. To study the effect of growth stage on carotenoid synthesis, Kadono et al. (2015) fused the *psy* gene with fluorescent protein to observe the changes in the carotenoid expression levels in *Phaeodactylum tricornutum* at different growth stages. The obtained results of the transformants were compared with the wild type and found that there was 1.45-fold increase in carotenoid content in the transformants. Further it was also concluded that the PSY mRNA levels at the log phase contributes to the increased carotenoid production in the stationary phase (Kadono et al., 2015). Such new findings will be useful large-scale cultivations, where the organism can be harvested at the right phase with maximum yield of the desired metabolite.

Multiple genes can also be transformed into a single organism. A study on single, double and triple transformation in

Phaeodactylum tricornutum using one, two and three carotenoid biosynthesis genes respectively shows enhanced carotenoid production. The genes used in the experiment were Violaxanthin de-epoxidase (Vde), Vde-related (Vdr) and Zeaxanthin epoxidase 3 (Zep3). Studies were performed to evaluate the change in the pigment content and the results suggest that the triple transformants showed 4-fold increase in fucoxanthin content (Manfellotto et al., 2020). In the same way, multiple genes involved in a metabolic pathway can be transformed and altered to alter the biochemical pathways in order to obtain higher production rates.

Secondary metabolite accumulations in response to induced-stress conditions are quite common and well-known. But, it is equally important to understand the underlying mechanisms which causes the change in metabolite levels inside the cells. A recent multi omics study on *Chromochloris zofingiensis* by (Mao et al., 2020a) was performed to study the effect and the underlying mechanisms of TAG and astaxanthin accumulations under salt stress. This study has optimized the salt concentrations and also identified the key regulators which cause the metabolic shifts (Mao et al., 2020b). This study was also helpful in finding that *Chromochloris zofingiensis* can tolerate moderate salt stress and thus sea water can be employed in large-scale productions instead of freshwater. Another study employed time-resolved transcriptional analysis on *Chromochloris zofingiensis* to study the transitions depending on the nutritional status. The transitions were observed between sulphur starved and sulphur-replenished conditions (Mao et al., 2020a). This study was helpful in finding the role of key regulators and its effect on redirection of biochemical pathways leading to TAG and astaxanthin accumulations. These regulators can be future targets for genetic engineering to produce potential mutants with higher yields. Each of the study discussed above employs specific transformation method suitable for the organism under study and further coupled with omic approaches to find the desired genes to be targeted. This is crucial as most of the metabolites are industrially important and to meet the existing demands higher production rates are required for commercialization processes.

INDUSTRIAL APPLICATIONS OF ALGAL SECONDARY METABOLITES

Microalgae and its metabolites can be used to produce a variety of industrially important products. These metabolites can be bio-pigments, MAAs, Isoprenoids, Alkaloids etc. In comparison to synthetically available pigments, microalgal bio-pigments are renewable, safe, and effective. Humans are not capable of denovo synthesis of pigments such as carotenoids. As a result, dietary consumption of such pigments is essential to meet the requirements (Fayyaz et al., 2020). Carotenoids are pigments that have a variety of medical properties and are found in many foods, cosmetics, and pharmaceuticals. Carotenoids are powerful antioxidants with anticancer properties. Carotenoids have

commercial importance due to several properties like antioxidant property, brilliant colors and health promoting factors (Chakdar and Pabbi, 2017). Major carotenoids of microalgae are astaxanthin, lutein and β -carotene. Other molecules like polyketides, phenolic compounds, polyhydroxyalkanoates, proteins and peptides also exhibit strong antioxidant characteristics. These are produced in high amounts to protect the cells from hydrogen peroxide and oxygen radicals produced due to oxidative stress (Vuppaladadiyam et al., 2018). The carotenoids lutein and zeaxanthin are found in the eye as protecting macular pigments. Studies have shown that, consuming more carotenoids through diet lowers the risk of age-related macular degeneration (Wu et al., 2015; Rosales-Mendoza, 2016). Further the β -carotene also known as orange carotenoid can functions as a precursor for Vitamin-A, a vitamin that is involved in important physiological processes involving lung development, tissue maintenance and regeneration and can cause serious disorders such as disturbing the normal lung functioning leading to tissue dysfunction, if deficient (Timoneda et al., 2018). Phytoene and β -Cryptoxanthin are carotenoids with anti-inflammatory properties (Mason et al., 2015). Consumption of metabolites like phenolics through dietary supplements can reduce the risk of certain degenerative disorders such as Alzheimer's and Parkinson's diseases (Machu et al., 2015; Deviram et al., 2020).

Species like *Chlorella zofingiensis*, *Chlorella vulgaris*, *Dunaliella salina* and *Haematococcus pluvialis* are common commercial producers of carotenoids. *Haematococcus pluvialis* is a commercial producer of astaxanthin. Large-scale cultivation of the organism is usually performed employing a two-stage cultivation system, where the cells are grown at optimum conditions in the first stage and later subjected to combinations of stress conditions for enhanced pigment accumulations (Markou and Nerantzis, 2013). Phycobilins have a good economic value due to their high coloration effects. They are used as biochemical tags, food colorants and in the cosmetics industries (Kannaujiya et al., 2018).

A terpenoid called Betulin is extracted from algal species like *Phaeodactylum tricornutum* with the potential to act against HIV and certain cancers such as lung cancer, colorectal cancer and cervical cancer (Schwiebs and Radeke, 2018; D'Adamo et al., 2019; Zehra et al., 2019). Important amino acids such as MAAs are also extracted from algal species such as *Chlamydomonas hedleyi*, *Alexandrium* sps and *Gymnodinium catenatum* (Raj et al., 2021). MAA are photoprotective compounds with wide range of applications due to their anti-inflammatory, antioxidant, and anticancer properties. Osmoregulation and wound healing properties are also reported from MAAs (Choi et al., 2015; Gharib et al., 2020). The MAAs can act against cancer cells by blocking their proliferation or by triggering apoptosis. When it comes to wound healing, MAAs stimulate a number of factors such as Focal Adhesion Kinases (FAKs) and Extracellular signal Regulated Kinases (ERKs) and activates the signalling pathways that help in the healing process (Raj et al., 2021).

Silver Nanoparticles are commonly employed in cancer treatment to induce cytotoxicity in cancer cells, but non-cancer cells are frequently damaged as well. To lessen such negative effects of nanoparticle application, combination of

metabolites from microalgal crude extract could benefit theranostics (Hussein et al., 2020) by limiting the damage to non-cancerous cells. Microalgal crude extracts can be made with a variety of solvents, including water, ethanol, diethylether, and others, to study their antibacterial and anticancer properties. Similarly, Alkaloids like sytonemin and hapalindole also have commercial importance. Sytonemin is photoprotective in nature while hapalindole has antibacterial, antituberculosis and anticancer properties (Jeong et al., 2020), which can have several applications starting from cosmetic industries to human therapeutics. Similarly the exopolysaccharides from microalgae such as *Synechocystis* and *Gloeocapsa* sp. have antipathogenic effect against food borne pathogens (Najdenski et al., 2013) and has been tested to control the growth of *Staphylococcus aureus*, *Escherichia coli* and *Bacillus cereus*. *Scenedesmus* species are commonly studied to explore the medicinal properties of their metabolites due to their higher growth rate and ease to harvest. Marrez et al. (2019) investigated the anticancer and antimicrobial properties of *Scenedesmus* crude extract and its fractions. The findings show that both the crude extract and its fractions have a substantial antibacterial and antifungal activity against the bacteria and fungi such as *Salmonella typhi*, *Pseudomonas aeruginosa*, *Aspergillus steinii* and *Aspergillus carbonarius*. These chemicals also showed cytotoxicity against human breast MCF7, hepatic HepG2 and colon HCT116 cancer cell lines (Marrez et al., 2019) which indicates the possible wider application in cancer treatments.

Algae derived lipid containing molecules such as PUFAs and sterols have high commercial importance due to their health benefits and potential applications in food industries. PUFAs are used in treatment for certain diseases such as atherosclerosis, Alzheimer's, psoriasis and rheumatoid arthritis (Bule et al., 2018). Algae like *Thraustochytrium* sp. and *Parietochloris incisa* are well recognized as industrial PUFA producers, which can accumulate high amounts of lipids under stress conditions especially in nitrogen deplete medium. Microalgae have a highly diverse sterol profiles, which include phytosterols, fucosterols and stenols. Phytosterols have been reported with properties like hepatoprotective, immunomodulatory, anti-inflammatory, anticancer, antioxidative and also can regulate high cholesterol levels (Vuppaladadiyam et al., 2018). Shanab et al. (2012) studied the effects of aqueous extracts of microalgae for its antioxidant and anticancer properties. The results show an antioxidant efficiency ranging from 32 to 76% and anticancer efficiency of 89.4% when tested in human hepatocellular cancer lines. Among the cultured strains, *Nostoc* and *Oscillatoria* sps. Showed high increase in the phycobilin content followed by increased antioxidant and anticancer properties (Shanab et al., 2012), which suggest that cyanobacterial diversity can also be a potential source for bioactive compounds.

The chemical-based formulations of cosmetics have several side-effects, which may cause hypersensitivity and anaphylactic reactions. These negative effects can be tackled by using microalgal metabolites as a promising alternative source of natural cosmetics. They are bio-compatible and are of high demand in cosmetic productions. This is due to their anti-blemish, antimicrobial, anti-aging, anti-inflammatory, UV

protectant and skin whitening properties. Microalgal bio-pigments can be used as natural colouring agents in products like shampoo, soap, eye-shadow, lipsticks and lotions. Bioactive compounds from *S. plantensis* have vital role in skin repair and help in preventing skin wrinkles (Gürlek and Oncel, 2020). Extracts from *Chlorella vulgaris* reported to promote tissue regeneration by stimulating collagen synthesis (Kumar et al., 2018). However the aging can be caused by many of the internal and external factors. The internal factors can be hormonal or genetic disorders and external factors affecting aging are exposure to UV and toxins or less care and moistening given to skin. These factors cause many changes to skin like formation of Reactive Oxygen Species (ROS), Advanced Glycation Endproducts (AGE) and Matrix Metallo Proteinases (MMPs) (Gürlek and Oncel, 2020). M2G, a rare MAA is recently known for its inhibitory effect on AGE formation and has potential to be used in anti-aging formulations. M2G accumulations can be enhanced by UV irradiations and salt stress. This indicates that M2G has both photoprotectant and osmoprotectant properties. It is a free radical scavenger and also can act against oxidative stress induced melanoma in humans (Tarasuntisuk et al., 2018).

Microalgae can also produce metabolites with potential antiviral properties. The demand for pharmaceutical industry is increasing as the severity of viral outbreaks increases. In particular, COVID 19 pandemic has had a significant impact, and substantial research is being conducted to combat the virus. However, the majority of investigations are conducted in common expression systems such as mammalian cells, which pose a significant risk of pathogen contamination. Algae can be used to produce and potentially deliver important biopharmaceuticals to tackle this problem (Rosales-Mendoza et al., 2020). Recent studies suggest that algae can also be employed to produce vaccine, serological kits, nasal sprays and respirators and act effectively against SARS-COV-2 (Chia et al., 2021). Human therapeutic proteins can also be expressed in algal cells with significant expression levels by recombinant technology. Furthermore, the produced proteins are bioactive and can be incorporated and expressed in the chloroplast genome for better expression (Rasala and Mayfield, 2015). The algal biomass or extracts showed immense potential to be used in biopharmaceutical and nutraceutical industries however in spite of that the utilization of algal extracts at industrial level is still limited. The production cost and the quantity of metabolites generation is a challenge, which can be counter with the help of genetic engineering. Although microalgae have a faster growth rate and higher productivity, genetic engineering technologies can aid in greater accumulations of the desired product. However, this comes with its own set of challenges and limitations.

CHALLENGES AND LIMITATIONS IN ALGAL GENETIC ENGINEERING

Although algal genetic engineering is known for enhanced metabolite productions, it also has certain challenges and

limitations. Firstly, the challenge lies in the biochemical pathways that are not very well known in microalgae. Moreover, metabolic drifts may occur resulting in a partial conservation in the process of evolution. In addition to it, genome manipulations in microalgae are quite challenging due to their complex cellular structures and for the same reason they are underexplored compared to simple organisms like bacteria. Moreover, the genome sequences are available only for few species. One of the whole genome sequenced organism being *Chlamydomonas reinhardtii*, which is considered as a model organism for molecular studies. This model organism has been studied for essential cellular processes like photosynthesis, light perception and engineering studies for enhanced metabolite productions. But, it has not yet been used for industrial productions (Chakdar et al., 2021). Recently, there is progress in genetic engineering and transformation studies in species other than model organisms but, all the transformation methods are not well studied in microalgae. Moreover, the efficiency of the transformation depends on the selection of suitable gene transfer method. This is because the cell wall composition of algae varies from species to species and the organisms with rigid cell wall is difficult to perform gene deliveries. Different parameters can be changed to increase the permeability of the cell wall, but the product recovery and efficiency will be very less.

Transformation efficiency also depends on the organism under study. For example, *Haematococcus lacustris* is well recognised as an excellent astaxanthin producer, but the efficiency of transformation is less due to certain features like its slow growth rate, sensitivity to stress and its thick cell wall (Tran and Kaldenhoff, 2020). After transformation, the next challenge lies in the selection of transformants, which is commonly performed using selectable markers, which confers a survival advantage. Insertion of antibiotic resistance genes is a widely used method for selection of transformants. The antibiotics should be chosen considering the native habitat of the microalgae under study. Marine microalgae transformant selection has an additional challenge because high salt concentrations reduce the antibiotic activity and certain antibiotics like streptomycin and kanamycin cannot be used even in low salt concentrations (Vazquez-Villegas et al., 2018). Following transformant selection, transcriptomic and proteomic analysis to compare it with the wild type is carried out. But, there might be a difference in the comparative data between these analyses. This is because, not every gene in the mRNA is translated into protein or a single gene can code for multiple proteins.

In algal genome editing, the foreign gene insertion can be done either into the nuclear genome or into the chloroplast genome. Chloroplast expressions have shown higher and a broad range of metabolite accumulations compared to nuclear genome transformations. But, among the successful transformations, only few proteins accumulate and others do not. This may be due to the susceptibility of the recombinant proteins to proteases or the folds of mRNA which blocks the translation initiation. Other limitation is that the proteins expressed in chloroplast are not secreted and the cells must be lysed to isolate the metabolite followed by purification (Rasala and Mayfield, 2015). All these challenges can be tackled to some extent with specific strategies.

FUTURE PERSPECTIVES

Microalgal engineering has progressed in recent decades, with the majority of studies focusing on primary metabolites, particularly lipid metabolism. Algal secondary metabolites should be explored in every sector, with further research being performed to overcome the challenges using advanced strategies. Until now, traditional engineering, which involves random insertion into the host genome followed by screening is the widely used strategy in applied research. Target specific gene editing has become popular in recent years as a result of the development of powerful gene editing technologies. Advanced techniques can act on critical enzymes, which are involved in the rate limiting steps. Such techniques include Transcription Activator Like Receptors (TALEs), Clustered Regularly Interspaced Short Palindromic Repeats (CRISPR), Zinc Finger Nucleases (ZFNs), etc. which can alter the metabolite production rates at higher rates. RNAi and riboswitch engineering are also efficient in microalgal research.

Along with the advancements in gene editing techniques, sequencing technologies should also improve to make sequences more accessible and to study non-model organisms that are industrially important. Further, advanced bioinformatics approach in combination with genomic and metabolomic data analysis should progress to study the metabolic drifts. Such drifts may cause due to the non-orthologous gene displacement or a change in the main enzyme resulting in the same phenotype (Belcour et al., 2020). These drifts are naturally occurring, but can be a strategy in future to redesign a metabolic pathway to produce multiple enzymes involved in the targeted pathway. Artificial Intelligence (AI), which has recently acquired prominence in the field of microalgal research, can be used to make molecular predictions with respect to gene sequencing and editing. AI and microalgal informatics have the potential to improve current approaches to study genetic information while can also bridge the gap in microalgal engineering (Yong et al., 2020).

The gene delivery systems are critical for successful transformation of microalgal cells to insert foreign genes. The chosen system must be appropriate for the organism being studied, which is selected depending on the cell wall composition. Recent research has found the ideal approaches for algal cells with hard cell walls, such as the zinc oxide nanowire array microdevice system, are much more efficient than conventional transformation methods (Guihéneuf et al., 2016). Algal nuclear and chloroplast engineering in combination with synthetic biology can help in commercialising algal secondary metabolites with therapeutic importance. As microalgae are free of infectious agents, most of them remain biocompatible and have several advantages over common expression systems. These features of algae can provide a scope in heterologous production of algae-based vaccines (Kumar et al., 2020).

Plants are more complicated than algae, with advanced metabolic pathways capable of producing a variety of biotechnologically relevant metabolites. However, gene editing studies are difficult to conduct due to their complexity. To obtain higher yields of the plant metabolites, respective genes can be transformed into organisms with higher growth rate like microalgae. The genes can be inserted into either the nuclear or

chloroplast genomes. Chloroplast transformation results in a larger accumulation of recombinant proteins in algae and plants than nuclear transformation (Rasala and Mayfield, 2015). Optimised gene design combined with codon optimization and synthetic intron spreading can be employed to combat the low levels of expression in the nuclear transformation (Lauersen et al., 2018).

All the above mentioned strategies are mostly performed on only a few organisms for commercial product productions due to the ease of cultivation and harvesting of some common species. There is a need for more research to be performed to explore the potential of other species as well.

CONCLUSION

Microalgae have the ability to produce a variety of secondary metabolites of commercial importance. Using genetic engineering, large-scale microalgae production can be made feasible. There are several studies performed on algal gene manipulations which resulted in higher yields of the target metabolites. The new technologies, when coupled with metabolic, genetic engineering methodologies and optimised culture conditions will help to improve metabolite production efficiency. In addition to it, accurate metabolic profiling also should progress to explore several secondary metabolites of industrial importance, which remain undiscovered till today. The proper handling and disposal of residual biomass can make

industrial production of genetically altered microalgae eco-friendly.

AUTHOR CONTRIBUTIONS

AB designed the concept for the review article and further interpret the literature in the relevant field. AS and SR drafted the article and draw the figures and tables. AB, AS, PG, and RBJ corrected and refined the drafts. AB supervised the writing process. All authors have read and agreed the manuscript.

FUNDING

This review is supported by SERB-SRG Grant, Govt. of India.

ACKNOWLEDGMENTS

AB would like to thank *Science and Engineering Research Board, Govt. of India* for SERB-SRG research grant. AS would like to thank SERB for project fellowship and SR would like to thank CSIR for PhD fellowship. All authors would also like to thank Department of Microbiology, School of Life sciences, Central University of Tamil Nadu for supporting this work.

REFERENCES

- Arias, C., Obudulu, O., Zhao, X., Ansolia, P., Zhang, X., Paul, S., et al. (2020). Nuclear Proteome Analysis of *Chlamydomonas* with Response to CO₂ Limitation. *Algal Res.* 46, 101765. doi:10.1016/j.algal.2019.101765
- Bajhaiya, A. K., Ziehe Moreira, J., and Pittman, J. K. (2017). Transcriptional Engineering of Microalgae: Prospects for High-Value Chemicals. *Trends Biotechnol.* 35, 95–99. doi:10.1016/j.tibtech.2016.06.001
- Bajhaiya, A. S. (2021). *Abstract Algae Based Bio-Plastics: Future of Green Economy*.
- Banerjee, C., Singh, P. K., and Shukla, P. (2016). Microalgal Bioengineering for Sustainable Energy Development: Recent Transgenesis and Metabolic Engineering Strategies. *Biotechnol. J.* 11, 303–314. doi:10.1002/biot.201500284
- Belcour, A., Girard, J., Aite, M., Delage, L., Trotter, C., Marteau, C., et al. (2020). Inferring Biochemical Reactions and Metabolite Structures to Understand Metabolic Pathway Drift. *iScience* 23, 100849. doi:10.1016/j.isci.2020.100849
- Bule, M. H., Ahmed, I., Maqbool, F., Bilal, M., and Iqbal, H. M. N. (2018). Microalgae as a Source of High-Value Bioactive Compounds. *Front. Biosci. (Schol. Ed.)* 10, 197–216. doi:10.2741/s509
- Cerezo, J., Zúñiga, J., Bastida, A., Requena, A., Cerón-Carrasco, J. P., and Eriksson, L. A. (2012). Antioxidant Properties of β -Carotene Isomers and Their Role in Photosystems: Insights from Ab Initio Simulations. *J. Phys. Chem. A* 116, 3498–3506. doi:10.1021/jp301485k
- Chakdar, H., Hasan, M., Pabbi, S., Nevalainen, H., and Shukla, P. (2021). High-throughput Proteomics and Metabolomic Studies Guide Re-engineering of Metabolic Pathways in Eukaryotic Microalgae: A Review. *Bioresour. Technology* 321, 124495. doi:10.1016/j.biortech.2020.124495
- Chakdar, H., and Pabbi, S. (2017). Algal Pigments for Human Health and Cosmeceuticals. *Algal Green. Chem.* 1, 171–188. doi:10.1016/B978-0-444-63784-0.00009-6
- Chia, W. Y., Kok, H., Chew, K. W., Low, S. S., and Show, P. L. (2021). Can Algae Contribute to the War with Covid-19? *Bioengineered* 12, 1226–1237. doi:10.1080/21655979.2021.1910432
- Choi, Y.-H., Yang, D., Kulkarni, A., Moh, S., and Kim, K. (2015). Mycosporine-Like Amino Acids Promote Wound Healing through Focal Adhesion Kinase (FAK) and Mitogen-Activated Protein Kinases (MAP Kinases) Signaling Pathway in Keratinocytes. *Mar. Drugs* 13, 7055–7066. doi:10.3390/md13127056
- D'Adamo, S., Schiano di Visconte, G., Lowe, G., Szaub-Newton, J., Beacham, T., Landels, A., et al. (2019). Engineering the Unicellular Alga *Phaeodactylum Tricornutum* for High-Value Plant Triterpenoid Production. *Plant Biotechnol. J.* 17, 75–87. doi:10.1111/pbi.12948
- Deviram, G., Mathimani, T., Anto, S., Ahamed, T. S., Ananth, D. A., and Pugazhendhi, A. (2020). Applications of Microalgal and Cyanobacterial Biomass on a Way to Safe, Cleaner and a Sustainable Environment. *J. Clean. Prod.* 253, 119770. doi:10.1016/j.jclepro.2019.119770
- Enamala, M. K., Enamala, S., Chavali, M., Donepudi, J., Yadavalli, R., Kolapalli, B., et al. (2018). Production of Biofuels from Microalgae - A Review on Cultivation, Harvesting, Lipid Extraction, and Numerous Applications of Microalgae. *Renew. Sustainable Energ. Rev.* 94, 49–68. doi:10.1016/j.rser.2018.05.012
- Fabiola, J., Garc, P., Palma-ram, D., Alfonso, C., Paredes-rojas, J. C., and Facundo, J. M. (2020). Continuous Microalgal Cultivation for Antioxidants Production. *Molecules* 25, 4171. doi:10.3390/molecules25184171
- Fabris, M., George, J., Kuzhiumparambil, U., Lawson, C. A., Jaramillo-Madrid, A. C., Abbriano, R. M., et al. (2020). Extrachromosomal Genetic Engineering of the Marine Diatom *Phaeodactylum Tricornutum* Enables the Heterologous Production of Monoterpenoids. *ACS Synth. Biol.* 9, 598–612. doi:10.1021/acssynbio.9b00455
- Fajardo, C., Donato, M., Carrasco, R., Martínez-Rodríguez, G., Mancera, J. M., and Fernández-Acero, F. J. (2020). Advances and Challenges in Genetic Engineering of Microalgae. *Rev. Aquacult.* 12, 365–381. doi:10.1111/raq.12322
- Fayyaz, M., Chew, K. W., Show, P. L., Ling, T. C., Ng, I.-S., and Chang, J.-S. (2020). Genetic Engineering of Microalgae for Enhanced Biorefinery Capabilities. *Biotechnol. Adv.* 43, 107554. doi:10.1016/j.biotechadv.2020.107554
- Fu, W., Nelson, D. R., Mystikou, A., Daakour, S., and Salehi-Ashtiani, K. (2019). Advances in Microalgal Research and Engineering Development. *Curr. Opin. Biotechnol.* 59, 157–164. doi:10.1016/j.copbio.2019.05.013

- Gan, F., and Bryant, D. A. (2015). Adaptive and Acclimative Responses of Cyanobacteria to Far-Red Light. *Environ. Microbiol.* 17, 3450–3465. doi:10.1111/1462-2920.12992
- Gharib, R., Tabarza, M., and Hosseinabadi, T. (2020). *Trends in Peptide and Protein Sciences*.
- Gimpel, J. A., Henriquez, V., and Mayfield, S. P. (2015). In Metabolic Engineering of Eukaryotic Microalgae: Potential and Challenges Come with Great Diversity. *Front. Microbiol.* 6, 1–14. doi:10.3389/fmicb.2015.01376
- Guilhénuef, F., Khan, A., and Tran, L.-S. P. (2016). Genetic Engineering: A Promising Tool to Engender Physiological, Biochemical, and Molecular Stress Resilience in green Microalgae. *Front. Plant Sci.* 7, 1–8. doi:10.3389/fpls.2016.00400
- Gutiérrez, S., and Lauersen, K. J. (2021). Gene Delivery Technologies with Applications in Microalgal Genetic Engineering. *Biology* 10, 265. doi:10.3390/biology10040265
- Hadizadeh, M., Ofoghi, H., Kianirad, M., and Amidi, Z. (2019). Elicitation of Pharmaceutical Alkaloids Biosynthesis by Salicylic Acid in marine Microalgae *Arthrospira Platensis*. *Algal Res.* 42, 101597. doi:10.1016/j.algal.2019.101597
- Hartmann, A., Becker, K., Karsten, U., Remias, D., and Ganzera, M. (2015). Analysis of Mycosporine-like Amino Acids in Selected Algae and Cyanobacteria by Hydrophilic Interaction Liquid Chromatography and a Novel MAA from the Red Alga *Catenella Repens*. *Mar. Drugs* 13, 6291–6305. doi:10.3390/md13106291
- Hussein, H. A., Maulidiani, M., and Abdullah, M. A. (2020). Microalgal Metabolites as Anti-cancer/anti-oxidant Agents Reduce Cytotoxicity of Elevated Silver Nanoparticle Levels against Non-cancerous Vero Cells. *Heliyon* 6, e05263. doi:10.1016/j.heliyon.2020.e05263
- Im, D. J., Jeong, S.-N., Yoo, B. S., Kim, B., Kim, D.-P., Jeong, W.-J., et al. (2015). Digital Microfluidic Approach for Efficient Electroporation with High Productivity: Transgene Expression of Microalgae without Cell Wall Removal. *Anal. Chem.* 87, 6592–6599. doi:10.1021/acs.analchem.5b00725
- Jeong, Y., Cho, S.-H., Lee, H., Choi, H.-K., Kim, D.-M., Lee, C.-G., et al. (2020). Current Status and Future Strategies to Increase Secondary Metabolite Production from Cyanobacteria. *Microorganisms* 8, 1849. doi:10.3390/microorganisms8121849
- Joannes, C., Sipaut, C. S., Dayou, J., Yasir, S. M., Mansa, R. F., and Effendi, H. (2015). Review Paper on Cell Membrane Electroporation of Microalgae Using Electric Field Treatment Method for Microalgae Lipid Extraction. *IOP Conf. Ser. Mater. Sci. Eng.* 78, 012034. doi:10.1088/1757-899X/78/1/012034
- Kadono, T., Kira, N., Suzuki, K., Iwata, O., Ohama, T., Okada, S., et al. (2015). Effect of an Introduced Phytoene Synthase Gene Expression on Carotenoid Biosynthesis in the Marine Diatom *Phaeodactylum Tricornutum*. *Mar. Drugs* 13, 5334–5357. doi:10.3390/md13085334
- Kannaujiya, V. K., Kumar, D., Pathak, J., and Sinha, R. P. (2019). Phycobiliproteins and Their Commercial Significance. *Cyanobacteria* 1, 207–216. doi:10.1016/B978-0-12-814667-5.00010-6
- Karas, B. J., Diner, R. E., Lefebvre, S. C., Mcquaid, J., Phillips, A. P. R., Noddings, C. M., et al. (2015). Designer Diatom Episomes Delivered by Bacterial Conjugation. *Nat. Commun.* 6, 6925. doi:10.1038/ncomms7925
- Kato, Y., Oyama, T., Inokuma, K., Vavricka, C. J., Matsuda, M., Hidese, R., et al. (2021). Enhancing Carbohydrate Repartitioning into Lipid and Carotenoid by Disruption of Microalgae Starch Debranching Enzyme. *Commun. Biol.* 4, 450. doi:10.1038/s42003-021-01976-8
- Koch, M., Duigou, T., Carbonell, P., and Faulon, J.-L. (2017). Molecular Structures Enumeration and Virtual Screening in the Chemical Space with RetroPath2.0. *J. Cheminform.* 9 (1), 64. doi:10.1186/s13321-017-0252-9
- Kumar, G., Shekh, A., Jakhu, S., Sharma, Y., Kapoor, R., and Sharma, T. R. (2020). Bioengineering of Microalgae: Recent Advances, Perspectives, and Regulatory Challenges for Industrial Application. *Front. Bioeng. Biotechnol.* 8, 914. doi:10.3389/fbioe.2020.00914
- Lauersen, K. J., Wichmann, J., Baier, T., Kampranis, S. C., Pateraki, I., Möller, B. L., et al. (2018). Phototrophic Production of Heterologous Diterpenoids and a Hydroxy-Functionalized Derivative from *Chlamydomonas Reinhardtii*. *Metab. Eng.* 49, 116–127. doi:10.1016/j.ymben.2018.07.005
- Machu, L., Misurcova, L., Vavra Ambrozova, J., Orsavova, J., Mlcek, J., Sochor, J., et al. (2015). Phenolic Content and Antioxidant Capacity in Algal Food Products. *Molecules* 20, 1118–1133. doi:10.3390/molecules20011118
- Manfellotto, F., Stella, G. R., Falcione, A., Brunet, C., and Ferrante, M. I. (2020). Engineering the Unicellular Alga *Phaeodactylum Tricornutum* for Enhancing Carotenoid Production. *Antioxidants* 9, 757. doi:10.3390/antiox9080757
- Mao, X., Lao, Y., Sun, H., Li, X., Yu, J., and Chen, F. (2020a). Time-resolved T-ranscriptome A-nalysis during T-ransitions of S-ulfur N-utritional S-tatus P-rovides I-sight into T-riacylglycerol (TAG) and A-staxanthin A-ccumulation in the green A-lga *Chromochloris Z-ofingensis*. *Biotechnol. Biofuels* 13, 1–18. doi:10.1186/s13068-020-01768-y
- Mao, X., Zhang, Y., Wang, X., and Liu, J. (2020b). Novel Insights into Salinity-Induced Lipogenesis and Carotenogenesis in the Oleaginous *Staxanthin-Producing Alga Chromochloris Zofingensis*: a Multi-Omics Study. *Biotechnol. Biofuels* 13, 1–24. doi:10.1186/s13068-020-01714-y
- Markou, G., and Nerantzis, E. (2013). Microalgae for High-Value Compounds and Biofuels Production: A Review with Focus on Cultivation under Stress Conditions. *Biotechnol. Adv.* 31, 1532–1542. doi:10.1016/j.biotechadv.2013.07.011
- Marrez, D. A., Naguib, M. M., Sultan, Y. Y., and Higazy, A. M. (2019). Antimicrobial and Anticancer Activities of *Scenedesmus Obliquus* Metabolites. *Heliyon* 5, e01404. doi:10.1016/j.heliyon.2019.e01404
- Mason, J. B., Sanders, D., Greiner, T., Shrimpton, R., and Yukich, J. (2015). Vitamin A Deficiency: Policy Implications of Estimates of Trends and Mortality in Children. *Lancet Glob. Health* 4, e21. doi:10.1016/S2214-109X(15)00246-6
- Muñoz, C. F., Sturme, M. H. J., D'Adamo, S., Weusthuis, R. A., and Wijffels, R. H. (2019). Stable Transformation of the green Algae *Acutodesmus Obliquus* and *Neochloris Oleoabundans* Based on *E. coli* Conjugation. *Algal Res.* 39, 101453. doi:10.1016/j.algal.2019.101453
- Najdenski, H. M., Gigova, L. G., Iliev, I. I., Pilarski, P. S., Lukavský, J., Tsvetkova, I. V., et al. (2013). Antibacterial and Antifungal Activities of Selected Microalgae and Cyanobacteria. *Int. J. Food Sci. Technol.* 48, 1533–1540. doi:10.1111/ijfs.12122
- Nowruzi, B., Sarvari, G., and Blanco, S. (2020). The Cosmetic Application of Cyanobacterial Secondary Metabolites. *Algal Res.* 49, 101959. doi:10.1016/j.algal.2020.101959
- Ohta, K., and Ichihashi, N. (2019). Liposome Fragment-Mediated Introduction of Multiple Plasmids into *Bacillus Subtilis*. *Biochem. Biophys. Rep.* 18, 100646. doi:10.1016/j.bbrep.2019.100646
- Patil, L., and Kaliwal, B. B. (2019). Microalga *Scenedesmus Bajacalifornicus* BBKLP-07, a New Source of Bioactive Compounds with *In Vitro* Pharmacological Applications. *Bioproc. Biosyst. Eng.* 42, 979–994. doi:10.1007/s00449-019-02099-5
- Pralhad Rathod, J., M. Gade, R., Rathod, D., and Dudhare, M. (2017). A Review on Molecular Tools of Microalgal Genetic Transformation and Their Application for Overexpression of Different Genes. *Int. J. Curr. Microbiol. App. Sci* 6, 3191–3207. doi:10.20546/ijcmas.2017.612.373
- Pratheesh, P. T., Vineetha, M., and Kurup, G. M. (2014). An Efficient Protocol for the Agrobacterium-Mediated Genetic Transformation of Microalga *Chlamydomonas Reinhardtii*. *Mol. Biotechnol.* 56, 507–515. doi:10.1007/s12033-013-9720-2
- Rabinovich, P., and Peng, B. (1997). Characterization of Liposome-Mediated Gene Delivery: Expression, Stability and Pharmacokinetics of Plasmid. *Gene Ther.* 43, 226–237. doi:10.1038/sj.gt.3300350
- Raj, S., Kuniyil, A. M., Sreenikethanam, A., and Gugulothu, P. (2021). Microalgae as a Source of Mycosporine-like Amino Acids (MAAs): Advances and Future Prospects. *Int. J. Environ. Res. Public Health* 18 (23), 12402. doi:10.3390/ijerph182312402
- Rasala, B. A., and Mayfield, S. P. (2011). The microalga *Chlamydomonas Reinhardtii* as a Platform for the Production of Human Protein Therapeutics. *Bioengineered Bugs* 2, 50–54. doi:10.4161/bbug.2.1.13423
- Rosales-Mendoza, S. (2016). *Algae-Based Biopharmaceuticals*. Cham: Springer Nature Switzerland. doi:10.1007/978-3-319-32232-2
- Rosales-Mendoza, S., García-Silva, I., González-Ortega, O., Sandoval-Vargas, J. M., Malla, A., and Vilmolmangkang, S. (2020). The Potential of Algal Biotechnology to Produce Antiviral Compounds and Biopharmaceuticals. *Molecules* 25, 4049. doi:10.3390/molecules25184049

- Ruiz-Ruiz, F., Torres-Acosta, M. A., Garcia-Echauri, S. A., Aguilar-Yanez, J. M., Rito-Palomares, M., and Ruiz-Ruiz, F. (2018). Genetic Manipulation of Microalgae for the Production of Bioproducts. *Front. Biosci.* 10, 254–275. doi:10.2741/e821
- Sabarathan, K. G., and Gomathy, M. (2011). Cyanobacterial Biopigments – A Review. *Agric. Rev.* 32, 146–149.
- Saini, D. K., Chakdar, H., Pabbi, S., and Shukla, P. (2020). Enhancing Production of Microalgal Biopigments through Metabolic and Genetic Engineering. *Crit. Rev. Food Sci. Nutr.* 60, 391–405. doi:10.1080/10408398.2018.1533518
- San, C. T., Yee, W., and Ahmad, A. (2011). *Assessment of Factors Affecting Agrobacterium-Mediated Transformation of Microalgae LSP93 Assessment of Factors Affecting Agrobacterium -Mediated Transformation of Microalgae.*
- Sasso, S., Pohnert, G., Lohr, M., Mittag, M., and Hertweck, C. (2012). Microalgae in the Postgenomic Era: a Blooming Reservoir for New Natural Products. *FEMS Microbiol. Rev.* 36, 761–785. doi:10.1111/j.1574-6976.2011.00304.x
- Schwies, A., and Radeke, H. H. (2018). Immunopharmacological Activity of Betulin in Inflammation-Associated Carcinogenesis. *Acamc* 18, 645–651. doi:10.2174/1871520617666171012124820
- Shanab, S. M., Mostafa, S. S., Shalaby, E. A., and Mahmoud, G. I. (2012). Aqueous Extracts of Microalgae Exhibit Antioxidant and Anticancer Activities. *Asian Pac. J. Trop. Biomed.* 2, 608–615. doi:10.1016/S2221-1691(12)60106-3
- Sharma, A. K., Nymark, M., Sparstad, T., Bones, A. M., and Winge, P. (2018). Transgene-free Genome Editing in marine Algae by Bacterial Conjugation - Comparison with Biolistic CRISPR/Cas9 Transformation. *Sci. Rep.* 8, 1–11. doi:10.1038/s41598-018-32342-0
- Simon, D. P., Narayanan, A., Mallikarjun Gouda, K. G., and Sarada, R. (2015). Vir Gene Inducers in *Dunaliella salina*; an Insight in to the *Agrobacterium* -mediated Genetic Transformation of Microalgae. *Algal Res.* 11, 121–124. doi:10.1016/j.algal.2015.06.007
- Stucken, K., Koch, R., and Dagan, T. (2013). Cyanobacterial Defense Mechanisms against Foreign DNA Transfer and Their Impact on Genetic Engineering. *Biol. Res.* 46, 373–382. doi:10.4067/s0716-97602013000400009
- Tarasuntisuk, S., Patipong, T., Hibino, T., Waditee-Sirisattha, R., and Kageyama, H. (2018). Inhibitory Effects of Mycosporine-2-glycine Isolated from a Halotolerant Cyanobacterium on Protein Glycation and Collagenase Activity. *Lett. Appl. Microbiol.* 67, 314–320. doi:10.1111/lam.13041
- Teng, S. Y., Yew, G. Y., Sukačová, K., Show, P. L., Máša, V., and Chang, J.-S. (2020). Microalgae with Artificial Intelligence: A Digitalized Perspective on Genetics, Systems and Products. *Biotechnol. Adv.* 44, 107631. doi:10.1016/j.biotechadv.2020.107631
- Timoneda, J., Rodríguez-Fernández, L., Zaragoza, R., Marín, M. P., Cabezuolo, M. T., Torres, L., et al. (2018). Vitamin A Deficiency and the Lung. *Nutrients* 10 (9), 1132. doi:10.3390/nu1001132
- Tran, N. T., and Kaldenhoff, R. (2020). Achievements and Challenges of Genetic Engineering of the Model green Alga *Chlamydomonas Reinhardtii*. *Algal Res.* 50, 101986. doi:10.1016/j.algal.2020.101986
- Vavitsas, K., Fabris, M., and Vickers, C. (2018). Terpenoid Metabolic Engineering in Photosynthetic Microorganisms. *Genes* 9, 520. doi:10.3390/genes9110520
- Vuppaladadiyam, A. K., Prinsen, P., Raheem, A., Luque, R., and Zhao, M. (2018). *Microalgae Cultivation and Metabolites Production*. Wiley, 1–21. doi:10.1002/bbb.1864
- Wu, J., Cho, E., Willett, W. C., Sastry, S. M., and Schaumberg, D. A. (2015). Intakes of Lutein, Zeaxanthin, and Other Carotenoids and Age-Related Macular Degeneration during 2 Decades of Prospective Follow-Up. *JAMA Ophthalmol.* 133, 1415–1424. doi:10.1001/jamaophthalmol.2015.3590
- Yarkent, Ç., Gürlük, C., and Oncel, S. S. (2020). Potential of Microalgal Compounds in Trending Natural Cosmetics: A Review. *Sustainable Chem. Pharm.* 17, 100304. doi:10.1016/j.scp.2020.100304
- Zaragoza, R., Marín, M. P., Rodríguez-Fernández, L., Zaragoza, R., Cabezuolo, M. T., and Torres, L. (2018). Vitamin A Deficiency and the Lung. *Nutrients* 10 (9), 1132. doi:10.3390/nu10091132
- Zehra, B., Ahmed, A., Sarwar, R., Khan, A., Farooq, U., Abid Ali, S., et al. (2019). Apoptotic and Antimetastatic Activities of Betulin Isolated from *Quercus Incana* against Non-small Cell Lung Cancer Cells. *Cmar* 11, 1667–1683. doi:10.2147/cmar.s186956

Conflict of Interest: The authors declare that the research was conducted in the absence of any commercial or financial relationships that could be construed as a potential conflict of interest.

Publisher's Note: All claims expressed in this article are solely those of the authors and do not necessarily represent those of their affiliated organizations, or those of the publisher, the editors and the reviewers. Any product that may be evaluated in this article, or claim that may be made by its manufacturer, is not guaranteed or endorsed by the publisher.

Copyright © 2022 Sreenikethanam, Raj, J, Gugulothu and Bajhaiya. This is an open-access article distributed under the terms of the Creative Commons Attribution License (CC BY). The use, distribution or reproduction in other forums is permitted, provided the original author(s) and the copyright owner(s) are credited and that the original publication in this journal is cited, in accordance with accepted academic practice. No use, distribution or reproduction is permitted which does not comply with these terms.



Evaluation of *Euglena gracilis* 815 as a New Candidate for Biodiesel Production

Zixi Chen^{1†}, Yehua Chen^{1†}, Hua Zhang^{1,2}, Huan Qin¹, Jiayi He¹, Zezhou Zheng¹, Liqing Zhao³, Anping Lei¹ and Jiangxin Wang^{1*}

¹Shenzhen Key Laboratory of Marine Bioresources and Eco-environmental Science, Shenzhen Engineering Laboratory for Marine Algal Biotechnology, Guangdong Provincial Key Laboratory for Plant Epigenetics, College of Life Sciences and Oceanography, Shenzhen University, Shenzhen, China, ²Shenzhen Academy of Environmental Science, Shenzhen, China, ³College of Chemistry and Environmental Engineering, Shenzhen University, Shenzhen, China

OPEN ACCESS

Edited by:

Kanhaiya Kumar,
Norwegian University of Science and
Technology, Norway

Reviewed by:

Ihana Aguiar Severo,
Federal University of Paraná, Brazil
Ankush Karemore,
Georgia Institute of Technology,
United States
Marcin Debowski,
University of Warmia and Mazury in
Olsztyn, Poland

*Correspondence:

Jiangxin Wang
jxwang@szu.edu.cn

[†]These authors have contributed
equally to this work

Specialty section:

This article was submitted to
Bioprocess Engineering,
a section of the journal
Frontiers in Bioengineering and
Biotechnology

Received: 02 December 2021

Accepted: 07 March 2022

Published: 25 March 2022

Citation:

Chen Z, Chen Y, Zhang H, Qin H, He J,
Zheng Z, Zhao L, Lei A and Wang J
(2022) Evaluation of *Euglena gracilis*
815 as a New Candidate for
Biodiesel Production.
Front. Bioeng. Biotechnol. 10:827513.
doi: 10.3389/fbioe.2022.827513

Euglena comprises over 200 species, of which *Euglena gracilis* is a model organism with a relatively high fatty acid content, making it an excellent potential source of biodiesel. This study isolated and characterized a new strain named *E. gracilis* 815. *E. gracilis* 815 cells were cultivated under light and dark conditions, with either ethanol or glucose as an external carbon source and an autotrophic medium as control. To achieve maximum active substances within a short period i.e., 6 days, the effects of the light condition and carbon source on the accumulation of bioactive ingredients of *E. gracilis* 815 were explored, especially fatty acids. In comparison with the industrially used *E. gracilis* Z strain, *E. gracilis* 815 exhibited high adaptability to different carbon sources and light conditions, with a comparable biomass and lipid yield. The content and composition of fatty acids of *E. gracilis* 815 were further determined to assess its potential for biodiesel use. Results suggested that *E. gracilis* 815 has biodiesel potential under glucose addition in dark culture conditions and could be a promising source for producing unsaturated fatty acids. Therefore, *E. gracilis* 815 is a candidate for short-chain jet fuel, with prospects for a wide variety of applications.

Keywords: microalgae, *Euglena gracilis* 815 strain, paramylon, fatty acids, biodiesel

INTRODUCTION

Extensive global industrialization has driven an increasing energy demand and caused a severe energy crisis. Therefore, alternative and renewable sources of energy are urgently needed. Estimates suggest they can provide 30% of the worldwide energy demand without compromising on food production (Koonin, 2006). Since biomass energy is massive, renewable, and environmentally friendly (Wu et al., 2012; Chew et al., 2017; Chandra et al., 2019; Dębowski et al., 2020a), it has become an essential source of alternative energy (Williams, 2007; Li et al., 2008).

Biodiesels are complex in composition and mainly include palmitic acid, stearic acid, oleic acid, linoleic acid, and other long-chain fatty acids and esters formed by alcohol (Vicente et al., 2007). Rising demand for traditional biofuels, which were originated from food crops such as soybeans, corn, rapeseed, and castor oil, has inadvertently worsened the food crisis. Microalgae biodiesel may be a solution to this problem (Brennan and Owende, 2010; Lei et al., 2012). Microalgae convert light energy into chemical energy, subsequently storing energy as lipids in their cells (Chisti, 2007; Lam and Lee, 2012; Kang et al., 2022; Li et al., 2022). Since the carbon chain lengths of these lipids are

similar to that of diesel, these lipids can be transformed into biodiesel via transesterification (Chisti, 2007; Ramos et al., 2009; Jung et al., 2021; de Carvalho Silvello et al., 2022). Because fatty acids are the precursors for biodiesel production, many researchers in this area have focused on comparing the content and composition of fatty acids among different oleaginous algae (Harwood and Guschina, 2009). Other studies have shown that fatty acid composition significantly impacts the fuel characteristics of biodiesel (Ramos et al., 2009), including essential indicators for evaluating biodiesel potentials such as cetane number (CN), iodine value (IN), and saponification value (SN) (Lei et al., 2012).

Euglena species lack cell walls and have high nutrient availability (Zakryś et al., 2017; Shao et al., 2019). They could be cultivated on a large scale and used in various industrial applications (Mahapatra et al., 2013; Sun et al., 2018; Wu et al., 2020; Wu et al., 2021b). Some *Euglena* species produce medium and long-chain fatty acids, making them potential candidates for having biodiesels to meet the demands of the energy market, and such as in jet fuel (Zeng et al., 2016; Gupta et al., 2021).

Euglena species are highly adaptable and evolutionarily distinct. Notably, *Euglena* species possess characteristics of both plants and animals, and they can grow autotrophically, mixotrophically or heterotrophically with glucose, ethanol, glutamic acid, malate, pyruvate, lactate, and other carbon sources (Barsanti et al., 2000). Some studies on *Euglena* have shown that the addition of a carbon source can induce cell division and promote growth (Hurlbert and Rittenberg, 1962; Rodríguez-Zavala et al., 2006; Wu et al., 2021b), as well as increase the content of total lipids, mainly neutral lipids (Coleman et al., 1988; Thuillier-Bruston et al., 1990). Mainly, organic carbon sources such as ethanol and glucose have been found to participate in different metabolic pathways of *Euglena* and strongly influence their growth and accumulation of active substances. When *Euglena* metabolizes ethanol, it is rapidly oxidized to acetate and converted into acetyl-CoA and participates in the tricarboxylic acid cycle (TCA cycle) (Garlaschi et al., 1974; Zimorski et al., 2017). In comparison, glucose is mainly metabolized through glycolysis and pentose phosphate pathways (PPP) similar to that of other organisms (Hurlbert and Rittenberg, 1962).

The industrial use of *Euglena* has developed rapidly in recent years owing to its commercial potential and value. However, the selection and culture of different *Euglena* species remain a significant obstacle, and most strains have limited application capabilities. Therefore, efforts to screen and identify excellent *Euglena* strains are crucial to expand the range of potential industrial applications for *Euglena* and reduce production costs (Suzuki et al., 2015).

In this study, a new *E. gracilis* strain, *E. gracilis* 815, which uses glucose and ethanol as additional carbon sources, was isolated and cultured under both dark and light conditions. To achieve a high yield of active substances within a short period (i.e., a 6-day culture period), the effects of nutrient and light conditions on the growth, biomass, paramylon, and total lipid accumulation of *E. gracilis* 815 were investigated. Meanwhile its fatty acid composition and contents were also determined. To assess the

potential value of *E. gracilis* 815 for biodiesel applications, its properties were compared with that of the industrially used *E. gracilis* Z strain. Finally, the potential for the industrial application of *E. gracilis* 815 was discussed and evaluated.

MATERIALS AND METHODS

Isolation and Cultivation of *Euglena* Strains

The *Euglena* strain was collected from water samples taken from a fishpond in Fuzhou, China (26°08'N, 119°28'E) in August 2018. Single cells were separated using a capillary pipette and cultured in 96-well plates. They were cultivated autotrophically using Cramer-Myers (CM) medium (Cramer and Myers, 1952) under 25°C and 80 $\mu\text{mol photons}\cdot\text{m}^{-2}\cdot\text{s}^{-1}$.

Culture Medium and Growth Conditions

The culture of *E. gracilis* 815 strain at log phase were inoculated into a 1 L Erlenmeyer flasks containing 250 ml fresh CM medium. Two carbon sources which were commonly used in the cultivation of *E. gracilis* Z (Rodríguez-Zavala et al., 2006; Rodríguez-Zavala et al., 2010), glucose (15 g/L) or ethanol (1% v/v), were added after the medium was autoclaved and cooled for the static culture of *E. gracilis* 815. The autotrophic group was cultured under autotrophic light conditions (CM(L), 80 $\mu\text{mol photons}\cdot\text{m}^{-2}\cdot\text{s}^{-1}$), while the mixotrophic and heterotrophic groups were cultured as follows: ethanol + light (CM + E(L), 1% v/v, 80 $\mu\text{mol photons}\cdot\text{m}^{-2}\cdot\text{s}^{-1}$), glucose + light (CM + G(L), 15 g/L, 80 $\mu\text{mol photons}\cdot\text{m}^{-2}\cdot\text{s}^{-1}$), ethanol + darkness (CM + E(D), 1% v/v, 0 $\mu\text{mol photons}\cdot\text{m}^{-2}\cdot\text{s}^{-1}$), and glucose + darkness (CM + G(D), 15 g/L, 0 $\mu\text{mol photons}\cdot\text{m}^{-2}\cdot\text{s}^{-1}$). Apart from the parameters described above, all groups were statically cultured under 25°C. The initial density in each group was set to 1.7×10^5 cells/ml. Three replicates of each group were cultured simultaneously.

To further compare the biomass accumulation between *E. gracilis* 815 and *E. gracilis* Z, these two strains were cultivated in 1.2 L photobioreactors containing 600 ml fresh CM medium and 1% v/v ethanol as carbon sources. All samples were grown under 25°C, with 80 $\mu\text{mol photons}\cdot\text{m}^{-2}\cdot\text{s}^{-1}$ white light and bubbled with 12 L/min air, while the initial density was 1.1×10^6 cells/mL. After 6 days, cells were collected, dried, and weighted to compare the biomass.

Cell Growth Monitoring

From Day 0 to the day when all groups came to the plateau phase, samples were collected daily. Before sampling, the algae culture in the Erlenmeyer flask was shaken gently. Then, 1 ml of the algae liquid was transferred into a 1.5-ml EP microtube, and counted using a phase-contrast inverted microscope.

Measurement of Biomass

The photosynthetic autotrophic group reached the plateau phase on Day 6 of cultivation. To ensure data integrity, physiological and biochemical analyses of *E. gracilis* 815 cells were only carried out on Day 6. Totally 50 ml of *E. gracilis* 815 or *E. gracilis* Z cells were transferred from each flask to a pre-

weighted 50-ml centrifuge tube. Algal cells were centrifuged at 8,000 rpm for 3 min, collected, lyophilized, and weighted for biomass.

Determination of Paramylon Content

20 mg of *E. gracilis* 815 lyophilized algae powder was transferred into a 15-ml glass centrifuge tube, mixed with 4 ml acetone on a vortex mixer twice (15 s each time), shook at 150 rpm for 1 h, and centrifuged at 5,000 rpm for 5 min. After aspirating the supernatant, the pellet was resuspended with 1 ml of 1% SDS solution, transferred to a pre-weighed 1.5-ml EP tube, and kept at 85°C for 30 min. Then the sample was centrifuged at 2000 rpm for 5 min. After discarding the supernatant, the sample was placed in an oven at 50°C for drying to a constant weight, and the dried powder was paramylon (Takenaka et al., 1997; Wu et al., 2020; Wu et al., 2021b).

Total Lipids Determination

The modified Bligh-Dyer method extracted and determined the total lipids (Bligh and Dyer, 1959). Totally 20 mg of *E. gracilis* 815 dry algae powder was transferred into a 15-ml centrifuge tube. To lyse the algal cells and extract the lipids, 9.5 ml of mixed solvent (chloroform: methanol: distilled water = 1: 2: 0.8) was added to the powder. Then the sample was shaken vigorously for 5 min, ultrasonicated for 30 min, and centrifuged at 5,000 rpm for 2 min. After collecting the supernatant, the remaining algae cells were precipitated, followed by repeating the extraction step twice. Then distilled water and chloroform were added to the collected extract and mixed to achieve a final ratio of chloroform: methanol: distilled water as 1:1:0.9. After mixing, the sample was centrifuged at 5,000 rpm for 10 min. The lower chloroform layer containing lipids was collected to a pre-weighed 50-ml glass tube and dried to constant weight by nitrogen blowing. The total lipid yield was then calculated based on the biomass.

Fatty Acid Composition Analysis

Totally 10 mg of *E. gracilis* 815 dry algae powder was used to quantitatively analyze fatty acid composition. To lyse the algae cells, algae powder was transferred into a glass tube, followed by adding 1 ml of 2 mol/L NaOH-CH₃OH solutions and 50 µl of methyl nonadecanoate working solution (5 mg of methyl nonadecanoate dissolved in 10 ml of dichloromethane) as the internal standard, vortexing for 30 s on a vortex shaker, and shaking for a further 1 h on a shaker at 110 rpm. Cell lysate was placed in a 75°C water bath for 30 min for saponification, and cooled down naturally at room temperature. For methyl esterification, 1 ml of 4 mol/L HCl-CH₃OH solution and 0.5 ml of concentrated HCl (mass fraction of 38%) were added to the saponified lysate to achieve the sample pH < 2, then the sample was kept in a water bath at 75°C for 30 min, and cooled down naturally at room temperature. Then, 1 ml of n-hexane was added for extracting the lipids, followed by vortexing the sample for 5 min. The sample was centrifuged at 4,000 rpm for 2 min, and the supernatant was transferred to a new glass tube, followed by repeating the extraction step twice. The supernatants were combined, filtered through a 0.22 µm PVDF filter into a new test

tube, and the solvent was blown dry with nitrogen. A total of 500 µl of dichloromethane was added into the test tube to fully dissolve the fatty acid methyl ester. The dissolved sample was quickly transferred to the chromatography injection bottle for GC-MS analysis.

A gas chromatography-mass spectrometer (GC-MS, Agilent 7890A-5975C) detected the fatty acid composition. The chromatographic column VF-23 ms (30 m × 320 µm × 0.25 µm) was used, and high-purity helium gas with the purity greater than 99.999% was used as the carrier gas. The injection volume was 2 µl, with a 3 min solvent delay. The injection port temperature was 240°C, the injection port pressure was 1.2 psi, the column flow rate was 1.2299 ml/min, and the split ratio was 10:1. The heating program was as follows: the initial temperature was set at 70°C and held for 1 min, increased to 180°C at a rate of 25°C/min and held for 2 min, increased to 205°C at a rate of 3°C/min and held for 2 min, then increased to 230°C at a rate of 8°C/min and kept for 5 min (Wang et al., 2013; Zeng et al., 2016).

Before loading each batch of samples, 37 kinds of fatty acid mixed standards (Sigma, catalog number: CRM47885) were tested. The chromatographic peaks of the mixed standard samples were qualitatively and quantitatively analyzed in combination with Agilent ChemStation software (Shao et al., 2019).

Calculation of CN, IN, and SN Values

The SN, IN, and CN values were calculated according to the fatty acid composition and content on Day 6 to evaluate the biodiesel potential of *E. gracilis* 815 cultured under different conditions. The SN, IN, and CN values were calculated using the empirical using the empirical formulae (1–3) (Krisnangkura, 1986; Azam et al., 2005).

$$SN = \sum (560 \times P_i) / MW_i \quad (1)$$

$$IN = \sum (254 \times D \times P_i) / MW_i \quad (2)$$

$$CN = 46.3 + 5458 / SN - 0.225 \times IN \quad (3)$$

P_i refers to the weight percentage of each fatty acid, MW_i refers to the molecular weight of each fatty acid, and D refers to the number of double bonds in each fatty acid (Lei et al., 2012).

Statistical Analysis

The mean value and standard deviation (SD) across the three replicates in each group were calculated. One-way analysis of variance (ANOVA) was used to test the significance of differences in cell density, cell biomass, paramylon and total lipids, fatty acid composition, SN, IN, and CN under different conditions. When the variances were homogeneous, and the differences among other states were significant ($p \leq 0.05$), the Student-Newman-Keuls multiple comparison tests were used to determine the source of the differences. When the variances were not homogeneous, the Dunnett's C test was used for analysis and comparison. SPSS 17.0 software (SPSS Inc., United States) was used for all the statistical analyses.

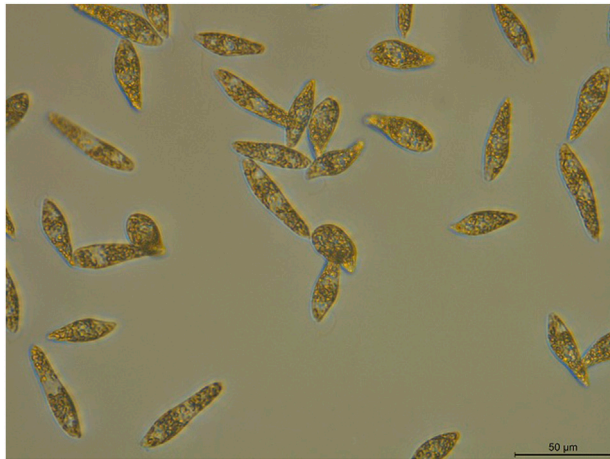


FIGURE 1 | Morphology of *E. gracilis* 815. Scale bar: 50 μ m.

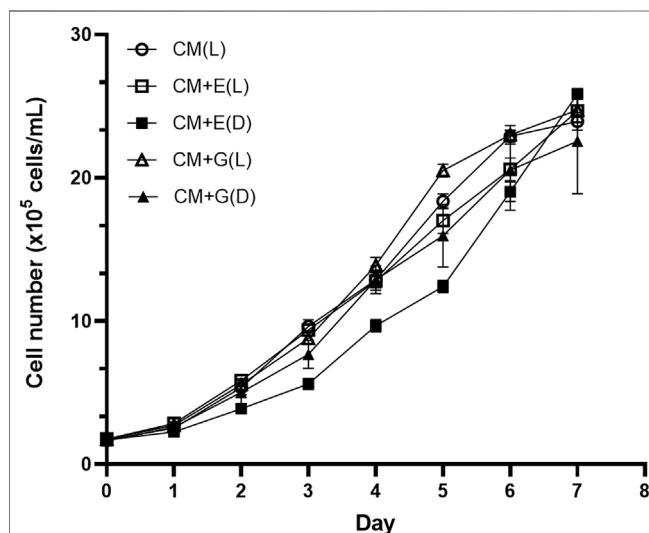


FIGURE 2 | Growth of *E. gracilis* 815 under different conditions. Abbreviations: CM(L), CM medium + light; CM + E(L), CM medium + ethanol (light); CM + E(D), CM medium + ethanol (dark); CM + G(L), CM medium + glucose (light); CM + G(D), CM medium + glucose (dark). Values correspond to the mean \pm standard deviation ($n = 3$).

RESULTS

Species Identification and Morphological Observation

To identify the newly isolated algal strain, the 18S rRNA sequence of the samples were sequenced. According to the 18S rRNA sequencing results (GenBank sequence numbers LSU: MW690035; SSU: MW690034), the samples were identified as *E. gracilis*, and this strain was designated as *E. gracilis* 815. Individual *E. gracilis* 815 algal cells, with approximately 30–50 μ m in length and 10–20 μ m in width, were slender and spindle-shaped with tapered ends, lacked cell walls (**Figure 1**), and could swim freely.

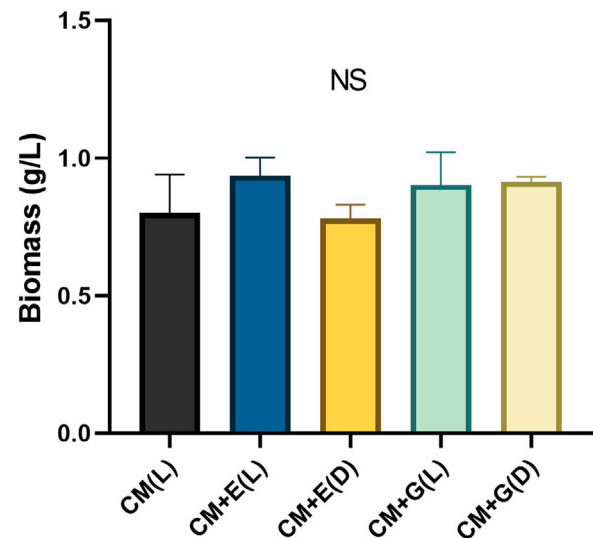


FIGURE 3 | Biomass (g/L) of *E. gracilis* 815 cultured under different conditions on Day 6. NS indicates no significant difference according to ANOVA test at $p > 0.05$.

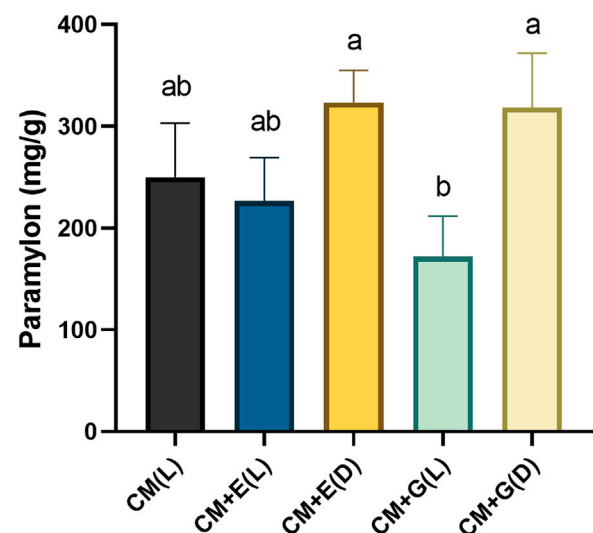
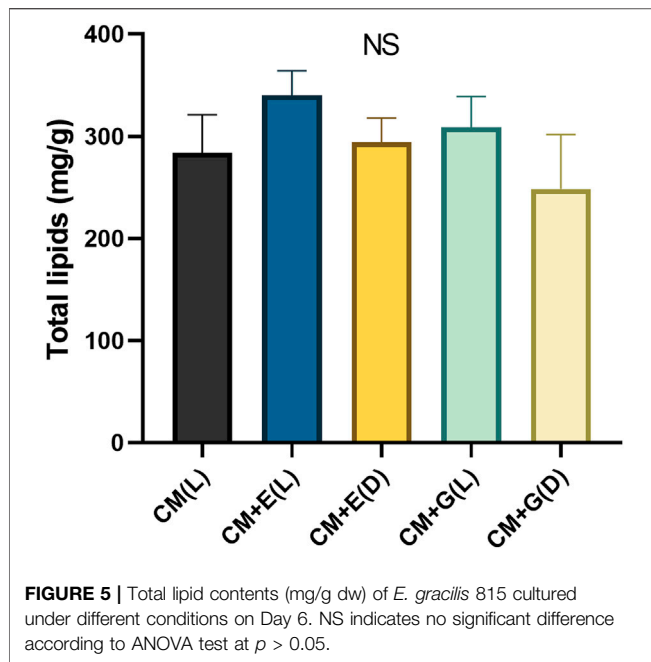


FIGURE 4 | Paramylon content (mg/g dw) of *E. gracilis* 815 cultured under different conditions on Day 6. Different letters indicate significant difference according to ANOVA test at $p \leq 0.05$.

Growth and Biomass of *E. gracilis* 815 Under Different Conditions

To evaluate the ability of using different carbon sources under light or dark conditions, *E. gracilis* 815 was cultured under autotrophic (CM(L)), mixotrophic (CM + E(L) and CM + G(L)), and heterotrophic (CM + E(D) and CM + G(D)) conditions. Growth of the autotrophic groups reached the plateau phase on Day 6, when cell densities ranged from 1.90×10^6 cells/ml (CM + E(D)) to 2.30×10^6 cells/mL (CM + G(L)).



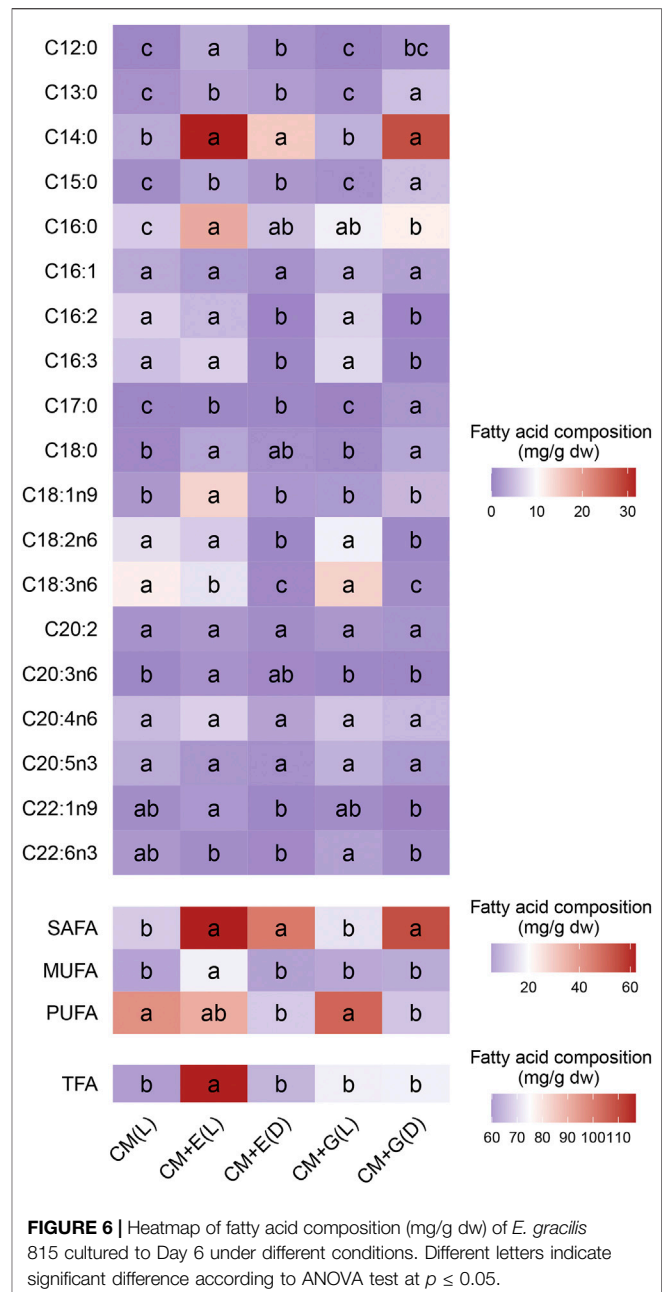
The CM + E(D) group grew slowly between Day2 to Day5, but there were no significant differences among different conditions on Day 6 (Figure 2). In addition, no significant differences were observed among different conditions in the accumulation of cell biomass, which ranged between 0.78–0.94 g/L on Day 6 of incubation (Figure 3).

Paramylon Quantification

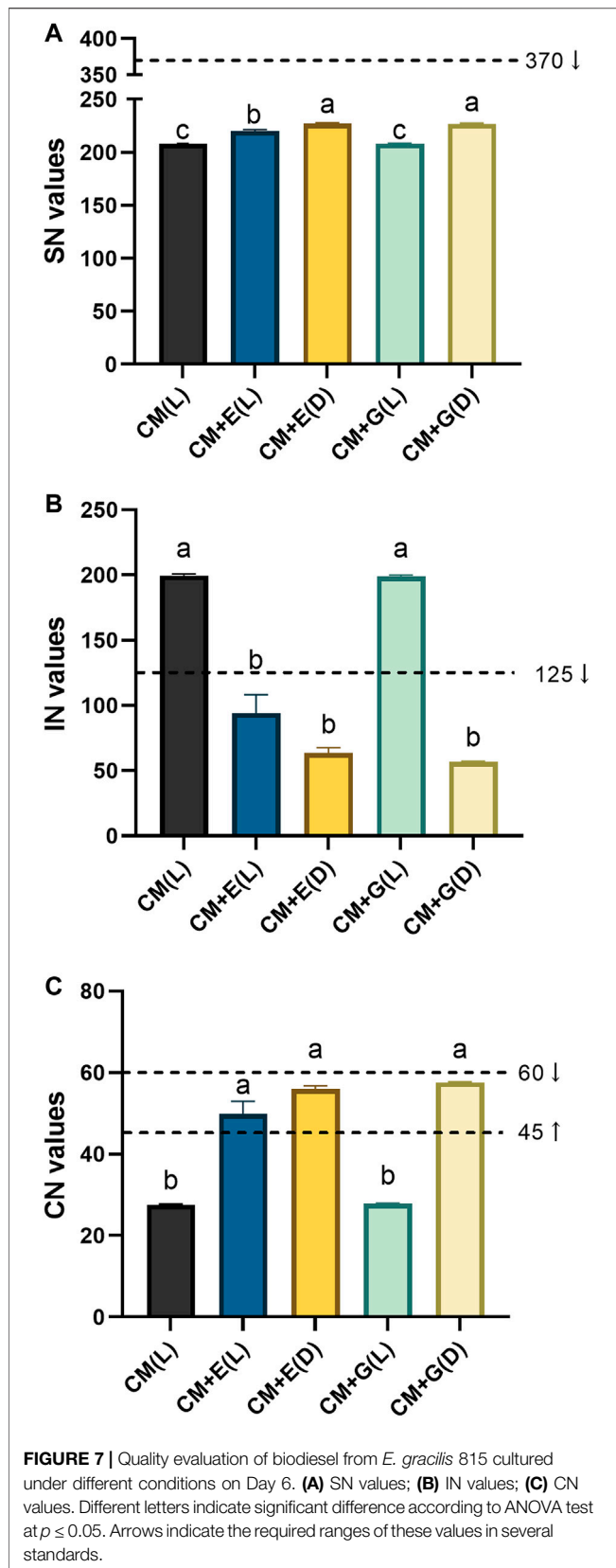
E. gracilis 815 cells were collected on Day 6, and lyophilized algae powder was used for extracting paramylon according to the methods described above. Heterotrophic groups, using ethanol or glucose as carbon sources and cultivated in the dark, significantly accumulated more paramylon than the mixotrophic group using glucose and cultivated in light ($p \leq 0.05$) (Figure 4). However, no significant differences were observed among the three autotrophic and mixotrophic groups cultivated in light. Quantitatively, the paramylon content of the two heterotrophic groups ranged between 318.3–323.3 mg/g dw (dried weight), and the three autotrophic and mixotrophic groups yielded paramylon between 171.7–250 mg/g dw (Figure 4). In summary, heterotrophic cultivation should be used to produce paramylon in *E. gracilis* 815, which agreed to the previous results in *E. gracilis* Z (Zeng et al., 2016).

Total Lipids Quantification, Fatty Acid Content and Composition

The five groups yielded total lipids between 248.67–340.33 mg/g dw on Day 6 (24.87–34.03% total lipids in dry weight), but no significant differences were observed. However, yields from the two mixotrophic groups (340.33 mg/g dw for CM + E(L) and 309 mg/g dw for CM + G(L)) were slightly higher than those from the autotrophic group (284 mg/g dw for CM(L)) and two



heterotrophic groups (294.33 mg/g dw for CM + E(D) and 248.67 mg/g dw for CM + G(D)) (Figure 5). To further evaluate the potential of producing fatty acids using *E. gracilis* 815, the fatty acid contents and compositions cultivated under different conditions according to the methods described above (Figure 6 and Supplementary Table S1). Totally 19 individual fatty acids were detected, and the fatty acid carbon chain composition was C12–C22. Although only the mixotrophic group with ethanol exhibited significantly higher total fatty acid (TFA) content ($p \leq 0.05$), there were significant differences in the contents of different types of fatty acids among all groups. Compared with the autotrophic group, cells cultivated with ethanol significantly accumulated more saturated



fatty acids (SAFAs) ($p \leq 0.05$), which accounted for 50–70% of total fatty acid content. In addition, the content of monounsaturated fatty acids (MUFAs) in the mixotrophic group using ethanol were significantly higher ($p \leq 0.05$) than the others. In groups using glucose, polyunsaturated fatty acids (PUFAs) were mainly found to accumulate in the presence of light, while SAFAs accumulated primarily in the dark. The autotrophic and the mixotrophic groups using glucose accumulated significantly higher ($p \leq 0.05$) levels of PUFAs, which accounted up to 70% of total fatty acid content, and these two conditions could be the candidates for the further study evaluation of producing PUFAs.

When *E. gracilis* 815 were cultured in light, significant differences in fatty acid content were observed between the autotrophic and mixotrophic groups. Compared with the autotrophic group, most types of fatty acids in the mixotrophic group using ethanol were significantly higher ($p \leq 0.05$). These included medium and long-chain SAFAs (C12–C18), as well as unsaturated fatty acids (UFAs), such as oleic acid (C18:1n9), and C20:3n6. However, the contents of most types of fatty acids in the mixotrophic group using glucose did not differ significantly from those of the autotrophic group.

When *E. gracilis* 815 was cultured in the dark, the heterotrophic group using ethanol significantly accumulated fewer fatty acids than the mixotrophic groups cultured in light ($p \leq 0.05$). Most of these differences were attributed to a decrease in the contents of UFAs, such as C16:2, C16:3, oleic acid (C18:1n9), linoleic acid (C18:2n6), α -linolenic acid (C18:3n6), erucic acid (C22:1n9), and others. Similarly, the heterotrophic group using glucose also significantly accumulated less UFAs than the mixotrophic group, such as C16:2, C16:3, linoleic acid (C18:2n6), α -linolenic acid (C18:3n6), and DHA (C22:6n3). In addition, the two heterotrophic groups accumulated significantly higher ($p \leq 0.05$) levels of medium and long-chain SAFAs such as C13–C18.

Evaluation for the Biodiesel Potential of *E. gracilis* 815

As *E. gracilis* 815 accumulated various kinds of fatty acids under different conditions, several critical properties of biodiesels, including SN, IN, and CN values were assessed. SN refers to the mass of potassium hydroxide required for the complete saponification of one unit of oil, IN refers to the number of grams of iodine absorbed per 100 g of oil (reflecting the degree of unsaturation of the oil), and CN is an essential indicator for evaluating the ignition performance of diesel. SN and IN can be used to characterize the possibility of fatty acids or fatty acid methyl esters as raw materials for biodiesel and are related to the length of the fatty acid carbon chain and the degree of unsaturation. CN, the leading indicator of biodiesel quality, can be used to evaluate the impact of biodiesel on the stability and combustion process of diesel engines (Lu et al., 2012).

The SN values of each group of *E. gracilis* 815 ranged between 208.1–227.1 (Figure 7A). The current American ASTM D6751 standard requires an SN standard of biodiesel to be less than 370

(Sakthivel et al., 2018). While there were significant differences between different groups, all groups met this requirement. The IN values of mixotrophic and heterotrophic groups varied substantially, ranging between 56.6–200 (Figure 7B). National biodiesel standards require an IN value not exceeding 125 (Luo et al., 2006). The heterotrophic groups and the mixotrophic group using ethanol, met this requirement. The CN values of each group ranged between 27.6–57.6 (Figure 7C). The international minimum standard for biodiesel CN is set at a value of 45, and values between 45–60 are considered suitable. Similar to IN, the heterotrophic groups and the mixotrophic group using ethanol met this requirement. Based on these results, the heterotrophic cultivation and the mixotrophic cultivation using ethanol could be the candidates for the further evaluation of producing biodiesel.

DISCUSSION

Carbon sources and photosynthesis influence the growth of *Euglena*. No significant differences in cell density between groups of *E. gracilis* 815 using photosynthetic autotrophy, as well as groups using ethanol or glucose as carbon sources were observed on Day 6. However, as observed in *E. gracilis* Z (Zeng et al., 2016), *E. gracilis* 815 was found to exhibit a comparable cell density among all the conditions in result. Studies on *E. gracilis* Z under different culture conditions have shown that adding the carbon sources can promote biomass accumulation under dark conditions (Rodríguez-Zavala et al., 2006; Sun et al., 2018). In the present study, however, no significant difference was observed across conditions of *E. gracilis* 815 in biomass accumulation by Day 6, indicating that this new strain shows strong adaptability to environmental conditions when biomass is harvested in the short term. Since we have proved the possibility of water reuse in the cultivation of *E. gracilis* Z recently (Wu et al., 2021a), further evaluations in *E. gracilis* 815 could be expanded to reusing the wastes from other process, such as exhaust gases or wastewater from factories or livestock, in the cultivation of microalgae (Tsolcha et al., 2018; Amenorfenyo et al., 2019; Dębowski et al., 2020b; Geremia et al., 2021; Mathew et al., 2021; Cheng et al., 2022; Lopez-Sanchez et al., 2022; Singh and Singh, 2022).

The biomass of various *E. gracilis* 815 groups ranged between 0.78–0.94 g/L when their cell density ranged between 1.90×10^6 – 2.3×10^6 cells/ml. In comparison, the biomass of *E. gracilis* Z has been recorded to reach 6.61 g/L and 10.8 g/L at cell densities of 1.86×10^7 cells/ml and 2.45×10^7 cells/ml, respectively, with the initial inoculated densities at 1×10^6 cells/ml. Due to the differences in initial inoculated densities and culture conditions between the experiment of *E. gracilis* 815 and the reference of *E. gracilis* Z (Zeng et al., 2016), modifications such as increasing the initial inoculated density or optimizing the cultivation conditions can be adopted to increase the biomass accumulation in *E. gracilis* 815, and are worthy of further research and exploration. When cultivated with the same initial inoculated densities at 1.1×10^6 cells/ml, no significant difference of biomass was found between *E. gracilis* 815 and *E. gracilis* Z (Supplementary Figure S1). Previous studies have reported that glucose was more conducive to cell density and

biomass accumulation than ethanol in *E. gracilis* Z (Afiukwa and Ogbonna, 2007; Kim et al., 2021). For example, the cell density of the mixotrophic group with ethanol was only half of that with glucose in *E. gracilis* Z after being cultivated for 6 days (Afiukwa and Ogbonna, 2007). However, there were no significant differences in cell density and biomass in *E. gracilis* 815. From the perspective of growth and biomass accumulation, we proposed that *E. gracilis* 815 has prospects for a wide range of applications and is a potential application-type algae strain.

Paramylon is a product of photosynthesis and the main product of carbon storage in *Euglena*. Previous work in *E. gracilis* Z reported that the highest paramylon content was about 200–250 mg/g on Day 4 under heterotrophic conditions (Zeng et al., 2016), which was close to the paramylon content of *E. gracilis* 815 in autotrophic conditions on Day 6. Garlaschi et al. (1974) have shown that ethanol can benefit the synthesis of paramylon in *E. gracilis* Z. The accumulation of paramylon was related to the consumption of ethanol in the medium (Garlaschi et al., 1974). Other studies identified that glucose was the best carbon source for the growth of *Chromochloris zofingiensis* and *E. gracilis* Z, owing to its ability to increase photosynthetic yield (Santek et al., 2010; Ivušić and Šantek, 2015; Roth et al., 2019). Here, by 6 Days of culture, the accumulation of *E. gracilis* 815 under light conditions was not significantly correlated with carbon source. Under dark heterotrophic conditions, the accumulation of paramylon in *E. gracilis* 815 using glucose was considerably higher than that achieved in light. Notably, Schwartzbach et al. (1975) showed that paramylon in *E. gracilis* Z and the non-photosynthetic mutant W3BUL induced by light, with darkness being conducive to paramylon synthesis (Schwartzbach et al., 1975). This agrees with the results of this paper. No significant differences were observed in the accumulation of paramylon when ethanol was added to the culture, suggesting that the accumulation of paramylon in *E. gracilis* 815 may not significantly depend on light or dark when using ethanol. However, as the biomass and total lipid accumulation among all the groups did not differ significantly, differences in paramylon accumulation may be related to differences in protein synthesis in *E. gracilis* 815.

Although there was no significant difference in total lipid accumulation across the non-autotrophic groups, total lipid contents ranged between 24.87–34.03%. Previous studies on other common lipid-producing algae yield have reported similar or even lower lipid contents. For instance, the typical lipid yield of *Chlorella* was 18.59–37.78%, the lipid content of *Scenedesmus obliquus* was 30.25–36.17%. In comparison, diatoms (*Nitzschia minor* and *Phaeodactylum tricornutum*) and *Isochrysis* were approximately 20% (Yang et al., 2011). Meanwhile, studies conducted in *Euglena* showed that the total lipid content of *E. gracilis* (NIES-48) varied within the range of 18–22% (Wang et al., 2018), and that of *Euglena* species varied within the scope of 10–30% (Mahapatra et al., 2013). Furthermore, Jung et al. (2021) found that the maximum lipid content of *E. gracilis* Z during autotrophic culture did not exceed 5%. Under mixotrophic and heterotrophic culture conditions, lipid accumulation in *E. gracilis* Z strain could not exceed 15 and 25%, respectively. Thus, *E. gracilis* 815 has a higher total lipids content than common oleaginous algae and *E. gracilis* Z (Jung et al., 2021).

Moreover, *Euglena* species do not contain cell walls, which could significantly reduce the lipid production costs and enhance production efficiency.

Results showed that *E. gracilis* 815 accumulated significantly more total fatty acid content when using ethanol than either using glucose or photosynthetic, indicating that *E. gracilis* 815 has a higher utilization rate of ethanol in the fatty acid synthesis pathway. SAFAs of the ethanol mixotrophic group and two heterotrophic groups were significantly higher than the autotrophic group. In contrast, the autotrophic group and the glucose mixotrophic group promoted the production of PUFAs. According to the result, the addition of ethanol may be involved in the fatty acid saturation process of *E. gracilis* 815, and light may be involved in the fatty acid desaturation process of *E. gracilis* 815. Studies have also shown that light-induced culture can significantly increase the content of UFAs in *E. gracilis* Z, with SAFAs accounting for the primary product in the dark (Barsanti et al., 2000). This observation indicates that the synthesis of UFAs in *Euglena* is related to the photosynthetic activity.

Previous studies on *E. gracilis* Z have examined the contents of different types of fatty acids, and these results were compared with the levels achieved in *E. gracilis* 815. When *E. gracilis* Z was cultured to Day 7, SAFA contents under mixotrophic and heterotrophic conditions reached 23.7 and 88.3 mg/g dw, respectively (Zeng et al., 2016). In comparison, *E. gracilis* 815 obtained SAFA contents of 62.1 and 54.9 mg/g dw under mixotrophic and heterotrophic conditions on Day 6, respectively. *E. gracilis* Z has been reported to reach MUFA contents of up to 9.51 mg/g dw under mixotrophic conditions (Zeng et al., 2016), while *E. gracilis* 815 reached 17.8 mg/g dw when using ethanol in light. *E. gracilis* Z has reached PUFA contents of 94 and 42.6 mg/g dw in mixotrophic and heterotrophic conditions (Zeng et al., 2016), whereas *E. gracilis* 815 reached 50.2 mg/g dw in mixotrophic condition. Therefore, in comparison with *E. gracilis* Z, the novel strain *E. gracilis* 815 has a relatively higher capacity for producing MUFA, a relatively lower capacity for producing PUFA, and a similar power for making SAFA.

Since PUFAs have more functions than SAFAs, their value has received widespread attention. PUFAs are essential nutrients for the human body and will cause various diseases if they are lacking. PUFAs can thus be used as nutritional supplements in different food and beverages (Simopoulos, 2000; Nessel et al., 2020). In medicine, PUFAs serve a variety of physiological functions such as anti-inflammation and blood lipid regulation while also necessary for the prevention of cardiovascular diseases and treating schizophrenia (Marion-Letellier et al., 2015). PUFAs are also used in beauty and skin-care products. Here, various types of PUFAs were found in different non-autotrophic groups of *E. gracilis* 815, for instance α -linolenic acid, AA (arachidonic acid), EPA (eicosapentaenoic acid), and DHA (docosahexaenoic acid). As α -linolenic acid (C18:3n6) is a product of active photosynthesis (Reitz and Moore, 1972; Barsanti et al., 2000), it was higher in *E. gracilis* 815 cultured in light, regardless of carbon source. In comparison, the observed changes in the content of AA, EPA, and DHA do not seem to be directly related to the carbon source or light. Studies have shown that arachidonic acid and EPA synthesis do not depend on the light. The synthesis of these polyenoic acids is related to non-

photosynthetic organelles, such as mitochondria and microsomes. When cultured with CM medium under mixotrophic conditions, *E. gracilis* Z contained 5.3–23.9, 3.9–5.8, and 0.7–3.4 mg/g dw of AA, EPA, and DHA, respectively, on Day 4 (Barsanti et al., 2000). Here, on Day 6 of *E. gracilis* 815 culture, the contents of these PUFAs were at 7.71–14.47, 1.53–3.79, and 0.8–2.4 mg/g dw, respectively. Another study culturing *E. gracilis* Z to the seventh day reported PUFA contents of 23.54, 6.07, and 5.95 mg/g dw in the mixotrophic condition, respectively. However, when *E. gracilis* 815 was cultured to the sixth day, the contents of these PUFAs were the highest in the mixotrophic group at 14.47, 3.79, and 2.4 mg/g dw, respectively (Zeng et al., 2016). While *E. gracilis* 815 produces slightly lower PUFAs than *E. gracilis* Z, the former may still be developed as an essential source of PUFA production. Overall, the differences in fatty acid composition between different carbon sources and trophic conditions in *E. gracilis* 815 were quite similar to *E. gracilis* Z, suggesting that these two strains shared similar a pattern of metabolic regulation (Reitz and Moore, 1972). Especially when environmental conditions are reasonably controlled and diversified metabolism characteristics are used, fatty acid production can be achieved purposefully for specific applications in *E. gracilis* 815.

In this study, some critical properties of biodiesels in *E. gracilis* 815 were also considered. Based on these indicators of feedstock oil, the actual production process can be assessed. Comparison of SN values of *E. gracilis* 815 to the American ASTM D6751 standard suggested that *E. gracilis* 815 is suitable for direct use as a biodiesel feedstock oil. The SN values of *E. gracilis* 815 were quite similar to those of other familiar sources of biodiesel, such as chicken fat (251.23), mutton fat (244.50), and waste fat oil (204.16) (Sakthivel et al., 2018). Only *E. gracilis* 815 using ethanol (in both light and dark conditions) and those using glucose in the dark met the standards required for IN and CN. If *E. gracilis* 815 were to be used as a biodiesel source under other conditions, problems such as diesel engine ignition difficulties and carbon deposits could emerge, making it unsuitable for direct use as feedstock oil. Notably, *E. gracilis* 815 using glucose in the dark reported the lowest IN and the highest CN. Both values reached the highest, most elevated international biodiesel standards and corresponded to reasonable levels of combustibility. Previous studies have conducted similar biodiesel evaluations on other industrial algae. For instance, *Haematococcus pluvialis*, a high commercial value algae strain, was evaluated under different environmental stresses and found to achieve SN values between 201.9–205.7, IN values between 100–120, and CN values between 45.9–51.6 (Lei et al., 2012). *Chlorella sorokiniana*, a potential biodiesel algae strain, was evaluated under different inoculation amounts and growth periods and found to achieve SN values between 197.8–199.4. The majority of IN values fell between 130–150, with the lowest at 113. CN values of only a few groups exceeded the minimum international standard of 45 (the highest CN value was 48.2) (Lu et al., 2012). Compared with these algae species, *E. gracilis* 815 has a superior CN value of 57.6 (when cultured on glucose in the dark). Totally, under most culture conditions, *E. gracilis* 815 attained SN, IN, and CN values that meet the required standards, suggesting a good biodiesel performance.

CONCLUSION

In conclusion, a new strain of *E. gracilis*, *E. gracilis* 815, was found to have strong adaptability to the environment, fast-growing, relatively high biomass accumulation, and total lipid yield. The accumulation of biomass and total lipids showed no significant differences among all the groups. In contrast, the paramylon content in the mixotrophic group using glucose is lower than the heterotrophic group. Accumulation of total fatty acids and MUFAs in *E. gracilis* 815 was highest when cultured with ethanol in the presence of light. In contrast, when cultured in the dark, overall fatty acid production showed biodiesel potential. As a novel strain, further research is needed to ascertain the full biodiesel potential of *E. gracilis* 815. Future research on this strain could focus on combining transcriptomic and metabolic analyses to explore the mechanisms, determine the best environmental conditions for accumulating active substances, and achieve the production goals in a rapid, controllable, purposeful, and large-scale manner. Overall, *E. gracilis* 815 has demonstrated the potential of industrial production capacity and prospects for broad applications, making it an ideal candidate for industrial biodiesel.

DATA AVAILABILITY STATEMENT

The original contributions presented in the study are included in the article/**Supplementary Material**, further inquiries can be directed to the corresponding author.

REFERENCES

- Afiukwa, C. A., and Ogbonna, J. C. (2007). Effects of Mixed Substrates on Growth and Vitamin Production by *Euglena Gracilis*. *Afr. J. Biotechnol.* 6 (22), 2612–2615. doi:10.5897/AJB2007.000-2417
- Amenorfenyo, D. K., Huang, X., Zhang, Y., Zeng, Q., Zhang, N., Ren, J., et al. (2019). Microalgae Brewery Wastewater Treatment: Potentials, Benefits and the Challenges. *Ijerph* 16 (11), 1910. doi:10.3390/ijerph16111910
- Barsanti, L., Bastianini, A., Passarelli, V., Tredici, M. R., and Gualtieri, P. (2000). Fatty Acid Content in Wild Type and WZSL Mutant of *Euglena Gracilis* - Effects of Carbon Source and Growth Conditions. *J. Appl. Phycology* 12 (3-5), 515–520. doi:10.1023/a:1008187514624
- Bligh, E. G., and Dyer, W. J. (1959). A Rapid Method of Total Lipid Extraction and Purification. *Can. J. Biochem. Physiol.* 37 (8), 911–917. doi:10.1139/o59-099
- Brennan, L., and Owende, P. (2010). Biofuels from Microalgae-A Review of Technologies for Production, Processing, and Extractions of Biofuels and Co-products. *Renew. Sustainable Energ. Rev.* 14 (2), 557–577. doi:10.1016/j.rser.2009.10.009
- Chandra, R., Iqbal, H. M. N., Vishal, G., Lee, H.-S., and Nagra, S. (2019). Algal Biorefinery: A Sustainable Approach to Valorize Algal-Based Biomass towards Multiple Product Recovery. *Bioresour. Technology* 278, 346–359. doi:10.1016/j.biortech.2019.01.104
- Cheng, P., Li, Y., Wang, C., Guo, J., Zhou, C., Zhang, R., et al. (2022). Integrated marine Microalgae Biorefineries for Improved Bioactive Compounds: A Review. *Sci. Total Environ.* 817, 152895. doi:10.1016/j.scitotenv.2021.152895
- Chew, K. W., Yap, J. Y., Show, P. L., Suan, N. H., Juan, J. C., Ling, T. C., et al. (2017). Microalgae Biorefinery: High Value Products Perspectives. *Bioresour. Technology* 229, 53–62. doi:10.1016/j.biortech.2017.01.006
- Chisti, Y. (2007). Biodiesel from Microalgae. *Biotechnol. Adv.* 25 (3), 294–306. doi:10.1016/j.biotechadv.2007.02.001

AUTHOR CONTRIBUTIONS

JW conceived and designed the experiments. YC and HZ performed the experiments. ZC, HQ, JH and ZZ analyzed the data. ZC and YC wrote the manuscript. AL, JW and LZ revised the manuscript. All authors have read and approved the final manuscript.

FUNDING

This work was supported by the National Key R&D Program of China (2020YFA0908703; 2021YFA0910800; 2018YFA0902500), the National Natural Science Foundation of China (41876188).

ACKNOWLEDGMENTS

We would like to thank TopEdit (www.topeditsci.com) for the English language editing of this manuscript. We thank the Instrument Analysis Center of Shenzhen University for assistance with the inverted microscope analysis.

SUPPLEMENTARY MATERIAL

The Supplementary Material for this article can be found online at: <https://www.frontiersin.org/articles/10.3389/fbioe.2022.827513/full#supplementary-material>

- Coleman, L. W., Rosen, B. H., and Schwartzbach, S. D. (1988). Environmental Control of Carbohydrate and Lipid Synthesis in *Euglena*. *Plant Cell Physiol.* 29, 423–432. doi:10.1093/oxfordjournals.pcp.a077510
- Cramer, M., and Myers, J. (1952). Growth and Photosynthetic Characteristics of *Euglena Gracilis*. *Archiv Für Mikrobiologie* 17 (1-4), 384–402. doi:10.1007/bf00410835
- de Carvalho Silvello, M. A., Severo Gonçalves, I., Patrícia Held Azambuja, S., Silva Costa, S., Garcia Pereira Silva, P., Oliveira Santos, L., et al. (2022). Microalgae-based Carbohydrates: A green Innovative Source of Bioenergy. *Bioresour. Technology* 344 (Pt B), 126304. doi:10.1016/j.biortech.2021.126304
- Dębowski, M., Zieliński, M., Kazimierowicz, J., Kujawska, N., and Talbierz, S. (2020a). Microalgae Cultivation Technologies as an Opportunity for Bioenergetic System Development—Advantages and Limitations. *Sustainability* 12 (23), 9980. doi:10.3390/su12239980
- Dębowski, M., Zieliński, M., Kisielińska, M., Kazimierowicz, J., Dudek, M., Świca, I., et al. (2020b). The Cultivation of Lipid-Rich Microalgae Biomass as Anaerobic Digestate Valorization Technology—A Pilot-Scale Study. *Processes* 8 (5), 517. doi:10.3390/pr8050517
- Garlaschi, F. M., Garlaschi, A. M., Lombardi, A., and Forti, G. (1974). Effect of Ethanol on the Metabolism of *Euglena Gracilis*. *Plant Sci. Lett.* 2 (1), 29–39. doi:10.1016/0304-4211(74)90035-2
- Geremia, E., Ripa, M., Catone, C. M., and Ulgiati, S. (2021). A Review about Microalgae Wastewater Treatment for Bioremediation and Biomass Production-A New Challenge for Europe. *Environments* 8 (12), 136. doi:10.3390/environments8120136
- Gupta, S. P., KhushbooGupta, V. K., Gupta, V. K., Minhas, U., Kumar, R., and Sharma, B. (2021). *Euglena* Species: Bioactive Compounds and Their Varied Applications. *Ctmc* 21 (29), 2620–2633. doi:10.2174/1568026621666210813111424
- Harwood, J. L., and Guschina, I. A. (2009). The Versatility of Algae and Their Lipid Metabolism. *Biochimie* 91 (6), 679–684. doi:10.1016/j.biochi.2008.11.004

- Hurlbert, R. E., and Rittenberg, S. C. (1962). Glucose Metabolism of *Euglena gracilis* var. *Bacillaris*; Growth and Enzymatic Studies*. *J. Protozool* 9, 170–182. doi:10.1111/j.1550-7408.1962.tb02602.x
- Ivušić, F., and Santek, B. (2015). Optimization of Complex Medium Composition for Heterotrophic Cultivation of *Euglena Gracilis* and Paramylon Production. *Bioproc. Biosyst Eng* 38 (6), 1103–1112. doi:10.1007/s00449-015-1353-3
- Jung, J.-M., Kim, J. Y., Jung, S., Choi, Y.-E., and Kwon, E. E. (2021). Quantitative Study on Lipid Productivity of *Euglena Gracilis* and its Biodiesel Production According to the Cultivation Conditions. *J. Clean. Prod.* 291, 125218. doi:10.1016/j.jclepro.2020.125218
- Kang, N. K., Baek, K., Koh, H. G., Atkinson, C. A., Ort, D. R., and Jin, Y.-S. (2022). Microalgal Metabolic Engineering Strategies for the Production of Fuels and Chemicals. *Bioresour. Technology* 345, 126529. doi:10.1016/j.biortech.2021.126529
- Kim, S., Wirasmita, R., Lee, D., Yu, J., and Lee, T. (2021). Enhancement of Growth and Paramylon Production of *Euglena Gracilis* by Upcycling of Spent Tomato Byproduct as an Alternative Medium. *Appl. Sci.* 11 (17), 8182. doi:10.3390/app11178182
- Koonin, S. E. (2006). Getting Serious About Biofuels. *Science* 311 (5760), 435. doi:10.1126/science.1124886
- Krisnangkura, K. (1986). A Simple Method for Estimation of Cetane index of Vegetable Oil Methyl Esters. *J. Am. Oil Chem. Soc.* 63 (4), 552–553. doi:10.1007/bf02645752
- Lam, M. K., and Lee, K. T. (2012). Microalgae Biofuels: A Critical Review of Issues, Problems and the Way Forward. *Biotechnol. Adv.* 30 (3), 673–690. doi:10.1016/j.biotechadv.2011.11.008
- Lei, A., Chen, H., Shen, G., Hu, Z., Chen, L., and Wang, J. (2012). Expression of Fatty Acid Synthesis Genes and Fatty Acid Accumulation in *Haematococcus pluvialis* under Different Stressors. *Biotechnol. Biofuels* 5 (1), 18. doi:10.1186/1754-6834-5-18
- Li, Y., Horsman, M., Wu, N., Lan, C. Q., and Dubois-Calero, N. (2008). Biofuels From Microalgae. *Biotechnol. Prog.* 24 (4), 815–820. doi:10.1021/bp070371k
- Li, S., Li, X., and Ho, S.-H. (2022). Microalgae as a Solution of Third World Energy Crisis for Biofuels Production from Wastewater toward Carbon Neutrality: An Updated Review. *Chemosphere* 291 (Pt 1), 132863. doi:10.1016/j.chemosphere.2021.132863
- López-Sánchez, A., Silva-Gálvez, A. L., Aguilar-Juárez, Ó., Senés-Guerrero, C., Orozco-Nunnally, D. A., Carrillo-Nieves, D., et al. (2022). Microalgae-based Livestock Wastewater Treatment (MbWT) as a Circular Bioeconomy Approach: Enhancement of Biomass Productivity, Pollutant Removal and High-Value Compound Production. *J. Environ. Manage.* 308, 114612. doi:10.1016/j.jenvman.2022.114612
- Lu, S., Wang, J., Niu, Y., Yang, J., Zhou, J., and Yuan, Y. (2012). Metabolic Profiling Reveals Growth Related FAME Productivity and Quality of *Chlorella Sorokiniana* with Different Inoculum Sizes. *Biotechnol. Bioeng.* 109 (7), 1651–1662. doi:10.1002/bit.24447
- Luo, W., Yuan, Z. H., and Liao, C. P. (2006). *Biodiesel Standard and Quality Assessment*. Yingkou, China: Renewable Energy 4, 33–37.
- Mahapatra, D. M., Chanakya, H. N., and Ramachandra, T. V. (2013). *Euglena* Sp. As a Suitable Source of Lipids for Potential Use as Biofuel and Sustainable Wastewater Treatment. *J. Appl. Phycol* 25 (3), 855–865. doi:10.1007/s10811-013-9979-5
- Marion-Letellier, R., Savoye, G., and Ghosh, S. (2015). Polyunsaturated Fatty Acids and Inflammation. *Iubmb Life* 67 (9), 659–667. doi:10.1002/iub.1428
- Mathew, M. M., Khatana, K., Vats, V., Dhanker, R., Kumar, R., Dahms, H.-U., et al. (2021). Biological Approaches Integrating Algae and Bacteria for the Degradation of Wastewater Contaminants-A Review. *Front. Microbiol.* 12, 801051. doi:10.3389/fmicb.2021.801051
- Mohibbeazam, M., Waris, A., and Nahar, N. (2005). Prospects and Potential of Fatty Acid Methyl Esters of Some Non-traditional Seed Oils for Use as Biodiesel in India. *Biomass and Bioenergy* 29 (4), 293–302. doi:10.1016/j.biombioe.2005.05.001
- Nessel, I., De Rooy, L., Khashu, M., Murphy, J. L., and Dyall, S. C. (2020). Long-Chain Polyunsaturated Fatty Acids and Lipid Peroxidation Products in Donor Human Milk in the United Kingdom: Results from the LIMIT 2-Centre Cross-Sectional Study. *J. Parenter. Enteral Nutr.* 44 (8), 1501–1509. doi:10.1002/jpen.1773
- Ramos, M. J., Fernández, C. M., Casas, A., Rodríguez, L., and Pérez, Á. (2009). Influence of Fatty Acid Composition of Raw Materials on Biodiesel Properties. *Bioresour. Technology* 100 (1), 261–268. doi:10.1016/j.biortech.2008.06.039
- Reitz, R. C., and Moore, G. S. (1972). Effects of Changes in the Major Carbon Source on the Fatty Acids of *Euglena gracilis*. *Lipids* 7 (3), 217–220. doi:10.1007/BF02533068
- Rodríguez-Zavala, J. S., Ortiz-Cruz, M. A., Mendoza-Hernández, G., and Moreno-Sánchez, R. (2010). Increased Synthesis of α -tocopherol, Paramylon and Tyrosine by *Euglena Gracilis* under Conditions of High Biomass Production. *J. Appl. Microbiol.* 109 (6), 2160–2172. doi:10.1111/j.1365-2672.2010.04848.x
- Rodríguez-Zavala, J. S., Ortiz-Cruz, M. A., and Moreno-Sánchez, R. (2006). Characterization of an Aldehyde Dehydrogenase from *Euglena Gracilis*. *J. Eukaryot. Microbiol.* 53 (1), 36–42. doi:10.1111/j.1550-7408.2005.00070.x
- Roth, M. S., Westcott, D. J., Iwai, M., and Niyogi, K. K. (2019). Hexokinase Is Necessary for Glucose-Mediated Photosynthesis Repression and Lipid Accumulation in a green Alga. *Commun. Biol.* 2, 347. doi:10.1038/s42003-019-0577-1
- Santek, B., Felski, M., Friehs, K., Lotz, M., and Flaschel, E. (2010). Production of Paramylon, a β -1,3-glucan, by Heterotrophic Cultivation of *Euglena gracilis* on Potato Liquor. *Eng. Life Sci.* 10 (2), NA. doi:10.1002/elsc.200900077
- Sakthivel, R., Ramesh, K., Purnachandran, R., and Mohamed Shameer, P. (2018). A Review on the Properties, Performance and Emission Aspects of the Third Generation Biodiesels. *Renew. Sustainable Energ. Rev.* 82, 2970–2992. doi:10.1016/j.rser.2017.10.037
- Schwartzbach, S. D., Schiff, J. A., and Goldstein, N. H. (1975). Events Surrounding the Early Development of *Euglena* Chloroplasts. *Plant Physiol.* 56 (2), 313–317. doi:10.1104/pp.56.2.313
- Shao, Q., Hu, L., Qin, H., Liu, Y., Tang, X., Lei, A., et al. (2019). Metabolomic Response of *Euglena Gracilis* and its Bleached Mutant Strain to Light. *PLoS One* 14 (11), e0224926. doi:10.1371/journal.pone.0224926
- Simopoulos, A. P. (2000). Human Requirement for N-3 Polyunsaturated Fatty Acids. *Poult. Sci.* 79 (7), 961–970. doi:10.1093/ps/79.7.961
- Singh, A., and Singh, A. (2022). Microbial Degradation and Value Addition to Food and Agriculture Waste. *Curr. Microbiol.* 79 (4), 119. doi:10.1007/s00284-022-02809-5
- Sun, A., Hasan, M. T., Hobba, G., Nevalainen, H., and Te'o, J. (2018). Comparative Assessment of the *Euglena Gracilis* Var. *Saccharophila* Variant Strain as a Producer of the β -1,3-glucan Paramylon under Varying Light Conditions. *J. Phycol.* 54 (4), 529–538. doi:10.1111/jpy.12758
- Suzuki, K., Mitra, S., Iwata, O., Ishikawa, T., Kato, S., and Yamada, K. (2015). Selection and Characterization of *Euglena Anabaena* Var. *Minor* as a New Candidate *Euglena* Species for Industrial Application. *Biosci. Biotechnol. Biochem.* 79 (10), 1730–1736. doi:10.1080/09168451.2015.1045828
- Takenaka, S., Kondo, T., Nazeri, S., Tamura, Y., Tokunaga, M., Tsuyama, S., et al. (1997). Accumulation of Trehalose as a Compatible Solute under Osmotic Stress in *Euglena Gracilis* Z. *J. Eukaryot. Microbiol. (Usa)* 44, 609–613. doi:10.1111/j.1550-7408.1997.tb05967.x
- Thuillier-Bruston, F., Briand, J., and Laval-Martin, D. (1990). Effects of a First Exposure to Ethanol on the Compositions of Neutral and Polar Lipids in *Euglena Gracilis* Z, Taken as a Hepatic Cell Model: Equilibration by Citrulline-Malate. *Biochem. Med. Metab. Biol.* 44 (2), 159–174. doi:10.1016/0885-4505(90)90057-8
- Tsolcha, O., Tekerlekopoulou, A., Akratos, C., Aggelis, G., Genitsaris, S., Moustaka-Gouni, M., et al. (2018). Agroindustrial Wastewater Treatment with Simultaneous Biodiesel Production in Attached Growth Systems Using a Mixed Microbial Culture. *Water* 10 (11), 1693. doi:10.3390/w10111693
- Vicente, G., Martínez, M., and Aracil, J. (2007). Optimisation of Integrated Biodiesel Production. Part I. A Study of the Biodiesel Purity and Yield. *Bioresour. Technology* 98 (9), 1724–1733. doi:10.1016/j.biortech.2006.07.024
- Wang, J., Chen, L., Tian, X., Gao, L., Niu, X., Shi, M., et al. (2013). Global Metabolomic and Network Analysis of *Escherichia coli* Responses to Exogenous Biofuels. *J. Proteome Res.* 12 (11), 5302–5312. doi:10.1021/pr400640u
- Wang, Y., Seppänen-Laakso, T., Rischer, H., and Wiebe, M. G. (2018). *Euglena Gracilis* Growth and Cell Composition under Different Temperature, Light and

- Trophic Conditions. *PLoS One* 13 (4). e0195329. doi:10.1371/journal.pone.0195329
- Williams, P. J. (2007). Biofuel: microalgae cut the social and ecological costs. *Nature* 450 (7169). 478. doi:10.1038/450478a
- Wu, M., Du, M., Wu, G., Lu, F., Li, J., Lei, A., et al. (2021a). Water Reuse and Growth Inhibition Mechanisms for Cultivation of Microalga *Euglena Gracilis*. *Biotechnol. Biofuels* 14 (1), 132. doi:10.1186/s13068-021-01980-4
- Wu, M., Li, J., Qin, H., Lei, A., Zhu, H., Hu, Z., et al. (2020). Pre-concentration of Microalga *Euglena Gracilis* by Alkaescent pH Treatment and Flocculation Mechanism of $\text{Ca}_3(\text{PO}_4)_2$, $\text{Mg}_3(\text{PO}_4)_2$, and Derivatives. *Biotechnol. Biofuels* 13 (3), 98. doi:10.1186/s13068-020-01734-8
- Wu, M., Qin, H., Deng, J., Liu, Y., Lei, A., Zhu, H., et al. (2021b). A New Pilot-Scale Fermentation Mode Enhances *Euglena Gracilis* Biomass and Paramylon (β -1,3-Glucan) Production. *J. Clean. Prod.* 321, 128996. doi:10.1016/j.jclepro.2021.128996
- Wu, X., Ruan, R., Du, Z., and Liu, Y. (2012). Current Status and Prospects of Biodiesel Production from Microalgae. *Energies* 5 (8), 2667–2682.
- Yang, J., Jiang, J. C., and Zhang, N. (2011). *Oil Productivity Capabilities of Several Microalgae Strains in Different Cultivation Methods*. Nanjing, China: Biomass Chemical Engineering 45 (02), 15–19.
- Zakryś, B., Milanowski, R., and Karnkowska, A. (2017). Evolutionary Origin of *Euglena*. *Adv. Exp. Med. Biol.* 979, 3–17. doi:10.1007/978-3-319-54910-1_1
- Zeng, M., Hao, W., Zou, Y., Shi, M., Jiang, Y., Xiao, P., et al. (2016). Fatty Acid and Metabolomic Profiling Approaches Differentiate Heterotrophic and Mixotrophic Culture Conditions in a Microalgal Food Supplement 'Euglena'. *BMC Biotechnol.* 16 (1), 49. doi:10.1186/s12896-016-0279-4
- Zimorski, V., Rauch, C., van Hellemond, J. J., Tielens, A. G. M., and Martin, W. F. (2017). The Mitochondrion of *Euglena Gracilis*. *Adv. Exp. Med. Biol.* 979, 19–37. doi:10.1007/978-3-319-54910-1_2

Conflict of Interest: The authors declare that the research was conducted in the absence of any commercial or financial relationships that could be construed as a potential conflict of interest.

Publisher's Note: All claims expressed in this article are solely those of the authors and do not necessarily represent those of their affiliated organizations, or those of the publisher, the editors and the reviewers. Any product that may be evaluated in this article, or claim that may be made by its manufacturer, is not guaranteed or endorsed by the publisher.

Copyright © 2022 Chen, Chen, Zhang, Qin, He, Zheng, Zhao, Lei and Wang. This is an open-access article distributed under the terms of the Creative Commons Attribution License (CC BY). The use, distribution or reproduction in other forums is permitted, provided the original author(s) and the copyright owner(s) are credited and that the original publication in this journal is cited, in accordance with accepted academic practice. No use, distribution or reproduction is permitted which does not comply with these terms.



Comparative Proteomics Reveals Evidence of Enhanced EPA Trafficking in a Mutant Strain of *Nannochloropsis oculata*

Wan Aizuddin Wan Razali^{1,2}, Caroline A. Evans¹ and Jagroop Pandhal^{1*}

¹Department of Chemical and Biological Engineering, University of Sheffield, Sheffield, United Kingdom, ²Faculty of Fisheries and Food Science, Universiti Malaysia Terengganu, Terengganu, Malaysia

OPEN ACCESS

Edited by:

Kanhaiya Kumar,
Norwegian University of Science and
Technology, Norway

Reviewed by:

Hongli Cui,
Shanxi Agricultural University, China
Elvis Chua,
The University of Queensland,
Australia
Anandita Pal,
University of North Carolina at Chapel
Hill, United States

*Correspondence:

Jagroop Pandhal
j.pandhal@sheffield.ac.uk

Specialty section:

This article was submitted to
Industrial Biotechnology,
a section of the journal
Frontiers in Bioengineering and
Biotechnology

Received: 17 December 2021

Accepted: 29 March 2022

Published: 12 May 2022

Citation:

Wan Razali WA, Evans CA and
Pandhal J (2022) Comparative
Proteomics Reveals Evidence of
Enhanced EPA Trafficking in a Mutant
Strain of *Nannochloropsis oculata*.
Front. Bioeng. Biotechnol. 10:838445.
doi: 10.3389/fbioe.2022.838445

The marine microalga *Nannochloropsis oculata* is a bioproducer of eicosapentaenoic acid (EPA), a fatty acid. EPA is incorporated into monogalactosyldiacylglycerol within *N. oculata* thylakoid membranes, and there is a biotechnological need to remodel EPA synthesis to maximize production and simplify downstream processing. In this study, random mutagenesis and chemical inhibitor-based selection method were devised to increase EPA production and accessibility for improved extraction. Ethyl methanesulfonate was used as the mutagen with selective pressure achieved by using two enzyme inhibitors of lipid metabolism: cerulenin and galvestine-1. Fatty acid methyl ester analysis of a selected fast-growing mutant strain had a higher percentage of EPA (37.5% of total fatty acids) than the wild-type strain (22.2% total fatty acids), with the highest EPA quantity recorded at 68.5 mg/g dry cell weight, while wild-type cells had 48.6 mg/g dry cell weight. Label-free quantitative proteomics for differential protein expression analysis revealed that the wild-type and mutant strains might have alternative channeling pathways for EPA synthesis. The mutant strain showed potentially improved photosynthetic efficiency, thus synthesizing a higher quantity of membrane lipids and EPA. The EPA synthesis pathways could also have deviated in the mutant, where fatty acid desaturase type 2 (13.7-fold upregulated) and lipid droplet surface protein (LDSP) (34.8-fold upregulated) were expressed significantly higher than in the wild-type strain. This study increases the understanding of EPA trafficking in *N. oculata*, leading to further strategies that can be implemented to enhance EPA synthesis in marine microalgae.

Keywords: *Nannochloropsis*, eicosapentaenoic acid (EPA), ethyl methanesulfonate (EMS) random mutagenesis, cerulenin, galvestine-1, label-free quantitative (LFQ) proteomic analysis

INTRODUCTION

Eicosapentaenoic acid (EPA) is an omega-3 long-chain polyunsaturated fatty acid (LC-PUFA) found in fish oils and well documented to provide multiple benefits for human health (Shi et al., 2021). However, the use of fish oils as a source of EPA has many issues, including declining fish stocks, contamination by heavy metals and organic pollutants, unpleasant smells, and unsuitability for vegetarian markets (Kaye et al., 2015; Shi et al., 2021). Therefore, there is a drive to obtain omega-3 (ω -3) directly from their primary source, microalgae. Microalgae are well-known sources of various high-value bioactive compounds, including LC-PUFA, carotenoids, proteins, polyphenols,

phytosterols, hormones, and vitamins (Levasseur et al., 2020). Due to their metabolic capacity and relatively simple structures, microalgae are considered the most efficient “plants” on Earth in capturing sunlight energy (Vecchi et al., 2020), growing up to five to ten times faster than land plants (Adamczyk et al., 2016) and enhancing biological carbon fixation by utilizing carbon dioxide in the atmosphere (Kumar et al., 2010). A few microalgae species have been identified to synthesize relatively high amounts of LC-PUFA, although efforts to increase titers are increasingly sought to improve economic viability.

Nannochloropsis species are relatively small (2–4 μm diameter) unicellular microalgae that contain ovoid- or cup-shape chloroplasts (Iwai et al., 2015). Reports demonstrate species with a relatively high concentration of ω -3 EPA of up to 40 mg/g dry cell weight (DCW) (Chini Zittelli et al., 1999; Kent et al., 2015). In an *N. oceanica* strain, 30% of total fatty acids (TFA) were quantified as ω -3 EPA (Kaye et al., 2015), while an *N. oculata* strain produced the highest reported percentage at 40% EPA of TFA (Renaud et al., 1991). However, in order to increase EPA production in microalgae, it is important to understand its synthesis from a metabolic and spatial perspective.

Fatty acid (FA) synthesis occurs in chloroplasts, producing up to 18 carbon chain lengths, whereafter EPA is reportedly elongated in the endoplasmic reticulum (ER) prior to being imported back into the chloroplasts for incorporation into the thylakoid membrane polar lipid, monogalactosyldiacylglycerol (MGDG) (Sayanova et al., 2017). The initial synthesis of FAs is catalyzed by fatty acid synthase (FAS) and acetyl CoA carboxylase (Chaturvedi and Fujita, 2006). Ketoacyl-acyl carrier protein (ACP) synthase (KAS) is responsible for the elongation of medium-chain FAs up to C16:0 in the chloroplasts (Nofiani et al., 2019). The elongation of C18:0 to EPA in *Phaeodactylum* consists of two routes, while one route is suggested for *N. gaditana* (Dolch et al., 2017). The main suggested route for *N. gaditana* is via the ω -6 pathway (Janssen et al., 2020). The process consists of step-wise conversion from C16:0 to C18:0, C18:1 Δ^9 , C18:2 $\Delta^{9,12}$ (linoleic acid), C18:3 $\Delta^{6,9,12}$ (γ -linolenic acid), C20:3 $\Delta^{8,11,14}$ (dihomo- γ -linolenic acid), C20:4 $\Delta^{5,8,11,14}$ (arachidonic acid), and C20:5 $\Delta^{5,8,11,14,17}$ (EPA) via the actions of Δ^0 -elongase (ELO), stroma stearyl-ACP Δ^9 -desaturase (SAD), or an ER fatty acid desaturase (ERA9FAD), Δ^{12} FAD, ERA6FAD, Δ^6 -ELO, ERA5FAD, and ER ω 3FAD, respectively (Dolch et al., 2017).

A study on *N. oceanica* found that during the exponential growth phase, MGDG, phosphatidylcholine (PC), and phosphatidylglycerols (PG) are the main membrane polar lipids (Han et al., 2017). However, in the thylakoid membranes, MGDG contributes approximately 40–50% to these membrane lipids. A study in the same strain found that 60% of MGDG is enriched EPA (Junpeng et al., 2020). In a related strain, *N. gaditana*, it was found that EPA resides in membrane polar lipids during the exponential phase but translocates to neutral lipids, triacylglycerols (TAG), toward the end of batch growth (Janssen et al., 2019). An attempt to discover the relationship between EPA and membrane polar lipids in *N. gaditana* demonstrated that MGDG production relies on EPA supplied from the ER to the chloroplast (Dolch et al., 2017).

Hence, EPA synthesis and translocation is a highly regulated and complex process. This means that cell engineering approaches to increase EPA content in microalgae have resulted in limited success. Gene overexpression studies in *N. oceanica* included targeting Δ^{12} desaturase (Kaye et al., 2015), Δ^6 desaturase (Yang F. et al., 2019), Δ^6 elongase (Shi et al., 2021), and combined Δ^5 , Δ^9 , and Δ^{12} desaturase (Poliner et al., 2018). Most of these genetically engineered strains showed a slight increase in the EPA content compared to the wild-type strain, although overexpression of Δ^6 desaturase even reduced the EPA percentage of TFA in total lipids compared to the wild type (Yang F. et al., 2019).

When highly regulated metabolic pathways are involved or genetic tool kits for engineering specific strains are not available, random mutagenesis with selection or screening is an attractive option to generate desirable phenotypes. Gamma-ray (Park et al., 2021), UV ray (Bougaran et al., 2012), ^{137}Cs - γ nuclear radiation (Lu et al., 2020), atmospheric and room temperature plasma (ARTP) (Zhang et al., 2014), heavy-ion irradiation-mediated mutagenesis (Song et al., 2018), and chemicals (Chaturvedi et al., 2004; Wu et al., 2019) are mutagens that have successfully been used to generate genetic diversity in microalgae. The challenge then becomes the implementation of successful selection strategies. Enzyme inhibitors have shown increasing promise as a strategic selection method following random mutagenesis (Chaturvedi et al., 2004; Chaturvedi and Fujita, 2006; Li et al., 2015; Fu et al., 2016). This is because enzyme inhibitors can limit the function of a single targeted enzyme without influencing the operation of other enzymes (Kukorelli et al., 2013; Arora et al., 2020).

FAS inhibitors have been used previously to select microbial strains with re-wired metabolism that have enhanced the accumulation of specific FAs. For example, cerulenin, a FAS inhibitor, and an oxidant triphenyl tetrazolium chloride (TTC) were used in combination to screen *Mortierella alpina* mutant cells to select strains with higher arachidonic acid (ARA) content, an omega-6 component that has the same carbon length as EPA (Li et al., 2015). TTC is an oxidant that can be ingested and oxidized to a red molecule by living cells. Cerulenin changed the FA composition by affecting FA degradation in a *Colwellia psychrerythraea* strain, where C16:1 was reduced by 12.6% of TFA, and DHA increased by 7.8% of TFA (Wan et al., 2016). Mutants with a standard growth rate in the presence of cerulenin were identified as having higher FAS activity than wild-type species (Li et al., 2015). Cerulenin was also reported to interfere with the lipid metabolism, which caused the increase in ARA in *Mortierella alpina* from 39 to 45.6% of TFA (Li et al., 2015). Cerulenin is also effective in inhibiting β -ketoacyl-ACP synthase (KAS I, KAS II, and KAS III) (Meng et al., 2018). Cerulenin was also reported as the first treatment followed by N-methyl-N-nitrosoguanidine (NTG) mutagenesis in *Shewanella electrodiphila*, where the EPA increased from 20 to 30 mg/g DCW (Zhang and Burgess, 2017). However, equivalents are not known for selecting long-chain FA changes in microalgae species. Another inhibitor previously tested to screen for *N.*

oculata mutants with elevated lipid content was acetyl-CoA carboxylase (ACCase) inhibitor Quizalofop. The quantity of EPA in the mutant was not measured; however, the level of ARA in the mutant was considerably higher than the wild-type strain (Moha-León et al., 2019). Considering the EPA content in MGDG; MGDG synthase inhibitors could also be used as selective agents. MGDG synthase inhibitors include citraconic anhydride, N-ethylmaleimide, ortho-phenanthroline, S-nitroso-N-acetyl penicillamine, and galvestine-1 (Coves et al., 1988; Marechal et al., 1995; Boudière et al., 2012). Although galvestine-1 was shown to effectively inhibit MGDG synthase, reducing MGDG quantity in *Arabidopsis thaliana* (Botté et al., 2011), no previous research has been conducted to investigate the effect of galvestine-1 on MGDG synthesis in microalgae.

In this study, *N. oculata* was selected as it can synthesize relatively high levels of EPA content compared to other microalgae species (Adarme-Vega et al., 2012), and previous studies have successfully applied random mutagenesis in this strain (Chaturvedi et al., 2004; Chaturvedi and Fujita, 2006). Moreover, *N. oculata* is one of the most widely used microalgae in aquaculture hatcheries demonstrating industrial robustness (Babuskin et al., 2014). This work reports a random mutagenesis approach by chemical mutagen ethyl methanesulfonate (EMS), combined with the combined use of two specific enzyme inhibitors of lipid metabolism, cerulenin, and galvestine-1, for the first time, for screening the mutants. The initial aim was to develop an improved *N. oculata* strain that is able to produce enhanced EPA levels compared to wild-type cells without comprising growth rates and subsequently apply cross-species quantitative proteomics to generate specific hypotheses on how metabolism has been re-wired to generate the phenotype.

MATERIALS AND METHODS

Algal Strain and Culture Conditions

N. oculata (849/1) was provided by the Culture Center of Algae and Protozoa (CCAP, Scotland) and was cultured in modified f/2 medium composed of the following: 33.5 g/L artificial seawater salt (Ulramarine Synthetic Sea Salt, Waterlife, United Kingdom), 75 mg/L NaNO₃, 4.35 mg/L NaH₂PO₄·2H₂O, enriched with trace elements (4.16 mg/L Na₂EDTA, 3.16 mg/L FeCl₃·6H₂O, 0.01 mg/L CuSO₄·5H₂O, 0.022 mg/L ZnSO₄·7H₂O, 0.01 mg/L CoCl₂·6H₂O, 0.18 mg/L MnCl₂·4H₂O, and 0.006 mg/L Na₂MoO₄·2H₂O) and vitamins (0.1 mg/L thiamine HCl (B₁), 0.005 mg/L cyanocobalamin (B₁₂), and 0.0005 mg/L biotin). The stock culture was maintained in a 500 ml conical flask and bubbled with 0.22 µm filtered air for aeration and mixing. The incubation temperature was 20°C, and the light intensity was 100 to 110 µmol m⁻² s⁻¹ range for 12-h light/dark cycles. The stock culture was refreshed every week to maintain the culture in the exponential growth phase. All the chemicals used in this study were purchased from Sigma-Aldrich, unless otherwise stated.

Mutagenesis and Selection of EPA-Overproducing Mutant Strains

Cells in the early exponential phase (7×10^6 cells/ml) were refreshed with sterile f/2 medium and centrifuged at $3,488 \times g$ for 5 min, and EMS was added to make a final concentration of 100, 200, and 300 mM. The cells were mutagenized for 60 min, washed three times with sterile f/2 medium, and allowed to grow for seven days before initiating selection. The sub-lethal chemical concentrations were determined by measuring optical density (OD) at 595 nm using a GENios Tecan plate reader (TECAN, Germany) (Supplementary Figures S1A, S1B). Equal cell numbers (2×10^7 cells/ml) were spread uniformly on f/2 medium plates (1.5% w/v) containing 50 µM of cerulenin. After three weeks of incubation at 20°C, the number of resistant colonies from each plate was counted. The countable plate was selected, and each colony was inoculated in a 3 ml f/2 medium containing 50 µM of cerulenin in 24-well plates placed under light ($130 \mu\text{mol m}^{-2} \text{s}^{-1}$). The absorbance was measured at 595 nm on the plate reader for ten days. The mutant colonies with a higher optical density at 595 nm than wild-type *N. oculata* were selected and cultured in f/2 media containing a higher concentration of cerulenin, 60 µM. The three fastest-growing mutants were selected for the next stage using an MGDG synthase inhibitor, galvestine-1 (Botté et al., 2011; Boudière et al.,

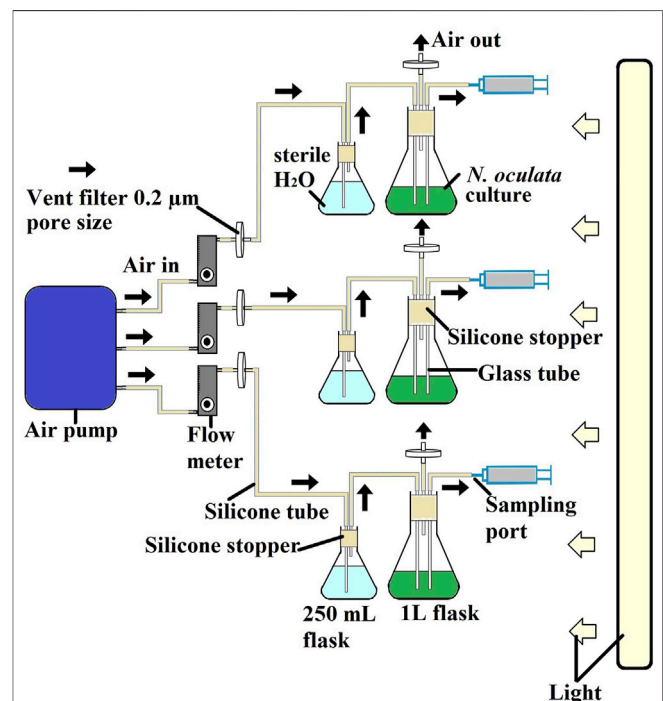


FIGURE 1 | Schematic diagram of experimental cultivation system for selecting two-time points for LFQ proteomics experiments. All experiments were conducted at room temperature at 20°C and illuminated under $130 \mu\text{mol m}^{-2} \text{s}^{-1}$ under a 12-h/12-h (day/night) cycle. The cultures were subjected to continuous filtered aeration and bubbled at 2 L/min.

2012). The mutants were cultured in *f/2* media containing 10 μM of galvestine-1, and the fastest-growing mutant was selected for further studies. The growth rate (μ/day) was calculated as follows:

$$\mu = \frac{\ln(W_f/W_i)}{\Delta t},$$

where W_f and W_i were the final and initial OD at 595 nm, respectively, and Δt was the cultivation time in the day (Chiu et al., 2009). The mutant with the fastest growth and EPA content was selected for further studies.

Photobioreactor Setup for Selecting Two-Time Points for Label-Free Quantification Proteomics Experiments

N. oculata cultures were set up in triplicates using a 1-L flask photobioreactor system (Figure 1). The starting optical density at 595 nm was 0.3. All flasks were maintained at a temperature of 20°C and illuminated under 130 $\mu\text{mol } \mu\text{mol m}^{-2} \text{ s}^{-1}$ under a 12-h/12-h (day/night) cycle. Cultures were subjected to continuous filtered aeration and bubbling at 2 L/minute. The algal culture was aerated and mixed in the same way as the pre-culture. The optical density at 595 nm, and pH was monitored using a portable pH meter LAQUA B-712 (Horiba, Moulton Park, United Kingdom) every day throughout the experiments over a 12-day period. The samples were taken on days 3, 5, 7, 9, and 12 for wild-type *N. oculata* and days 2, 5, 7, 9, and 12 for the selected mutant *N. oculata*. The sample was taken on day 2, considering that the selected mutant grew faster than the wild-type *N. oculata*. Then 5 ml culture was taken for each analysis of DCW, proteins and chlorophylls, lipids, and EPA. A sample volume of 50 ml was taken for LFQ proteomics analysis. The samples were collected in three biological replicates for all analyses. All the sampling was done during the dark period, 2 h before the light period started. Harvested cells pellets (centrifuge at 4,415 $\times g$ for 5 min) were washed with phosphate-buffered saline and centrifuged (11,337 $\times g$ for 2 min) prior to storage at -20°C, while proteomic samples were kept at -80°C until further analysis.

Analytical Methods

Cell pellets were freeze-dried for 24 h by using a freeze drier (LyoQuest, Telstar, United Kingdom), and the DCW was measured using a microbalance (CPA2P, Sartorius, OH, United States).

Chlorophylls and proteins were quantified by using the spectrophotometric method in triplicate (Chen and Vaidyanathan, 2013). In brief, cell pellets were lysed by glass bead-beating using a cell disruptor (DISRUPTOR GENIE®, United States). The samples were saponified by heating at 100°C for 30 min (Digital Drybath, Thermo Fisher Scientific, United Kingdom). An aliquot was used for protein assay, and the remaining sample was mixed with chloroform and methanol (ratio 2:1, v/v), vortexed (2 min), centrifuged (12,000 $\times g$, 2 min), and the top aqueous phase was used for chlorophyll assays.

Methods for quantification of nitrate (Collos et al., 1999) and phosphate (Strickland and Parsons, 1972) in an *f/2* medium were adapted from previous studies. The supernatants from the harvested samples were kept after filtration through a 0.22 μm syringe filter (Millex, United Kingdom). The concentrations of nitrate and phosphate were determined for each sampling day by measuring the absorbance values at 220 and 885 nm, respectively.

Determination of Fatty Acid Methyl Ester

The method for determining fatty acid methyl ester (FAME) was adapted from a previous study with slight modifications (Griffiths et al., 2010). In brief, 300 μl toluene was added to the 2 ml Eppendorf tube containing wet microalga biomass. The Eppendorf tube then vortexed for 2 min and continued by adding 300 μl of sodium methoxide. The mixture was then transferred into the 2 ml glass vial and incubated at 80°C for 20 min. After that, the vials were kept a while at room temperature for cooling. 300 μl boron trifluoride was added to the vial and incubated again at 80°C for 20 min. In the meantime, 300 μl HPLC-grade water and 600 μl hexane were added to other prepared empty 2 ml Eppendorf tubes. The mixture in the vial was transferred to the prepared Eppendorf tube containing water and hexane and then centrifuged at 7,916 $\times g$ for 10 min. Then, 750 μl organic phase (upper hexane-toluene layer) was transferred to a new labeled Eppendorf tube. The extract was then dried using inert nitrogen gas and stored at -20°C until further analysis.

A measure of 80 μl of toluene was added to the extracted sample and vortexed to ensure that all the extracts were well-mixed. The mixture was then centrifuged at 11,337 $\times g$ for 2 min. A quantity of 35 μl FAME was transferred into a GC vial and was identified and quantified using a Thermo Finnigan TRACE 1300 GC-FID System (Thermo Fisher Scientific, United Kingdom) onto a TR-FAME capillary column (25 m \times 0.32 mm \times 0.25 μm). Then 1 μl of Supelco 37 Component FAME Mix standard was injected as a reference and 1 μl of sample volume was injected in split injection mode at 250°C. The split flow was 75 ml/min. The GC was operated at a constant flow of 1.5 ml/min helium. The temperature program was started at 150°C for 1 min, followed by temperature ramping at 10°C/min to a final temperature of 250°C, and held constant at 250°C for 1 min. The total analysis time was 15 min, and the standard 37 FAME was injected for all 24 samples to ensure that the system was working correctly.

The peak identities were ascertained for data interpretation and analysis using external Supelco 37 Component FAME Mix standard, C16, C18, and C20:5 standards. The peak areas were integrated using a chromatography data system, Chromeleon 7 software (Thermo Fisher Scientific, United Kingdom). Based on the known amount value of 37 FAME components, C16, C18, and C20:5 standards, a ratio was established between the area and the amount. The amount of unknown components in the microalgal extract was then determined by their peak areas and calculated in mg/g DCW.

The quantification of FAME within TAG and polar lipids was adapted from a previous study with modifications (Janssen et al., 2019). In brief, total lipids were extracted from wet microalgae

biomass using a standard Folch method (Axelsson and Gentili, 2014). C17:0 PC and C17:0 triheptadecanoin were added to the samples prior to the extraction of total lipids. Then 2 ml of methanol was added to the samples and homogenized for 1 min using a homogenizer Ultra-Turrax® T 25 (Ultra-Turrax, Germany), followed by the addition of 4 ml of chloroform and further homogenization for 2 min. The total lipid solution was filtered through a 0.22- μ m filter (SLS, United Kingdom). The cell debris were rinsed with 2 ml fresh solvent (chloroform and methanol, ratio 2:1, v/v) and combined with the previous filtrate. 2 ml of potassium chloride solution (8.8 g/L) was added, and the mixture vortexed for 1 min. The top solvent layer was discarded, and the bottom solvent was evaporated using a centrifugal evaporator (Jouan, United States). The total lipid extract was dissolved in chloroform and spotted onto a thin liquid chromatography (TLC) plate along with TAG and polar lipid standard. The mobile phase used was iso-hexane, ether, and formic acid (80:20:2, v/v/v) to separate the TAG and polar lipids. The TAG and polar lipid fractions were removed by scraping the silica into test tubes, followed by re-extraction using iso-hexane and ether (1:1, v/v) and chloroform, methanol, and distilled water (5:5:1, v/v/v), respectively. A total of 1 ml of toluene and 2 ml of 1% sulfuric acid in methanol were added for transesterification, and the samples were incubated at 50°C for 16 h. Then 5 μ l FAME sample was identified and quantified using a GG, Agilent 6890 model (Agilent Technologies, United States), onto a CP-Wax (52 CB) GC column (30 m \times 0.25 mm \times 0.15 μ m). In total, 1 μ l of FAME standard (Nu-Chek Prep, United States) was injected as a reference, and 1 μ l of sample volume was injected in split injection mode at 230°C. The GC was operated at a constant flow of 1 ml/min hydrogen. The temperature program was started at 170°C for 3 min, followed by temperature ramping at 4°C/min to a final temperature of 220°C and held constant at 220°C for 10 min. Peak areas were integrated using a chromatography data system, Agilent Chemstation software (Agilent Technologies, United States). The EPA of TFA in TAG and polar lipids were determined by their peak areas and quantified against the added internal standard.

Statistical Analysis for Growth Profiles

Statistical differences for all growth profiles data, percentages, and quantification of EPA were performed by Student's *t*-test, with three replicates (*n* = 3). Array 1 was for wild-type *N. oculata*, and array 2 was for the selected mutant *N. oculata*; 2-tails and type 1 were set using Microsoft® Excel® for Microsoft 365 MSO (Washington, United States). The data were considered significant when the *p*-value was at least <0.05.

Protein Extraction and Quantification

In total, 50 ml microalga samples were harvested at early exponential phase on day 2 and late exponential phase on day 12 for the selected mutant *N. oculata*, and at early exponential phase on day 3 and late exponential phase on day 12 for wild-type *N. oculata* in triplicates via centrifugation at 4,000 *g* for 15 min at 4°C. The supernatants were discarded, and the samples were kept at –80°C until further use. Crude proteins were extracted as described previously

(Posch, 2014). A measure of 1 ml of lysis buffer (2% sodium dodecyl sulfate (SDS), 40 mM Tris base, and 60 mM dithiothreitol (DTT)) and 10 μ l Halt™ protease inhibitor cocktail (Thermo Fisher Scientific, United Kingdom) were added to the samples pellets and put on ice for thawing. 500 μ l glass beads having sizes 425–600 μ m were added to the sample tubes. The samples were vortexed for 20 cycles (30 s vortexed and then 30 s cooled on ice). Lysed samples were centrifuged at 18,000 \times *g* for 5 min at 4°C. The samples were kept on ice for 30 min until the foam subsided. The supernatants (crude protein) were transferred to 1.5-ml protein LoBind Eppendorf tubes and stored at –80°C.

Two sets of samples were purified from lipids, pigments, and other contaminants by using a protein 2D clean-up kit (GE Healthcare, United States) by following the manufacturer's protocols. The 2D cleaned-up protein pellets were resuspended in 100 μ l urea buffer (8 M urea, 100 mM Tris-HCl (pH 8.5), and 5 mM DTT) for 1D SDS-PAGE and in-solution digestion, respectively. The samples were incubated in a sonication bath for 5 min to dissolve protein into the urea buffer. Then, the proteins samples were quantified using a NanoDrop™ 2000 (Thermo Fisher Scientific, United Kingdom) spectrophotometer. The spectrophotometer setting was set as 1 mg/ml equals to 1 optical density reading at 280 nm. BSA was used to create a standard curve with urea buffer (1, 0.8, 0.6, 0.4, 0.2, 0.1 mg/ml) (Supplementary Figures S2A, S2B).

In-Solution Digestion

A measure of 50 μ g protein was transferred to a sterile protein LoBind Eppendorf tube. Protein samples were diluted to 10 μ l with urea buffer and incubated at 37°C for 30 min. Then 1 μ l 100 mM iodoacetamide was added and incubated in the dark for 30 min at 20°C to S-alkylate the protein samples. A measure of 2 μ g Trypsin/Lys-C mix (Promega, United States) was added to the protein solutions and incubated for 3 h at 37°C; 75 μ l (50 mM Tris-HCl (pH 8.5), 10 mM CaCl₂) was added to the protein solution and incubated overnight (16–20 h) at 37°C for trypsin digestion (Hitchcock et al., 2016); 5 μ g of protein samples were run via 1D SDS-PAGE to confirm that the protein was digested; 4.8 μ l (5% of the total protein solution) of 10% TFA was added to the protein solution to stop the digestion process. Pierce® C18 spin columns (Thermo Fisher Scientific, United Kingdom) were used for desalting the samples by following the manufacturer's protocols; and 60 μ l purified protein samples were collected from the spin columns. The samples were dried using a vacuum evaporator (Concentrator plus, Eppendorf, Germany) and stored at –80°C for further mass spectrometry analysis.

LC-MS/MS for Proteomics

LC-MS/MS was performed and analyzed by nano-flow liquid chromatography (U3000 RSLCnano, Thermo Fisher Scientific, United Kingdom) coupled to a hybrid quadrupole-orbitrap mass spectrometer (Q Exactive HF, Thermo Fisher Scientific, United Kingdom). Peptides were separated on an Easy-Spray C18 column (75 μ m \times 50 cm) using a 2-step gradient from 3% solvent A (0.1% formic acid in water) to 10% B over 5 min and

then to 50% solvent B (0.1% formic acid in 80% acetonitrile) over 180 min at 300 nl min⁻¹, 40°C. The mass spectrometer was programmed for data-dependent acquisition with 10 product ion scans (resolution 30,000, automatic gain control 1e5, maximum injection time 60 ms, isolation window 1.2 Th, normalized collision energy 27, and intensity threshold 3.3e4) per full MS scan (resolution 120,000, automatic gain control 1e6, maximum injection time 60 ms) with a 20-s exclusion time. Each sample was run in triplicate.

Protein Identification and Generation of Label-Free Quantification Quantitative Proteomic Data

Mass spectrometry data in *.raw format were processed using MaxQuant v. 1.6.17 integrated with the MaxLFQ algorithm. Proteins were identified by searching the MS data files against an in-house constructed *Nannochloropsis* proteome database. The proteome database is a combination of *Nannochloropsis* strains downloaded from NCBI (December 2020), UniProt (December 2020), and extracted from the MSPnr100 database (Tran et al., 2016). The total number of protein sequences in the combined *Nannochloropsis* proteome database was 16,270 proteins. A 1% FDR was applied, and default settings were applied. Search parameters specified tryptic cleavage, carbamidomethyl-Cys (fixed modification), Met oxidation, and protein N-terminal acetylation (variable modifications) with a maximum of two missed cleavages. In total, seven amino acids were set at the minimum peptide length.

Statistical Analysis of Label-Free Quantification Quantitative Proteomic Data

Statistical analyses were performed using LFQ-Analyst (<https://bioinformatics.erc.monash.edu/apps/LFQ-Analyst/>), whereby the LFQ intensity values were used for protein quantification. The missing values were replaced by values drawn from a normal distribution of 1.8 standard deviations and a width of 0.3 for each sample (Perseus-type). Differential expression analysis was performed using protein-wise linear models combined with empirical Bayesian statistics using the Bioconductor package limma. The Benjamini–Hochberg method of FDR correction was used. The adjusted *p*-value cutoff was set at 0.05, and the log2 fold change cutoff was set at 1.

RESULTS AND DISCUSSION

Growth Profiles of Wild-Type and M1 Mutant *N. oculata*

Mutants of wild-type *N. oculata* were randomly generated using EMS, and desirable phenotypes were first screened using the FAS inhibitor, cerulenin, with the hypothesis that traits such as alternative mechanisms or increased synthesis of EPA and TAG would be selected. A total of 82 colonies were counted on f/2 medium agar plates with 200 mM EMS and

50 μ M cerulenin after three weeks of incubation (**Supplementary Figure S3B**); 100 and 300 mM EMS concentrations generated too many or no mutants, respectively (**Supplementary Figures S3A, S3C**). Finally, 200 mM EMS was selected as the concentration to generate mutants. All 82 colonies from the 200 mM EMS agar plate were isolated and grown in 24-well plates in f/2 media containing 50 μ M cerulenin and cultivated under 130 μ mol m⁻² s⁻¹ illumination (12-h light/dark cycle) at 20°C. After ten days, 20 mutants were recorded with a higher OD (595 nm) than the wild-type *N. oculata* cells (**Figure 2A**). These 20 mutants were subsequently cultivated in f/2 media containing a higher cerulenin concentration, 60 μ M, and three mutants (labeled M1, M18, and M45) that reached the highest OD (595 nm) were further selected for the next stage of screening using galvestine-1 (**Figure 2B**). The selected three mutants were cultured for ten days in an f/2 medium containing 10 μ M galvestine-1, the sub-lethal concentration for wild-type *N. oculata*. M1 and M18 mutants' growth rate per day were statistically significantly higher than wild-type cells, with a *p*-value less than 0.01 (**Figure 3**). The FA profile of M1, M18, and M45 mutant strains showed elevated levels of EPA compared to the wild-type strain (**Supplementary Figures S4, S5**). M1 mutant recorded the highest EPA (33.6%) of TFA in total lipids compared to other mutants and the wild-type strain. Hence, M1 mutant *N. oculata* was selected for further growth and FAME analysis before LFQ proteomics analysis.

Wild-type and M1 mutant *N. oculata* cells were cultivated in 1-L flasks in triplicate at 150 μ mol m⁻² s⁻¹ under a 12-h/12-h (day/night) cycle for 12 days. The growth performance, nutrient uptake, and changes of FAME profiles were monitored in order to select two-time points where EPA and TAG synthesis were at an optimum level and where differential protein expression analysis would provide insight into novel cellular adaptations. Even though the M1 mutant showed a higher growth rate than wild-type cells during screening in 24-well plates, and despite a higher final DCW in the mutant strain (day 12), no statistical significance was observed (**Figures 4A,B**). However, chlorophyll *a* in the M1 mutant was statistically significantly higher than wild-type cells from day 7 onward (**Figure 4C**), suggesting more efficient light-harvesting and photosynthetic capability than the wild-type.

The pH was recorded around 7–8.5 for both the wild-type and M1 mutant cultures, suggesting that the aeration was sufficient to control the pH at the optimum conditions. A pH of 8.5 was previously reported to be optimal for *Nannochloropsis* sp. growth (Khatoun et al., 2014).

Nitrate and phosphate concentrations in the f/2 medium were also monitored during growth. Although these macronutrients are essential for microalgae growth (Hu and Gao, 2006), their uptake rates could affect the FA profiles (Rasdi and Qin, 2015). Nitrate was rapidly consumed until day 5 and was below detection limits by day 9 of culturing (**Figure 4D**). The M1 mutant displayed a faster nitrate uptake, with the nitrate concentration decreasing in the media from 330 to 255 μ M during two days of culturing, whereas the nitrate in the wild-

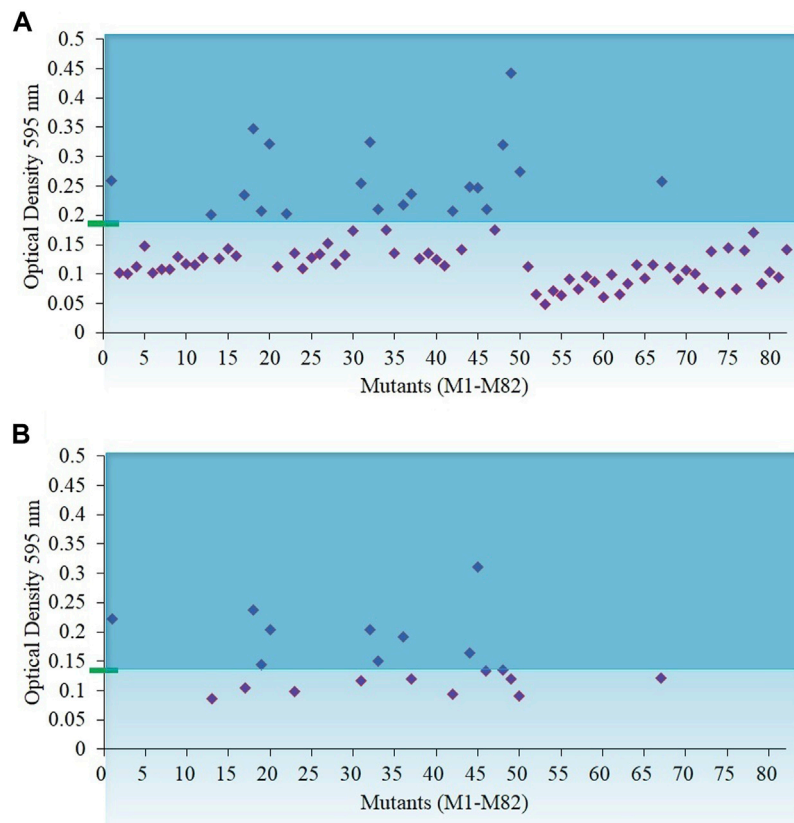


FIGURE 2 | Biomass density of *N. oculata* mutants after eight days of growth in f/2 medium containing cerulenin. The initial optical density of 595 nm was 0.15 at day 0 **(A)** Optical density of 82 *N. oculata* mutants in 50 µM cerulenin. **(B)** Optical density of 20 *N. oculata* mutants containing 60 µM cerulenin. The cultures were incubated at 130 µmol m⁻²s⁻¹, 20°C, under a 12-h/12-h (light/dark) cycle. The green rectangle and blue line represent the biomass density of the wild-type *N. oculata*.

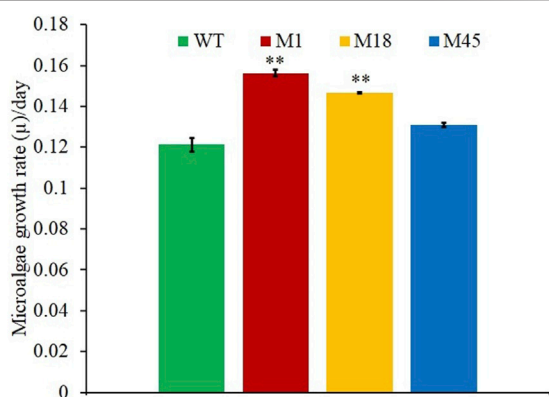


FIGURE 3 | Growth rate per day comparisons of mutants M1, M18, M45, and wild-type *N. oculata*, incubated at 130 µmol m⁻²s⁻¹, 20°C, under a 12-h/12-h (light/dark) cycle and 160 RPM shaking for ten days. Mean ± standard deviation is shown ($n = 3$) and t -tests determine the statistical significance ($p < 0.05$ [*]; $p < 0.01$ [**]; and $p < 0.001$ [***]) of the M1 mutant strain compared to the wild-type strain.

type *N. oculata* flasks reduced from 330 to 299 µM within three days. Nitrate limited condition in the f/2 medium after day 9 could trigger the synthesis of neutral lipids, as observed in

several oleaginous microalgae (Burch and Franz, 2016; Tran et al., 2016; Remmers et al., 2017).

Similarly, phosphate concentrations reduced to below detectable limits during growth within 2 and 3 days for M1 mutant and wild-type cells, respectively (Figure 4D). Overall, the nitrate and phosphate results suggested that the wild-type and M1 mutant strains had completed their batch growth over nine days of culturing.

Fatty Acid Methyl Ester Profiles

The compositions of FAME in wild-type and M1 mutant *N. oculata* cells were measured by GC-FID analysis. In terms of percentage composition (Figures 5A,B), the major FAME observed in both wild-type and M1 mutant strains were C16:0 (palmitic acid), C16:1 (palmitoleic acid), and C20:5 (EPA). The other FAMES identified were C14:0 (myristic acid), C18:0 (stearic acid), C18:1 (oleic acid), C18:2 (linoleic acid), C18:3 (α/γ-linolenic-acid), and C20:4 (arachidonic acid/eicosatetraenoic acid). At the early exponential phase, the percentage of EPA was highest at 37.5 and 22.2% for M1 mutant and wild-type *N. oculata*, respectively (Figures 5A,B). This percentage of EPA in M1 mutant *N. oculata* was considerably higher than quantified at the mid-exponential phase in a previous *N. oceanica* study (Poliner et al., 2018). The higher percentage of EPA of TFA in

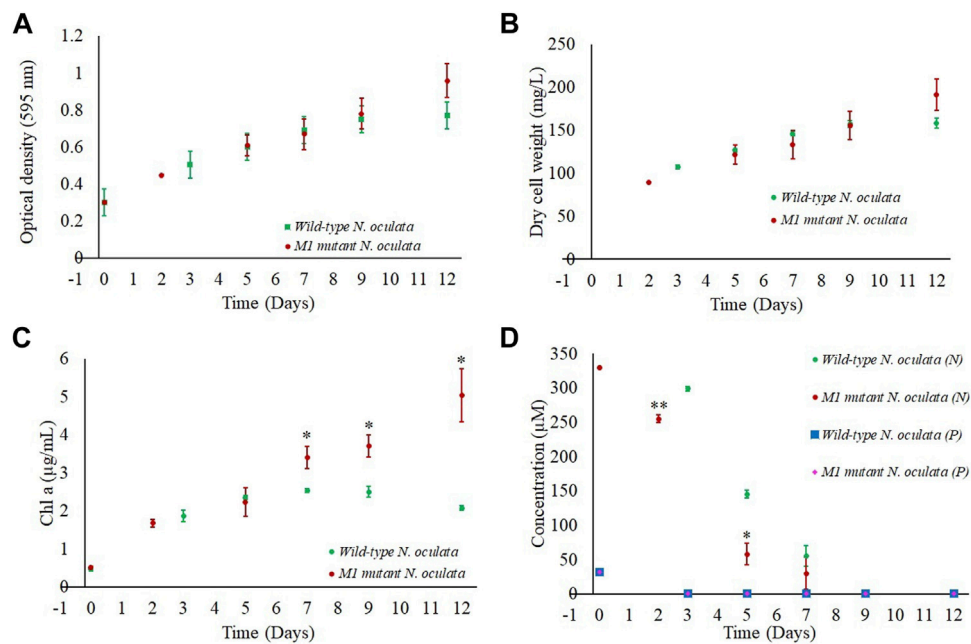


FIGURE 4 | Growth profiles for wild-type and M1 mutant *N. oculata* cultivated in 1-L flasks under $150 \mu\text{mol m}^{-2} \text{s}^{-1}$, 20°C , and aerated bubbling for mixing and carbon source for 12 days. **(A)** Growth curves illustrated by optical density at 595 nm and **(B)** DCW. Comparison of wild-type and M1 mutant *N. oculata* over 12 days of culturing for **(C)** chlorophyll concentration and **(D)** phosphate (P) and nitrate (N) uptake profiles. Mean \pm standard deviation is shown ($n = 3$) and *t*-tests determine the statistical significance ($p < 0.05$ [*]; $p < 0.01$ [**]; and $p < 0.001$ [***]) of the M1 mutant strain compared to the wild-type strain.

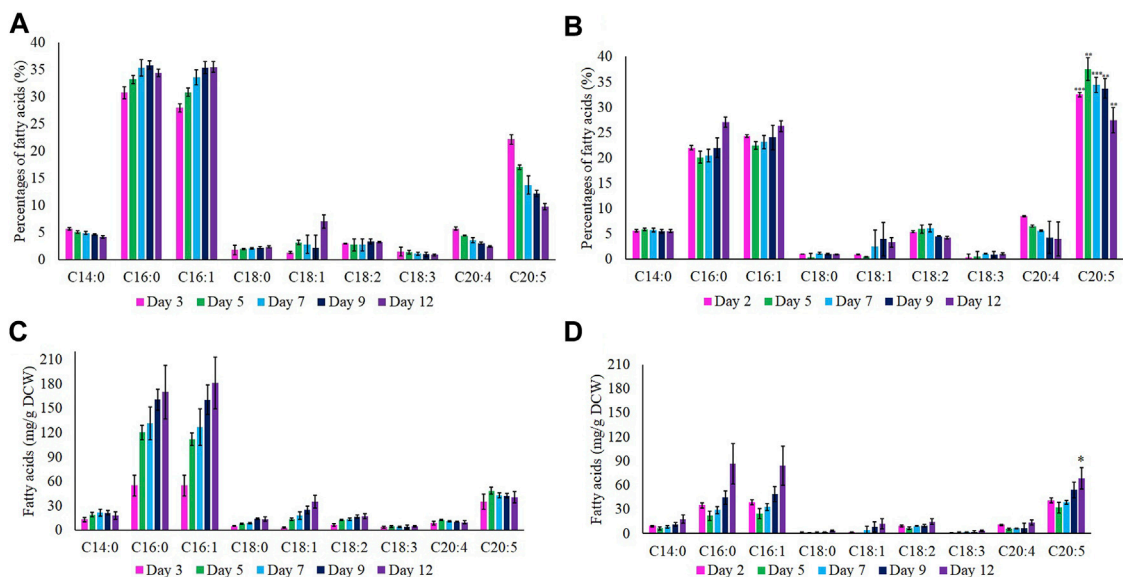


FIGURE 5 | Percentages (%) of fatty acids at day 12. **(A)** Wild-type and **(B)** M1 mutant *N. oculata*. Quantification (mg/g) of fatty acids at day 12. **(C)** Wild-type and **(D)** M1 mutant *N. oculata*. Mean \pm standard deviation is shown ($n = 3$) and *t*-tests determine the statistical significance ($p < 0.05$ [*]; $p < 0.01$ [**]; $p < 0.001$ [***]) for EPA content in the M1 mutant strain compared to the wild-type strain.

total lipids at the early exponential phase in both strains suggested that EPA synthesis prefers favorable growth conditions. A previous study showed the chlorophyll *a* was directly proportional to MGDG quantity, where day 8 (exponential

phase) had a higher chlorophyll *a* and MGDG quantity than day 12 in *N. salina* (Koh et al., 2019).

Total FAME amounts (mg/g DCW) were calculated by referring to the standard FAME intensity, as shown in **Figures**

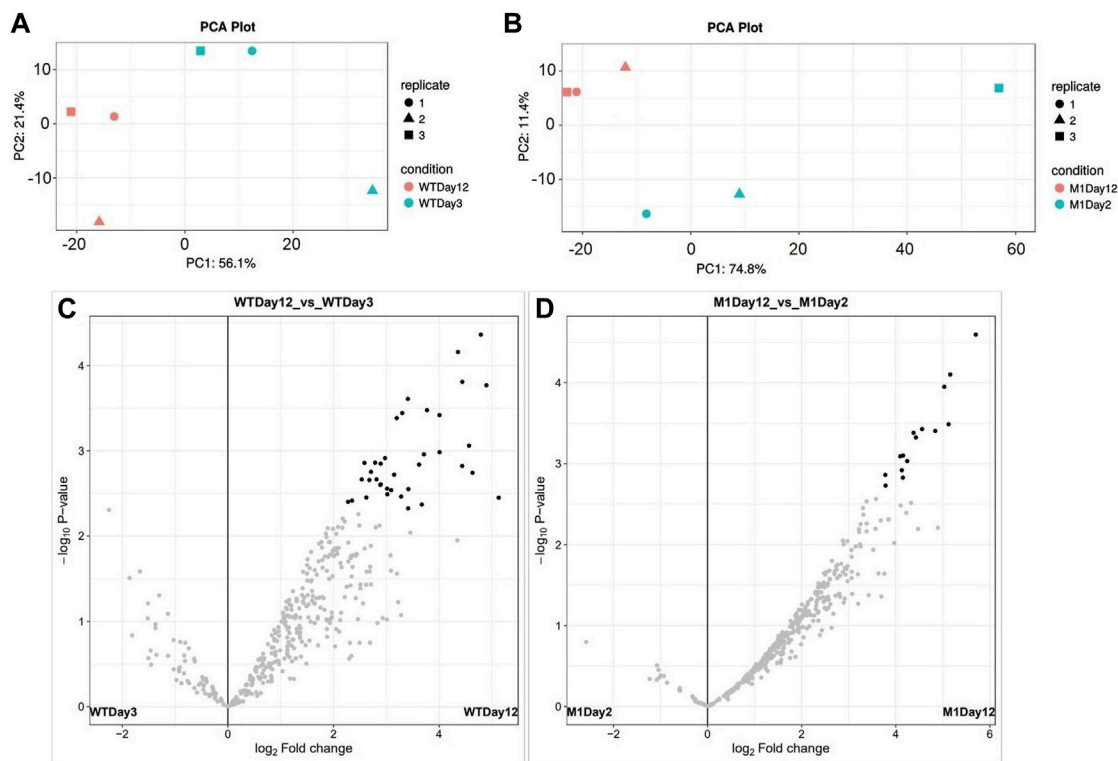


FIGURE 6 | PCA plots show 12 samples clustered by biological replicates: **(A)** Wild-type *N. oculata* samples day 3 (light blue) and day 12 (pink) and **(B)** M1 mutant *N. oculata* samples day 2 (light blue) and day 12 (pink). Volcano plots show the significant protein distributions in wild-type **(C)** and M1 mutant **(D)** *N. oculata*.

5C,D. The EPA concentration increased gradually after day 2 and reached the highest (68.5 mg/g DCW) on day 12 for M1 mutant *N. oculata*. In contrast, the wild-type strain showed the highest EPA of 48.6 mg/g DCW on day 5. The EPA quantity recorded in M1 mutant was considerably higher than those in previous studies. Shi et al. (2021) recorded EPA at 40 and 45 mg/g DCW on day 4 for a wild-type *N. oceanica* strain and a $\Delta 6$ elongase overexpression strain, respectively. Yang et al. (2019a) described a $\Delta 6$ desaturase overexpression *N. oceanica* strain with 62.35 mg/g DCW on day 10, which decreased to around 50 mg/g DCW on day 13, while the wild-type strain had approximately 40 mg/g DCW on day 10, which increased to around 60 mg/g DCW on day 13.

An increase in neutral lipids (C16:0 and C16:1) was observed during batch growth in both strains and, as predicted, were inversely proportional to the nutrients level in the *f/2* medium. The percentage of neutral lipids gradually increased for both wild-type and M1 mutant strain and reached the highest (35 and 27%, respectively) on day 12. Nutrient limitation is known to induce TAG accumulation as a stress response, and a previous study showed that C16:0 reached the maximum of around 40% of TFA under these conditions (Wei and Huang, 2017). In order to further investigate the increase in EPA content, two time-points were chosen based on the FAs profiles between TAG and EPA, EPA percentages, and absolute EPA quantifications. The two most significant time points were when the EPA content was measured at the highest and the lowest level compared to C16:0

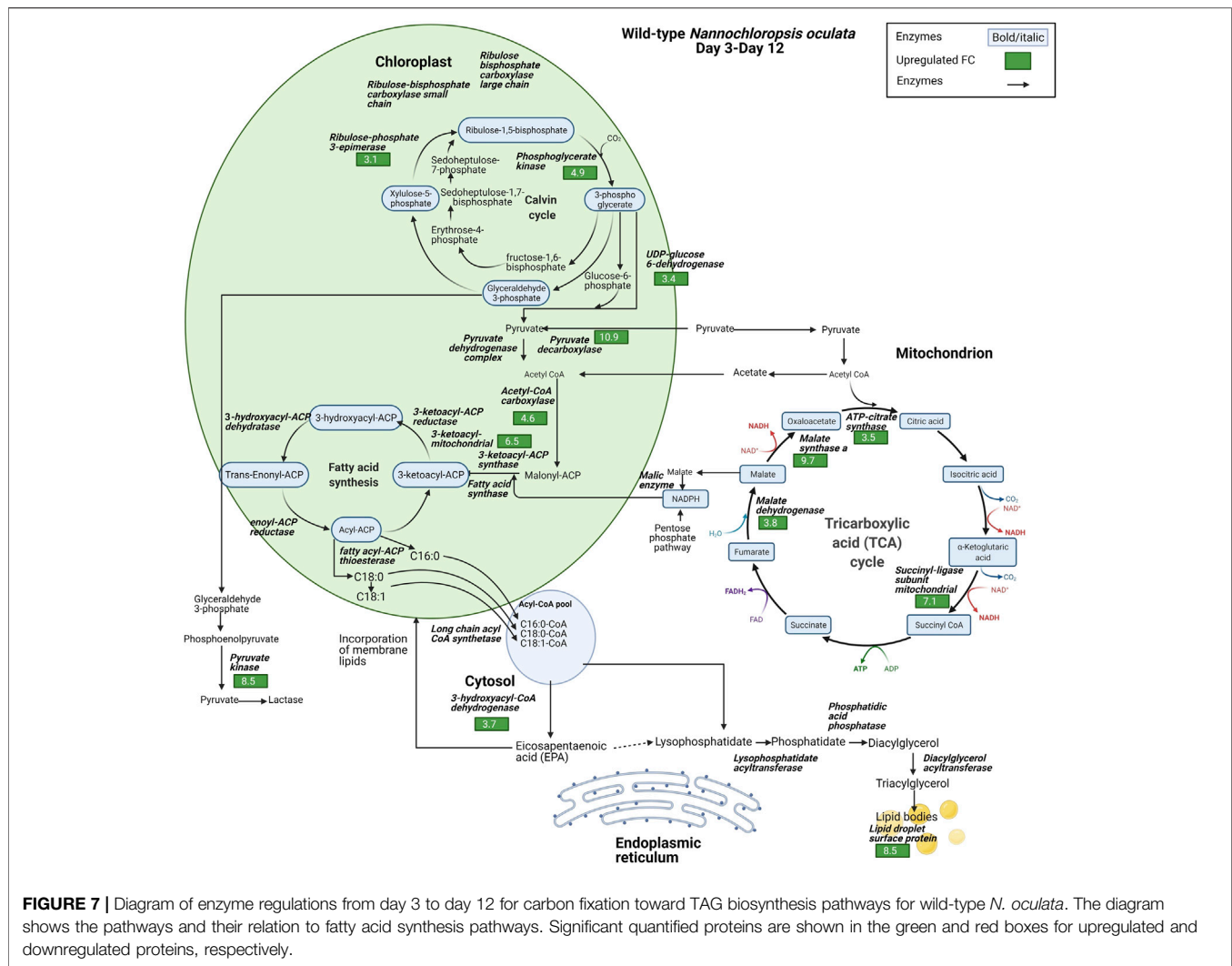
and C16:1 components. Hence, the early exponential phase (days 2 and 3) and late exponential phase (day 12) were chosen as two-time points for LFQ proteomics analysis.

LFQ Proteomic Overview

LFQ proteomics was conducted at two-time points, early and late exponential phase, in order to investigate differential protein expression patterns that could contribute to higher EPA synthesis in our M1 mutant *N. oculata* strain. Days 2 and 3 were selected for the early exponential phase in M1 mutant and wild-type *N. oculata*, respectively, while day 12 was selected for the late exponential phase.

MS/MS scans for LFQ experiments for wild-type and M1 mutant *N. oculata* in early exponential phase and end of exponential phase samples are shown in **Supplementary Table S1**. The UniProt proteome database (December 2020) contains only 219 proteins for *N. oculata*, although there are 15,363 proteins for *Nannochloropsis gaditana*. Hence, for this study, a *Nannochloropsis* genus proteome database was created by combining sequences from UniProt, NCBI, and MSPnr100 (Tran et al., 2016; Wang and Jia, 2020). The combined proteome database of the *Nannochloropsis* genus consisted of 16,270 protein sequences, and our identification process relied on matching identical peptide sequences.

A PCA plot for sample clustering and volcano plots displaying significantly differentially quantified proteins are shown in **Figure 6**. The number of protein groups with

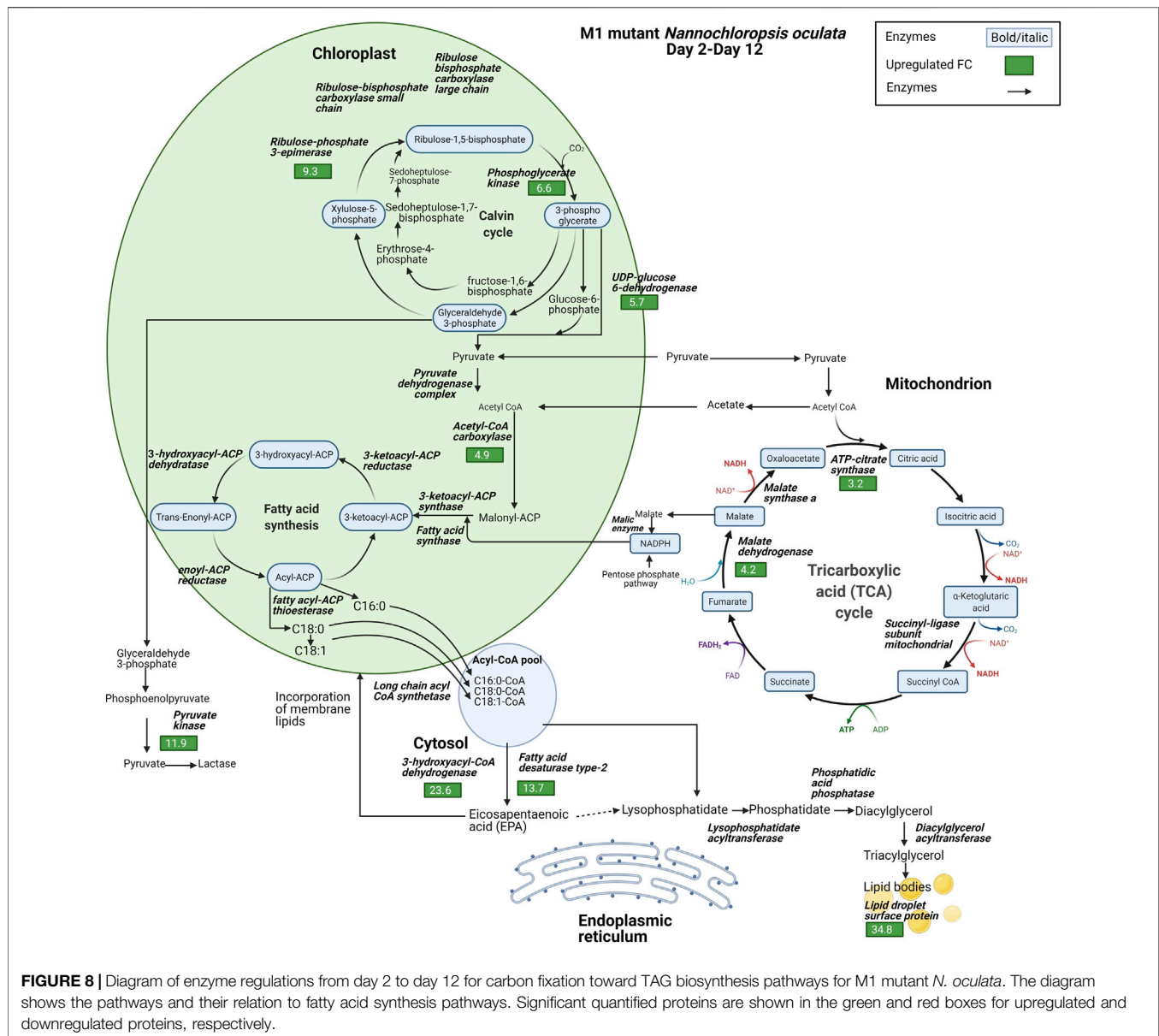


at least two peptides was 422 and 434 for wild-type and M1 mutant *N. oculata*, respectively. The numbers of significant proteins (> 2 -fold changes and p -value < 0.05) were 123 and 103 for the wild-type and M1 mutant strain, respectively (Supplementary Tables S2, S3). Differential protein analyses will be discussed in relation to growth and stress, photosynthetic systems, FA, TAG and EPA synthesis, and membrane remodeling. The data were analyzed by comparing the early versus late exponential phase for the wild-type strain and subsequently the same switch in the growth phase in the mutant strain, following a discussion on how these differed.

Photosynthetic System

Photosynthesis is the process where microalgae convert and store solar energy as energy-rich organic molecules as a source of energy for microalgae cell growth. Cell growth is associated with cell division and complex biochemical processes, including cell cycle machinery, cytoskeletal elements, chromosomes, and membranes (Kagiali et al., 2017). In this study, cell division protein was a 10.4-fold increased in abundance in the M1

mutant strain from early to late exponential phase, while 7-fold upregulated in the wild-type strain. The higher cell division protein level in the M1 mutant could be related to faster cell division in the M1 mutant than in the wild-type strain. During autotrophic growth, microalgae cells utilize light energy harvested by chlorophyll molecules and convert carbon dioxide and water to carbohydrates and oxygen. Photosynthetic (rates) are different across microalgae species and culture conditions (Costache et al., 2013). The photosynthetic mechanism is organized in organelles, thylakoids, and stroma in chloroplasts. Different species of microalgae have specific preferences for the chlorophyll-binding group. For example, Chl *a/b*-binding proteins found in Viridiplantae (LHCA/LHCB), fucoxanthin Chl *a/c*-binding protein (FCP or LHCF) in diatoms, and LHCR in red algae (Carbonera et al., 2014). *N. oculata* has only chlorophyll *a* as a primary photosynthetic pigment and one plastid (Szabó et al., 2014). Maximizing the light absorption of light-harvesting antennae is a sustainable way to increase the growth rate and biomass production of microalgae cells (Szabó et al., 2014). Photosynthetic proteins in the M1



mutant were mostly upregulated from the early to late exponential phase, including photosystem I iron-sulfur center (22.3-fold increase), photosystem I subunit III (15.7-fold increase), chlorophyll A-B-binding protein (13.6-fold increase), photosystem II 12 kDa extrinsic protein (12.9-fold increase), photosystem II 11 kDa protein (12.4-fold increase), photosystem II CP43 reaction center protein (5.6-fold increase), chloroplast light-harvesting protein isoform 4 (5.5-fold increase), photosystem I reaction center subunit IV (5.2-fold increase), and photosystem I reaction center subunit XI (4.6-fold increase). The only photosynthetic protein found to increase significantly in the wild-type strain during the period of exponential phase was photosystem I reaction center subunit IV (3-fold increase). The results suggest that a faster photosynthetic efficiency was achieved in the M1 mutant. This

increase in photosynthetic proteins led to the hypothesis that more NADPH could be available for reductive synthesis processes in the M1 mutant, hence contributing to the high efficiency of EPA synthesis. This is because the availability of NADPH has previously been shown to increase the reaction velocity of NADPH-requiring enzymes involved in FA synthesis such as acetyl-CoA carboxylase (ACCase) and ATP citrate lyase (ATP: CL) (Mühlroth et al., 2013). In *N. salina*, the increase in NADPH has recently been linked to higher FA synthesis (Jeon et al., 2021).

Rieske (2f3-2s) region protein and ferredoxin are common proteins involved in electron transfer chains in the mitochondria and chloroplast for NADPH generation (Fukuyama, 2004; Kameda et al., 2011). Rieske (2f3-2s) region protein was 52-fold upregulated, and ferredoxin was 29.7-fold upregulated in the

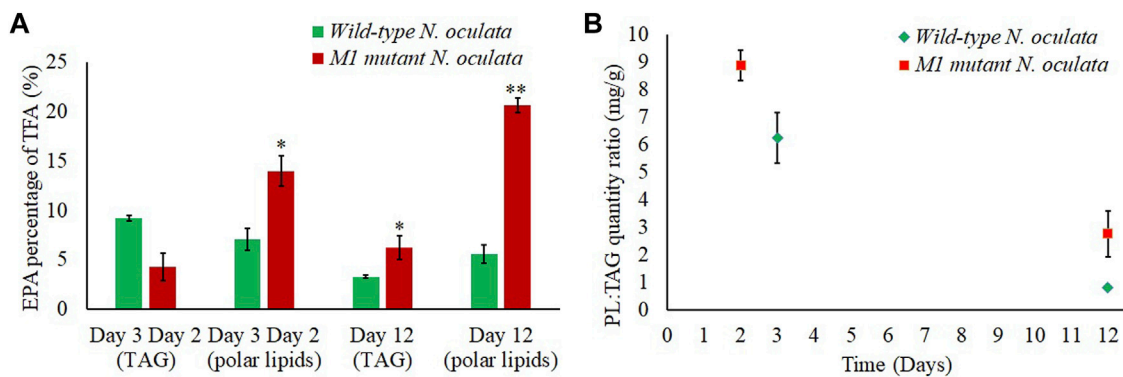


FIGURE 9 | Fatty acid content. **(A)** EPA percentages (%) of TFA in polar lipids and TAG at day 2 (M1 mutant), day 3 (wild-type), and day 12 (wild-type and M1 mutant) *N. oculata*. **(B)** Polar lipid (PL):TAG quantity ratio (mg/g) at day 2 (M1 mutant), day 3 (wild-type), and day 12 (wild-type and M1 mutant) *N. oculata*. Mean \pm standard deviation is shown ($n = 3$) and t-tests determine the statistical significance ($p < 0.05$ [*]; $p < 0.01$ [**]; $p < 0.001$ [***]) for EPA content in the M1 mutant strain compared to the wild-type strain.

M1 mutant strain, from early exponential to late exponential phase. However, Rieske (2f3-2s) region protein and ferredoxin were not significantly regulated in wild-type strain over the same growth phase.

FA, TAG, and EPA Synthesis

The proteomic data highlighted the differences in the relative expression of key enzymes associated with the synthesis of FAs, TAG, and EPA. Lipid droplet surface protein (LDSP) was identified as one of the most differentially expressed proteins in both wild-type and M1 mutant *N. oculata*. LDSP are novel proteins associated with lipid droplets in *Nannochloropsis* sp., previously linked to the TAG storage compartment (Vieler et al., 2012). Moreover, lipid droplet structure is highly dynamic and involved in various cellular processes, such as regulation of energy homeostasis, remodeling of membranes and signaling (Zienkiewicz and Zienkiewicz, 2020). LDSP was 8.5-fold upregulated from day 3 to day 12 in wild-type *N. oculata* (Figure 7). However, LDPS was 34.8-fold upregulated in M1 mutant *N. oculata* from day 2 to day 12 (Figure 8). The increase in LDPS in wild-type cells was expected where the C16:0 quantity (mg/g DCW) had a 2.7-fold increase at the late exponential phase. This level of change was seen previously in *N. oculata* cells (Tran et al., 2016), where LDSP was 2.4-fold upregulated after 11 days of cultivation. However, the much larger fold change LDSP in the M1 mutant strain implies a major alteration in cell regulation that leads to an increase in FAs.

In contrast, acyl-coenzyme A dehydrogenase (ACAD) had a 35-fold increase in the wild-type strain compared to a smaller 9.2-fold increase in the M1 mutant. ACAD is responsible for FA β -oxidation in mitochondria (Tan and Lee, 2016), and therefore a reduced rate of FA degradation in the mutant relative to the wild-type appears probable. Acetyl CoA carboxylase (ACCase) converts acetyl-CoA to malonyl-CoA and serves as a carbon donor for FA chain extension in the plastid (Li et al., 2014). 3-hydroxyacyl-CoA dehydrogenase (HCDH) is involved in FA metabolism and catalyzes the reduction of 3-hydroxyacyl-CoA to 3-oxoacyl-CoA. Short- and medium-chain HCDH reside in the

mitochondrial matrix, while long-chain HCDH is part of the membrane-associated multifunction protein in the mitochondria and peroxisome (Xu et al., 2014). HCDH had a 23.6-fold increase in the M1 mutant, significantly higher than the increase observed in wild-type *N. oculata* (3.7-fold). Although several enzymes are involved in FA elongation, for example, 3-oxoacyl-reductase, 3-hydroacyl-CoA dehydratase and enoyl-CoA reductase (process palmitic acid (C16:0) to stearic acid (C18:0)) (Kapase et al., 2018), these proteins were not detected here.

Fatty acid desaturase type 2 (FAD2) was 13.7-fold upregulated in the M1 mutant strain, whereas it was not significantly regulated in the wild-type strain. FAD2 enzyme is part of integral membrane protein in ER, responsible for the biological switch from oleic acid (C18:1) to linoleic acid (C18:2) (Dar et al., 2017). This finding suggests that FAD2 protein may be actively involved in EPA synthesis in the ER. On the contrary, 3-ketoacyl-mitochondrial was 6.5-fold upregulated in wild-type and not differentially expressed in the M1 mutant. With reference to the UniProt database and gene ontology functions, 3-ketoacyl-CoA thiolase and 3-ketoacyl-mitochondrial share a similar function that enables acetyl-CoA C-acyltransferase activity. 3-ketoacyl-CoA thiolase enzyme is involved in FA β -oxidation, whereas acetyl-CoA is catalyzed in the chloroplast for FA synthesis (Osumi et al., 1992; Kechasov et al., 2020). Another protein with a potential role is 3-ketoacyl-ACP synthase (KAS), an important enzyme involved in FA elongation in plastids (Chaturvedi and Fujita, 2006; Morales-Sánchez et al., 2016).

Three possible spatial routes have been previously suggested for EPA synthesis (Mühlroth et al., 2013): 1) chloroplast \rightarrow acetyl-CoA \rightarrow ER \rightarrow membrane lipids, 2) chloroplast \rightarrow mitochondrion \rightarrow acetyl-CoA \rightarrow ER \rightarrow membrane lipids, and 3) chloroplast \rightarrow citrate \rightarrow acetyl-CoA \rightarrow ER \rightarrow membrane lipids. Due to the nature of proteomics data with missing proteins, it is difficult to confirm which route is likely for *N. oculata* wild-type and M1 mutant cells. However, based on differential protein expression, it is possible that wild-type *N. oculata* undertook the first or second route when 3-ketoacyl-mitochondrial was 6.5-fold upregulated in the chloroplast-mitochondria pathway. In the M1 mutant, EPA

synthesis may be maximized outside the chloroplast; in the cytosol and ER. The EPA may be incorporated into membrane lipids during the exponential phase. The highest EPA was quantified on day 12 with 68.5 mg/g DCW, suggesting that EPA could be translocated from membrane lipids to TAG at the end exponential phase period.

Membrane Lipid Remodeling

Lipidomic analyses have shown increased accumulation of neutral lipids during nitrogen-deprived conditions, in addition to a decrease in the level of membrane lipids (Han et al., 2017; Liang et al., 2019). This implies that cellular responses responsible for TAG accumulation are related to the modification of membrane lipids. Under nitrogen constraint, MGDG was the predominant membrane lipid component that was reduced in *N. oceanica*, which was proposed as a protective mechanism to prevent the degradation of the thylakoid and chloroplast envelope membranes (Han et al., 2017). The membrane lipid composition was also remodeled under phosphate starvation in the same strain, where phospholipids were replaced by betaine lipids (Murakami et al., 2020). Our methodology of combined mutagenesis and selection with galvestine-1 also remodeled membrane lipids in *N. oculata*. A high level of LDSP expression in M1 mutant *N. oculata* cells suggests that the membrane lipids were modified and converted to TAG at significantly higher levels, and hence EPA that is usually enriched in membrane lipids were transported to TAG. Both biomass growth and FA synthesis compete for the same substrates, acetyl-CoA and NADPH; hence substrate availability is a rate-limiting step in balancing growth rate and FA accumulation (Tan and Lee, 2016). Acetyl-CoA conversion is derived from the glycolytic process, and pyruvate kinase (PK) and enolase are identified as primary photosynthate (Tran et al., 2016). Carbohydrates in the form of pyruvate are converted to acetyl-CoA to supply the cell with energy and reduced carbon (Mühlroth et al., 2013). Acetyl-CoA also is a key metabolite in both the TCA cycle in the mitochondrion and FA synthesis in the chloroplast (Mühlroth et al., 2013). Phosphoglucosyltransferase is involved in chrysolaminarin synthesis and functions as a critical node in sharing the carbon precursors between carbohydrate and lipid metabolism (Yang Y.-F. et al., 2019) and had an 11.5-fold increase in the M1 mutant cells, whereas it was only 4-fold upregulated in the wild-type strain. A higher carbohydrate metabolic process in M1 mutant might suggest a higher quantity of membrane lipids is present in M1 mutant cells, which could be used to facilitate higher EPA quantities, than in the wild-type strain.

Identifying protein changes that contribute to membrane lipid composition remains challenging because a relatively small number of membrane proteins have been sequenced and studied in algae (Garibay-Hernández et al., 2017). MGDG and DGDG are the major lipids of the photosynthetic membrane, where MGDG is synthesized in the chloroplast (Dolch et al., 2017), and DGDG is synthesized in both chloroplast and ER (Cecchin et al., 2020). The formation of membrane polar lipids is intrinsically linked to photosynthesis, for example, there is evidence to suggest that the light-harvesting complex may stabilize the MGDG component in thylakoids membranes (Han et al., 2017). A greater membrane lipid content in M1 mutant could be due to more efficient light-harvesting within

photosynthesis. As a result, during the early exponential phase growth, more EPA might be produced. When the mutant cells approached the end of the exponential phase, the lower MGDG led to more EPA being translocated outside the membrane lipid, resulting in a greater overall EPA level. The cell wall architecture of *N. oculata* is primarily composed of polysaccharides, with 68% as glucose subunits (Scholz et al., 2014). Through glycolysis, glucose sourced from the cell wall can be oxidized to generate energy that can be diverted to FA synthesis. In a recent study, during nitrogen starvation, the *N. oceanica* cell wall altered from two layers with a thickness of 32.9 nm to a one-layer cell wall with a thickness of 37.8 nm (Roncaglia et al., 2021). This implied that the cell wall degradation might also contribute to FA synthesis.

Cellular Location of EPA

The absolute quantity and percentage composition of FAME were also investigated within the TAG and polar lipid cellular components, as the proteomic data implied the EPA in M1 mutant *N. oculata* could be translocated outside the chloroplast. The ratio of polar membrane lipids to TAG (Figure 9B) decreased on day 12, indicating that TAG was accumulated in both wild-type and M1 mutant strains at the end of 12 days of culturing. In the M1 mutant, the EPA percentage in TAG was 1.9-fold higher than the wild-type strain (Figure 9A). This provided additional evidence for the enhanced translocation of EPA to TAG in the M1 mutant strain and could be linked to the elevated abundance of LDSP in this strain. The EPA percentage in M1 mutant was 2-fold and 3.7-fold increased at the early and late exponential phase, respectively, compared to the wild-type strain. The enhanced EPA quantity in the M1 mutant is likely linked to the relatively high synthesis of polar lipids, particularly MGDG. A high MGDG content was preserved until the late exponential phase and could be due to the abundance of polar lipids synthesized in the M1 mutant compared to the wild-type strain. Hence, the EPA could be partially translocated to TAG at day 12 in M1 mutant, while in the wild-type strain, the EPA and MGDG could be converted to TAG, resulting in a lower EPA. In the FAs pathways, membrane lipids were previously observed to translocate to TAG, especially under limited nutrient conditions (Janssen et al., 2020). Hence, the EPA could be translocated with membrane lipids to TAG with a structural modification to saturated FA. On the contrary, the EPA could be directly translocated to TAG from the ER (Ma et al., 2016); however, this mechanism is less studied in the literature.

CONCLUSION

A novel strategy to increase EPA productivity in *N. oculata* was devised using a combination of EMS-induced random mutagenesis and screening with FAS chemical inhibitors, which have not been applied together previously. LFQ proteomic analysis was conducted and highlighted metabolic pathways that could contribute to enhance EPA synthesis and alternative translocation routes between a selected mutant strain and the wild-type strain. Overall, the developed method could be used as an alternative to genetic engineering methods for increasing EPA production, although cell engineering targets were highlighted for further improvement studies. Increasing

EPA productivity in industrially relevant microalgal strains increases the sustainable manufacturing of this LC-PUFA.

DATA AVAILABILITY STATEMENT

The original contributions presented in the study are included in the article/**Supplementary Material**, further inquiries can be directed to the corresponding author.

AUTHOR CONTRIBUTIONS

WR, CE, and JP planned the project. WR performed all the experiments. CE prepared and performed LC-MS/MS for LFQ proteomics. WR, CE, and JP wrote the manuscript.

FUNDING

The authors would like to acknowledge funding from the Malaysian government, Universiti Malaysia Terengganu, and

the Natural Environment Research Council (NE/PO16820/1). This work was supported by the University of Sheffield, United Kingdom, and the Ministry of Higher Education, Malaysia.

ACKNOWLEDGMENTS

The authors are thankful to Dr. Eric Maréchal for providing galvestine-1 for this project and Dr. Josselin Noirel for assisting in combining and filtering all the *Nannochloropsis* proteomes for LFQ proteomics analysis. The authors also thank Katarzyna Okurowska for culturing and biochemical assay methodologies.

SUPPLEMENTARY MATERIAL

The Supplementary Material for this article can be found online at: <https://www.frontiersin.org/articles/10.3389/fbioe.2022.838445/full#supplementary-material>

REFERENCES

- Adamczyk, M., Lasek, J., and Skawińska, A. (2016). CO₂ Biofixation and Growth Kinetics of *Chlorella Vulgaris* and *Nannochloropsis Gaditana*. *Appl. Biochem. Biotechnol.* 179, 1248–1261. doi:10.1007/s12010-016-2062-3
- Adarme-Vega, T. C., Lim, D. K. Y., Timmins, M., Vernen, F., Li, Y., and Schenk, P. M. (2012). Microalgal Biofactories: a Promising Approach towards Sustainable omega-3 Fatty Acid Production. *Microb. Cel Fact.* 11, 96. doi:10.1186/1475-2859-11-96
- Arora, N., Yen, H.-W., and Philippidis, G. P. (2020). Harnessing the Power of Mutagenesis and Adaptive Laboratory Evolution for High Lipid Production by Oleaginous Microalgae and Yeasts. *Sustainability* 12, 5125. doi:10.3390/su12125125
- Axelsson, M., and Gentili, F. (2014). A Single-step Method for Rapid Extraction of Total Lipids from green Microalgae. *PLoS One* 9, e89643–20. doi:10.1371/journal.pone.0089643
- Babuskin, S., Krishnan, K. R., Babu, P. A. S., Sivarajan, M., and Sukumar, M. (2014). Functional Foods Enriched with marine Microalga *Nannochloropsis Oculata* as a Source of ω -3 Fatty Acids. *Food Technol. Biotechnol.* 52, 292–299.
- Balzano, S., Villanueva, L., De Bar, M., Sahonero Canavesi, D. X., Yildiz, C., Engelmann, J. C., et al. (2019). Biosynthesis of Long Chain Alkyl Diols and Long Chain Alkenols in *Nannochloropsis* Spp. (Eustigmatophyceae). *Plant Cel Physiol* 60, 1666–1682. doi:10.1093/pcp/pcz078
- Botté, C. Y., Deligny, M., Roccia, A., Bonneau, A.-L., Saïdani, N., Hardré, H., et al. (2011). Chemical Inhibitors of Monogalactosyldiacylglycerol Synthases in *Arabidopsis thaliana*. *Nat. Chem. Biol.* 7, 834–842. doi:10.1038/nchembio.658
- Boudière, L., Botté, C. Y., Saidani, N., Lajoie, M., Marion, J., Bréhélin, L., et al. (2012). Galvestine-1, a Novel Chemical Probe for the Study of the Glycerolipid Homeostasis System in Plant Cells. *Mol. Biosyst.* 8, 2023–2035. doi:10.1039/c2mb25067e
- Bougaran, G., Rouxel, C., Dubois, N., Kaas, R., Grouas, S., Lukomska, E., et al. (2012). Enhancement of Neutral Lipid Productivity in the microalga *IsochrysisaffinisGalbana*(T-Iso) by a Mutation-Selection Procedure. *Biotechnol. Bioeng.* 109, 2737–2745. doi:10.1002/bit.24560
- Burch, A. R., and Franz, A. K. (2016). Combined Nitrogen Limitation and Hydrogen Peroxide Treatment Enhances Neutral Lipid Accumulation in the marine Diatom *Phaeodactylum Tricornutum*. *Bioresour. Technol.* 219, 559–565. doi:10.1016/j.biortech.2016.08.010
- Carbonera, D., Agostini, A., Di Valentin, M., Gerotto, C., Basso, S., Giacometti, G. M., et al. (2014). Photoprotective Sites in the Violaxanthin-Chlorophyll a Binding Protein (VCP) from *Nannochloropsis Gaditana*. *Biochim. Biophys. Acta (Bba) - Bioenerg.* 1837, 1235–1246. doi:10.1016/j.bbabbio.2014.03.014
- Cecchin, M., Berteotti, S., Paltrinieri, S., Vigliante, L., Iadarola, B., Giovannone, B., et al. (2020). Improved Lipid Productivity in *Nannochloropsis Gaditana* in Nitrogen-Replete Conditions by Selection of Pale green Mutants. *Biotechnol. Biofuels* 13, 1–14. doi:10.1186/s13068-020-01718-8
- Chaturvedi, R., and Fujita, Y. (2006). Isolation of Enhanced Eicosapentaenoic Acid Producing Mutants of *Nannochloropsis Oculata* ST-6 Using Ethyl Methane Sulfonate Induced Mutagenesis Techniques and Their Characterization at mRNA Transcript Level. *Phycological Res.* 54, 208–219. doi:10.1111/j.1440-1835.2006.00428.x
- Chaturvedi, R., Uppalapati, S. R., Alamsjah, M. A., and Fujita, Y. (2004). Isolation of Quiazalofop-Resistant Mutants of *Nannochloropsis Oculata* (Eustigmatophyceae) with High Eicosapentaenoic Acid Following N-Methyl-N-Nitrosourea-Induced Random Mutagenesis. *J. Appl. Phycology* 16, 135–144. doi:10.1023/B:JAPH.0000044826.70360.8e
- Chen, Y., and Vaidyanathan, S. (2013). Simultaneous Assay of Pigments, Carbohydrates, Proteins and Lipids in Microalgae. *Analytica Chim. Acta* 776, 31–40. doi:10.1016/j.aca.2013.03.005
- Chini Zittelli, G., Lavista, F., Bastianini, A., Rodolfi, L., Vincenzini, M., and Tredici, M. R. (1999). Production of Eicosapentaenoic Acid by *Nannochloropsis* Sp. Cultures in Outdoor Tubular Photobioreactors. *J. Biotechnol.* 70, 299–312. doi:10.1016/S0168-1656(99)00082-6
- Chiu, S.-Y., Kao, C.-Y., Tsai, M.-T., Ong, S.-C., Chen, C.-H., and Lin, C.-S. (2009). Lipid Accumulation and CO₂ Utilization of *Nannochloropsis Oculata* in Response to CO₂ Aeration. *Bioresour. Technol.* 100, 833–838. doi:10.1016/j.biortech.2008.06.061
- Collos, Y., Mornet, F., Sciandra, A., Waser, N., Larson, A., and Harrison, P. J. (1999). An Optical Method for the Rapid Measurement of Micromolar Concentrations of Nitrate in marine Phytoplankton Cultures. *J. Appl. Phycol.* 11, 179–184. doi:10.1023/A:1008046023487
- Costache, T. A., Ación Fernández, F. G., Morales, M. M., Fernández-Sevilla, J. M., Stamatin, I., and Molina, E. (2013). Comprehensive Model of Microalgae Photosynthesis Rate as a Function of Culture Conditions in Photobioreactors. *Appl. Microbiol. Biotechnol.* 97, 7627–7637. doi:10.1007/s00253-013-5035-2
- Covés, J., Joyard, J., and Douce, R. (1988). Lipid Requirement and Kinetic Studies of Solubilized UDP-Galactose:diacylglycerol Galactosyltransferase Activity from

- Spinach Chloroplast Envelope Membranes. *Proc. Natl. Acad. Sci. U.S.A.* 85, 4966–4970. doi:10.1073/pnas.85.14.4966
- Dar, A. A., Choudhury, A. R., Kancharla, P. K., and Arumugam, N. (2017). The FAD2 Gene in Plants: Occurrence, Regulation, and Role. *Front. Plant Sci.* 8, 1–16. doi:10.3389/fpls.2017.01789
- Dolch, L.-J., Rak, C., Perin, G., Tourcier, G., Broughton, R., Letierrier, M., et al. (2017). A Palmitic Acid Elongase Affects Eicosapentaenoic Acid and Plastidial Monogalactosyldiacylglycerol Levels in Nannochloropsis. *Plant Physiol.* 173, 742–759. doi:10.1104/pp.16.01420
- Fu, W., Chaiboonchoe, A., Khraiweh, B., Nelson, D., Al-Khairi, D., Mystikou, A., et al. (2016). Algal Cell Factories: Approaches, Applications, and Potentials. *Mar. Drugs* 14, 225. doi:10.3390/md14120225
- Fukuyama, K. (2004). Structure and Function of Plant-type Ferredoxins. *Photosynthesis Res.* 81, 289–301. doi:10.1023/B:PRES.0000036882.19322.0a
- Garibay-Hernández, A., Barkla, B. J., Vera-Estrella, R., Martinez, A., and Pantoja, O. (2017). Membrane Proteomic Insights into the Physiology and Taxonomy of an Oleaginous green Microalga. *Plant Physiol.* 173, 390–416. doi:10.1104/pp.16.01240
- Griffiths, M. J., Van Hille, R. P., and Harrison, S. T. L. (2010). Selection of Direct Transesterification as the Preferred Method for Assay of Fatty Acid Content of Microalgae. *Lipids* 45, 1053–1060. doi:10.1007/s11745-010-3468-2
- Han, D., Jia, J., Li, J., Sommerfeld, M., Xu, J., and Hu, Q. (2017). Metabolic Remodeling of Membrane Glycerolipids in the Microalga Nannochloropsis Oceanica under Nitrogen Deprivation. *Front. Mar. Sci.* 4, 1–15. doi:10.3389/fmars.2017.00242
- Hitchcock, A., Jackson, P. J., Chidgey, J. W., Dickman, M. J., Hunter, C. N., and Canniffe, D. P. (2016). Biosynthesis of Chlorophyll a in a Purple Bacterial Phototroph and Assembly into a Plant Chlorophyll-Protein Complex. *ACS Synth. Biol.* 5, 948–954. doi:10.1021/acssynbio.6b00069
- Hu, H., and Gao, K. (2006). Response of Growth and Fatty Acid Compositions of *Nannochloropsis* sp. to Environmental Factors Under Elevated CO₂ Concentration. *Biotechnol. Lett.* 28, 987–992. doi:10.1007/s10529-006-9026-6
- Iwai, M., Hori, K., Sasaki-Sekimoto, Y., Shimojima, M., and Ohta, H. (2015). Manipulation of Oil Synthesis in Nannochloropsis Strain NIES-2145 with a Phosphorus Starvation-Inducible Promoter from Chlamydomonas Reinhardtii. *Front. Microbiol.* 6, 1–15. doi:10.3389/fmicb.2015.00912
- Janssen, J. H., Lamers, P. P., de Vos, R. C. H., Wijffels, R. H., and Barbosa, M. J. (2019). Translocation and De Novo Synthesis of Eicosapentaenoic Acid (EPA) during Nitrogen Starvation in Nannochloropsis Gaditana. *Algal Res.* 37, 138–144. doi:10.1016/j.algal.2018.11.025
- Janssen, J. H., Spoelder, J., Koehorst, J. J., Schaap, P. J., Wijffels, R. H., and Barbosa, M. J. (2020). Time-dependent Transcriptome Profile of Genes Involved in Triacylglycerol (TAG) and Polyunsaturated Fatty Acid Synthesis in Nannochloropsis Gaditana during Nitrogen Starvation. *J. Appl. Phycol.* 32, 1153–1164. doi:10.1007/s10811-019-02021-2
- Jeon, S., Koh, H. G., Cho, J. M., Kang, N. K., and Chang, Y. K. (2021). Enhancement of Lipid Production in Nannochloropsis salina by Overexpression of Endogenous NADP-dependent Malic Enzyme. *Algal Res.* 54, 102218. doi:10.1016/j.algal.2021.102218
- Junpeng, J., Xupeng, C., Miao, Y., and Song, X. (2020). Monogalactosyldiacylglycerols with High PUFA Content from Microalgae for Value-Added Products. *Appl. Biochem. Biotechnol.* 190, 1212–1223. doi:10.1007/s12010-019-03159-y
- Kagali, Z. C. Ü., Şentürk, A., Özkan Küçük, N. E., Qureshi, M. H., and Özlü, N. (2017). Proteomics in Cell Division. *Proteomics* 17, 1600100. doi:10.1002/pmic.201600100
- Kameda, H., Hirabayashi, K., Wada, K., and Fukuyama, K. (2011). Mapping of Protein-Protein Interaction Sites in the Plant-type [2Fe-2S] Ferredoxin. *PLoS One* 6, e21947. doi:10.1371/journal.pone.0021947
- Kapase, V. U., Nesamma, A. A., and Jutur, P. P. (2018). Identification and Characterization of Candidates Involved in Production of OMEGAs in Microalgae: a Gene Mining and Phylogenomic Approach. *Prep. Biochem. Biotechnol.* 48, 619–628. doi:10.1080/10826068.2018.1476886
- Kaye, Y., Grundman, O., Leu, S., Zarka, A., Zorin, B., Didi-Cohen, S., et al. (2015). Metabolic Engineering toward Enhanced LC-PUFA Biosynthesis in Nannochloropsis Oceanica : Overexpression of Endogenous Δ12 Desaturase Driven by Stress-Inducible Promoter Leads to Enhanced Deposition of Polyunsaturated Fatty Acids in TAG. *Algal Res.* 11, 387–398. doi:10.1016/j.algal.2015.05.003
- Kechasov, D., de Grahl, I., Endries, P., Reumann, S., Biochemistry, P., Biology, I., et al. (2020). Evolutionary Maintenance of the PTS2 Protein Import Pathway in the Stramenopile Alga Nannochloropsis. *Front. Cel Dev. Biol.* 8, 1–33. doi:10.3389/fcell.2020.593922
- Kent, M., Welladsen, H. M., Mangott, A., and Li, Y. (2015). Nutritional Evaluation of Australian Microalgae as Potential Human Health Supplements. *PLoS One* 10, e0118985–14. doi:10.1371/journal.pone.0118985
- Khatoun, H., Abdu Rahman, N., Banerjee, S., Harun, N., Suleiman, S. S., Zakaria, N. H., et al. (2014). Effects of Different Salinities and pH on the Growth and Proximate Composition of Nannochloropsis Sp. And Tetraselmis Sp. Isolated from South China Sea Cultured under Control and Natural Condition. *Int. Biodeterioration Biodegradation* 95, 11–18. doi:10.1016/j.ibiod.2014.06.022
- Koh, H. G., Kang, N. K., Jeon, S., Shin, S.-E., Jeong, B.-r., and Chang, Y. K. (2019). Heterologous Synthesis of Chlorophyll B in Nannochloropsis salina Enhances Growth and Lipid Production by Increasing Photosynthetic Efficiency. *Biotechnol. Biofuels* 12, 1–15. doi:10.1186/s13068-019-1462-3
- Kukorelli, G., Reisinger, P., and Pinke, G. (2013). ACCase Inhibitor Herbicides - Selectivity, weed Resistance and Fitness Cost: A Review. *Int. J. Pest Manage.* 59, 165–173. doi:10.1080/09670874.2013.821212
- Kumar, A., Ergas, S., Yuan, X., Sahu, A., Zhang, Q., Dewulf, J., et al. (2010). Enhanced CO₂ Fixation and Biofuel Production via Microalgae: Recent Developments and Future Directions. *Trends Biotechnol.* 28, 371–380. doi:10.1016/j.tibtech.2010.04.004
- Levasseur, W., Perré, P., and Pozzobon, V. (2020). A Review of High Value-Added Molecules Production by Microalgae in Light of the Classification. *Biotechnol. Adv.* 41, 107545. doi:10.1016/j.biotechadv.2020.107545
- Li, J., Han, D., Wang, D., Ning, K., Jia, J., Wei, L., et al. (2014). Choreography of Transcriptomes and Lipidomes of Nannochloropsis Reveals the Mechanisms of Oil Synthesis in Microalgae. *Plant Cell* 26, 1645–1665. doi:10.1105/tpc.113.121418
- Li, X., Liu, R., Li, J., Chang, M., Liu, Y., Jin, Q., et al. (2015). Enhanced Arachidonic Acid Production from Mortierella Alpina Combining Atmospheric and Room Temperature Plasma (ARTP) and Diethyl Sulfate Treatments. *Bioresour. Technol.* 177, 134–140. doi:10.1016/j.biortech.2014.11.051
- Liang, J., Wen, F., and Liu, J. (2019). Transcriptomic and Lipidomic Analysis of an EPA-Containing Nannochloropsis Sp. PJ12 in Response to Nitrogen Deprivation. *Sci. Rep.* 9, 1–18. doi:10.1038/s41598-019-41169-2
- Lu, H., Cheng, J., Wang, Z., Zhang, X., Chen, S., and Zhou, J. (2020). Enhancing Photosynthetic Characterization and Biomass Productivity of Nannochloropsis Oceanica by Nuclear Radiation. *Front. Energ. Res.* 8, 1–9. doi:10.3389/fenrg.2020.00143
- Ma, X.-N., Chen, T.-P., Yang, B., Liu, J., and Chen, F. (2016). Lipid Production from Nannochloropsis. *Mar. Drugs* 14, 61. doi:10.3390/md14040061
- Maréchal, E., Miège, C., Block, M. A., Douce, R., and Joyard, J. (1995). The Catalytic Site of Monogalactosyldiacylglycerol Synthase from Spinach Chloroplast Envelope Membranes. *J. Biol. Chem.* 270, 5714–5722. doi:10.1074/jbc.270.11.5714
- Meng, Q., Liang, H., and Gao, H. (2018). Roles of Multiple KASIII Homologues of Shewanella Oneidensis in Initiation of Fatty Acid Synthesis and in Cerulenin Resistance. *Biochim. Biophys. Acta (Bba) - Mol. Cel Biol. Lipids* 1863, 1153–1163. doi:10.1016/j.bbalip.2018.06.020
- Moha-León, J. D., Pérez-Legaspi, I. A., Ortega-Clemente, L. A., Rubio-Franchini, I., and Ríos-Leal, E. (2019). Improving the Lipid Content of Nannochloropsis Oculata by a Mutation-Selection Program Using UV Radiation and Quizalofop. *J. Appl. Phycol.* 31, 191–199. doi:10.1007/s10811-018-1568-1
- Morales-Sánchez, D., Kyndt, J., Ogden, K., and Martinez, A. (2016). Toward an Understanding of Lipid and Starch Accumulation in Microalgae: A Proteomic Study of Neochloris Oleoabundans Cultivated under N-Limited Heterotrophic Conditions. *Algal Res.* 20, 22–34. doi:10.1016/j.algal.2016.09.006
- Mühlroth, A., Li, K., Rökke, G., Winge, P., Olsen, Y., Hohmann-Marriott, M., et al. (2013). Pathways of Lipid Metabolism in marine Algae, Co-expression Network, Bottlenecks and Candidate Genes for Enhanced Production of EPA and DHA in Species of Chromista. *Mar. Drugs* 11, 4662–4697. doi:10.3390/md11114662
- Murakami, H., Kakutani, N., Kuroyanagi, Y., Iwai, M., Hori, K., Shimojima, M., et al. (2020). MYB-like Transcription Factor NoPSR1 Is Crucial for Membrane Lipid Remodeling under Phosphate Starvation in the Oleaginous Microalga Nannochloropsis Oceanica. *FEBS Lett.* 594, 3384–3394. doi:10.1002/1873-3468.13902
- Nofiani, R., Philmus, B., Nindita, Y., and Mahmud, T. (2019). 3-Ketoacyl-ACP Synthase (KAS) III Homologues and Their Roles in Natural Product Biosynthesis. *Med. Chem. Commun.* 10, 1517–1530. doi:10.1039/c9md00162j
- Osumi, T., Tsukamoto, T., and Hata, S. (1992). Signal Peptide for Peroxisomal Targeting: Replacement of an Essential Histidine Residue by Certain Amino

- Acids Converts the Amino-Terminal Presequence of Peroxisomal 3-Ketoacyl-CoA Thiolase to a Mitochondrial Signal Peptide. *Biochem. Biophysical Res. Commun.* 186, 811–818. doi:10.1016/0006-291x(92)90818-6
- Park, S.-B., Yun, J.-H., Ryu, A. J., Yun, J., Kim, J. W., Lee, S., et al. (2021). Development of a Novel Nannochloropsis Strain with Enhanced Violaxanthin Yield for Large-scale Production. *Microb. Cel Fact.* 20, 1–11. doi:10.1186/s12934-021-01535-0
- Poliner, E., Pulman, J. A., Zienkiewicz, K., Childs, K., Benning, C., and Farré, E. M. (2018). A Toolkit for Nannochloropsis Oceanica CCMP 1779 Enables Gene Stacking and Genetic Engineering of the Eicosapentaenoic Acid Pathway for Enhanced Long-chain Polyunsaturated Fatty Acid Production. *Plant Biotechnol. J.* 16, 298–309. doi:10.1111/pbi.12772
- Posch, A. (2014). Sample Preparation Guidelines for Two-Dimensional Electrophoresis. *Arch. Physiol. Biochem.* 120, 192–197. doi:10.3109/13813455.2014.955031
- Rasdi, N. W., and Qin, J. G. (2015). Effect of N:P Ratio on Growth and Chemical Composition of Nannochloropsis Oculata and Tisochrysis Lutea. *J. Appl. Phycol.* 27, 2221–2230. doi:10.1007/s10811-014-0495-z
- Remmers, I. M., Martens, D. E., Wijffels, R. H., and Lamers, P. P. (2017). Dynamics of Triacylglycerol and EPA Production in Phaeodactylum Tricornutum under Nitrogen Starvation at Different Light Intensities. *PLoS One* 12, e0175630–13. doi:10.1371/journal.pone.0175630
- Renaud, S. M., Parry, D. L., Thinh, L.-V., Kuo, C., Padovan, A., and Sammy, N. (1991). Effect of Light Intensity on the Proximate Biochemical and Fatty Acid Composition of Isochrysis Sp. And Nannochloropsis Oculata for Use in Tropical Aquaculture. *J. Appl. Phycol.* 3, 43–53. doi:10.1007/BF00003918
- Roncaglia, B., Papini, A., Chini Zittelli, G., Rodolfi, L., and Tredici, M. R. (2021). Cell wall and Organelle Modifications during Nitrogen Starvation in Nannochloropsis Oceanica F&M-M24. *J. Appl. Phycol.* 33, 2069–2080. doi:10.1007/s10811-021-02416-0
- Sabzi, S., Shamsaie Mehrgan, M., Rajabi Islami, H., and Hosseini Shekarabi, S. P. (2021). Changes in Biochemical Composition and Fatty Acid Accumulation of Nannochloropsis Oculata in Response to Different Iron Concentrations. *Biofuels* 12, 1–7. doi:10.1080/17597269.2018.1489672
- Sayanova, O., Mimouni, V., Ulmann, L., Morant-Manceau, A., Pasquet, V., Schoefs, B., et al. (2017). Modulation of Lipid Biosynthesis by Stress in Diatoms. *Phil. Trans. R. Soc. B* 372, 20160407. doi:10.1098/rstb.2016.0407
- Scholz, M. J., Weiss, T. L., Jinkerson, R. E., Jing, J., Roth, R., Goodenough, U., et al. (2014). Ultrastructure and Composition of the Nannochloropsis Gaditana Cell wall. *Eukaryot. Cel* 13, 1450–1464. doi:10.1128/EC.00183-14
- Shi, Y., Liu, M., Pan, Y., Hu, H., and Liu, J. (2021). $\Delta 6$ Fatty Acid Elongase Is Involved in Eicosapentaenoic Acid Biosynthesis via the $\omega 6$ Pathway in the Marine Alga Nannochloropsis Oceanica. *J. Agric. Food Chem.* 69, 9837–9848. doi:10.1021/acs.jafc.1c04192
- Song, X., Wang, J., Wang, Y., Feng, Y., Cui, Q., and Lu, Y. (2018). Artificial Creation of Chlorella Pyrenoidosa Mutants for Economic Sustainable Food Production. *Bioresour. Technol.* 268, 340–345. doi:10.1016/j.biortech.2018.08.007
- Strickland, J. D. H., and Parsons, T. R. (1972). Determination of Reactive Phosphorus. *A. Pract. Handb. Seawater Anal.* 167, 49–55. doi:10.1007/978-1-4615-5439-4_19
- Szabó, M., Parker, K., Guruprasad, S., Kuzhiumparambil, U., Lilley, R. M., Tamburic, B., et al. (2014). Photosynthetic Acclimation of Nannochloropsis Oculata Investigated by Multi-Wavelength Chlorophyll Fluorescence Analysis. *Bioresour. Technol.* 167, 521–529. doi:10.1016/j.biortech.2014.06.046
- Tan, K. W. M., and Lee, Y. K. (2016). The Dilemma for Lipid Productivity in green Microalgae: Importance of Substrate Provision in Improving Oil Yield without Sacrificing Growth. *Biotechnol. Biofuels* 9, 1–14. doi:10.1186/s13068-016-0671-2
- Tran, N.-A. T., Padula, M. P., Evenhuis, C. R., Commault, A. S., Ralph, P. J., and Tamburic, B. (2016). Proteomic and Biophysical Analyses Reveal a Metabolic Shift in Nitrogen Deprived Nannochloropsis Oculata. *Algal Res.* 19, 1–11. doi:10.1016/j.algal.2016.07.009
- Vecchi, V., Barera, S., Bassi, R., and Dall'Osto, L. (2020). Potential and Challenges of Improving Photosynthesis in Algae. *Plants* 9, 67. doi:10.3390/plants9010067
- Vieler, A., Wu, G., Tsai, C.-H., Bullard, B., Cornish, A. J., Harvey, C., et al. (2012). Genome, Functional Gene Annotation, and Nuclear Transformation of the Heterokont Oleaginous Alga Nannochloropsis Oceanica CCMP1779. *Plos Genet.* 8, e1003064. doi:10.1371/journal.pgen.1003064
- Wan, X., Peng, Y.-F., Zhou, X.-R., Gong, Y.-M., Huang, F.-H., and Moncalián, G. (2016). Effect of Cerulenin on Fatty Acid Composition and Gene Expression Pattern of DHA-Producing Strain Colwellia Psychrerythraea Strain 34H. *Microb. Cel Fact.* 15, 1–13. doi:10.1186/s12934-016-0431-9
- Wang, B., and Jia, J. (2020). Photoprotection Mechanisms of Nannochloropsis Oceanica in Response to Light Stress. *Algal Res.* 46, 101784. doi:10.1016/j.algal.2019.101784
- Wang, Q., Feng, Y., Lu, Y., Xin, Y., Shen, C., Wei, L., et al. (2021). Manipulating Fatty-Acid Profile at Unit Chain-Length Resolution in the Model Industrial Oleaginous Microalgae Nannochloropsis. *Metab. Eng.* 66, 157–166. doi:10.1016/j.ymben.2021.03.015
- Wei, L., and Huang, X. (2017). Long-duration Effect of Multi-Factor Stresses on the Cellular Biochemistry, Oil-Yielding Performance and Morphology of Nannochloropsis Oculata. *PLoS One* 12, e0174646–20. doi:10.1371/journal.pone.0174646
- Wu, M., Zhang, H., Sun, W., Li, Y., Hu, Q., Zhou, H., et al. (2019). Metabolic Plasticity of the Starchless Mutant of Chlorella Sorokiniana and Mechanisms Underlying its Enhanced Lipid Production Revealed by Comparative Metabolomics Analysis. *Algal Res.* 42, 101587. doi:10.1016/j.algal.2019.101587
- Xu, Y., Li, H., Jin, Y.-H., Fan, J., and Sun, F. (2014). Dimerization Interface of 3-Hydroxyacyl-CoA Dehydrogenase Tunes the Formation of its Catalytic Intermediate. *PLoS One* 9, e95965. doi:10.1371/journal.pone.0095965
- Yang, F., Yuan, W., Ma, Y., Balamurugan, S., Li, H.-Y., Fu, S., et al. (2019a). Harnessing the Lipogenic Potential of $\Delta 6$ -Desaturase for Simultaneous Hyperaccumulation of Lipids and Polyunsaturated Fatty Acids in Nannochloropsis Oceanica. *Front. Mar. Sci.* 6, 1–8. doi:10.3389/fmars.2019.00682
- Yang, Y.-F., Li, D.-W., Chen, T.-T., Hao, T.-B., Balamurugan, S., Yang, W.-D., et al. (2019b). Overproduction of Bioactive Algal Chrysolaminarin by the Critical Carbon Flux Regulator Phosphoglucosyltransferase. *Biotechnol. J.* 14, 1800220–1800228. doi:10.1002/biot.201800220
- Zhang, J., and Burgess, J. G. (2017). Enhanced Eicosapentaenoic Acid Production by a New Deep-Sea marine Bacterium Shewanella Electrodephila MAR441T. *PLoS One* 12, e0188081–19. doi:10.1371/journal.pone.0188081
- Zhang, X., Zhang, X.-F., Li, H.-P., Wang, L.-Y., Zhang, C., Xing, X.-H., et al. (2014). Atmospheric and Room Temperature Plasma (ARTP) as a New Powerful Mutagenesis Tool. *Appl. Microbiol. Biotechnol.* 98, 5387–5396. doi:10.1007/s00253-014-5755-y
- Zienkiewicz, K., and Zienkiewicz, A. (2020). Degradation of Lipid Droplets in Plants and Algae-Right Time, Many Paths, One Goal. *Front. Plant Sci.* 11, 1–14. doi:10.3389/fpls.2020.579019

Conflict of Interest: The authors declare that the research was conducted in the absence of any commercial or financial relationships that could be construed as a potential conflict of interest.

Publisher's Note: All claims expressed in this article are solely those of the authors and do not necessarily represent those of their affiliated organizations, or those of the publisher, the editors, and the reviewers. Any product that may be evaluated in this article, or any claim that may be made by its manufacturer, is not guaranteed or endorsed by the publisher.

Copyright © 2022 Wan Razali, Evans and Pandhal. This is an open-access article distributed under the terms of the Creative Commons Attribution License (CC BY). The use, distribution or reproduction in other forums is permitted, provided the original author(s) and the copyright owner(s) are credited and that the original publication in this journal is cited, in accordance with accepted academic practice. No use, distribution or reproduction is permitted which does not comply with these terms.



Pilot-Scale Cultivation of the Snow Alga *Chloromonas typhlos* in a Photobioreactor

Floris Schoeters^{1*}, Jornt Spit¹, Rahmasari Nur Azizah^{1,2} and Sabine Van Miert¹

¹Radius, Thomas More University of Applied Sciences, Geel, Belgium, ²I-BioStat, Data Science Institute, Hasselt University, Hasselt, Belgium

OPEN ACCESS

Edited by:

Kanhaiya Kumar,
Norwegian University of Science and
Technology, Norway

Reviewed by:

Dominik Refardt,
Zurich University of Applied Sciences,
Switzerland

Sergio Revah,
Metropolitan Autonomous University,
Mexico

Helena Melo Amaro,
University of Porto, Portugal
Fantao Kong,
Dalian University of Technology, China

*Correspondence:

Floris Schoeters
floris.schoeters@thomasmore.be

Specialty section:

This article was submitted to
Bioprocess Engineering,
a section of the journal
Frontiers in Bioengineering and
Biotechnology

Received: 14 March 2022

Accepted: 02 May 2022

Published: 09 June 2022

Citation:

Schoeters F, Spit J, Azizah RN and
Van Miert S (2022) Pilot-Scale
Cultivation of the Snow Alga
Chloromonas typhlos in
a Photobioreactor.
Front. Bioeng. Biotechnol. 10:896261.
doi: 10.3389/fbioe.2022.896261

The most studied and cultivated microalgae have a temperature optimum between 20 and 35°C. This temperature range hampers sustainable microalgae growth in countries with colder periods. To overcome this problem, psychrotolerant microalgae, such as the snow alga *Chloromonas typhlos*, can be cultivated during these colder periods. However, most of the research work has been carried out in the laboratory. The step between laboratory-scale and large-scale cultivation is difficult, making pilot-scale tests crucial to gather more information. Here, we presented a successful pilot-scale growth test of *C. typhlos*. Seven batch mode growth periods were compared during two longer growth tests in a photobioreactor of 350 L. We demonstrated the potential of this alga to be cultivated at colder ambient temperatures. The tests were performed during winter and springtime to compare ambient temperature and sunlight influences. The growth and CO₂ usage were continuously monitored to calculate the productivity and CO₂ fixation efficiency. A maximum dry weight of 1.082 g L⁻¹ was achieved while a maximum growth rate and maximum daily volumetric and areal productivities of 0.105 d⁻¹, 0.110 g L⁻¹ d⁻¹, and 2.746 g m⁻² d⁻¹, respectively, were measured. Future tests to optimize the cultivation of *C. typhlos* and production of astaxanthin, for example, will be crucial to explore the potential of biomass production of *C. typhlos* on a commercial scale.

Keywords: biomass production, greenhouse, microalgae, psychrotolerant, year-round cultivation, CO₂ utilization, cold climate

INTRODUCTION

Microalgae are a diverse group of single-celled eukaryotic organisms that are ubiquitously present in a wide range of habitats and conditions. They can use CO₂ as a carbon source and sunlight as an energy source to produce organic matter through photosynthesis (Benedetti et al., 2018; Abo et al., 2019; Vale et al., 2020; Vecchi et al., 2020). Their photosynthetic efficiency can be 10 times more efficient than that of terrestrial plants, and when combined with their fast growth rates, they are a promising source of renewable feedstock for different applications (Singh and Ahluwalia, 2013; Benedetti et al., 2018; Khan et al., 2018). It is, thus, no surprise that the cultivation of microalgae has bloomed in recent years due to its vast potential (Richmond, 2000; Chisti, 2007; Singh and Ahluwalia, 2013; Benedetti et al., 2018; Khan et al., 2018). The true potential of microalgae, however, remains untapped on a larger scale. For many microalgae species, several challenges remain to reach sustainable and economically viable cultivation (Richmond, 2000; Chisti, 2007; Mata et al., 2010; Sayre, 2010; Tredici, 2010).

Currently, only a few selective microalgae are commercially cultivated (Garrido-Cardenas et al., 2018; Dolganyuk et al., 2020; Wang et al., 2021). This is often attributed to the legislative burden associated with the cultivation of novel species, for example, the European Novel Foods Regulation (Araújo et al., 2021). Next to the aforementioned, only a select few of the thousands of species are studied (Guiry, 2012; Garrido-Cardenas et al., 2018). Most of this research is carried out on the laboratory scale and often in well-controlled small volumes, making the extrapolation to larger-scale cultivation difficult (Tredici, 2010; Quinn et al., 2011; Moody et al., 2014). Furthermore, most microalgae studied or commercially cultivated are microalgae with optimal growth temperatures between 20 and 35°C (Kvíděrová et al., 2017; Cheregi et al., 2019; Suzuki et al., 2019; Dolganyuk et al., 2020). Nevertheless, many countries have a colder climate, making year-round cultivation difficult unless cultures are heated during colder months. Since the production costs of microalgae are still a bottleneck in the expansion of commercialization, a year-round microalgae cultivation, without the need for excessive heating, can support sustainability and economic feasibility (Matsumoto et al., 2017; Garrido-Cardenas et al., 2018; Cheregi et al., 2019; Suzuki et al., 2019).

Cold-adapted microalgae could bridge the colder periods during year-round microalgae cultivation (Kvíděrová et al., 2017; Matsumoto et al., 2017; Suzuki et al., 2019). While, cold-adapted microalgae, often referred to as snow algae, are being studied more in recent years (Remias et al., 2016; Kvíděrová et al., 2017; Hoham and Remias, 2020); most studies focus on the ecology and taxonomy. A few studies describe the cultivation of snow algae in a laboratory setting, but knowledge of their cultivation on a larger scale is largely absent (Kvíděrová, 2010; Kvíděrová et al., 2017; Matsumoto et al., 2017). Aside from being able to grow in colder temperatures, snow algae can be a source of polyunsaturated fatty acids (PUFAs) and other valuable compounds such as astaxanthin (Varshney et al., 2015; Kvíděrová et al., 2017; Cheregi et al., 2019; Sathasivam et al., 2019; Suzuki et al., 2019). Snow algae, many belonging to the *Chloromonas*–*Chlamydomonas* complex, are polyextremophiles adapted to survive in regions with harsh conditions such as low temperatures, high irradiation, and lack of nutrients and liquid water (Remias et al., 2005; Kvíděrová, 2010; Kvíděrová et al., 2017; Procházková et al., 2018; Hoham and Remias, 2020).

One snow alga with a potential commercial value is the red snow alga *Chloromonas typhlos* (*Chlamydomonas nivalis*). It is one of the most studied snow algae and is known to cause the phenomenon of red patches of snow (Mosser et al., 1977; Remias et al., 2005; Cvetkovska et al., 2017). This phenomenon of red snow, often called “watermelon snow”, is caused by the red pigment astaxanthin and its acid ester derivatives (Remias et al., 2005; Cvetkovska et al., 2017). However, to the best of our knowledge, no studies describe the large-scale cultivation of this alga in a photobioreactor. In order to help close the gap between laboratory experiments and large-scale cultivation of the snow alga *C. typhlos*, we performed a proof-of-concept study in which we grew *C. typhlos* in a photobioreactor installed in a minimally heated (frost-protection) greenhouse during colder periods.

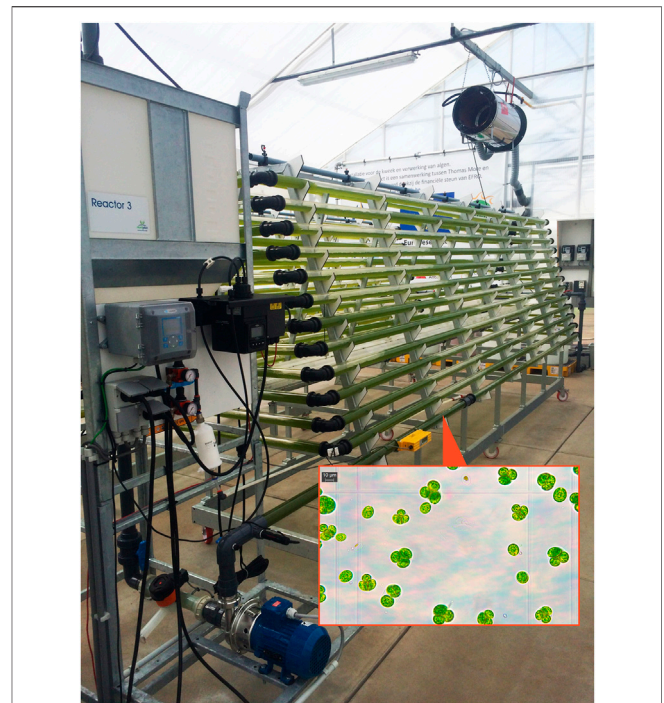


FIGURE 1 | Picture of the photobioreactor used to perform the growth experiments with *C. typhlos*. The red frame shows the *C. typhlos* cells as seen throughout the experiments. The cells were always green.

MATERIALS AND METHODS

Microalga Strain and Culture Conditions

Chloromonas typhlos (SAG 26.68) was purchased from SAG (Department Experimental Phycology and Culture Collection of Algae, University of Göttingen, Germany). The culture was maintained in the laboratory in a sterilized (autoclaved at 121°C for 20 min) freshwater medium based on the SAG basal medium (version 10.2008). It was kept in a 250-ml Erlenmeyer flask on an orbital shaker at 90 rpm with $70 \mu\text{mol m}^{-2} \text{s}^{-1}$ light exposure (cool-white fluorescent) in a climate-controlled room at 22°C (± 0.2 SD) under a 16/8-h day/night regime. For upscaling, the cultures were transferred, respectively, to aerated 1, 2, and 40 L recipients. Ambient air was used for aeration, and no extra CO_2 was provided during upscaling of the cultures. Cultures in the photobioreactors were grown in the same medium sterilized by filtration (0.1 μm). The freshwater medium had the following composition: $152 \text{ mg L}^{-1} \text{ HNO}_3$, $22 \text{ mg L}^{-1} \text{ H}_3\text{PO}_4$, $148 \text{ mg L}^{-1} \text{ KOH}$, $6.3 \text{ mg L}^{-1} \text{ Fe-DTPA}$, $42 \text{ pg L}^{-1} \text{ CuSO}_4 \cdot 5\text{H}_2\text{O}$, $2.8 \mu\text{g L}^{-1} \text{ ZnSO}_4$, $7.2 \mu\text{g L}^{-1} \text{ MnSO}_4$, $4.3 \mu\text{g L}^{-1} \text{ Na}_2\text{MoO}_4$, $40 \mu\text{g L}^{-1} \text{ Na}_2\text{B}_4\text{O}_7$, $0.2 \text{ g L}^{-1} \text{ NaHCO}_3$, and $23 \text{ mg L}^{-1} \text{ MgSO}_4 \cdot 7\text{H}_2\text{O}$. Furthermore, nitrogen and phosphorus were added to the culture when needed, based on the regular measurement of their concentrations, to maintain non-nutrient conditions. The medium was prepared autonomously by a central computer control unit in the greenhouse and fed to the cultures by a feed supply unit (FertiMiX 600, Hortimax).

Horizontal Tubular Multilayer Photobioreactor

A tubular multilayer photobioreactor with a volume of 350 L was used for the cultivation of *C. typhlos*. The reactor is part of the pilot plant of the EU project “Sunbuilt” and is located in a greenhouse in Geel, Belgium. The photobioreactor consists of transparent unplasticized polyvinylchloride (PVC-u) tubes with an external diameter of 5 cm. To avoid shading of lower located tubes, a triangle-like configuration of the tubes was used (Figure 1). For the inoculation of the photobioreactor, approximately 40 L of a 0.5–1 g L⁻¹ *C. typhlos* culture was used.

Modus Operandi of the Photobioreactor

C. typhlos was cultivated in a 350-L (V_r) bioreactor during two growth tests ranging from March to May 2019 (growth test 1) and from December 2019 to February 2020 (growth test 2) in non-nutrient limiting conditions. To evaluate the growth of *C. typhlos* during these two tests, seven (three during the first test and four during the second test) 9-day growth periods were selected and compared. Prior to starting a 9-day growth period, *C. typhlos* was partially harvested, and the culture was refreshed with a new medium and permitted to regrow before a new 9-day growth period started. The first period at the start of growth test 2 (December 2019), however, started right from inoculation, giving a lower start concentration.

The growth was monitored continuously online with a turbidity sensor (Georg Fischer Signet 4,150 turbidimeter 0–1000 NTU) and offline by dry weight measurements. The medium was circulated by using a centrifugal pump (900 rpm), and filter-sterilized (0.1 µm) ambient air was injected into the lowest tube at a continuous rate for mixing. The working pH was set at 8, continuously measured, and maintained by the injection of CO₂ on demand, in the airflow, with a maximum flow of 885.9 ml normal per minute. The total CO₂ injected into the photobioreactors was measured during the growth periods (IN-FLOW mass flow meter/controller Bronkhorst, the Netherlands). The ambient temperature inside the greenhouse was monitored (Ektron III-C, Hortiplan) continuously and maintained at night at a minimal temperature of 10°C for frost protection with a gas heater (HHB-100A-230V, Holland Heaters).

When the temperature inside the greenhouse reached 23°C, foggers inside the greenhouse and sprinklers on the roof were turned on automatically to prevent an excessive rise in temperature. Photosynthetically active radiation (PAR) was measured continuously with a PAR sensor (LI-COR LI-190 R Quantum sensor) installed inside the greenhouse, on top of the reactor. A solar irradiance meter (LP02-TR pyranometer) was installed outside the greenhouse to measure total solar radiation. At a measured value of 400 W m⁻², a sunscreen inside the greenhouse was automatically partially closed to reduce irradiation by 20–30%. The effect of additional lighting to prolong the length of daytime was studied between 10 December 2019 and 19 February 2020 by providing extra lighting (Philips TL-D 58 W 865; 504 mmol m⁻²) from 6.30 to 10.30 and 15.30 to 22.00 during 3–4 days to lengthen the day

and simulate a 16/8-h day/night cycle. During the other days, the extra lighting was not switched on to see if there was a difference between days with extra lighting versus days without extra lighting. Control, logging, and steering were carried out automatically by computer (MultiMate series III, Hortiplan).

Growth Determination

The algal growth in the bioreactor was monitored online every 30 min with a turbidity meter. The measured turbidity was correlated with a dry weight value based on a correlation described previously (Thoré et al., 2021). In addition to the continuous monitoring by turbidity, the dry weight (g L⁻¹) was determined at the start (C_s) and end (C_e) of each batch and at random moments during the growth periods. For this, samples (5 ml/sample) were filtered over pre-dried and pre-weighed Whatman GF/C glass microfiber filter papers (0.45 µm) and washed. After drying for 24 h at 70°C, the samples were cooled in a desiccator before weighing.

Calculations of Volumetric and Areal Productivities, Specific Growth Rate, CO₂ Fixation, Influence of Total PAR, and CO₂ Utilization Efficiency

The total volumetric biomass productivity P_v (dry g L⁻¹ d⁻¹) for the batch mode was calculated by the formula:

$$P_v = (C_e - C_s) / t_d,$$

with C_s and C_e, the start and end biomass (g L⁻¹), respectively, and t_d was the cultivation period (9 days for total and 1 day for (maximum) daily volumetric biomass productivity). The total areal biomass productivity P_a (dry g m⁻² d⁻¹) was calculated as follows:

$$P_a = 350 (C_e - C_s) / 14 t_d,$$

with 350 L being the volume of the reactor, t_d being 9 days for the total or 1 day for the (maximum) daily biomass areal productivity, and 14 m² being the total area covered by the reactor.

The specific growth rate was calculated over the 9-day period:

$$\mu = \ln(N_e - N_s) / t_d,$$

with N_e being the biomass at the end and N_s being the biomass at the start of the 9-day period and t_d being 9 days.

To know the daily yield on light (P_L), the daily areal productivity (P_a) was divided by the total PAR (PAR_T) received for that specific day, resulting in P_L:

$$P_L = P_a / PAR_T.$$

The total CO₂ injected was measured during each 9-day period by using a mass flow meter (IN-FLOW mass flow meter/controller Bronkhorst, the Netherlands). The theoretical total CO₂ fixation (CO_{2th}, g) by the algae for each batch was calculated as follows:

TABLE 1 | Volumetric and areal biomass productivities in dry weight of *C. typhlos* grown in batch for 9-day periods in a 350-L horizontal tubular reactor and the specific growth rates are shown. The specific growth rate (μ) is calculated over the 9-day period. The total volumetric (P_v) and areal (P_a) productivities are calculated over the 9-day period by dividing the total dry weight produced by 9. The maximum volumetric (Max P_v) or areal (Max P_a) productivity is the maximum value obtained for the daily productivity during that 9-day period.

Period	μ d^{-1}	P_v $g\ L^{-1}\ d^{-1}$	Max P_v $g\ L^{-1}\ d^{-1}$	P_a $g\ m^{-2}\ d^{-1}$	Max P_a $g\ m^{-2}\ d^{-1}$
19–28 March 2019	0.050	0.028	0.075	0.694	1.871
1–10 April 2019	0.066	0.046	0.110	1.147	2.746
17–26 April 2019 ^a	0.020	0.010	0.055	0.252	1.384
10–19 December 2019 ^b	0.105	0.032	0.063	0.791	1.561
17–26 January 2020 ^b	0.072	0.057	0.069	1.431	1.717
27 January–5 February 2020 ^b	0.091	0.067	0.069	1.680	1.720
10–19 February 2020 ^b	0.091	0.060	0.108	1.508	2.695
Mean	0.0707 \pm 0.029	0.043 \pm 0.021	0.078 \pm 0.021	1.072 \pm 0.514	1.956 \pm 0.543

^aGrowth during this period was comparable with other periods during the first 4–5 days but halted afterward. This is most likely due to 5 consecutive days of ambient temperatures over 30°C. See text for more details.

^bDenotes periods in which artificial lighting was provided; see text for more details.

$$CO_{2th} = 0.5 (C_e - C_s) V_r \left(\frac{m_{CO_2}}{m_C} \right),$$

with m_{CO_2} and m_C being the molar masses of CO_2 and C, respectively, V_r the volume of the reactor, and 0.5 being the average percentage of the carbon content in the biomass (Mirón et al., 2003; Tang et al., 2011). Higher or lower carbon content is nonetheless possible (Mandalam and Palsson, 1998; Patil et al., 2012; Rendón-Castrillón et al., 2021) which might lead to significant differences (Adamczyk et al., 2016).

The CO_2 fixation rate CO_{2fr} was calculated as $1.833P_v$, with 1.833 derived from multiplying the average carbon content (50%) per unit of biomass with the CO_2 carbon ratio (44/12).

To have an idea about the CO_2 uptake efficiency, the calculated CO_{2th} was divided by the total CO_2 (CO_{2t} , g) injected (influent CO_2) and multiplied by 100 to know the utilization efficiency percentage ($U_{\%}$):

$$U_{\%} = 100CO_{2th}/CO_{2t}.$$

The aforementioned formula is a simplified version of the formula: $\frac{\text{Influent of } CO_2 - \text{effluent } CO_2}{\text{influent } CO_2} \times 100$ (Klinthong et al., 2015), in which the numerator is replaced by the theoretical total CO_2 fixation since the photobioreactor had no measurement of CO_2 in the outgoing gases. The total loss of CO_2 (CO_{2tL}) was calculated by subtracting CO_{2th} from CO_{2t} :

$$CO_{2tL} = CO_{2t} - CO_{2th}.$$

Statistical Analysis

To compare the differences in temperatures, received PAR, and daily biomass production between the seven batches, a one-way analysis of variance (ANOVA) with *post hoc* Tukey HSD with a significance level of 0.05 was performed. Normality was tested with a Shapiro–Wilk test. Data are given as mean \pm SD.

RESULTS AND DISCUSSION

Growth and Biomass Productivity

To analyze the 9-day periods, the daily productivities were compared, and a difference was found ($p < 0.05$): the period 17–26 April was significantly different from periods 17–26 January 2020 and 27 January–5 February 2020, while the period 27 January–5 February 2020 was also significantly different from the period 10–19 December 2019. To further assess the biomass obtained during the cultivation of *C. typhlos* in the seven 9-day periods, we looked at the specific growth rate and total and maximum volumetric and areal biomass productivities. **Table 1** summarizes these results. The highest growth rate was achieved during the 10–19 December period, which was five times higher than the 17–26 April period. **Figure 2** shows that the growth halted after 6 days in the 17–26 April period, leading to a lower growth rate. The highest total volumetric biomass productivity ($0.067\ g\ L^{-1}\ d^{-1}$) was obtained during the period 27 January–5 February 2020. While a maximum biomass productivity of $0.110\ g\ L^{-1}\ d^{-1}$ was obtained during the period 1–10 April 2019, the total volumetric productivity ($0.046\ g\ L^{-1}\ d^{-1}$) was lower than that of three other periods during the winter (**Table 1**).

A potential explanation for the lower total volumetric productivity during the 1–10 April period could be that a maximum ambient temperature of 30.5°C was reached inside the greenhouse on 7 April 2019, causing temperature stress on the cells and leading to a decline in growth. This can be seen in **Figure 2** between days 8 and 9. A similar effect could be observed from day 6 during the period 17–26 April 2019. During this period, the lowest total volumetric biomass productivity ($0.010\ g\ L^{-1}\ d^{-1}$) and growth rate ($0.020\ d^{-1}$) were obtained. This growth period had the highest average temperature (22.5°C), the highest maximum temperature (35.2°C), and several (5) consecutive days with temperatures above 30°C (**Figure 3**). A stress response at a temperature around 30°C is in line with what others have reported (Teoh et al., 2013; Lukeš

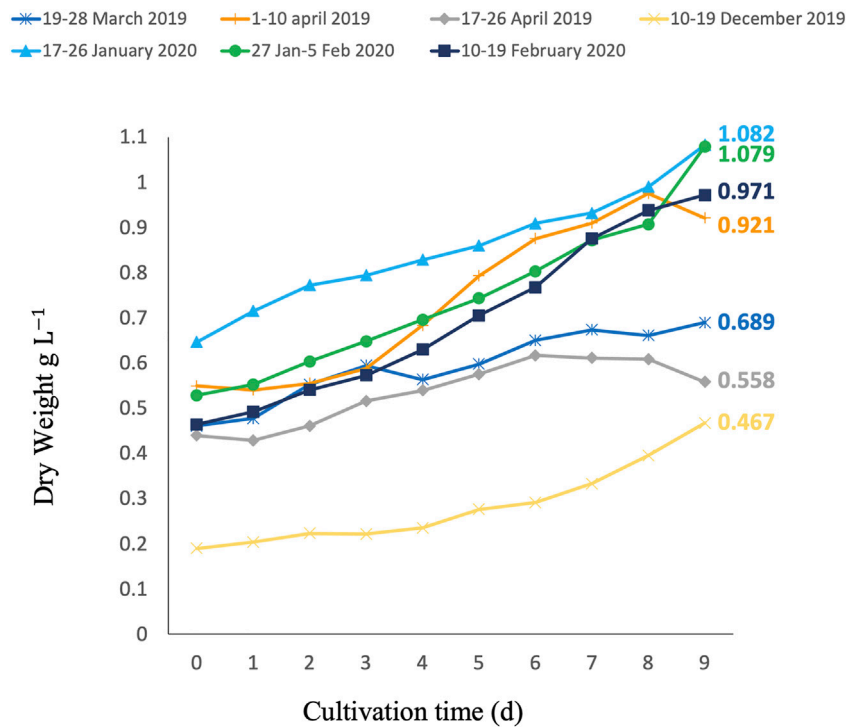


FIGURE 2 | Growth curves of *C. typhlos* during seven different 9-day batch growth tests in a 350-L photobioreactor. The end concentration (C_e) of each growth period is depicted next to the respective lines in g L⁻¹.

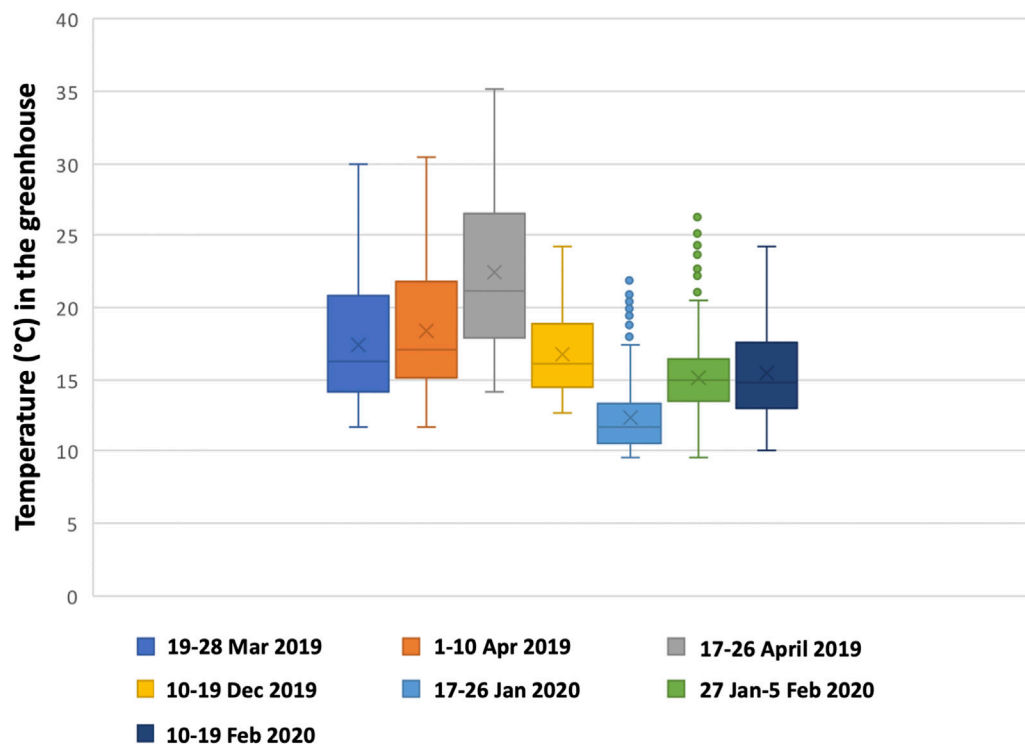


FIGURE 3 | Box plot of the temperature for each period. Outliers are shown by dots above the maximum. See also **Table 2**.

TABLE 2 | Average total PAR, average daily yield in light (P_L) for each growth period, and greenhouse temperatures measured during the batch tests. A significance between groups is also shown with $p < 0.05$. The identifier is used to show the significant differences between periods.

Period (ID)	Average total PAR	Significant versus	Average PL	Significant versus	Average temperature	Significant versus
	Mmol m^{-2}		$\text{g } \mu\text{mol}^{-1} \text{d}^{-1}$		$^{\circ}\text{C}$	
19–28 March 2019 (A)	$3,074 \pm 365$	C	0.22 ± 20	/	17.5 ± 0.9	C, E, and F
1–10 April 2019 (B)	$3,446 \pm 467$	G	0.31 ± 29	/	18.4 ± 1.4	C, E, F, and G
17–26 April 2019 (C)	$4,283 \pm 509$	A, D, E, and F	0.1 ± 0.12	E, F	22.5 ± 2.5	A, B, D, E, F, and G
10–19 December 2019 ^a (D)	$2,709 \pm 449$	C and G	0.26 ± 0.24	/	16.7 ± 1.8	C and E
17–26 January 2020 ^a (E)	$2,888 \pm 770$	C and G	0.39 ± 0.15	C	12.4 ± 1.4	A, B, C, D, F, and G
27 January–5 February 2020 ^a (F)	$3,379 \pm 925$	C and G	0.40 ± 0.25	C	15.1 ± 1.0	A, B, C, and E
10–19 February 2020 ^a (G)	$5,039 \pm 727$	B, D, E, and G	0.25 ± 0.16	/	15.5 ± 1.5	B, C, and E

^aDuring these periods artificial light was provided. The artificial light is included in the average totals depicted here.

et al., 2014). Contrary to Teoh et al. (2013) and Lukeš et al. (2014), we measured the ambient temperature in the greenhouse rather than the culture temperature itself. Since multiple parameters can influence the culture temperature and large differences between ambient and culture temperature are possible (Tredici and Materassi, 1992; González-Camejo et al., 2019), future laboratory and pilot-scale tests that measure both the ambient and culture temperatures are required to fully understand the temperature impact on *C. typhlos*.

Productivities and growth rates for the *Chloromonas* species were lower than the literature values: over the nine batches average volumetric and areal productivities of $0.043 \pm 0.021 \text{ g L}^{-1} \text{ d}^{-1}$ and $1.072 \pm 0.514 \text{ g m}^{-2} \text{ d}^{-1}$, respectively, were obtained, while growth rates varied between 0.020 and 0.105 d^{-1} . However, a comparison is difficult to obtain due to insufficient information or the different cultivation techniques used (Teoh et al., 2013; Idrissi Abdelkhalek et al., 2016; Hulatt et al., 2017; Onuma et al., 2018; Morales-Sánchez et al., 2020; Peng et al., 2021). Compared to commercially cultivated algae, the production and growth rate is lower and needs to be improved to be competitive (de Vree et al., 2015; Barka and Blecker, 2016; Benedetti et al., 2018; Darvehei et al., 2018; Metsovit et al., 2019).

Aside from temperature stress, algae, in general, react to light stress (Minhas et al., 2016; Shi et al., 2020; Zheng et al., 2020), although *C. typhlos* has mechanisms; for example, the production of astaxanthin to cope with high light intensities (Gorton et al., 2007; Remias et al., 2010; Zheng et al., 2020). To estimate the influence of total PAR on the growth of *C. typhlos*, the total averaged PAR was measured. Table 2 shows the average PAR received during the periods, the average daily yield on light (P_L), average temperatures, and whether they differ significantly between growth periods.

During the 10–19 February period, the total PAR was higher than the spring growth periods. There was a higher total PAR during the February 2020 period due to a few exceptional sunny days throughout this period and the extra artificial lighting. In addition, the sun screens in the greenhouse did not partly close since the minimal closing limit of 400 W m^{-2} was most often not reached, contrary to the spring periods. Table 2 shows that the growth period 17–26 of January had the lowest temperature and second lowest total PAR light, yet the total volumetric and areal productivities were above the averages of the growth periods (see Table 1). This shows that even at lower temperatures and

sunlight, *C. typhlos* can still be cultivated at comparable productivities to higher temperature and sunlight conditions.

The total PAR received differed significantly between the growth periods. To normalize the growth for PAR received, we looked at the yield per light. Only period 17–26 April 2019 was significantly different from periods 17–26 January 2020 and 27 January–5 February 2020. The time period of 16–26 April 2019 was also significantly different from all other periods in regard to the temperatures reached (Table 2). The period 17–26 April 2019 was also different than most other growth periods for the total light received (only periods 1–10 April 2019 and 10–19 February 2020 were similar). This shows the influence of higher temperatures ($>30^{\circ}\text{C}$) on the growth of *C. typhlos*. Table 2 also shows that at lower temperatures, *C. typhlos* still had a high yield in light.

Like many cold adapted algae, *C. typhlos* is a potential source of lipids and carotenoids produced at lower temperatures and high light intensities as a mechanism to protect the cells (Gorton et al., 2007; Remias et al., 2010; Liu and Nakamura, 2019; Hoham and Remias, 2020; Shi et al., 2020; Peng et al., 2021). If *C. typhlos* can produce sufficient biomass and valuable products such as astaxanthin at a low temperature with high light intensities, it can be a sustainable approach to cultivate microalgae during colder periods without excessive heating.

During our growth experiments, *C. typhlos* cells were green (Figure 1). We did not notice the typical red color indicative of astaxanthin. All experiments were performed in non-nutrient limiting batches, and no attempts were made during these experiments to stress the cells specifically to produce astaxanthin and color red. As no analysis was performed on the astaxanthin content, we cannot rule out that it was produced at levels too low to give the cells their typical red color. For future work, it will be vital to characterize the specific parameters, such as low nitrogen, that produce red *C. typhlos* cells as astaxanthin is an important and valuable carotenoid (Leya et al., 2009; Han et al., 2013; Sathasivam et al., 2019).

Turbidity Measurements to Monitor Growth and Influence of (Artificial) Light

During the winter period, artificial lights were turned on for several days in each period to simulate a 16/8 day-night regime. These days

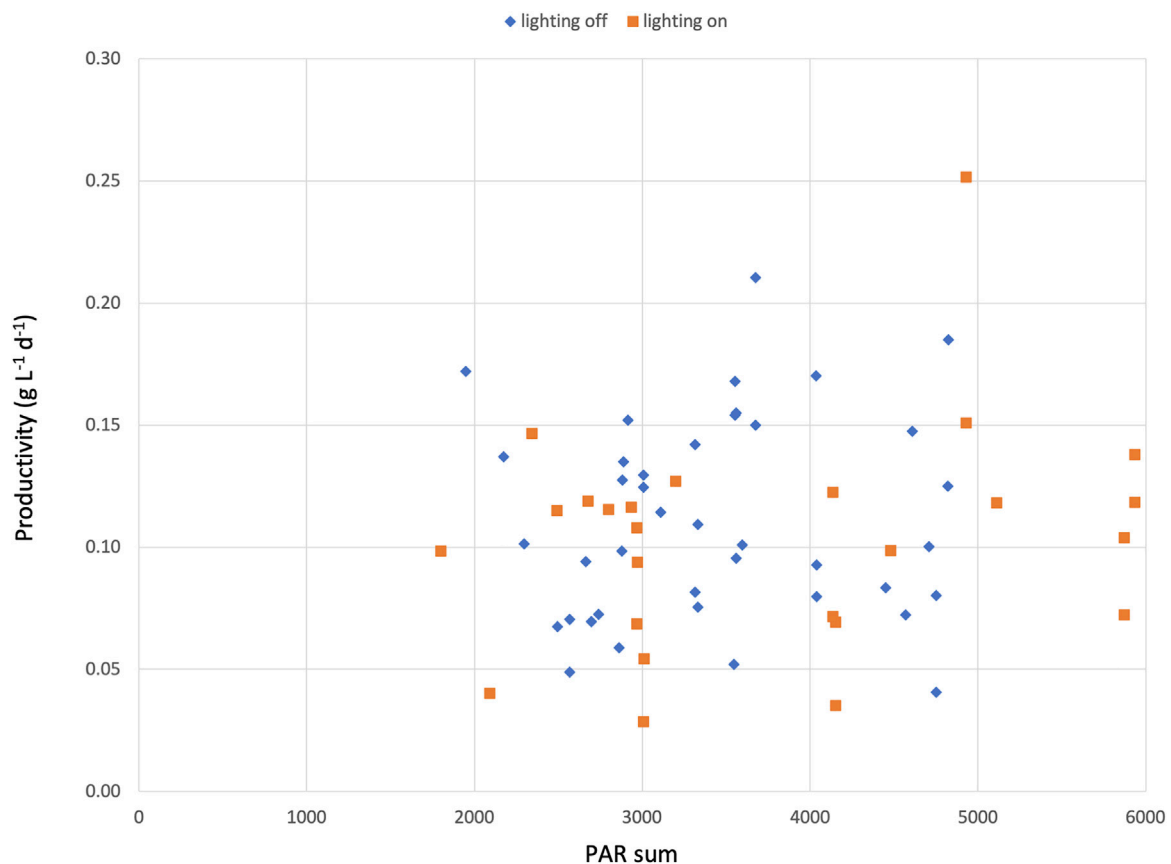


FIGURE 4 | Daily productivity of *C. typhlos* ($\text{g L}^{-1} \text{d}^{-1}$) and PAR sum of each specific day during the two growth periods. Each square represents 1 day.

were then compared to days without artificial light. However, no significant difference in biomass productivity was found between the days with artificial light versus the days without (**Figure 4**). Several reasons might explain why the extra lighting had no effect. One explanation could be that our 9-day test periods were too short to detect a difference. A second reason could be the high variance of received sunlight between the days. The PAR sum from the sunlight ranged from 1,588 to 5,431 mmol m^{-2} . On days with the addition of artificial light, the PAR sum increased by 10–31%; however, due to the high variance, the effect was limited. A third reason could be the use of insufficient or non-specific lighting. The reactors were constructed in 2014 and equipped with fluorescent lamps (6500 K) that only provided minimal extra lighting during the dark period. However, in recent years, more attention has been given to the use of modern LED lamps with a specific light spectrum to optimize the growth of microalgae (Glemser et al., 2016); using better lights might therefore have a significant impact on growth. A last final reason could be the placing of the lights. They were fixed underneath the PBR tubes and only reached a small area of the total PBR tubes. Placing LED lamps closer to each individual tube could increase the effects substantially.

Figure 5A shows a typical growth pattern based on turbidity measurements (NTU). A general increase in turbidity can be seen over the course of several days (the black arrow in **Figure 5A**),

indicating an increase in cells and biomass. When looking at a 24-h period, without artificial light added on days 3, 4, and 5, a typical pattern can be observed, pointing toward a diurnal rhythm. The cell cycle of photosynthetic microalgae is influenced by a day-night regime in which cell growth (G1) takes place during the light phase (daytime), and the reproductive, cell division phase (S/M) occurs during the dark period (nighttime) (Cross and Umen, 2015; Ivanov et al., 2019; Zou and Bozhkov, 2021). The NTU profile (**Figure 5A**) can be linked to this diurnal rhythm. The steady increase in NTU a few hours after sunrise to sunset follows the cell growth: the enlargement of the cells and increase in dry weight (Lien and Knutsen, 1979; Spudich and Sager, 1980; Ostgaard and Jensen, 1982; Bišová and Zachleder, 2014; de Winter et al., 2017b). After sunset and during the night, the NTU fluctuated little, which can be linked to the cells no longer growing but dividing within the parental cell (Harper, 1999; Cross and Umen, 2015; Ivanov et al., 2019; Zou and Bozhkov, 2021). Throughout warmer periods, the NTU decreased more overnight, which can be linked to the loss of biomass during the night. During warmer nights, the respiration rates can be higher than on colder nights (De-Luca et al., 2019; Masojádek et al., 2021), leading to more biomass loss and potentially explaining the more pronounced decrease in NTU during warmer nights.

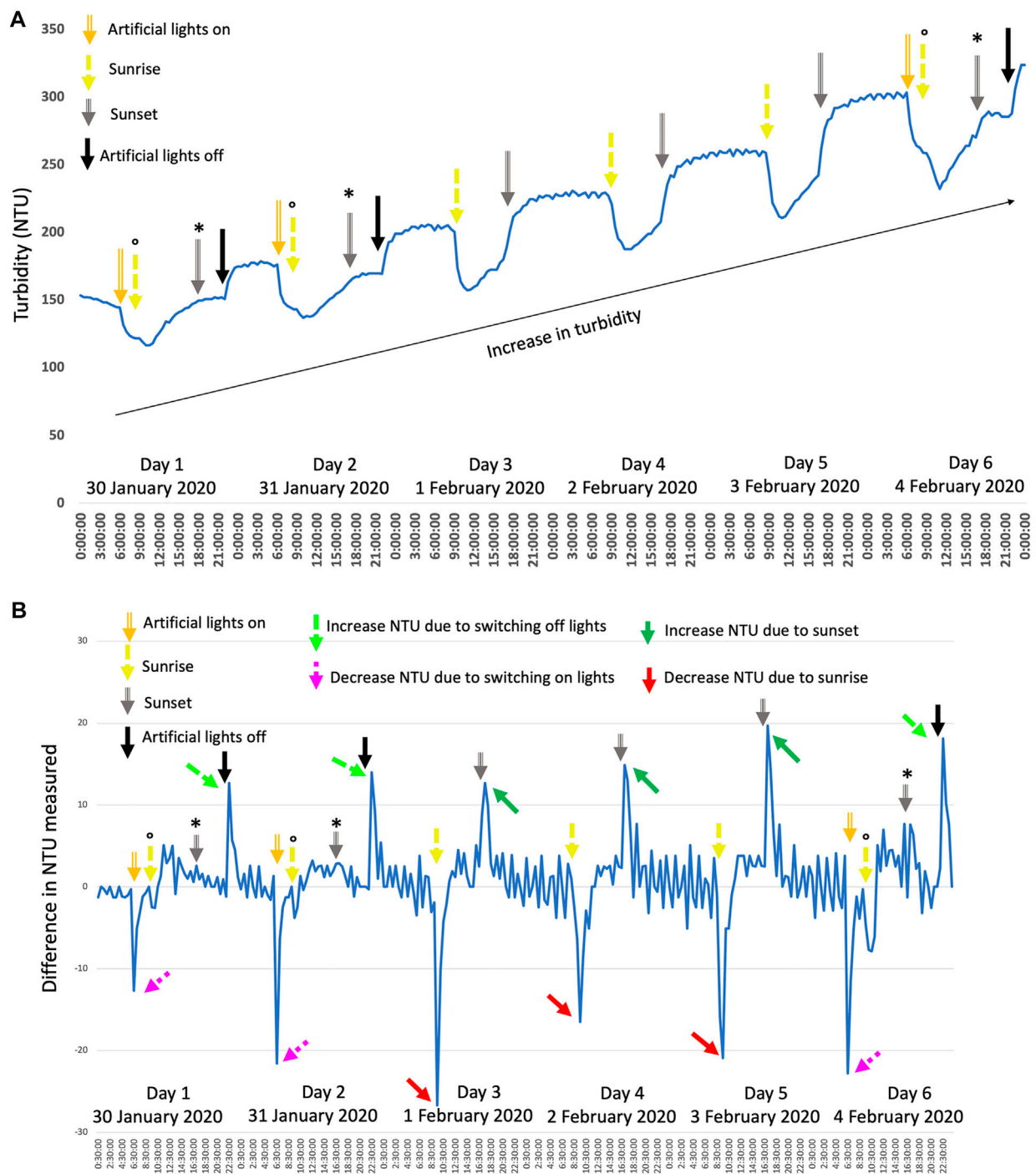


FIGURE 5 | (A) shows the typical growth pattern of *C. typhlos* observed over several days. A representative period during one of the winter periods is shown here with artificial lights being used to extend the day. Artificial lights were kept on between 6.30–10.30 and 15.30–22.00, although slight variances were possible depending on the real sunset and sunrise times of the specific days. **(B)** shows the difference in the NTU value calculated for every 30 min ($NTU_{x+30min} - NTU_x$) plotted over time. Arrows indicate specific time points or substantial increases/decreases. The symbol 'o' denotes the artificial light switching off at sunrise, while the symbol '*' denotes the artificial lights switching on at sunset. See text for more details.

This nightly biomass loss is often attributed to respiration using compounds like carbohydrates during the night (Ogbonna and Tanaka, 1996; Michels et al., 2014;

Edmundson and Huesemann, 2015; Åkerström et al., 2016). Next to the aforementioned, general pattern, a rapid and substantial drop or increase in turbidity, respectively, at

TABLE 3 | Overview of the total CO₂ injected during each batch growth test, pH was set at 8, and CO₂ was injected on demand to maintain a steady pH. The two periods in bold show the highest CO₂ utilization efficiency.

Period	Average pH	Average temperature	$(C_e - C_s)$ g L ⁻¹	CO _{2t} g	CO _{2th} g	CO _{2tL} g	U% %	CO _{2fr} g L ⁻¹ d ⁻¹
19–28 March 2019	8.21 ± 0.49	17.5 ± 0.9	0.250	5,390	160	5,220	2.97	0.05
1–10 April 2019	8.00 ± 0.25	18.4 ± 1.4	0.413	7,620	265	7,355	3.48	0.08
17–26 April 2019	7.93 ± 0.18	22.5 ± 2.5	0.091	2,430	58	2,372	2.40	0.02
10–19 December 2019	7.86 ± 0.25	16.7 ± 1.8	0.285	610	182	428	29.97	0.06
17–26 January 2020	7.80 ± 0.30	12.4 ± 1.4	0.515	860	330	530	38.42	0.11
27 January–5 February 2020	7.88 ± 0.24	15.1 ± 1.0	0.605	4,260	388	3,872	9.11	0.12
10–19 February 2020	7.96 ± 0.39	15.5 ± 1.5	0.543	3,980	348	3,632	8.75	0.11

sunrise and sunset, is seen. To highlight this, **Figure 5B** shows the difference in NTU between each half-hour registered. The drop in turbidity at sunrise is indicated with red arrows, while the increase at sunset is visualized with green arrows. A rapid decrease or increase points toward a strong and swift reaction of the algae to the presence or absence of light. The NTU is monitored with a nephelometric sensor that uses white light (400–700 nm) that can readably be used by microalgae (Carvalho et al., 2006; de Mooij et al., 2016). Potentially, *C. typhlos* is able to activate and upregulate its photosynthetic system very fast, leading to a substantial increase in absorption of light while reducing the scattered light and causing a rapid and substantial drop in turbidity (Thorne and Nannestad, 1959; Kourti, 2000; Gregory, 2009). For extremophiles, a fast activation or deactivation of their metabolism can be crucial to cope with harsh conditions (Harel et al., 2004; Peng et al., 2021).

As daughter cells are released from the parental cell at the end of the dark period (Mihara and Hase, 1971; Vítová and Zachleder, 2005; Harris et al., 2009; Bišová and Zachleder, 2014; Zou and Bozhkov, 2021), although it can extend into the light period (Eschbach et al., 2005), many new cells are present and able to influence the turbidity measurements when their photosynthetic apparatus is turned on at sunrise. See also **Figure 1** for daughter cells still inside the parental cell after multiple fission. A similar explanation can be given for the substantial rise in NTU at sunset. As the cells switch their metabolism from the light phase to the dark phase, less light is absorbed, thereby increasing the scattering of light and giving a higher NTU value at sunset and during the night.

When artificial light was provided (days 1, 2, and 6), a similar pattern could be observed. A steep decrease in turbidity was observed when the artificial light was turned on prior to sunset (purple dashed arrows), and an increase was seen when turning off the artificial light after sunset (light green dashed arrow; **Figure 5B**). **Figure 5A** shows that the effect of the artificial light was similar but not exactly the same. The steady increase of turbidity (NTU) during the growth phase was lower when only artificial light was present as compared to sunlight (plateau between gray and black arrow). However, the substantial increase in turbidity was similar when turning off the artificial light compared to at sunset (**Figure 5B**, dashed light green arrows). **Figure 5B** also shows that after turning on the artificial light before sunrise a second, lower drop in turbidity

was observable at sunrise (yellow arrows with the symbol “o” on top). Although no significant effect of artificial light was detected on the biomass production of *C. typhlos*, artificial light did, however, have a noticeable impact on the growth pattern of *C. typhlos*.

It is possible to use a continuous turbidity measurement in combination with the correlation between turbidity and dry weight to track the dry weight evolution (Thoré et al., 2021). Our results, however, also indicate that caution is needed when interpreting and linking turbidity measurements with the dry weight of the microalga cultivated. However, the growth (turbidity) pattern of *C. typhlos* was also different compared to other non-snow algae tested. Both *P. purpureum* and *N. gaditana* showed a substantial decrease in turbidity during the night (unpublished data) but no substantial decrease or increase respectively at sunrise and sunset. This could potentially indicate a different and faster response of snow algae to a night and day cycle. Like biomass loss overnight, the influence of the day/night cycles of microalgae and their effect on the cells, cell division, and biomass are still understudied and can vary between algae (Edmundson and Huesemann, 2015; de Winter et al., 2017a; León-Saiki et al., 2018). To optimize microalgae cultivation, the nightly biomass loss and circadian rhythm can be important factors to establish the optimal time of harvesting. Future studies should address this.

CO₂ Fixation and Utilization Efficiency

To investigate the CO₂ fixation and utilization efficiency, the total CO₂ injected into the photobioreactor was monitored. Using the total biomass produced during each period, the efficiency of CO₂ uptake could be calculated (**Table 3**).

During the periods 10–19 December 2019 and 17–26 January 2020, the CO₂ utilization efficiency was the highest at 29.97 and 38.42%, respectively. The other periods achieved lower utilization efficiencies with percentages between 2.4 and 9.11%. The exact reasons for this difference are unclear as many factors can influence the CO₂ utilization efficiency (Ryu et al., 2009; Daneshvar et al., 2022). Both periods have the lowest total PAR received ($2,379 \pm 345$ and $2,604 \pm 791$ mmol/m²); however, they do not differ significantly from the periods 19–28 March 2019 and 10–19 February (**Table 2**).

A second observation is that the maximum greenhouse temperatures reached during these two periods were also the

two lowest registered maximum temperatures, but the average temperature of the period 10–19 December was higher than that of three other periods (Table 2). During our tests, the worst efficiencies were seen during the three warmest periods (19–28 March 2019, $17.46 \pm 0.9^\circ\text{C}$; 1–10 April 2019, $18.4 \pm 1.4^\circ\text{C}$; and 17–26 April 2019, $22.4 \pm 2.5^\circ\text{C}$). This is in line with the lower solubility of CO_2 at higher temperatures (Singh and Singh, 2014). While we observed a wide range of CO_2 fixation rates and utilization efficiency, they are in accord with what others have already found for other algal species (Tang et al., 2011; Ketheesan and Nirmalakhandan, 2012; Lam et al., 2012). In laboratory conditions and smaller working volumes, one can easily maintain specific parameters such as total PAR, pH, temperature, or a day/night period; however, it is less possible in a greenhouse pilot plant or outdoors. In order to truly find a correlation between different parameters and CO_2 utilization to improve the utilization efficiency, more pilot plant studies are needed. CO_2 utilization efficiency can be very low and is influenced by many parameters such as the temperature, pH, and growth rate, making the design of a reactor with optimal gas exchange expensive and very difficult (Carvalho et al., 2006; Klinthong et al., 2015; Fu et al., 2019), if not impossible. In different (seasonal) weather conditions outdoors or in a greenhouse, it can particularly be arduous. Thus, a more interesting approach for improved sustainability might be to capture the CO_2 in the effluent gas and reuse it for the influent, lowering the total CO_2 lost into the air.

CONCLUSION

The psychrotolerant microalga *C. typhlos* was successfully cultivated in a greenhouse in a photobioreactor with a working volume of 350 L during several batch periods, ranging from winter to spring. A maximum dry weight and growth rate of 1.082 g L^{-1} and 0.105 d^{-1} , respectively, were achieved while maximum volumetric and areal productivities of $0.110 \text{ g L}^{-1} \text{ d}^{-1}$ and $2.746 \text{ g m}^{-2} \text{ d}^{-1}$, respectively, were measured. Being one of the first pilot-scale cultivation tests of a snow alga in a photobioreactor, it is difficult to compare with known data from snow algae. One critical factor, negatively influencing the growth, was shown to be ambient temperatures of $>30^\circ\text{C}$. Lower temperatures ($11\text{--}15^\circ\text{C}$), however, had no detrimental effect on the

growth. Due to the distinct growth pattern influenced by sunset or artificial light, it will be crucial to determine how to use artificial lights to find the optimal light/dark regime. While these experiments were carried out at a set pH of 8, future tests at different pH values will be crucial to determine the optimal pH and CO_2 uptake efficiency. Future tests to optimize the cultivation and production of *C. typhlos* biomass are, thus, crucial to estimate its commercial value. Furthermore, the production of astaxanthin or PUFAs has to be studied to fully explore the potential of *C. typhlos*.

DATA AVAILABILITY STATEMENT

The raw data supporting the conclusions of this article will be made available by the authors, without undue reservation.

AUTHOR CONTRIBUTIONS

FS: formal analysis and interpretation, writing—original draft, and writing—review and editing; JS: conceptualization, acquisition of data, and writing—review and editing; RA: formal analysis and writing—review and editing; SM: funding acquisition and writing—review and editing.

FUNDING

This research was funded by NORTH-WEST EUROPE INTERREG, grant number NWE 639 as part of the IDEA project (Implementation and development of economically viable algae-based value chains in North-West Europe).

ACKNOWLEDGMENTS

The authors would like to thank E. Gebruers, I. Noyens, and S. Goossens for helping with sampling for the acquisition of data, A. Wuyts for helping with the cultivation and upscaling of *C. typhlos*, and A. De Cuyper and E. Van Cantfort for improvement of the manuscript. Furthermore, we would also like to thank the reviewers for aiding in improving the manuscript.

REFERENCES

- Abo, B. O., Odey, E. A., Bakayoko, M., and Kalakodio, L. (2019). Microalgae to Biofuels Production: a Review on Cultivation, Application and Renewable Energy. *Rev. Environ. Health* 34, 91–99. doi:10.1515/reveh-2018-0052
- Adamczyk, M., Lasek, J., and Skawińska, A. (2016). CO_2 Biofixation and Growth Kinetics of *Chlorella Vulgaris* and *Nannochloropsis Gaditana*. *Appl. Biochem. Biotechnol.* 179, 1248–1261. doi:10.1007/s12010-016-2062-3
- Åkerström, A. M., Mortensen, L. M., Rusten, B., and Gislerød, H. R. (2016). Biomass Production and Removal of Ammonium and Phosphate by *Chlorella* Sp. In Sludge Liquor at Natural Light and Different Levels of Temperature Control. *Springerplus* 5, 676. doi:10.1186/s40064-016-2266-6
- Araújo, R., Vázquez Calderón, F., Sánchez López, J., Azevedo, I. C., Bruhn, A., Fluch, S., et al. (2021). Current Status of the Algae Production Industry in Europe: An Emerging Sector of the Blue Bioeconomy. *Front. Mar. Sci.* 7, 626389. doi:10.3389/fmars.2020.626389
- Barka, A., and Blecker, C. (2016). Microalgae as a Potential Source of Single-Cell Proteins. A Review. *Biotechnol. Agron. Soc. Environ.* 20, 427–436. doi:10.25518/1780-4507.13132
- Benedetti, M., Vecchi, V., Barera, S., and Dall'Osto, L. (2018). Biomass from Microalgae: the Potential of Domestication towards Sustainable Biofactories. *Microb. Cell Fact.* 17, 173. doi:10.1186/s12934-018-1019-3

- Bišová, K., and Zachleder, V. (2014). Cell-cycle Regulation in Green Algae Dividing by Multiple Fission. *J. Exp. Bot.* 65, 2585–2602. doi:10.1093/jxb/ert466
- Carvalho, A. P., Meireles, L. A., and Malcata, F. X. (2006). Microalgal Reactors: A Review of Enclosed System Designs and Performances. *Biotechnol. Prog.* 22, 1490–1506. doi:10.1021/bp060065r
- Cheregi, O., Ekdahl, S., Engelbrektsson, J., Strömberg, N., Godhe, A., and Spetea, C. (2019). Microalgae Biotechnology in Nordic Countries - the Potential of Local Strains. *Physiol. Plant.* 166, 438–450. doi:10.1111/ppl.12951
- Chisti, Y. (2007). Biodiesel from Microalgae. *Biotechnol. Adv.* 25, 294–306. doi:10.1016/j.biotechadv.2007.02.001
- Cross, F. R., and Umen, J. G. (2015). The *Chlamydomonas* Cell Cycle. *Plant J.* 82, 370–392. doi:10.1111/tpj.12795
- Cvetkovska, M., Hüner, N. P. A., and Smith, D. R. (2017). Chilling Out: the Evolution and Diversification of Psychrophilic Algae with a Focus on *Chlamydomonadales*. *Polar Biol.* 40, 1169–1184. doi:10.1007/s00300-016-2045-4
- Daneshvar, E., Wicker, R. J., Show, P.-L., and Bhatnagar, A. (2022). Biologically-mediated Carbon Capture and Utilization by Microalgae towards Sustainable CO₂ Biofixation and Biomass Valorization - A Review. *Chem. Eng. J.* 427, 130884. doi:10.1016/j.cej.2021.130884
- Darvehei, P., Bahri, P. A., and Moheimani, N. R. (2018). Model Development for the Growth of Microalgae: A Review. *Renew. Sustain. Energy Rev.* 97, 233–258. doi:10.1016/j.rser.2018.08.027
- de Mooij, T., de Vries, G., Latsos, C., Wijffels, R. H., and Janssen, M. (2016). Impact of Light Color on Photobioreactor Productivity. *Algal Res.* 15, 32–42. doi:10.1016/j.algal.2016.01.015
- de Vree, J. H., Bosma, R., Janssen, M., Barbosa, M. J., and Wijffels, R. H. (2015). Comparison of Four Outdoor Pilot-Scale Photobioreactors. *Biotechnol. Biofuels* 8, 215. doi:10.1186/s13068-015-0400-2
- de Winter, L., Cabanelas, I. T. D., Martens, D. E., Wijffels, R. H., and Barbosa, M. J. (2017a). The Influence of Day/night Cycles on Biomass Yield and Composition of *Neochloris Oleoabundans*. *Biotechnol. Biofuels* 10, 104. doi:10.1186/s13068-017-0762-8
- de Winter, L., Cabanelas, I. T. D., Órfão, A. N., Vaessen, E., Martens, D. E., Wijffels, R. H., et al. (2017b). The Influence of Day Length on Circadian Rhythms of *Neochloris Oleoabundans*. *Algal Res.* 22, 31–38. doi:10.1016/j.algal.2016.12.001
- De-Luca, R., Bezzo, F., Béchet, Q., and Bernard, O. (2019). Meteorological Data-Based Optimal Control Strategy for Microalgae Cultivation in Open Pond Systems. *Complexity* 2019, 1–12. doi:10.1155/2019/4363895
- Dolganyuk, V., Belova, D., Babich, O., Prosekov, A., Ivanova, S., Katserov, D., et al. (2020). Microalgae: A Promising Source of Valuable Bioproducts. *Biomolecules* 10, 1153. doi:10.3390/biom10081153
- Edmundson, S. J., and Huesemann, M. H. (2015). The Dark Side of Algae Cultivation: Characterizing Night Biomass Loss in Three Photosynthetic Algae, *Chlorella Sorokiniana*, *Nannochloropsis Salina* and *Picochlorum* Sp. *Algal Res.* 12, 470–476. doi:10.1016/j.algal.2015.10.012
- Eschbach, E., John, U., Reckermann, M., Cembella, A., Edvardsen, B., and Medlin, L. (2005). Cell Cycle Dependent Expression of Toxicity by the Ichthyotoxic *Prymnesiophyte* *Chrysochromulina Polylepis*. *Aquat. Microb. Ecol.* 39, 85–95. doi:10.3354/ame039085
- Fu, J., Huang, Y., Liao, Q., Xia, A., Fu, Q., and Zhu, X. (2019). Photo-bioreactor Design for Microalgae: A Review from the Aspect of CO₂ Transfer and Conversion. *Bioresour. Technol.* 292, 121947. doi:10.1016/j.biortech.2019.121947
- Garrido-Cardenas, J. A., Manzano-Agugliaro, F., Acien-Fernandez, F. G., and Molina-Grima, E. (2018). Microalgae Research Worldwide. *Algal Res.* 35, 50–60. doi:10.1016/j.algal.2018.08.005
- Glemser, M., Heining, M., Schmidt, J., Becker, A., Garbe, D., Buchholz, R., et al. (2016). Application of Light-Emitting Diodes (LEDs) in Cultivation of Phototrophic Microalgae: Current State and Perspectives. *Appl. Microbiol. Biotechnol.* 100, 1077–1088. doi:10.1007/s00253-015-7144-6
- González-Camejo, J., Aparicio, S., Ruano, M. v., Borrás, L., Barat, R., and Ferrer, J. (2019). Effect of Ambient Temperature Variations on an Indigenous Microalgae-Nitrifying Bacteria Culture Dominated by *Chlorella*. *Bioresour. Technol.* 290, 121788. doi:10.1016/j.biortech.2019.121788
- Gorton, H. L., Williams, W. E., and Vogelmann, T. C. (2007). The Light Environment and Cellular Optics of the Snow Alga *Chlamydomonas Nivalis* (Bauer) Willet. *Photochem. Photobiol.* 73, 611–620. doi:10.1562/0031-8655(2001)0730611tleaco2.0.co2
- Gregory, J. (2009). Monitoring Particle Aggregation Processes. *Adv. Colloid Interface Sci.* 147–148, 109–123. doi:10.1016/j.cis.2008.09.003
- Guiry, M. D. (2012). How Many Species of Algae Are There? *J. Phycol.* 48, 1057–1063. doi:10.1111/j.1529-8817.2012.01222.x
- Han, D., Li, Y., and Hu, Q. (2013). Astaxanthin in Microalgae: Pathways, Functions and Biotechnological Implications. *Algae* 28, 131–147. doi:10.4490/algae.2013.28.2.131
- Harel, Y., Ohad, I., and Kaplan, A. (2004). Activation of Photosynthesis and Resistance to Photoinhibition in Cyanobacteria within Biological Desert Crust. *Plant Physiol.* 136, 3070–3079. doi:10.1104/pp.104.047712
- Harper, J. D. I. (1999). “*Chlamydomonas* Cell Cycle Mutants,” in *International Review of Cytology*. Editor K. W. Jeon (San Diego: Academic Press), 131–176. doi:10.1016/B/S0074-7696(08)61387-X
- Harris, E. H., Stern, D. B., and Witman, G. B. (2009). “Cell Division,” in *The Chlamydomonas Sourcebook*. Editors E. H. Harris, D. B. Stern, and G. B. Witman. Second Edition (London: Academic Press), 65–87. doi:10.1016/B978-0-12-370873-1.00003-4
- Hoham, R. W., and Remias, D. (2020). Snow and Glacial Algae: A Review1. *J. Phycol.* 56, 264–282. doi:10.1111/jpy.12952
- Hulatt, C. J., Berecz, O., Egeland, E. S., Wijffels, R. H., and Kiron, V. (2017). Polar Snow Algae as a Valuable Source of Lipids? *Bioresour. Technol.* 235, 338–347. doi:10.1016/j.biortech.2017.03.130
- Idrissi Abdelkhalak, E. A., Mohamed, B., Mohammed, A. M., and Lotfi, A. (2016). Growth Performance and Biochemical Composition of Nineteen Microalgae Collected from Different Moroccan Reservoirs. *Medit. Mar. Sci.* 17, 323–332. doi:10.12681/mms.1320
- Ivanov, I. N., Vitová, M., and Bišová, K. (2019). Growth and the Cell Cycle in Green Algae Dividing by Multiple Fission. *Folia Microbiol.* 64, 663–672. doi:10.1007/s12223-019-00741-z
- Ketheesan, B., and Nirmalakhandan, N. (2012). Feasibility of Microalgal Cultivation in a Pilot-Scale Airlift-Driven Raceway Reactor. *Bioresour. Technol.* 108, 196–202. doi:10.1016/j.biortech.2011.12.146
- Khan, M. I., Shin, J. H., and Kim, J. D. (2018). The Promising Future of Microalgae: Current Status, Challenges, and Optimization of a Sustainable and Renewable Industry for Biofuels, Feed, and Other Products. *Microb. Cell Fact.* 17, 1–36. doi:10.1186/s12934-018-0879-x
- Klinthong, W., Yang, Y.-H., Huang, C.-H., and Tan, C.-S. (2015). A Review: Microalgae and Their Applications in CO₂ Capture and Renewable Energy. *Aerosol Air Qual. Res.* 15, 712–742. doi:10.4209/aaqr.2014.11.0299
- Kourti, T. (2000). “Turbidimetry in Particle Size Analysis,” in *Encyclopedia of Analytical Chemistry* (New York: John Wiley & Sons). doi:10.1002/9780470027318.a1517
- Kvídová, J. (2010). Characterization of the Community of Snow Algae and Their Photochemical Performance in Situ in the Giant Mountains, Czech Republic. *Antarct. Alp. Res.* 42, 210–218. doi:10.1657/1938-4246-42.2.210
- Kvídová, J., Shukla, S. P., Pushparaj, B., and Elster, J. (2017). “Perspectives of Low-Temperature Biomass Production of Polar Microalgae and Biotechnology Expansion into High Latitudes,” in *Psychrophiles: From Biodiversity to Biotechnology*. Second Edition (New York: Springer International Publishing), 585–600. doi:10.1007/978-3-319-57057-0_25
- Lam, M. K., Lee, K. T., and Mohamed, A. R. (2012). Current Status and Challenges on Microalgae-Based Carbon Capture. *Int. J. Greenh. Gas Control* 10, 456–469. doi:10.1016/j.jggc.2012.07.010
- León-Saiki, G. M., Cabrero Martí, T., van der Veen, D., Wijffels, R. H., and Martens, D. E. (2018). The Impact of Day Length on Cell Division and Efficiency of Light Use in a Starchless Mutant of *Tetrademus Obliquus*. *Algal Res.* 31, 387–394. doi:10.1016/j.algal.2018.02.027
- Ley, T., Rahn, A., Lütz, C., and Remias, D. (2009). Response of Arctic Snow and Permafrost Algae to High Light and Nitrogen Stress by Changes in Pigment Composition and Applied Aspects for Biotechnology. *FEMS Microbiol. Ecol.* 67, 432–443. doi:10.1111/j.1574-6941.2008.00641.x
- Lien, T., and Knutsen, G. (1979). Synchronous Growth of *Chlamydomonas Reinhardtii* (Chlorophyceae): a Review of Optimal Conditions1. *J. Phycol.* 15, 191–200. doi:10.1111/j.1529-8817.1979.tb02984.x
- Liu, Y. C., and Nakamura, Y. (2019). Triacylglycerol Production in the Snow Algae *Chlamydomonas Nivalis* under Different Nutrient Conditions. *Lipids* 54, 255–262. doi:10.1002/lipd.12143

- Lukeš, M., Procházková, L., Schmidt, V., Nedbalová, L., and Kaftan, D. (2014). Temperature Dependence of Photosynthesis and Thylakoid Lipid Composition in the Red Snow Alga *Chlamydomonas* Cf. *Nivalis* (Chlorophyceae). *FEMS Microbiol. Ecol.* 89, 303–315. doi:10.1111/1574-6941.12299
- Mandalam, R. K., and Palsson, B. (1998). Elemental Balancing of Biomass and Medium Composition Enhances Growth Capacity in High-density *Chlorella Vulgaris* Cultures. *Biotechnol. Bioeng.* 59, 605–611. doi:10.1002/(sici)1097-0290(19980905)59:5<605::aid-bit11>3.0.co;2-8
- Masojidek, J., Ranglová, K., Lakatos, G. E., Silva Benavides, A. M., and Torzillo, G. (2021). Variables Governing Photosynthesis and Growth in Microalgae Mass Cultures. *Processes* 9, 820. doi:10.3390/pr9050820
- Mata, T. M., Martins, A. A., and Caetano, N. S. (2010). Microalgae for Biodiesel Production and Other Applications: A Review. *Renew. Sustain. Energy Rev.* 14, 217–232. doi:10.1016/j.rser.2009.07.020
- Matsumoto, M., Nojima, D., Nonoyama, T., Ikeda, K., Maeda, Y., Yoshino, T., et al. (2017). Outdoor Cultivation of Marine Diatoms for Year-Round Production of Biofuels. *Mar. Drugs* 15, 94. doi:10.3390/md15040094
- Metsoviti, M. N., Papapolymerou, G., Karapanagiotidis, I. T., and Katsoulas, N. (2019). Comparison of Growth Rate and Nutrient Content of Five Microalgae Species Cultivated in Greenhouses. *Plants* 8, 279. doi:10.3390/plants8080279
- Michels, M. H. A., Slegers, P. M., Vermuë, M. H., and Wijffels, R. H. (2014). Effect of Biomass Concentration on the Productivity of *Tetraselmis Suecica* in a Pilot-Scale Tubular Photobioreactor Using Natural Sunlight. *Algal Res.* 4, 12–18. doi:10.1016/j.algal.2013.11.011
- Mihara, S., and Hase, E. (1971). Studies on the Vegetative Life Cycle of *Chlamydomonas Reinhardtii* Dangeard in Synchronous Culture I. Some Characteristics of the Cell Cycle. *Plant Cell Physiology* 12 (2), 225–236. doi:10.1093/oxfordjournals.pcp.a074616
- Minhas, A. K., Hodgson, P., Barrow, C. J., and Adholeya, A. (2016). A Review on the Assessment of Stress Conditions for Simultaneous Production of Microalgal Lipids and Carotenoids. *Front. Microbiol.* 7, 546. doi:10.3389/fmicb.2016.00546
- Mirón, A. S., Garcí'a, M. C. C., Gómez, A. C., Camacho, F. G., Grima, E. M., and Chisti, Y. (2003). Shear Stress Tolerance and Biochemical Characterization of *Phaeodactylum Tricornutum* in Quasi Steady-State Continuous Culture in Outdoor Photobioreactors. *Biochem. Eng. J.* 16, 287–297. doi:10.1016/S1369-703X(03)00072-X
- Moody, J. W., McGinty, C. M., and Quinn, J. C. (2014). Global Evaluation of Biofuel Potential from Microalgae. *Proc. Natl. Acad. Sci. U.S.A.* 111, 8691–8696. doi:10.1073/pnas.1321652111
- Morales-Sánchez, D., Schulze, P. S. C., Kiron, V., and Wijffels, R. H. (2020). Production of Carbohydrates, Lipids and Polyunsaturated Fatty Acids (PUFA) by the Polar Marine Microalga *Chlamydomonas Malina* RCC2488. *Algal Res.* 50, 102016. doi:10.1016/j.algal.2020.102016
- Mosser, J. L., Mosser, A. G., and Brock, T. D. (1977). Photosynthesis in the Snow: the Alga *Chlamydomonas Nivalis* (Chlorophyceae)¹. *J. Phycol.* 13, 22–27. doi:10.1111/j.1529-8817.1977.tb02881.x
- Ogbonna, J. C., and Tanaka, H. (1996). Night Biomass Loss and Changes in Biochemical Composition of Cells during Light/dark Cyclic Culture of *Chlorella Pyrenoidosa*. *J. Ferment. Bioeng.* 82, 558–564. doi:10.1016/S0922-338X(97)81252-4
- Onuma, Y., Takeuchi, N., Tanaka, S., Nagatsuka, N., Niwano, M., and Aoki, T. (2018). Observations and Modelling of Algal Growth on a Snowpack in North-Western Greenland. *Cryosphere* 12, 2147–2158. doi:10.5194/tc-12-2147-2018
- Ostgaard, K., and Jensen, A. (1982). Diurnal and Circadian Rhythms in the Turbidity of Growing *Skeletonema Costatum* Cultures. *Mar. Biol.* 66, 261–268. doi:10.1007/BF00397031
- Patil, P. D., Reddy, H., Muppaneni, T., Mannarswamy, A., Schuab, T., Holguin, F. O., et al. (2012). Power Dissipation in Microwave-Enhanced *In Situ* Transesterification of Algal Biomass to Biodiesel. *Green Chem.* 14, 809–818. doi:10.1039/c2gc16195h
- Peng, Z., Liu, G., and Huang, K. (2021). Cold Adaptation Mechanisms of a Snow Alga *Chlamydomonas Nivalis* during Temperature Fluctuations. *Front. Microbiol.* 11, 611080. doi:10.3389/fmicb.2020.611080
- Procházková, L., Remias, D., Řezanka, T., and Nedbalová, L. (2018). *Chloromonas Nivalis* Subsp. *Tatrae*, Subsp. Nov. (Chlamydomonadales, Chlorophyta): Re-examination of a Snow Alga from the High Tatra Mountains (Slovakia). *Fottea* 18, 1–18. doi:10.5507/fot.2017.010
- Quinn, J., de Winter, L., and Bradley, T. (2011). Microalgae Bulk Growth Model with Application to Industrial Scale Systems. *Bioresour. Technol.* 102, 5083–5092. doi:10.1016/j.biortech.2011.01.019
- Remias, D., Karsten, U., Lütz, C., and Leya, T. (2010). Physiological and Morphological Processes in the Alpine Snow Alga *Chloromonas Nivalis* (Chlorophyceae) during Cyst Formation. *Protoplasma* 243, 73–86. doi:10.1007/s00709-010-0123-y
- Remias, D., Lütz-Meindl, U., and Lütz, C. (2005). Photosynthesis, Pigments and Ultrastructure of the Alpine Snow alga *Chlamydomonas Nivalis*. *Eur. J. Phycol.* 40, 259–268. doi:10.1080/09670260500202148
- Remias, D., Pichrtová, M., Pangratz, M., Lütz, C., and Holzinger, A. (2016). Ecophysiology, Secondary Pigments and Ultrastructure of *Chlamydomonas* (Chlorophyta) from the European Alps Compared with *Chlamydomonas Nivalis* forming Red Snow. *FEMS Microbiol. Ecol.* 92, fiv030. doi:10.1093/femsec/fiv030
- Rendón-Castrillón, L., Ramírez-Carmona, M., Ocampo-López, C., and Giraldo-Aristizabal, R. (2021). Evaluation of the Operational Conditions in the Production and Morphology of *Chlorella* Sp. *Braz. J. Biol.* 81, 202–209. doi:10.1590/1519-6984.228874
- Richmond, A. (2000). Microalgal Biotechnology at the Turn of the Millennium: A Personal View. *J. Appl. Phycol.* 12, 441–451. doi:10.1023/a:1008123131307
- Ryu, H. J., Oh, K. K., and Kim, Y. S. (2009). Optimization of the Influential Factors for the Improvement of CO₂ Utilization Efficiency and CO₂ Mass Transfer Rate. *J. Industrial Eng. Chem.* 15, 471–475. doi:10.1016/j.jiec.2008.12.012
- Sathasivam, R., Radhakrishnan, R., Hashem, A., and Abd_Allah, E. F. (2019). Microalgae Metabolites: A Rich Source for Food and Medicine. *Saudi J. Biol. Sci.* 26, 709–722. doi:10.1016/j.sjbs.2017.11.003
- Sayre, R. (2010). Microalgae: The Potential for Carbon Capture. *BioScience* 60, 722–727. doi:10.1525/bio.2010.60.9.9
- Shi, T.-Q., Wang, L.-R., Zhang, Z.-X., Sun, X.-M., and Huang, H. (2020). Stresses as First-Line Tools for Enhancing Lipid and Carotenoid Production in Microalgae. *Front. Bioeng. Biotechnol.* 8, 610. doi:10.3389/fbioe.2020.00610
- Singh, S. P., and Singh, P. (2014). Effect of CO₂ Concentration on Algal Growth: A Review. *Renew. Sustain. Energy Rev.* 38, 172–179. doi:10.1016/j.rser.2014.05.043
- Singh, U. B., and Ahluwalia, A. S. (2013). Microalgae: a Promising Tool for Carbon Sequestration. *Mitig. Adapt. Strateg. Glob. Change* 18, 73–95. doi:10.1007/s11027-012-9393-3
- Spudich, J. L., and Sager, R. (1980). Regulation of the *Chlamydomonas* Cell Cycle by Light and Dark. *J. Cell Biol.* 85, 136–145. doi:10.1083/jcb.85.1.136
- Suzuki, H., Hulatt, C. J., Wijffels, R. H., and Kiron, V. (2019). Growth and LC-PUFA Production of the Cold-Adapted Microalga *Koliella antarctica* in Photobioreactors. *J. Appl. Phycol.* 31, 981–997. doi:10.1007/s10811-018-1606-z
- Tang, D., Han, W., Li, P., Miao, X., and Zhong, J. (2011). CO₂ Biofixation and Fatty Acid Composition of *Scenedesmus Obliquus* and *Chlorella Pyrenoidosa* in Response to Different CO₂ Levels. *Bioresour. Technol.* 102, 3071–3076. doi:10.1016/j.biortech.2010.10.047
- Teoh, M.-L., Phang, S.-M., and Chu, W.-L. (2013). Response of Antarctic, Temperate, and Tropical Microalgae to Temperature Stress. *J. Appl. Phycol.* 25, 285–297. doi:10.1007/s10811-012-9863-8
- Thoré, E. S. J., Schoeters, F., Spit, J., and van Miert, S. (2021). Real-Time Monitoring of Microalgal Biomass in Pilot-Scale Photobioreactors Using Nephelometry. *Processes* 9, 1530. doi:10.3390/pr9091530
- Thorne, R. S. W., and Nannestad, I. (1959). Some Considerations on the Physical Significance of Turbidity Estimates. *J. Inst. Brew.* 65, 175–188. doi:10.1002/j.2050-0416.1959.tb01443.x
- Tredici, M. R., and Materassi, R. (1992). From Open Ponds to Vertical Alveolar Panels: the Italian Experience in the Development of Reactors for the Mass Cultivation of Phototrophic Microorganisms. *J. Appl. Phycol.* 4, 221–231. doi:10.1007/BF02161208
- Tredici, M. R. (2010). Photobiology of Microalgae Mass Cultures: Understanding the Tools for the Next Green Revolution. *Biofuels* 1, 143–162. doi:10.4155/bfs.09.10
- Vale, M. A., Ferreira, A., Pires, J. C. M., and Gonçalves, A. L. (2020). “CO₂ Capture Using Microalgae,” in *Advances in Carbon Capture* (Cambridge: Elsevier), 381–405. doi:10.1016/b978-0-12-819657-1.00017-7

- Varshney, P., Mikulic, P., Vonshak, A., Beardall, J., and Wangikar, P. P. (2015). Extremophilic Micro-algae and Their Potential Contribution in Biotechnology. *Bioresour. Technol.* 184, 363–372. doi:10.1016/j.biortech.2014.11.040
- Vecchi, V., Barera, S., Bassi, R., and Dall'Osto, L. (2020). Potential and Challenges of Improving Photosynthesis in Algae. *Plants* 9, 67. doi:10.3390/plants9010067
- Vítová, M., and Zachleder, V. (2005). Points of Commitment to Reproductive Events as a Tool for Analysis of the Cell Cycle in Synchronous Cultures of Algae. *Folia Microbiol.* 50, 141–149. doi:10.1007/BF02931463
- Wang, Y., Tibbetts, S., and McGinn, P. (2021). Microalgae as Sources of High-Quality Protein for Human Food and Protein Supplements. *Foods* 10, 3002. doi:10.3390/foods10123002
- Zheng, Y., Xue, C., Chen, H., He, C., and Wang, Q. (2020). Low-Temperature Adaptation of the Snow Alga *Chlamydomonas Nivalis* Is Associated with the Photosynthetic System Regulatory Process. *Front. Microbiol.* 11, 1233. doi:10.3389/fmicb.2020.01233
- Zou, Y., and Bozhkov, P. v. (2021). *Chlamydomonas* Proteases: Classification, Phylogeny, and Molecular Mechanisms. *J. Exp. Bot.* 72, 7680–7693. doi:10.1093/jxb/erab383

Conflict of Interest: The authors declare that the research was conducted in the absence of any commercial or financial relationships that could be construed as a potential conflict of interest.

Publisher's Note: All claims expressed in this article are solely those of the authors and do not necessarily represent those of their affiliated organizations, or those of the publisher, the editors, and the reviewers. Any product that may be evaluated in this article, or claim that may be made by its manufacturer, is not guaranteed or endorsed by the publisher.

Copyright © 2022 Schoeters, Spit, Azizah and Van Miert. This is an open-access article distributed under the terms of the Creative Commons Attribution License (CC BY). The use, distribution or reproduction in other forums is permitted, provided the original author(s) and the copyright owner(s) are credited and that the original publication in this journal is cited, in accordance with accepted academic practice. No use, distribution or reproduction is permitted which does not comply with these terms.



OPEN ACCESS

EDITED BY

Kanhaiya Kumar,
Indian Institute of Integrative Medicine
(CSIR), India

REVIEWED BY

Guodong Luan,
Chinese Academy of Sciences (CAS),
China
Neha Arora,
University of South Florida,
United States

*CORRESPONDENCE

Alexandre J. Paquette,
alexandre.paquette@ucalgary.ca

SPECIALTY SECTION

This article was submitted to Bioprocess
Engineering,
a section of the journal
Frontiers in Bioengineering and
Biotechnology

RECEIVED 13 May 2022

ACCEPTED 11 July 2022

PUBLISHED 11 August 2022

CITATION

Paquette AJ, Vadlamani A, Demirkaya C,
Strous M and De la Hoz Siegler H (2022),
Nutrient management and medium
reuse for cultivation of a cyanobacterial
consortium at high pH and alkalinity.
Front. Bioeng. Biotechnol. 10:942771.
doi: 10.3389/fbioe.2022.942771

COPYRIGHT

© 2022 Paquette, Vadlamani,
Demirkaya, Strous and De la Hoz Siegler.
This is an open-access article
distributed under the terms of the
Creative Commons Attribution License
(CC BY). The use, distribution or
reproduction in other forums is
permitted, provided the original
author(s) and the copyright owner(s) are
credited and that the original
publication in this journal is cited, in
accordance with accepted academic
practice. No use, distribution or
reproduction is permitted which does
not comply with these terms.

Nutrient management and medium reuse for cultivation of a cyanobacterial consortium at high pH and alkalinity

Alexandre J. Paquette^{1*}, Agasteswar Vadlamani¹,
Cigdem Demirkaya², Marc Strous¹ and
Hector De la Hoz Siegler²

¹Department of Geoscience, University of Calgary, Calgary, AB, Canada, ²Department of Chemical and Petroleum Engineering, University of Calgary, Calgary, AB, Canada

Alkaliphilic cyanobacteria have gained significant interest due to their robustness, high productivity, and ability to convert CO₂ into bioenergy and other high value products. Effective nutrient management, such as re-use of spent medium, will be essential to realize sustainable applications with minimal environmental impacts. In this study, we determined the solubility and uptake of nutrients by an alkaliphilic cyanobacterial consortium grown at high pH and alkalinity. Except for Mg, Ca, Co, and Fe, all nutrients are in fully soluble form. The cyanobacterial consortium grew well without any inhibition and an overall productivity of 0.15 g L⁻¹ d⁻¹ (AFDW) was achieved. Quantification of nutrient uptake during growth resulted in the empirical formula CH_{1.81}N_{0.17}O_{0.20}P_{0.013}S_{0.009} for the consortium biomass. We showed that spent medium can be reused for at least five growth/harvest cycles. After an adaptation period, the cyanobacterial consortium fully acclimatized to the spent medium, resulting in complete restoration of biomass productivity.

KEYWORDS

nutrient management, *Candidatus "Phormidium alkaliphilum"*, nutrient uptake, microalgae cultivation, reuse, spent medium

Introduction

Photosynthetic microorganisms such as cyanobacteria and eukaryotic microalgae have been proposed as a source of biomass for the production of bioenergy and bioproducts (Chisti, 2007; Mata et al., 2010; Khan et al., 2018). These microorganisms can grow on non-arable land and can potentially reach higher areal productivities than traditional food crops (Chisti, 2007; Brennan, 2010; Johnson and Wen, 2010; Christenson and Sims, 2012; Singh et al., 2017). While eukaryotic microalgae are investigated for their high lipid content, possibly contributing to renewable energy, cyanobacteria are mainly cultivated at large scale to produce high value products such as pigments, proteins, and vitamins (Chisti, 2007; Hoh et al., 2016; Singh et al., 2017).

Current large-scale systems for algal cultivation have a high-water footprint and nutrient demand (Scott et al., 2010; Zhang et al., 2014; Farooq et al., 2015; Lu et al., 2020). In fact, some studies have reported that to produce 1 L of microalgal biodiesel, over 3000 L of water is required (Farooq et al., 2015). Nutrient demand is typically associated with nitrogen and phosphorus, as they are energy intensive to obtain or their worldwide reserves are depleting (Rösch et al., 2012). Although carbon dioxide is less associated with the topic of nutrient demand, it is also crucial for algal biomass production and its supply to the culture needs to be considered. Depending on the growth conditions carbon can be supplied as CO₂ that is bubbled into the media or in the form of bicarbonate (HCO₃⁻) (Chi et al., 2011; Rafa et al., 2021; Zhu et al., 2021). For systems that bubble in CO₂ there are high capital and operating costs associated with CO₂ transportation and bubbling, as well as high energy requirements (Chi et al., 2011; Rafa et al., 2021; Zhu et al., 2021). In systems that use bicarbonate there are costs associated with the high concentration of bicarbonate in the growth medium. Some studies have shown that the use of bicarbonate may also avoid costs by preventing culture crashes (Rafa et al., 2021; Zhu et al., 2021). As the global demand for high value cyanobacterial products increases (Singh et al., 2017; Bhalamurugan et al., 2018), the water and nutrient requirements will only increase, potentially leading to an unsustainable process (Hannon et al., 2010; Farooq et al., 2015; Lu et al., 2020).

To implement an effective cultivation strategy and mitigate the high water and nutrient demand, multiple strategies have been proposed: 1) usage of nutrient-rich wastewater streams as a main source of nutrients and 2) re-use of spent media with supplementation of the depleted nutrients (Acien Fernández et al., 2012; Acien Fernández et al., 2018; Barbera et al., 2018). Although mitigation with nutrient-rich wastewater streams is a promising strategy, it could potentially introduce foreign substances (e.g., heavy metal ions, pathogenic microbes, etc.) into the cultivation system. Therefore, it might not be a viable option for biomass that is cultivated for food and pharmaceuticals (Barbera et al., 2018).

Cultivation of alkaliphilic, “high pH loving,” cyanobacteria has gained interest over the recent years because of their robustness and ability to capture carbon dioxide directly from the atmosphere (Bell et al., 2016; Canon-Rubio, 2016; Sharp et al., 2017; Zhu et al., 2018; Ataiean et al., 2019; Chowdhury et al., 2019; Kim et al., 2019; Berthold et al., 2020). Previously, we enriched a consortium consisting of the alkaliphilic filamentous cyanobacterium *Candidatus* “Phormidium alkaliphilum” (80–90%) and associated heterotrophs (Ataiean et al., 2021; Ataiean et al., 2022). It was enriched from soda lakes located on the Cariboo Plateau (British Columbia, Canada) and was cultivated at a pH of up to 11.2 and with 0.5 mol/L of combined carbonates. This pH was high enough to demonstrate regeneration of spent media with carbon dioxide captured directly from the air (Ataiean et al., 2019). Long-term, crash-

free productivity was shown in the laboratory (15.2 ± 1.0 g L⁻¹ d⁻¹, Ataiean et al. (2019)), as well as in an outdoor, high latitude pilot plant (5.8 g/m²/d, Haines et al. (2022)). The consortium contains 11–17% phycocyanin (Ataiean et al., 2021), which is a valuable, nutritious, and healthy blue pigment. Consortium composition at harvesting contains 60.9% protein, 13.4% lipids and 12% carbohydrates (Sharp et al., 2017; Demirkaya et al., 2022). Both productivity and biomass composition were typical of cyanobacteria, including *Arthrospira* (*Spirulina*). Although replenishing of inorganic carbon using air was a major step forward, reuse of other nutrients (P, N, Mg, S, Na, K, Ca, and Fe) is as important to make the cultivation system sustainable.

Using wastewater as a source of nutrients would not work for such a high-alkalinity cultivation system, because if an alkaline medium is combined with wastewater for cultivation, the alkalinity would be lost by dilution with non-alkaline wastewater. Re-use of spent media would mitigate both water and nutrient demand (Farooq et al., 2015; Lu et al., 2020). One study found that reusing spent media can reduce nutrient and water usage by 55 and 84%, respectively (Yang et al., 2011). The biggest advantage to reusing spent media is the cost savings on water, water pumping and nutrients (Yang et al., 2011; Farooq et al., 2015; Lu et al., 2020). Therefore, it is important to understand the effect of spent medium on biomass growth. Re-use of spent medium has been shown to increase, decrease or have no effect on biomass growth, depending on many factors such as culture conditions and harvesting methods (Lu et al., 2020). One area where the reuse of spent medium has not been well studied for biomass growth is in the cultivation of alkaliphilic cyanobacteria.

Here, we extend our previous work on the cultivation of an alkaliphilic cyanobacterial consortium and describe the nutrient solubility/availability and nutrient uptake rates at high pH (>10) and alkalinity (0.5 M). We also design and demonstrate cultivation conditions that allow re-use of the spent growth medium. The objectives of this study are to 1) determine the solubility of the provided nutrients at high pH, 2) investigate which nutrients are present at the end of a cultivation cycle and 3) determine if the alkaliphilic cyanobacterial consortium can be grown with recycled, spent media.

Materials and methods

Cultivation conditions

A laboratory grown microbial consortium dominated by cyanobacteria was used in all experiments (Ataiean et al., 2019; Ataiean et al., 2021; Ataiean et al., 2022). This consortium was originally enriched from photosynthetic microbial mats obtained from soda lakes located on the Cariboo Plateau (British Columbia, Canada) (Sharp et al.,

2017). A synthetic growth medium was formulated to simulate the high pH and alkalinity conditions of the soda lakes (Vadlamani et al., 2017; Ataiean et al., 2019). This medium, also used here, contained the following: Na_2CO_3 (210.98 mM), NaHCO_3 (77.85 mM), NaNO_3 (3.06 mM), NH_4Cl (0.92 mM), KH_2PO_4 (1.44 mM), $\text{MgSO}_4 \cdot 7\text{H}_2\text{O}$ (1 mM), $\text{CaCl}_2 \cdot 2\text{H}_2\text{O}$ (0.17 mM), NaCl (0.43 mM), KCl (6.04 mM), $\text{FeCl}_3 \cdot 6\text{H}_2\text{O}$ (0.04 mM) and 300 $\mu\text{L/L}$ of a trace metal solution. The trace metal solution contained H_3BO_3 (9.7 mM), $\text{MnCl}_2 \cdot 4\text{H}_2\text{O}$ (1.26 mM), ZnCl_2 anhydrous (0.15 mM), $\text{CuCl}_2 \cdot 2\text{H}_2\text{O}$ (0.11 mM), $\text{Na}_2\text{MoO}_4 \cdot 2\text{H}_2\text{O}$ (0.07 mM), $\text{CoCl}_2 \cdot 6\text{H}_2\text{O}$ (0.06 mM), $\text{NiCl}_2 \cdot 6\text{H}_2\text{O}$ (0.04 mM), KBr (0.08 mM).

Initial experiments to assess the nutrient uptake during growth was carried out in 1 L Erlenmeyer flasks, filled with 0.5 L of medium, for 4 days. In the second set of experiments, spent media was used for cultivation and the experiments were carried out in 12 L carboys for a growth period of 6 days. Both experiments were carried out in triplicates and full spectrum LED lights (T5H0, 6400K, Sunblaster Holdings ULC, Canada) were used to provide a light intensity of 200 $\mu\text{mol photons} \cdot \text{m}^{-2} \cdot \text{s}^{-1}$, operating with a light:dark cycle of 16:8 h (Ataiean et al., 2019). In both experiments the cyanobacterial consortium was cultivated as suspended cells and suspension cultures were continuously agitated using magnetic stir plates operating at 340 rpm.

Analytical methods

Supernatant analysis

The pH of the culture samples obtained during the incubation was measured using a pH meter (Seven Compact[™] S220, Mettler Toledo, United States). The cultures were then centrifuged for 10 min at 3,900 g (Allegra X-22R, Beckman Coulter, United States). The supernatant obtained after centrifugation was analysed for total alkalinity (TA), anions, cations, and total nitrogen concentrations. In brief, TA was measured using a G20 compact titrator (Mettler Toledo, United States); 40 ml of supernatant was taken in a beaker and titrated with 0.2N H_2SO_4 until the samples reached an endpoint of pH = 4.3 (Vadlamani et al., 2019). Bicarbonate and carbonate concentrations were calculated using the measured pH and total alkalinity (TA) (Vadlamani et al., 2017; Vadlamani et al., 2019).

The nitrate concentration was measured using an ion chromatograph equipped with an IonPac AS18 anion and a conductivity detector (DIONEX ICS 2000; Thermo Fisher, United States) (Vadlamani et al., 2017; Vadlamani et al., 2019). The ammonium concentration was determined colorimetrically as previously described (Sims et al., 1995). The total nitrogen concentration was assessed using a scaled down version of the Persulfate Digestion method (Hach Method 10071, Hach, United States) (Vadlamani et al., 2017; Vadlamani et al., 2019).

Quantification of cations

Sodium, potassium, phosphorus, sulfur, magnesium, calcium, and iron were analyzed in both freshly prepared medium, and supernatant obtained after growth. All measurements were performed using an Agilent 8800 Triple Quadrupole Inductively Coupled Plasma Mass Spectrometer (ICP-QQQ, Agilent Technologies, Tokyo, Japan). The ICP-QQQ was equipped with an SPS4 autosampler, which uptakes 3 ml of sample for analysis. Fresh media and culture samples obtained after each day of incubation were first centrifuged at 4500 rpm for 5 min to spin down cells. Next, the supernatant was split into two fractions. To one fraction, 5% HNO_3 was added, reducing the pH to less than 3 and dissolving any precipitated cations. The pH of the other fraction was not adjusted. By comparing the mineral content of these two fractions, the difference between the dissolved and total amounts could be determined for each ion (Hanifzadeh et al., 2018). Immediately before ICP analysis, samples were filtered through 0.2 μm mixed cellulose esters (MCE) membrane filters, to remove any remaining solids. The cation concentrations for both the fresh medium and supernatant were estimated from calibration curves generated by applying the same protocols to the standards. The relative standard deviation of ICP-QQQ measurements was within 4%.

X-ray mapping of precipitates

To determine the chemical nature of precipitates in the growth medium, an FEI Quanta FEG 250 environmental field emission scanning electron microscope (E-FESEM) in combination with a Bruker QUANTAX Energy Dispersive X-ray Spectroscopy (EDS) system was used. In brief, a freshly prepared medium was filtered using 0.2 μm mixed cellulose esters (MCE) membrane filter to separate the precipitates. Once all the media had passed through the filter, Milli-Q water was used to wash the filter. After washing the filter membrane two times, the filter was air dried for 24 h. A small portion of the dried filter membrane was mounted onto a stub using double sided carbon tape without any surface modification. The stub containing the filter membrane was then analyzed to obtain the elemental maps using the E-FESEM/EDS system (operated at primary energy – 15 KeV). These elemental maps were used to infer the chemical composition of the precipitates.

Visual MINTEQ modelling

Visual MINTEQ was used to estimate ion speciation in the high pH, alkaline medium. The chemical equilibrium model of Visual Minteq 3.1 (<https://vminteq.lwr.kth.se/>) is based on the program PC MINTEQA2 (Allison et al., 1991; Gustafsson, 2011). Computations were carried out using initial experimental conditions: 1) pH (10.46), 2) temperature (20°C), 3) Ion concentration and 4) Ionic strength (0.73 M) as input variables. With Visual Minteq we estimated, for each element: 1) the concentration of dissolved ions(s); 2) the fraction bound to ligands and 3) the fraction precipitated (Gustafsson, 2011).

Biomass productivity and elemental analysis

The wet biomass obtained after centrifugation was frozen at -80°C overnight and then freeze dried at -50°C at a pressure of 1 mPa using a bench top freeze dryer (Labconco, Kansas City, MO, United States) (Vadlamani et al., 2019). Ash content of the freeze-dried biomass was then analysed with a muffle oven as previously described (National Renewable Energy Laboratories, NREL, Sluiter et al., 2008). The ash content was used to estimate ash-free biomass concentrations and productivity using the equations provided in the [Supplementary Information](#).

Carbon, nitrogen, and hydrogen content of the freeze-dried biomass was determined as previously described (Ataiean et al., 2019). Other elements (K, P, S, Mg, Ca, and Fe) in the biomass were determined by ICP-MS analysis of the digested biomass. First, digestion of the biomass was carried out using a MARS 6 – Microwave Digestion System (CEM Corporation, United States) (Hanifzadeh et al., 2018). In brief, 10 ml of HNO_3 were added to about 50 mg of freeze-dried biomass and digested at 250°C and at a pressure of 55.16 bar for 30 min. These samples were then diluted with Milli-Q water (to fit in the calibration range) and analyzed for metallic (K, Mg, Ca, Fe) and some non-metallic (P, and S) elements using an ICP-MS (ICP-MS, Xseries 2, Thermo Scientific, United States) (Hanifzadeh et al., 2018). The measured elemental concentrations were then used to estimate nutrient uptake rates.

Carbohydrate content was analyzed by the sulfuric acid-phenol method; briefly, 5 mg of freeze-dried biomass was resuspended into 2 ml of DI water and then ultrasonicated using a 50 W Ultrasonic Homogenizer with a $\frac{1}{8}$ tip (VWR, United States) for 10 min. 200 μl of the ultrasonicated biomass were transferred into a 2 ml tube and 200 μl of 5% phenol and 1 ml of concentrated sulfuric acid were added. The tubes were incubated for 30 min at room temperature and then the absorbance was measured at 450 nm using a SpectraMax iD3 Multi-Mode Microplate Reader (Molecular Devices, San Jose, California, United States). The carbohydrate contents were estimated from a calibration curve generated by applying the same protocols to glucose standards (Masuko et al., 2005).

Protein content was measured following a modified Lowry assay as described by Slocombe et al. (2013). Briefly, 5 mg of freeze-dried biomass were added to 200 μl of 24% (v/v) trichloroacetic acid and incubated at 95°C for 15 min. After cooling to room temperature, 600 μl of water were added and tubes centrifuged at 15,000 g for 20 min at 4°C . The pellet was resuspended using 0.5 ml of Lowry Reagent D (24:0.5:0.5 ratio solution of Lowry reagent A (2% w/v of anhydrous Na_2CO_3 in 0.1 N NaOH), reagent B (1% w/v NaK tartrate tetrahydrate), and reagent C (0.5% w/v $\text{CuSO}_4 \cdot 5\text{H}_2\text{O}$ in H_2O)) and then incubated for 2 h at 55°C . After incubation the samples were cooled to room temperature and centrifuged at 15,000 g for 20 min. The supernatant was then transferred to new tubes and the pellet

was discarded. For quantification, 950 μl of Lowry Reagent D were added to 50 μl of the protein extract, mixed quickly by inversion, and incubated at room temperature for 10 min. Finally, 100 μl of diluted Folin-Ciocalteu phenol reagent (2N, Sigma-Aldrich, United States) were added, vortexed, and incubated at room temperature for 30 min (Slocombe et al., 2013). The absorbance was measured at 600 nm using a SpectraMax iD3 Multi-Mode Microplate Reader (Molecular Devices, United States). The protein content was estimated from a calibration curve generated by applying the same protocol to bovine serum albumin standards, prepared from a 30% solution (VWR, United States).

Statistical analysis

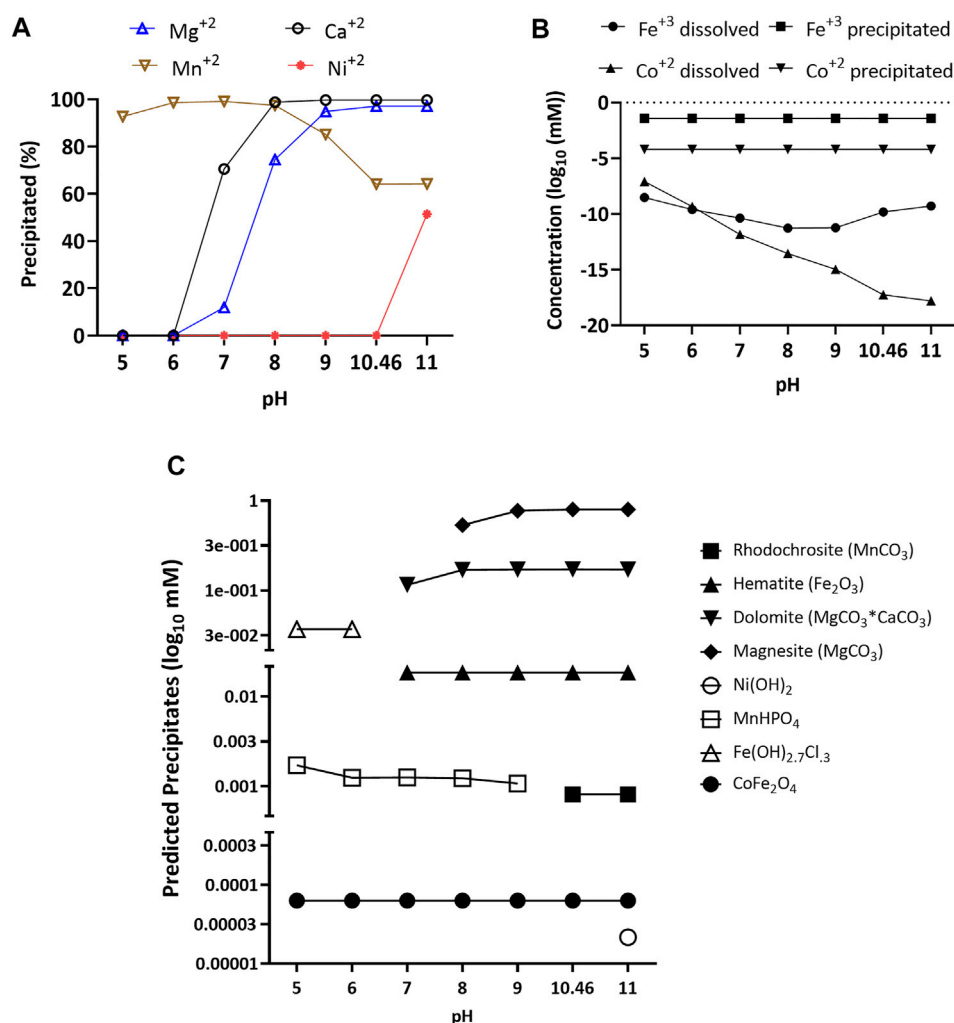
One-way analysis of variance (ANOVA) was conducted to identify significant differences between nutrient concentrations. In each case, a p value less than 0.05 was considered significant with a sample size, $n = 3$. Statistical analyses were performed using MS Excel.

Results and discussion

Nutrient solubility

Although it is hard to know to what extent an element is “bio-available,” at least we can be fairly confident that elements dissolved as ions in the medium are available for uptake by microorganisms (Suzuki et al., 1995; Lee et al., 2009). Because of the high pH (>10.4) and high ionic strength (0.73 M) of the growth medium, some elements (especially Mg, Ca, and Fe) were likely to precipitate (Vandamme et al., 2012). We performed a comprehensive analysis on the freshly prepared medium to determine the solubility of each element.

First, we used Visual Minteq 3.1 software (KTH, Sweden) to predict both the likelihood of precipitation and the nature of expected precipitates in the high alkalinity medium as a function of pH. For Mg^{2+} , Ca^{2+} , and especially Fe^{3+} and Co^{2+} , the salts added to the medium were expected to precipitate nearly completely at the actual medium pH of 10.46 (Figures 1A,B). For, Mn^{2+} , 64% of the added manganese was expected to precipitate. Lastly, nickel was only predicted to precipitate above pH 11. Further, under equilibrium conditions, the software predicted that above pH 7, both Mg and Ca would form carbonate salts such as dolomite ($\text{MgCO}_3 \cdot \text{CaCO}_3$) and magnesite (MgCO_3) (Figure 1C). For iron, it would mainly precipitate as hematite (Fe_2O_3 , Figure 1C), with production of a minor fraction of cobalt ferrite (CoFe_2O_4 , Figure 1C). Manganese would mainly precipitate as rhodochrosite (MnCO_3) from pH 10.46 to 11 and as MnHPO_4 from pH 5 to 9. Lastly, nickel at pH 11 would precipitate as $\text{Ni}(\text{OH})_2$.

**FIGURE 1**

Percentage of magnesium, calcium, nickel, and manganese precipitated (A), concentration dissolved and precipitated for iron and cobalt (B), and predicted precipitates (C) of calcium, magnesium, cobalt, nickel, and iron over a pH range of 5–11 with an ionic strength of 0.73 M. Data was obtained using Visual Minteq 3.1 equilibrium model.

To verify the equilibrium model's predictions, we collected precipitates from freshly prepared medium and analyzed them using a scanning electron microscope with energy-dispersive X-ray spectroscopy (SEM-EDS). The SEM images shown in Figures 2A,B indicate that the surface of the filter was covered with amorphous precipitates. EDS analysis confirmed experimentally that the amorphous precipitates mainly consisted of calcium carbonate and iron oxide (Figures 2A,B). For Mn, Co, and Mg it was difficult to identify the nature of the precipitates by using the EDS analysis, because the signals for Ca and Fe overpowered the spectrum. It was also possible that the precipitates formed from Mn, Co and Mg passed through the 0.2 μ m filter and for that reason weren't observed in the EDS analysis.

The fresh culture medium at pH = 10.46 was further analyzed using inductively coupled plasma mass spectrometry (ICP-MS) to determine the concentrations of dissolved sodium, potassium, phosphorus, sulfur, magnesium calcium, and iron. In parallel, the pH of the culture medium was decreased to less than 3, to dissolve any precipitated minerals, and analyzed it on ICP-MS. Together, these two measurements provided the dissolved and total amounts for each element, respectively. The ICP-MS analyses were compared with the Minteq predictions, and the amounts actually added to the growth medium (Table 1). ICP-MS showed that the added sodium, potassium, phosphate, and sulfate remained fully dissolved (Table 1). ICP-MS also showed that this was not the case for magnesium, calcium, and iron, indicating significant precipitation (ANOVA single factor, $p = 0.02$, Table 1). The experimentally determined concentration of

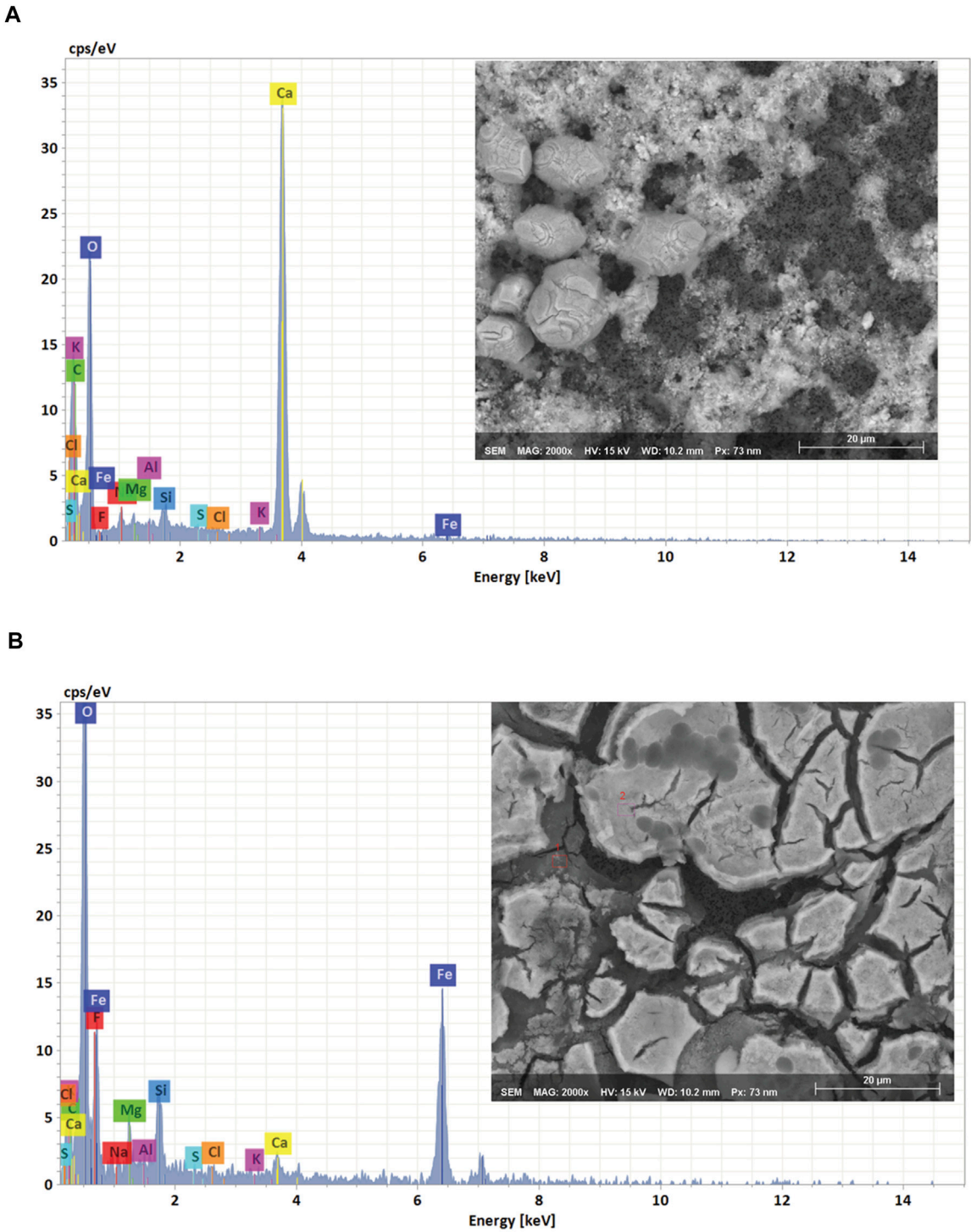


FIGURE 2
SEM image and EDS spectrum of the recovered precipitates **(A)** CaCO₃ and **(B)** Fe (OH)₃.

TABLE 1 Concentration (mM) of nutrients at high pH (10.4), reduced pH (<3), and solubility (%).

Elements	Expected concentration (mM)	Concentration in solution (mM)		Solubility (%)
		Analyzed at pH 10.4 ^a	Analyzed at pH < 3 ^b	
C-HCO ₃ ^{-c}	77.85	33.3 ± 0.8	N/A	N/A
N-NO ₃ ^{-d}	3.06	2.97 ± 0.07		100
N-NH ₄ ^{+e}	0.92	0.75 ± 0.04		82
Na	500	483.6 ± 5.5	476.5 ± 26.8	100
Mg	1	0.3 ± 0.04	1.0 ± 0.09	30
K	8.5	7.96 ± 0.42	8.0 ± 0.74	100
P	1.44	1.44 ± 0.05	1.4 ± 0.1	100
S	1	1.0 ± 0.07	0.88 ± 0.08	100
Ca	0.25	0.08 ± 0.02	0.25 ± 0.01	32
Fe	0.04	0.007 ± 0.001	0.02 ± 0.001	17

^aTo determine the total amounts of elements by ICP-MS, the pH of growth medium was reduced using 5% HNO₃.

^bHigh pH growth medium was directly analyzed on ICP-MS to obtain the concentration of dissolved elements.

^c(bi)carbonate was calculated using TA which was determined by titration with 0.2 H₂SO₄, and pH values.

^dNitrate was measured using an ion chromatograph.

^eAmmonium concentrations were determined using colorimetry.

dissolved Mg, Ca and Fe was still higher than the Minteq predictions. This indicated that the high pH culture medium was supersaturated in Mg, Ca, and Fe. Supersaturation of carbonate salts is a well-known phenomenon occurring in many natural waters (Minde et al., 2020). Despite supersaturation, the soluble fraction of Mg, Ca and Fe was significantly reduced due to precipitation in the high pH medium.

For inorganic carbon, it is well known that at pH 9–10, the dissolved CO₂ concentration is low and HCO₃⁻ is the dominant species. As the pH further increases (pH > 10), CO₃²⁻ becomes dominant. Since cyanobacteria have the ability to utilize both CO₂ and HCO₃⁻, but not CO₃²⁻ (Raven, 1994), it was important to determine the bicarbonate concentration in the high pH medium. The actual HCO₃⁻ concentration was calculated using the measured total alkalinity (TA, 0.5 ± 0.003 M) and pH (10.46 ± 0.02) values. The actual HCO₃⁻ concentration (33.3 ± 0.8 mM) was lower than the amount of bicarbonate added to the growth medium (77.9 mM, Table 1). This was caused by equilibration (outgassing) of dissolved CO₂ with ambient air, increasing pH and leading to the production of CO₃²⁻ (Wolf-Gladrow et al., 2007).

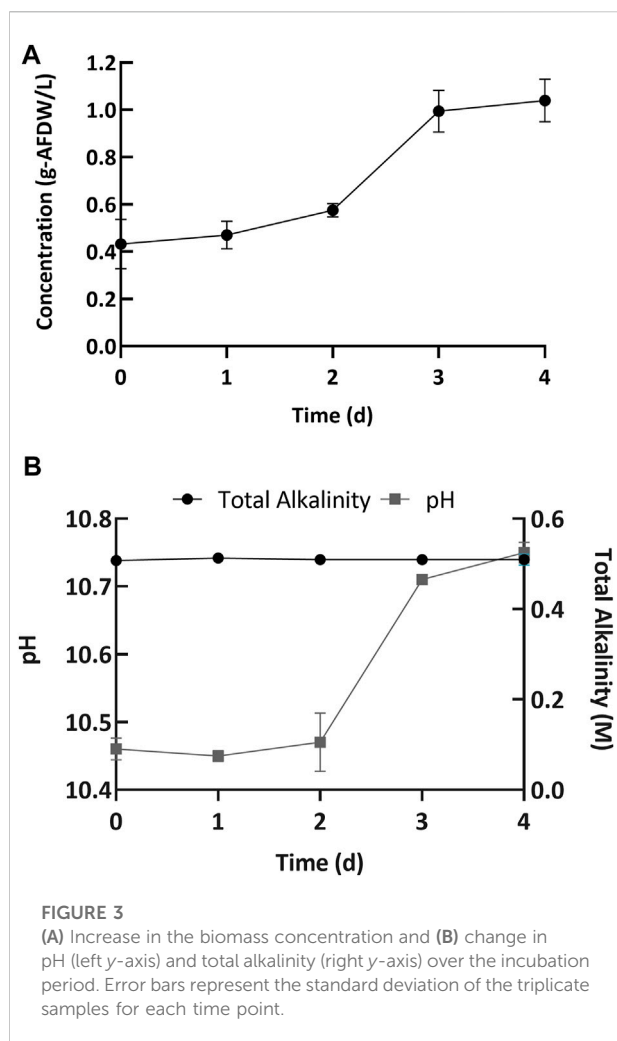
Nitrogen, another important nutrient, was also analysed for solubility. We added 3.98 mM total N to the medium, in the form of NaNO₃ (3.06 mM) and NH₄Cl (0.92 mM). Nitrate measurements indicated that close to 100% of the added NO₃⁻ remained dissolved in the medium (2.97 ± 0.07 mM, Table 1). On the other hand, measured NH₄⁺ concentrations indicated that the medium contained 20% less ammonium than was added (0.75 ± 0.04 mM compared to 0.92 mM, Table 1). The decrease in the N-NH₄⁺ could be explained by outgassing of

volatile NH₃ from the medium at high pH (Körner et al., 2001). Overall, more than 90% (3.72 mM) of the nitrogen added remained in the media to support cyanobacterial growth.

Biomass growth and nutrient uptake

Growth profile of cyanobacterial consortium

Next, we performed cultivation experiments to evaluate the biomass growth and nutrient uptake at high pH. The microbial consortium was grown in Erlenmeyer flasks (15 flasks) with a light:dark cycle of 16:8 h, with 4 days between harvests. Every day, three flasks were removed from the experiment and used for analysis. The consortium used in this study mainly consisted of (>90% relative DNA sequence abundance) the filamentous cyanobacterium *Candidatus* “Phormidium alkaliphilum” (Sharp et al., 2017; Ataeian et al., 2019; Ataeian et al., 2021; Ataeian et al., 2022). This cyanobacterial consortium was inoculated at an initial concentration of 0.43 ± 0.10 g/L AFDW (Day 0, Figure 3A). Initially the alkalinity was 0.5 ± 0.003 M, and the pH was 10.46 ± 0.02 (Day 0, Figure 3B). A 4-day incubation period was chosen because the biomass growth plateaued after 4 days of incubation in previous experiments, presumably due to nitrogen sources being fully depleted (Ataeian et al., 2019). The cultures exhibited an initial lag phase followed by growth (Figure 3A). A lag phase is common for many bacteria and algae, including the green algae *Desmodesmus* sp. F2 (Huang et al., 2012). Overall, cultures grew well without any apparent growth inhibition to a final biomass concentration of 1.04 ± 0.12 g/L AFDW. In parallel, the pH increased to 10.69 ± 0.1 (Day 4, Figures 3A,B). The corresponding volumetric biomass



productivity ($0.15 \text{ gL}^{-1}\text{d}^{-1}$ AFDW, estimated using Eq. 3) was higher than previously reported ($0.048 \text{ gL}^{-1}\text{d}^{-1}$ AFDW) (Vadlamani et al., 2017). The improvement in biomass productivity was likely due to a higher initial inoculum concentration and higher light intensities used in this report.

Nutrient analysis of supernatant and biomass

The estimated bicarbonate depletion observed at the end of the growth period was $16.4 \pm 1.4 \text{ mM}$ (Figure 4B). Simultaneously, an increase in carbonate concentration was also observed ($8.1 \pm 0.18 \text{ mM}$, Figure 4B). Since for every 1 mol of carbon fixed, 2 mol of bicarbonate are converted and 1 mol of carbonate is produced (Ataeian et al., 2019), the remainder of the bicarbonate decrease ($8.4 \pm 1.4 \text{ mM}$) was attributed to uptake by the cyanobacterial consortium. However, the net increase in organic carbon in the biomass (estimated from CHN analysis and gains in the ash free dry biomass concentration) was $22.9 \pm 0.72 \text{ mM}$ (Figure 4B). Thus, the net increase in organic carbon content was more than twice as

much as could be sourced from the bicarbonate added to the medium. Additional bicarbonate was most likely added to the medium by spontaneous air-capture of CO_2 during cultivation (Vadlamani et al., 2017; Ataeian et al., 2019; Vadlamani et al., 2019).

Uptake and depletion of nitrogen, phosphorus, sulfur, and potassium were analyzed along with carbon (See Figure 4). Figure 4A shows that the initial NO_3^- concentration was 2.97 ± 0.07 and the initial NH_4^+ concentration was $0.75 \pm 0.04 \text{ mM}$. By the end of the growth period the nitrogen was almost fully depleted with only $0.16 \pm 0.03 \text{ mM}$ of nitrate remaining in the media (Day 4, Figure 4A). Concomitantly, the amount of organic nitrogen in the biomass increased, equivalent to an uptake of $4.15 \pm 0.03 \text{ mM}$ (Day 4, Figure 4A). Although there was no significant increase in biomass during the lag phase (Figure 4A), 50% of the nitrogen supplied was consumed during this period (Figure 4A). The decoupling of nutrient uptake and biomass growth, known as luxurious uptake, is a well-documented phenomenon occurring in cyanobacteria and microalgae. See for example, Huang et al. (2012). The initial phosphorus concentration in the growth medium was $1.32 \pm 0.04 \text{ mM}$ (Day 0, Figure 4C). By the end of day 4, the final concentration of phosphorus in the media was $1.18 \pm 0.03 \text{ mM}$ (Figure 4D), which means nearly $0.14 \pm 0.01 \text{ mM}$ (Day 4, Figure 4C) of the phosphorus was depleted in the growth medium. This indicated that nearly 90% of the added phosphorus was left unused in the growth medium. Simultaneously, the concentration of phosphorus in the biomass increased by $0.25 \pm 0.10 \text{ mM}$ at the end of day 4 (Figure 4D). On day 0 the sulfur concentration in the growth medium was $1.1 \pm 0.04 \text{ mM}$ (Figure 4D) and by day 4 the final concentration was $0.95 \pm 0.02 \text{ mM}$ (Figure 4D), which means 86% of the initial sulfur added to the medium remained unused. This result was supported by the estimated uptake of sulfur in the biomass after 4 days, which was $0.16 \pm 0.07 \text{ mM}$. Finally, the initial potassium concentration in the media was $8.79 \pm 0.25 \text{ mM}$ (Day 0, Figure 4E) and by day 3 the concentration was $8.05 \pm 1.70 \text{ mM}$ (Day 3, Figure 4E). The potassium concentration on day 4 was not reported because it had a high margin of error. The concentration of potassium in the biomass increased by $0.36 \pm 0.13 \text{ mM}$ over 4 days (Day 4, Figure 4E).

ICP-MS measurements showed that the soluble fractions of Mg, Ca, and Fe in the fresh medium were 0.30, 0.32 and 0.17, respectively in the fresh medium (Table 1). A previous study showed that the concentration of these elements is also low in the alkaline Soda Lakes (Cariboo, BC) from which this microbial community was collected (Zorz et al., 2019). We hypothesize that the alkaliphilic microbial consortium is adapted to cope with low concentrations of Mg, Ca, Co, and Fe, for example by expressing high affinity ABC transporters, producing siderophores and siderophore receptors (Chakraborty et al., 2019; Årstad and Hohmann-Marriott, 2019). Results from Ataeian et al. (2021)

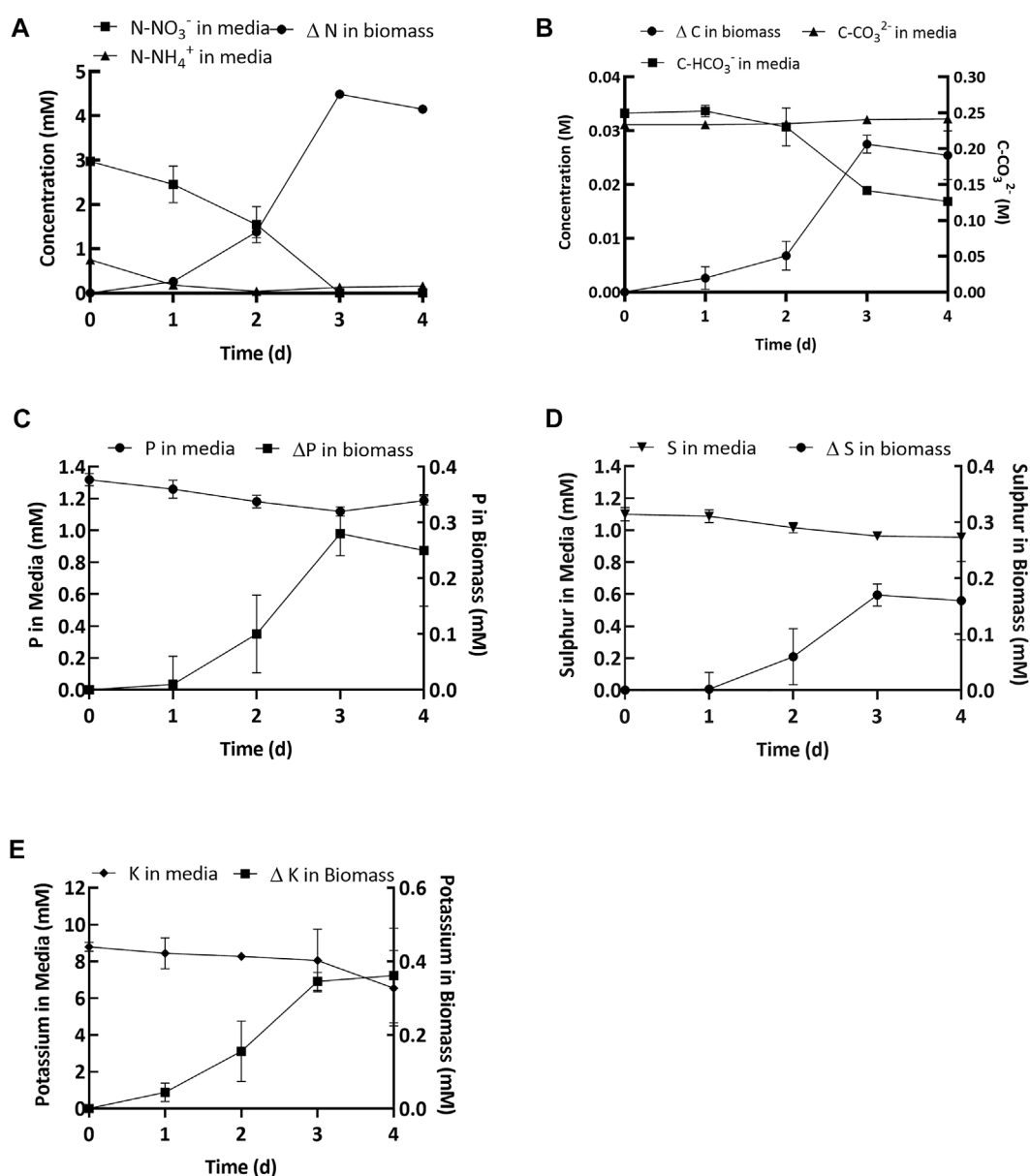


FIGURE 4

(A) Soluble nitrogen (NH₄⁺ and NO₃⁻) depleted in the media and change in biomass. (B) Bicarbonate (squares, left y-axis) and carbonate (circles, left y-axis) concentration in the media and change in carbon in the biomass (mM) (triangles, right y-axis). (C–E) Concentration of elements (P, S and K) in the spent media and change in the biomass. Values shown in the graphs are averages based on three replicates and error bars represent the standard deviation of the triplicate samples for each time point.

revealed that the dominant species in the cyanobacteria consortium (*Candidatus* “Phormidium alkaliphilum”) used in this study, contains the genes required for iron scavenging using ABC transporters, siderophores and siderophore receptors. The type of siderophores that would be produced are classified as hydroxamates (Ataiean et al., 2021). In addition, this cyanobacterium appeared to have minimized gene content dependent on Cobalt.

The concentration of Fe, Ca, and Mg in the growth medium was depleted over the incubation period (Supplementary Figure S2). However, as Mg, Ca, and Fe precipitate at high pH, it remains unknown if these elements were assimilated by cells or if the precipitates were trapped in the extracellular polymeric layer surrounding the cells. Consequently, the depletion rate of these three elements (Fe, Ca, and Mg) in the culture medium cannot be directly equated to assimilation.

TABLE 2 Comparison between elements in cultivated cyanobacteria consortium, microbial mats from soda lakes (Cariboo Plateau, British Columbia) and literature values.

Elements	Cyanobacterial consortium cultivated in lab environment		Microbial mats collected from soda lakes								Literature values ^a
	Day 3	Day 4	DL-M		PL-M		GEL-M		LC-M		
			2014	2017	2014	2017	2014	2017	2014	2017	
C (g/kg)	543.9 ± 2.6	503.0 ± 9.0	303.0	395.3	81.0	262.0	1288.12	528.0	412.0	364.9	175–650
H (g/kg)	72.6 ± 13.5	79.7 ± 31.2	43.8	55.7	11.2	34.2	192.6	73.4	54.1	51.0	ND
N (g/kg)	114.0 ± 17.45	85.2 ± 5.3	15.6	35.6	10.1	30.3	91.0	61.1	25.5	31.1	50–105
Ca (g/kg)	1.1 ± 0.4	1.5 ± 1.2	26.9	33.6	79.9	20.5	10.9	91.7	1.9	4.2	3–21
K (g/kg)	21.4 ± 3.6	14.9 ± 3.1	6.2	8.8	8.4	17.2	7.9	20.1	7.8	5.8	6–21
Mg (g/kg)	5.1 ± 0.1	4.2 ± 0.6	74.5	89.8	75.8	40.9	31.5	322.3	5.0	10.3	1–37
Na (g/kg)	63.7 ± 20.1	91.5 ± 10.1	251.4	110.4	178.1	135.3	129.6	281.8	71.6	51.9	7–321
P (g/kg)	13.3 ± 5.7	9.7 ± 3.1	1.4	4.5	6.3	17.6	3.0	11.0	1.0	2.3	0.9–30
S (g/kg)	8.1 ± 0.9	6.5 ± 1.2	5.7	9.3	36.1	10.7	81.4	18.8	21.6	9.2	4–14
Cu (mg/kg)	72.2 ± 0.4	14.7 ± 4.8	90.7	22.6	343.9	39.3	7.1	38.5	19.4	25.4	1–650
Mn (mg/kg)	88.2 ± 20.2	125.3 ± 55.3	313.9	385.1	1873.9	389.2	98.1	765.6	46.5	121.6	17–592
Zn (mg/kg)	49.5 ± 14.0	41.6 ± 9.2	51.7	50.1	212.6	51.6	16.3	75.5	14.8	30.3	2–64
Ni (mg/kg)	7.0 ± 5.7	7.1 ± 3.2	26.3	38.9	180.2	49.4	8.3	60.5	7.9	18.1	1–3
Co (mg/kg)	2.9 ± 0.9	5.9 ± 4.2	8.4	10.0	69.0	14.5	2.3	16.7	1.8	4.4	ND
Fe (mg/kg)	2.3 ± 0.5	2.9 ± 1.8	ND	ND	ND	ND	ND	ND	ND	ND	83–7,000

Deer Lake Microbial Mat (DL-M), Probe Lake Microbial Mat (PL-M), Goodenough Lake Microbial Mat (GEL-M) and Last Chance Lake Microbial Mat (LC-M). ND is no data.

^aFrom Silva et al. (2015), Tibbetts et al. (2015), Campanella et al. (1998), Volkman and Brown (2006).

Elemental composition and empirical formula of alkaline biomass

Using the experimental data obtained in this study, we estimated the elemental composition of the cyanobacterial consortium (Table 2). For comparison, we also analyzed the elemental composition of microbial mats collected from four different Soda Lakes located in the Cariboo Plateau, British Columbia, Canada: namely, Last Chance Lake (LCL-M), Probe Lake (PL-M), Deer Lake (DL-M), and Goodenough Lake (GEL-M). These mats were used as inoculum for the original enrichment of the cyanobacterial consortium (Sharp et al., 2017). Compared to the consortium, most mat samples were enriched in minerals, such as sodium, copper, manganese, and nickel. These were likely present as precipitates, concentrated by evaporation. Nitrogen and phosphorus were less abundant, likely because of a lower contribution of microbial cells to the mat biomass. Overall, the elemental composition obtained for both the cyanobacterial consortium and the microbial mats collected from the Soda Lakes were still comparable to previously reported pure cultures (Campanella et al., 1998; Volkman and Brown, 2006; Silva et al., 2015; Tibbetts et al., 2015).

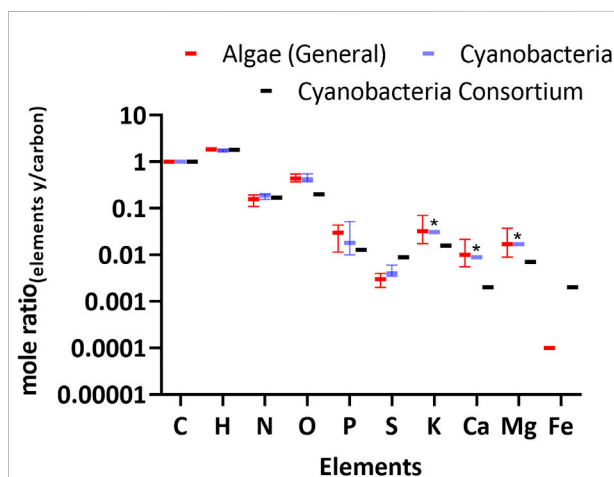


FIGURE 5

Biomass elemental composition of the cyanobacterial consortium relative to carbon. For comparison, literature values for Algae (Eukaryotes) and Cyanobacteria are shown. See Supplementary Table S2 for tabulated values and literature references. Error bars represent the interquartile range and solid lines represent the median. Asterisk represents the elements in the literature where only a single data point was collected for *M. aeruginosa*.

We used the elemental composition reported in Table 2 to calculate the empirical formula for the cyanobacterial consortium and microbial mats. The formula for the cyanobacterial consortium was $\text{CH}_{1.81}\text{N}_{0.17}\text{O}_{0.20}\text{P}_{0.013}\text{S}_{0.09}$; results for all empirical formulas are shown in Supplementary Table S1. Although this formula pertains to a microbial consortium, the stoichiometry of C to HNOPS was similar to cyanobacteria grown in pure culture (Figure 5 and Supplementary Table S2). With regards to CHNO, all forms of cellular biomass are very close, but many (eukaryotic) micro-algae have up to four times lower nitrogen content. This difference can be explained by the higher protein content of cyanobacteria.

Interestingly, the consortium's Ca and Mg was low compared to the values previously reported for other cyanobacteria such as *M. aeruginosa*. This may be due to the consortium originating from soda lakes with a pH >10 where the solubility of Ca and Mg is low. Therefore, it may be naturally adapted to use less Ca and Mg. The iron content in the consortium was up to five times higher than for most (eukaryotic) micro-algae, but it remains unknown if this Fe was cellular or was present in the extracellular polymeric matrix.

Regrowth of the cyanobacterial consortium in spent medium

One way to reduce the costs and improve the sustainability of algal cultivation is reusing the spent cultivation medium (Yang et al., 2011; Farooq et al., 2015; Lu et al., 2020). Depending on the culture and growth conditions, this may or may not be possible (Loftus and Johnson, 2017; Lu et al., 2020). In some cases, the reuse of spent cultivation medium has caused cultures to crash or suffer, while spent medium has also promoted growth (Lu et al., 2020).

Figure 4 shows that the inorganic carbon and nitrogen provided in the growth medium were significantly depleted. Therefore, to enable reuse of spent medium, inorganic carbon and nitrogen need to be supplemented. As more than 80% of the P, S and K remained unused (Figure 4), these nutrients would only need to be supplemented less than once every five growth cycles.

To investigate the consequences of reusing spent cultivation medium for growth, the cyanobacterial consortium was inoculated into freshly prepared media in a 12 L carboy (working volume = 10 L) at a pH of 10.5 and alkalinity of 500 mM. After 6 days the biomass was harvested by centrifugation. In the (unsterilized) spent medium, the nitrogen concentration was restored to 4 mM of combined nitrate and ammonium and the bicarbonate concentration was restored by sparging with CO_2 . The spent medium was not sterilized to mimic an actual commercial scale process more closely, where the high energy needs of sterilization would compromise both sustainability and economics. Part of the harvested biomass was added back to start the next growth cycle. In total, four growth cycles were carried out like this in

triplicate (three carboy's) using spent medium over a period of 24 days.

Biomass growth

Figure 6 shows the biomass growth in experiments with freshly prepared medium (cycle 1) and spent medium (cycles 2–5). The average biomass productivity (67.1 ± 0.4 mg-AFDW $\text{L}^{-1}\text{d}^{-1}$) in 12 L carboys during cycle 1 was lower than in 0.5 L Erlenmeyer flasks (150 ± 20 mg-AFDW $\text{L}^{-1}\text{d}^{-1}$), even though the same growth medium was used (Section 3.2). This decrease in productivity was likely caused by reduced light penetration due to the larger cultivation volume (Supplementary Figure S3). The width of the 12 L carboy was 10 inches, compared to four inches for the Erlenmeyers. With spent medium in cycle 2, both the biomass concentration (0.45 g-AFDW L^{-1} , see Figure 6B) and the estimated productivity (48.2 ± 5.7 mg-AFDW $\text{L}^{-1}\text{d}^{-1}$) decreased by 25% compared to with freshly prepared medium in cycle 1. In cultivation cycles 3 and 4, the biomass concentration and productivity recovered (Figure 6B). Nevertheless, it was still 20% lower than with fresh medium. In the final growth cycle, the biomass concentration (0.59 g-AFDW L^{-1}) and productivity (60.8 ± 8.0 mg-AFDW $\text{L}^{-1}\text{d}^{-1}$) were comparable to fresh medium ($p > 0.05$, ANOVA single factor) (Figure 6B). This showed that the consortium acclimatized to the spent media. All cycles (1–5) displayed a consistent relationship between growth and pH (Figure 6A).

Biomass and supernatant composition

Carbon uptake, measured as AFDW, was consistent with the carbon depletion in the media. Further, the carbon to nitrogen ratio across all cycles was 1:0.2, consistent with the carbon to nitrogen ratio reported above (Figures 6C,D). The carbohydrate, protein, and ash content of the harvested biomass at the end of each cycle is reported in Table 3. The most significant change was observed in the ash content, which decreased from 21% at the end of the first cycle to 12% at the end of the last cycle. This may be explained by decreasing amounts of precipitated minerals in the media after each cycle, as part of these minerals get removed when biomass is harvested. Carbohydrates and protein content only displayed minor variations, with carbohydrates varying in the range 9–12%, and proteins fluctuating around 56–68%. This was consistent with the stable carbon to nitrogen ratio that was reported above for all cycles. These results suggest that reusing spent media did not have a significant influence on the biochemical composition of the cyanobacterial consortium.

Throughout the experiments, the concentration of sodium in the media remained stable at around 500 mM, while potassium decreased from $4.72 \text{ mM} \pm 0.15$ to 3.80 ± 0.14 mM at the end of cycle 5 (Supplementary Figure S4). Both phosphorus and sulfate concentrations decreased drastically in cycle 1 compared to the cycles where spent medium was used (cycles 2–5). Overall, the decrease of both elements after each cycle declined. For example, in cycle 2 phosphorus decreased by 17%, but decreased by only

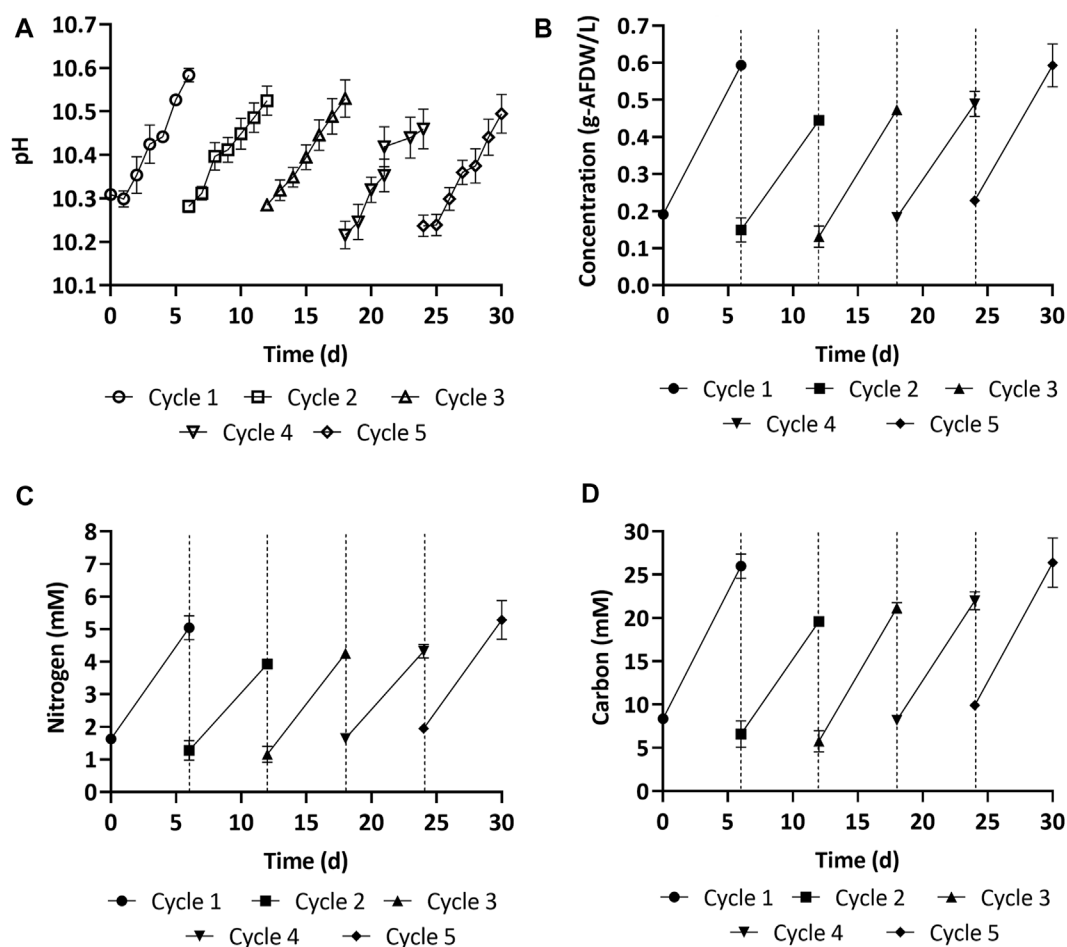


FIGURE 6

(A,B) Biomass growth and pH overtime in the fresh (cycle 1) and spent medium (cycle 2–5). (C,D) Nitrogen and carbon accumulated in the biomass overtime in the fresh (cycle 1) and spent medium (cycle 2–5). Error bars represent the standard deviation of the triplicate samples for each time point. The dashed vertical lines represent the transition between one growth cycle and the next.

TABLE 3 Biochemical composition (carbohydrates, protein, and ash) of the cyanobacterial consortium over five cycles of reusing spent medium.

Cycle	Carbohydrate (%)	Protein (%)	Ash (%)
1	10.15 ± 0.41	56.97 ± 6.19	21.19 ± 0.79
2	9.60 ± 1.06	63.35 ± 5.16	16.63 ± 0.44
3	10.58 ± 0.45	64.52 ± 1.16	15.05 ± 0.81
4	11.07 ± 0.69	64.11 ± 4.76	15.06 ± 2.23
5	11.48 ± 0.68	67.57 ± 4.58	12.05 ± 1.17

8% in cycle 3 (Supplementary Figure S4). The phenomenon that could explain this is called luxurious uptake (Solovchenko et al., 2019). This is when microorganisms such as cyanobacteria, which grow typically in low phosphorus and sulfur environments, assimilate more than they need of any nutrient

and store it. It is possible that at first, a large amount of both elements was uptaken and stored, but over time since so much was already assimilated the consortium needed less of these elements.

Previous studies using low-sodium (<20 mM) media (Mokashi et al., 2016; Barbera et al., 2018) have reported a loss of productivity due to evaporation, resulting in an increase in salinity (Discart et al., 2014; Church et al., 2017; Lu et al., 2019; Lu et al., 2020). This was not an issue for the cyanobacterial consortium used here, obtained from alkaline soda lakes, and grown in high alkalinity medium (0.5 mol L⁻¹ NaHCO₃), as shown by a complete recovery of productivity after five growth cycles. It is conceivable that the initial reduction in productivity was caused by the accumulation of organic compounds, as previously observed (Rodolfi et al., 2003; Discart et al., 2014; Depraetere et al., 2015; Lu et al., 2019; Lu et al., 2020). Indeed, the spent medium had a yellow/greenish

colour, likely associated with remains of cell lysis during harvesting by centrifugation, also observed previously (Rodolfi et al., 2003; Singh and Patidar, 2018). Some of these coloured compounds might have directly inhibited regrowth but could also simply have reduced light penetration, resulting in lower growth. In either case, if the accumulation of organic compounds was the cause of the initial loss of activity, it is likely that the heterotrophic bacteria, that were also part of the cyanobacterial consortium, started to consume these organic compounds and so facilitated the acclimatization of the culture. Many of these heterotrophs can grow on cyanobacterial metabolites and components such as cell walls, proteins, lipids and fatty acids (Ataeian et al., 2022).

Conclusion

Growth of cyanobacteria can benefit from high pH and alkalinity by improving carbon delivery. The low solubility of iron and cobalt was shown to potentially limit growth in alkaline media. A comprehensive empirical formula was determined for an alkaliphilic cyanobacterial consortium. Reuse of spent cultivation medium was successfully demonstrated. Future research should focus on determining the practical limits for medium reuse, either by establishing a maximum number of cycles or a bleeding rate. In-depth biochemical analysis of the spent medium could help identify potential inhibitors and their tolerable concentrations. This research provides a way of improving the economics and reducing the environmental footprint of cyanobacterial cultivation, with applications in production of phycocyanin, nutraceuticals, food, and animal feed.

Data availability statement

The raw data supporting the conclusions of this article will be made available by the authors, without undue reservation.

Author contributions

AJP, AV, CD, MS and HD conceived and planned the experiments. AJP, AV, and CD carried out the experiments. AJP, AV and CD contributed to sample preparation. AJP, AV, CD, MS, and HD contributed to the interpretation of the results. AJP and AV took the lead in writing the manuscript. All authors provided critical feedback and helped shape the research, analysis, and final version of the manuscript.

Funding

This study was supported by the Natural Sciences and Engineering Research Council (NSERC), Canada Foundation for Innovation (CFI), Canada First Research Excellence Fund (CFREF), Alberta Innovates, the Government of Alberta, the University of Calgary.

Acknowledgments

The authors are thankful for the assistance provided by Michael Nightingale and Bernhard Mayer in the use of Ion Chromatographer and G20 compact titrator; Brian Ballie for running the samples on ICP-MS; Pedro Pereira-Almao with the use of the MARS 6 microwave digester; and Christopher Debuhr for letting us use their facility for E-FESEM/EDS system. This research was undertaken thanks in part to funding from the Canada First Research Excellence Fund (CFREF), Alberta Innovates, the Government of Alberta, and the University of Calgary.

Conflict of interest

AJP, AV, CD, HD, and MS report a relationship with Synergia Biotech Inc. that includes equity or stocks. AV and MS have patent #WO2021102563 - Alkaliphilic consortium shifting for production of phycocyanins and biochemicals pending to Synergia Biotech Inc. AJP, AV, and MS have patent #63/246,811 - Method for cost and energy effective production of cyanobacterial consortium pending to Synergia Biotech Inc.

Publisher's note

All claims expressed in this article are solely those of the authors and do not necessarily represent those of their affiliated organizations, or those of the publisher, the editors and the reviewers. Any product that may be evaluated in this article, or claim that may be made by its manufacturer, is not guaranteed or endorsed by the publisher.

Supplementary material

The Supplementary Material for this article can be found online at: <https://www.frontiersin.org/articles/10.3389/fbioe.2022.942771/full#supplementary-material>

References

- Acién Fernández, F. G., Fernández, J. M., Magán, J. J., and Molina, E. (2012). Production cost of a real microalgae production plant and strategies to reduce it. *Biotechnol. Adv.* 30, 1344–1353. doi:10.1016/j.biotechadv.2012.02.005
- Acién Fernández, F. G., Gómez-Serrano, C., and Fernández-Sevilla, J. M. (2018). Recovery of Nutrients from wastewaters using microalgae. *Front. Sustain. Food Syst.* 2, 59. doi:10.3389/fsufs.2018.00059
- Allison, J., Brown, S. D., and Novo-Gradac, J. K. (1991). MINTEQA2/PRODEFA2, a geochemical assessment model for environmental systems: version 3.0 user's manual. U.S. Environmental Protection Agency Report EPA/600/3-91/021.
- Arata, S., Strazza, C., Lodi, A., and Del Borghi, A. (2013). *Spirulina platensis* culture with flue gas feeding as a cyanobacteria-based carbon sequestration option. *Chem. Eng. Technol.* 36, 91–97. doi:10.1002/ceat.201100722
- Årstøl, E., and Hohmann-Marriott, M. F. (2019). Cyanobacterial siderophores-physiology, structure, biosynthesis, and applications. *Mar. Drugs* 17, 281. doi:10.3390/md17050281
- Ataeian, M., Liu, Y., Canon-Rubio, K. A., Nightingale, M., Strous, M., Vadlamani, A., et al. (2019). Direct capture and conversion of CO₂ from air by growing a cyanobacterial consortium at pH up to 11.2. *Biotechnol. Bioeng.* 116, 1604–1611. doi:10.1002/bit.26974
- Ataeian, M., Vadlamani, A., Haines, M., Mosier, D., Dong, X., Kleiner, M., et al. (2021). Proteome and strain analysis of cyanobacterium *Candidatus* “Phormidium alkaliphilum” reveals traits for success in biotechnology. *iScience* 24, 103405. doi:10.1016/j.isci.2021.103405
- Ataeian, M., Liu, Y., Kouris, A., Hawley, A. K., and Strous, M. (2022). Ecological interactions of cyanobacteria and heterotrophs enhances the robustness of cyanobacterial consortium for carbon sequestration. *Front. Microbiol.* 13, 780346. doi:10.3389/fmicb.2022.780346
- Barbera, E., Sforza, E., Musolino, V., Kumar, S., and Bertucco, A. (2018). Nutrient recycling in large-scale microalgal production: Mass and energy analysis of two recovery strategies by process simulation. *Chem. Eng. Res. Des.* 132, 785–794. doi:10.1016/j.cherd.2018.02.028
- Bell, T. A. S., Prithiviraj, B., Wahlen, B. D., Fields, M. W., and Peyton, B. M. (2016). A lipid-accumulating alga maintains growth in outdoor, alkaliphilic raceway pond with mixed microbial communities. *Front. Microbiol.* 6, 1480. doi:10.3389/fmicb.2015.01480
- Berthold, D. E., Rosa, N. D. L., Engene, N., Jayachandran, K., Gantar, M., Laughinghouse, H. D., et al. (2020). Omega-7 producing alkaliphilic diatom *fistulifera* sp. (Bacillario-phyceae) from lake okeechobee, Florida. *ALGAE* 35, 91–106. doi:10.4490/algae.2020.35.12.16
- Bharamurugan, G. L., Valerie, O., and Mark, L. (2018). Valuable bioproducts obtained from microalgal biomass and their commercial applications: a review. *Environ. Eng. Res.* 23, 229–241. doi:10.4491/eer.2017.220
- Brennan, L., and Owende, P. (2010). Biofuels from microalgae—a review of technologies for production, processing, and extractions of biofuels and co-products. *Renew. Sustain. Energy Rev.* 14, 557–577. doi:10.1016/j.rser.2009.10.009
- Campanella, L., Crescentini, G., Avino, P., and Moauro, A. (1998). Determination of macrominerals and trace elements in the alga *Spirulina platensis*. *Analisis* 26, 210–214. doi:10.1051/analisis:1998136
- Canon-Rubio, K. A., Sharp, C. E., Bergerson, J., Strous, M., and De la Hoz Siegler, H. (2016). Use of highly alkaline conditions to improve cost-effectiveness of algal biotechnology. *Appl. Microbiol. Biotechnol.* 100, 1611–1622. doi:10.1007/s00253-015-7208-7
- Chakraborty, S., Verma, E., and Singh, S. S. (2019). “Chapter 19 - cyanobacterial siderophores: Ecological and biotechnological significance,” in *Cyanobacteria*. Editors A. K. Mishra, D. N. Tiwari, and A. N. Rai (Academic Press), 383–397. doi:10.1016/B978-0-12-814667-5.00019-2
- Chen, Y., Zhao, N., Wu, Y., Wu, K., Wu, X., Liu, J., et al. (2017). Distributions of organic compounds to the products from hydrothermal liquefaction of microalgae. *Environ. Prog. Sustain. Energy* 36, 259–268. doi:10.1002/ep.12490
- Chi, Z., O'fallon, J. V., and Chen, S. (2011). Bicarbonate produced from carbon capture for algae culture. *Trends Biotechnol.* 29, 537–541. doi:10.1016/j.tibtech.2011.06.006
- Chisti, Y. (2007). Biodiesel from microalgae. *Biotechnol. Adv.* 25, 294–306. doi:10.1016/j.biotechadv.2007.02.001
- Chowdhury, R., Keen, P. L., and Tao, W. (2019). Fatty acid profile and energy efficiency of biodiesel production from an alkaliphilic algae grown in the photobioreactor. *Bioresour. Technol. Rep.* 6, 229–236. doi:10.1016/j.biteb.2019.03.010
- Christenson, L. B., and Sims, R. C. (2012). Rotating algal biofilm reactor and spool harvester for wastewater treatment with biofuels by-products. *Biotechnol. Bioeng.* 109, 1674–1684. doi:10.1002/bit.24451
- Church, J., Hwang, J.-H., Kim, K.-T., Mclean, R., Oh, Y.-K., Nam, B., et al. (2017). Effect of salt type and concentration on the growth and lipid content of *Chlorella vulgaris* in synthetic saline wastewater for biofuel production. *Bioresour. Technol.* 243, 147–153. doi:10.1016/j.biortech.2017.06.081
- Cornet, J. F., Dussap, C. G., Cluzel, P., and Dubertret, G. (1992). A structured model for simulation of cultures of the cyanobacterium *spirulina platensis* in photobioreactors: II. Identification of kinetic parameters under light and mineral limitations. *Biotechnol. Bioeng.* 40, 826–834. doi:10.1002/bit.260400710
- Demirkaya, C., Vadlamani, A., Tervahauta, T., Strous, M., and De La Hoz Siegler, H. (2022). *Co-production of hydrogen and organic acids from alkaline cyanobacterial biomass via dark autofermentation*. Social Science Research Network. doi:10.2139/ssrn.4082772
- Depraetere, O., Pierre, G., Noppe, W., Vandamme, D., Foubert, I., Michaud, P., et al. (2015). Influence of culture medium recycling on the performance of *Arthrospira platensis* cultures. *Algal Res.* 10, 48–54. doi:10.1016/j.algal.2015.04.014
- Discart, V., Bilad, M. R., Marbelia, L., and Vankelecom, I. F. J. (2014). Impact of changes in broth composition on *Chlorella vulgaris* cultivation in a membrane photobioreactor (MPBR) with permeate recycle. *Bioresour. Technol.* 152, 321–328. doi:10.1016/j.biortech.2013.11.019
- Farooq, W., Suh, W. I., Park, M. S., and Yang, J.-W. (2015). Water use and its recycling in microalgae cultivation for biofuel application. *Bioresour. Technol.* 184, 73–81. doi:10.1016/j.biortech.2014.10.140
- Fontes, A. G., Moreno, J., and Vargas, M. A. (1989). Analysis of the biomass quality and photosynthetic efficiency of a nitrogen-fixing cyanobacterium grown outdoors with two agitation systems. *Biotechnol. Bioeng.* 34, 819–824. doi:10.1002/bit.260340611
- Gustafsson, J. P. (2011). *Visual MINTEQ 3.0 user guide*. Stockholm, Sweden: KTH, Department of Land and Water Resources.
- Haines, M., Vadlamani, A., Daniel Loty Richardson, W., and Strous, M. (2022). Pilot-scale outdoor trial of a cyanobacterial consortium at pH 11 in a photobioreactor at high latitude. *Bioresour. Technol.* 354, 127173. doi:10.1016/j.biortech.2022.127173
- Hanifzadeh, M., Garcia, E. C., and Viamajala, S. (2018). Production of lipid and carbohydrate from microalgae without compromising biomass productivities: role of Ca and Mg. *Renew. Energy* 127, 989–997. doi:10.1016/j.renene.2018.05.012
- Hannon, M., Gimpel, J., Tran, M., Rasala, B., and Mayfield, S. (2010). Biofuels from algae: challenges and potential. *Biofuels* 1, 763–784. doi:10.4155/bfs.10.44
- Hoh, D., Watson, S., and Kan, E. (2016). Algal biofilm reactors for integrated wastewater treatment and biofuel production: a review. *Chem. Eng. J.* 287, 466–473. doi:10.1016/j.cej.2015.11.062
- Huang, C.-C., Hung, J.-J., Peng, S.-H., and Chen, C.-N. N. (2012). Cultivation of a thermo-tolerant microalga in an outdoor photobioreactor: influences of CO₂ and nitrogen sources on the accelerated growth. *Bioresour. Technol.* 112, 228–233. doi:10.1016/j.biortech.2012.02.078
- Jena, U., Das, K. C., and Kastner, J. R. (2011). Effect of operating conditions of thermochemical liquefaction on biocrude production from *Spirulina platensis*. *Bioresour. Technol.* 102, 6221–6229. doi:10.1016/j.biortech.2011.02.057
- Johnson, M. B., and Wen, Z. (2010). Development of an attached microalgal growth system for biofuel production. *Appl. Microbiol. Biotechnol.* 85, 525–534. doi:10.1007/s00253-009-2133-2
- Khan, M. I., Shin, J. H., and Kim, J. D. (2018). The promising future of microalgae: current status, challenges, and optimization of a sustainable and renewable industry for biofuels, feed, and other products. *Microb. Cell Fact.* 17, 36. doi:10.1186/s12934-018-0879-x
- Kim, H. W., Vannela, R., Zhou, C., and Rittmann, B. E. (2011). Nutrient acquisition and limitation for the photoautotrophic growth of *Synechocystis* sp. PCC6803 as a renewable biomass source. *Biotechnol. Bioeng.* 108, 277–285. doi:10.1002/bit.22928
- Kim, G.-Y., Roh, K., and Han, J.-I. (2019). The use of bicarbonate for microalgae cultivation and its carbon footprint analysis. *Green Chem.* 21, 5053–5062. doi:10.1039/c9gc01107b

- Körner, S., Das, S. K., Veenstra, S., and Vermaat, J. E. (2001). The effect of pH variation at the ammonium/ammonia equilibrium in wastewater and its toxicity to *Lemna gibba*. *Aquat. Bot.* 71, 71–78. doi:10.1016/s0304-3770(01)00158-9
- Lee, J., Park, J. H., Shin, Y. S., Lee, B. C., Chang, N. I., Cho, J., et al. (2009). Effect of dissolved organic matter on the growth of algae, *pseudokirchneriella subcapitata*, in Korean lakes: the importance of complexation reactions. *Ecotoxicol. Environ. Saf.* 72, 335–343. doi:10.1016/j.ecoenv.2008.01.013
- Loftus, S. E., and Johnson, Z. I. (2017). Cross-study analysis of factors affecting algae cultivation in recycled medium for biofuel production. *Algal Res.* 24, 154–166. doi:10.1016/j.algal.2017.03.007
- Lu, Z., Sha, J., Wang, W., Li, Y., Wang, G., Chen, Y., et al. (2019). Identification of auto-inhibitors in the reused culture media of the Chlorophyta *Scenedesmus acuminatus*. *Algal Res.* 44, 101665. doi:10.1016/j.algal.2019.101665
- Lu, Z., Loftus, S., Sha, J., Wang, W., Park, M. S., Zhang, X., et al. (2020). Water reuse for sustainable microalgae cultivation: current knowledge and future directions. *Resour. Conservation Recycl.* 161, 104975. doi:10.1016/j.resconrec.2020.104975
- Masuko, T., Minami, A., Iwasaki, N., Majima, T., Nishimura, S.-I., Lee, Y. C., et al. (2005). Carbohydrate analysis by a phenol-sulfuric acid method in microplate format. *Anal. Biochem.* 339, 69–72. doi:10.1016/j.ab.2004.12.001
- Mata, T. M., Martins, A. A., and Caetano, N. S. (2010). Microalgae for biodiesel production and other applications: a review. *Renew. Sustain. Energy Rev.* 14, 217–232. doi:10.1016/j.rser.2009.07.020
- Minde, M. W., Zimmermann, U., Madland, M. V., Korsnes, R. I., Schulz, B., Gilbricht, S., et al. (2020). Mineral replacement in long-term flooded porous carbonate rocks. *Geochim. Cosmochim. Acta* 268, 485–508. doi:10.1016/j.gca.2019.09.017
- Mokashi, K., Shetty, V., George, S. A., and Sibi, G. (2016). Sodium bicarbonate as inorganic carbon source for higher biomass and lipid production integrated carbon capture in *Chlorella vulgaris*. *Achiev. Life Sci.* 10, 111–117. doi:10.1016/j.als.2016.05.011
- Picardo, M. C., De Medeiros, J. L., Monteiro, J. G. M., Chaloub, R. M., Giordano, M., De Queiroz Fernandes Araújo, O., et al. (2013). A methodology for screening of microalgae as a decision making tool for energy and green chemical process applications. *Clean. Technol. Environ. Policy* 15, 275–291. doi:10.1007/s10098-012-0508-z
- Popovic, M. (2019). Thermodynamic properties of microorganisms: determination and analysis of enthalpy, entropy, and Gibbs free energy of biomass, cells and colonies of 32 microorganism species. *Heliyon* 5, e01950. doi:10.1016/j.heliyon.2019.e01950
- Prajapati, S. K., Kumar, P., Malik, A., and Vijay, V. K. (2014). Bioconversion of algae to methane and subsequent utilization of digestate for algae cultivation: a closed loop bioenergy generation process. *Bioresour. Technol.* 158, 174–180. doi:10.1016/j.biortech.2014.02.023
- Rafa, N., Ahmed, S. F., Badruddin, I. A., Mofijur, M., and Kamangar, S. (2021). Strategies to produce cost-effective third-generation biofuel from microalgae. *Front. Energy Res.* 9, 749968. doi:10.3389/fenrg.2021.749968
- Raven, J. A. (1994). Carbon fixation and carbon availability in marine phytoplankton. *Photosynth. Res.* 39, 259–273. doi:10.1007/bf00014587
- Rodolfi, L., Zittelli, G. C., Barsanti, L., Rosati, G., and Tredici, M. R. (2003). Growth medium recycling in *Nannochloropsis* sp. mass cultivation. *Biomol. Eng.* 20, 243–248. doi:10.1016/s1389-0344(03)00063-7
- Rösch, C., Skarka, J., and Wegerer, N. (2012). Materials flow modeling of nutrient recycling in biodiesel production from microalgae. *Bioresour. Technol.* 107, 191–199. doi:10.1016/j.biortech.2011.12.016
- Scott, S. A., Davey, M. P., Dennis, J. S., Horst, I., Howe, C. J., Lea-Smith, D. J., et al. (2010). Biodiesel from algae: challenges and prospects. *Curr. Opin. Biotechnol.* 21, 277–286. doi:10.1016/j.copbio.2010.03.005
- Sharp, C. E., Urschel, S., Dong, X., Brady, A. L., Slater, G. F., Strous, M., et al. (2017). Robust, high-productivity phototrophic carbon capture at high pH and alkalinity using natural microbial communities. *Biotechnol. Biofuels* 10, 84. doi:10.1186/s13068-017-0769-1
- Silva, B. F., Wendt, E. V., Castro, J. C., Oliveira, A. E. D., Carrim, A. J. I., Vieira, J. D. G., et al. (2015). Analysis of some chemical elements in marine microalgae for biodiesel production and other uses. *Algal Res.* 9, 312–321. doi:10.1016/j.algal.2015.04.010
- Sims, G. K., Ellsworth, T. R., and Mulvaney, R. L. (1995). Microscale determination of inorganic nitrogen in water and soil extracts. *Commun. Soil Sci. Plant Analysis* 26, 303–316. doi:10.1080/00103629509369298
- Singh, G., and Patidar, S. K. (2018). Microalgae harvesting techniques: a review. *J. Environ. Manag.* 217, 499–508. doi:10.1016/j.jenvman.2018.04.010
- Singh, R., Parihar, P., Singh, M., Bajguz, A., Kumar, J., Singh, S., et al. (2017). Uncovering potential applications of cyanobacteria and algal metabolites in biology, agriculture and medicine: current status and future prospects. *Front. Microbiol.* 8, 515. doi:10.3389/fmicb.2017.00515
- Slocumbe, S. P., Ross, M., Thomas, N., McNeill, S., and Stanley, M. S. (2013). A rapid and general method for measurement of protein in micro-algal biomass. *Bioresour. Technol.* 129, 51–57. doi:10.1016/j.biortech.2012.10.163
- Solovchenko, A. E., Ismagulova, T. T., Lukyanov, A. A., Vasilieva, S. G., Konyukhov, I. V., Pogosyan, S. I., et al. (2019). Luxury phosphorus uptake in microalgae. *J. Appl. Phycol.* 31, 2755–2770. doi:10.1007/s10811-019-01831-8
- Sluiter, A., Hames, B., Ruiz, R., Scarlata, C., Sluiter, J., Templeton, D., et al. (2008). Determination of structural carbohydrates and lignin in biomass. *Laboratory analytical procedure* 1617, 1–16.
- Suzuki, Y., Kuma, K., and Matsunaga, K. (1995). Bioavailable iron species in seawater measured by macroalga (*Laminaria japonica*) uptake. *Mar. Biol.* 123, 173–178. doi:10.1007/bf00350337
- Tibbetts, S. M., Milley, J. E., and Lall, S. P. (2015). Chemical composition and nutritional properties of freshwater and marine microalgal biomass cultured in photobioreactors. *J. Appl. Phycol.* 27, 1109–1119. doi:10.1007/s10811-014-0428-x
- Vadlamani, A., Viamajala, S., Pendyala, B., and Varanasi, S. (2017). Cultivation of microalgae at extreme alkaline pH conditions: a novel approach for biofuel production. *ACS Sustain. Chem. Eng.* 5, 7284–7294. doi:10.1021/acssuschemeng.7b01534
- Vadlamani, A., Pendyala, B., Viamajala, S., and Varanasi, S. (2019). High productivity cultivation of microalgae without concentrated CO₂ input. *ACS Sustain. Chem. Eng.* 7, 1933–1943. doi:10.1021/acssuschemeng.8b04094
- Vandamme, D., Foubert, I., Fraeye, I., Meesschaert, B., and Muylaert, K. (2012). Flocculation of *Chlorella vulgaris* induced by high pH: role of magnesium and calcium and practical implications. *Bioresour. Technol.* 105, 114–119. doi:10.1016/j.biortech.2011.11.105
- Volkman, J. K., and Brown, M. R. (2006). *Nutritional value of microalgae and applications*. Enfield: Science Publishers, Inc., 407–457.
- Wolf-Gladrow, D. A., Zeebe, R. E., Klaas, C., Körtzinger, A., and Dickson, A. G. (2007). Total alkalinity: the explicit conservative expression and its application to biogeochemical processes. *Mar. Chem.* 106, 287–300. doi:10.1016/j.marchem.2007.01.006
- Yang, J., Xu, M., Zhang, X., Hu, Q., Sommerfeld, M., Chen, Y., et al. (2011). Life-cycle analysis on biodiesel production from microalgae: water footprint and nutrients balance. *Bioresour. Technol.* 102, 159–165. doi:10.1016/j.biortech.2010.07.017
- Zhang, T., Xie, X., and Huang, Z. (2014). Life cycle water footprints of nonfood biomass fuels in China. *Environ. Sci. Technol.* 48, 4137–4144. doi:10.1021/es404458j
- Zhu, C., Zhang, R., Cheng, L., and Chi, Z. (2018). A recycling culture of *Neochloris oleoabundans* in a bicarbonate-based integrated carbon capture and algae production system with harvesting by auto-flocculation. *Biotechnol. Biofuels* 11, 204. doi:10.1186/s13068-018-1197-6
- Zhu, C., Xi, Y., Zhai, X., Wang, J., Kong, F., Chi, Z., et al. (2021). Pilot outdoor cultivation of an extreme alkaliphilic Trebouxiaophyte in a floating photobioreactor using bicarbonate as carbon source. *J. Clean. Prod.* 283, 124648. doi:10.1016/j.jclepro.2020.124648
- Zorz, J. K., Sharp, C., Kleiner, M., Gordon, P. M. K., Pon, R. T., Dong, X., et al. (2019). A shared core microbiome in soda lakes separated by large distances. *Nat. Commun.* 10, 4230. doi:10.1038/s41467-019-12195-5



OPEN ACCESS

EDITED BY

Namita Khanna,
Birla Institute of Technology and
Science, India

REVIEWED BY

Muhammad Aamer Mehmood,
Government College University,
Faisalabad, Pakistan
Gopinath Halder,
National Institute of Technology,
Durgapur, India

*CORRESPONDENCE

Wasif Farooq,
wasif@kfupm.edu.sa

SPECIALTY SECTION

This article was submitted to Bioprocess
Engineering,
a section of the journal
Frontiers in Bioengineering and
Biotechnology

RECEIVED 21 April 2022

ACCEPTED 07 July 2022

PUBLISHED 18 August 2022

CITATION

Alatriki A, Ali I, Razzak SA, Ahmad I and
Farooq W (2022), Assessment of CO₂
biofixation and bioenergy potential of
microalga *Gonium pectorale* through its
biomass pyrolysis, and elucidation of
pyrolysis reaction via kinetics modeling
and artificial neural network.
Front. Bioeng. Biotechnol. 10:925391.
doi: 10.3389/fbioe.2022.925391

COPYRIGHT

© 2022 Alatriki, Ali, Razzak, Ahmad and
Farooq. This is an open-access article
distributed under the terms of the
[Creative Commons Attribution License
\(CC BY\)](https://creativecommons.org/licenses/by/4.0/). The use, distribution or
reproduction in other forums is
permitted, provided the original
author(s) and the copyright owner(s) are
credited and that the original
publication in this journal is cited, in
accordance with accepted academic
practice. No use, distribution or
reproduction is permitted which does
not comply with these terms.

Assessment of CO₂ biofixation and bioenergy potential of microalga *Gonium pectorale* through its biomass pyrolysis, and elucidation of pyrolysis reaction *via* kinetics modeling and artificial neural network

Ahmed Alatriki¹, Imtiaz Ali², Shaikh Abdur Razzak^{1,3},
Irshad Ahmad^{3,4} and Wasif Farooq^{1,3*}

¹Department of Chemical Engineering, King Fahd University of Petroleum and Minerals, Dhahran, Saudi Arabia, ²Department of Chemical and Materials Engineering, King Abdulaziz University, Rabigh, Saudi Arabia, ³Interdisciplinary Research Center for Membranes and Water Security, King Fahd University of Petroleum and Minerals (KFUPM), Dhahran, Saudi Arabia, ⁴Department of Bioengineering, King Fahd University of Petroleum and Minerals, Dhahran, Saudi Arabia

This study investigates CO₂ biofixation and pyrolytic kinetics of microalga *G. pectorale* using model-fitting and model-free methods. Microalga was grown in two different media. The highest rate of CO₂ fixation (0.130 g/L/day) was observed at a CO₂ concentration of 2%. The pyrokinetics of the biomass was performed by a thermogravimetric analyzer (TGA). Thermogravimetric (TG) and derivative thermogravimetric (DTG) curves at 5, 10 and 20°C/min indicated the presence of multiple peaks in the active pyrolysis zones. The activation energy was calculated by different model-free methods such as Friedman, Flynn-Wall-Ozawa (FWO), Kissinger-Akahira-Sunose (KAS), and Popescu. The obtained activation energy which are 61.7–287 kJ/mol using Friedman, 40.6–262 kJ/mol using FWO, 35–262 kJ/mol using KAS, and 66.4–255 kJ/mol using Popescu showed good agreement with the experimental values with higher than 0.96 determination coefficient (R²). Moreover, it was found that the most probable reaction mechanism for *G. pectorale* pyrolysis was a third-order function. Furthermore, the multilayer perceptron-based artificial neural network (MLP-ANN) regression model of the 4-10-1 architecture demonstrated excellent agreement with the experimental values of the thermal decomposition of the *G. pectorale*. Therefore, the study suggests that the MLP-ANN regression model could be utilized to predict thermogravimetric parameters.

KEYWORDS

microalgae, CO₂ bio-fixation, biomass pyrolysis, thermogravimetric analysis, reaction kinetics

1 Introduction

Microalgae are potential candidates for CO₂ biofixation and renewable energy. Microalgae can be cultivated in a closed photobioreactor located on non-arable land or in an open vast pond. It is a cost-effective source of carbon dioxide (CO₂) mitigation through photosynthesis (Aresta et al., 2005). The fixation of CO₂ by microalgae is sought as an attractive strategy to produce biofuels, aquaculture products, and renewable food. Furthermore, it can be processed into a variety of products, for example, fuel gases, soil modifiers, biodiesel, green diesel, and methane (Christenson and Sims, 2011). The fixation of CO₂ by microalgae depends on various biotic and abiotic factors, such as temperature, quality and quantity of light, pH of the solution, mode of cultivation, purity, and CO₂ concentration being supplied. Furthermore, CO₂ fixation is also affected by microalgae strain (Daneshvar et al., 2022; Farooq et al., 2022). Microalgae biomass after CO₂ fixation can be processed as an environmentally friendly renewable feedstock through different conversion technologies such as gasification, pyrolysis, liquefaction and bioethanol technology. Pyrolysis technology is a distinctive chemical reaction that produces valuable chemicals such as biochar, light olefins, and syngas. The pyrolysis of microalgae comprises numerous reactions in series and parallel. There are different pyrolysis processes for microalgae such as fast pyrolysis, slow pyrolysis, catalytic pyrolysis, and microwave-assisted pyrolysis (Farooq et al., 2021).

TGA examines the decomposition of materials by weight changes as a function of rising temperature. The relationship between temperature and weight loss due to oxidation, dehydration, and decomposition is recorded as the TGA plot, while derivative thermogravimetric (DTG) curve records the derivative of weight change with respect to temperature. The rate of the thermochemical reaction is represented by the peak of the DTG curve. The elevation of the DTG curve detects the potential to release volatile substances from a reaction during the slow process of pyrolysis (Yang et al., 2014). However, TGA technology only evaluates total weight loss due to reactions, restricts its usage, and provides general information on the overall kinetics of the reaction rather than individual reactions (Yang et al., 2019).

So far, commercialization of microalgae pyrolysis has been tested only on a bench scale although microalgae pyrolysis has been used since the early 1990s. TGA was extensively used to show the kinetics of the degradation process and to simulate the slow pyrolysis process (heating rate is usually lower than 1°C/s in a fixed-bed tubular reactor). Much research on pyrolysis of microalgae was conducted using a slow pyrolysis approach,

while only a few studies were conducted using fast pyrolysis. Fast pyrolysis with a heating rate greater than 10°C/s can be performed in the fluidized bed reactor (Yang et al., 2019).

The kinetic data of TGA can be analyzed by various methods. The two most commonly applied approaches are model-free and model-fitting. The model-fitting method cannot characterize non-isothermal data adequately compared to the model-free approach. The model-free approach is much simpler, it avoids errors related to the kinetic model choice and offers better fitting of thermogravimetric curves than the model-fitting method. One of the limitations of this method is that several kinetic curves are collected to perform the analysis. Reaction rates can be calculated based on data collected at different heating rates at the same conversion value, resulting in the calculation of the activation energy at each conversion point (Subagyono et al., 2021). No study on thermogravimetric analysis of *G. pectorale* is reported. Fewer studies on the genetic transformation of *G. pectorale* microalgae are available (Lerche and Hallmann, 2009; Hanschen et al., 2016). Lot of work has been done on CO₂ fixation of microalgae along with its bioenergy potential. Besides improving the cultivation and harvesting process to increase the yield of biomass, a search for new strain with better growth and CO₂ fixation potential is needed as well. To best of our knowledge, this strain has not been investigated for its CO₂ fixation potential and its bioenergy contents. We targeted this strain as there is no study on potential of the strain for CO₂ and bioenergy potential.

The objectives of this study were to 1) Investigate the potential of the *G. pectorale* microalga for its CO₂ fixation potential, which to best of our knowledge has not been reported in the literature, 2) Estimate its total energy content through higher heating value (HHV), and 3) Kinetic analysis of the conversion process using model-free and model-fitting methods, and 4) The conversion of *G. pectorale* was modeled using an artificial neural network (ANN) to predict the pyrolysis behavior. The input data were time, temperature, and weight loss, while the output data was the change in weight loss with respect to time.

2 Materials and methods

2.1 Media preparations

The microalga was cultivated in two different growth mediums, namely Tris-Acetate-Phosphate (TAP) medium and Modified Bold 3N medium (3NBBM). To test whether this microalga prefers organic carbon or not, the first medium contains an organic carbon compound (CH₃COOH) while the latter does not. Stock solutions for

the growth medium were prepared in a 250 ml volumetric flask. After that, the stock solutions were combined in a 2 L flask for the growth medium. Each prepared medium was autoclaved at 121°C for 4 h to eliminate bacterial contamination and then allowed to cool to room temperature before microalgae inoculation.

2.2 *G. pectorale* biomass growth and CO₂ fixation potential

G. pectorale (strain K3-F3–4, mating type minus, NIES-2863 obtained from the Microbial Culture Collection at the National Institute for Environmental Studies, Tsukuba, Japan; Available online: <http://mcc.nies.go.jp/>) was grown under continuous light (1,300 lux) in 50 ml of modified Bold's 3N medium (UTEX, Austin, TX, United States) (Guerriero et al., 2018). The Erlenmeyer flasks were incubated at 25°C and 120 RPM on a shaker under approximate illumination of 100 μmol m^{−2} s^{−1} using cool white florescent light (Liu et al., 2019). Then, both the optical density (OD) and dry weights were taken daily. After 14 days of incubation with a continuous light supply, algal biomass was harvested, dried, and then ground to powder. A standard calibration curve for *G. pectorale* was generated to estimate its biomass concentration in [g/L] at any measured OD by Eq. 1.

$$DW [g/L] = 0.263OD_{688} + 0.0104 \quad (1)$$

CO₂ bio-fixation rate can be measured using the equation of the reference (Adamczyk et al., 2016).

$$R_{CO_2} = P \cdot C_C \frac{MW_{CO_2}}{MW_C} \quad (2)$$

where R_{CO_2} is the fixation rate, and P is the productivity in [mg per L per Day], C_C is the average carbon content calculated by the elemental analyzer, MW_C is the molecular weight of one carbon atom, and MW_{CO_2} is the molecular weight of CO₂.

2.3 Ultimate analysis of *G. pectorale* and higher heating value

The ultimate analysis of the dried biomass was performed using (Perkin Elmer Model 2400 CHNS/O Elemental analyzer, Perkin Elmer Corporation). The harvested samples were dried in the drying oven at 60°C for 24 h. The dried biomass samples were weighted (0.75–1.5 mg) in clean tin capsules (5 mm × 8 mm, Perkin Elmer). The capsules were then heated to 975°C using oxygen gas as the combustion gas feed and helium gas as the purging gas in a furnace. The instrument was calibrated with different criteria of ±3.75 for hydrogen, ±0.15 for carbon and ±0.16 for nitrogen. Furthermore, the oxygen content was found by difference.

The higher heating value (HHV) was calculated from the equation of reference (Noushabadi et al., 2021).

$$\begin{aligned} HHV [MJ/kg] = & -0.8738 \times N \times H^{-1.3101} \\ & -0.1583 \times C \times O^{0.3497} \\ & +0.3856 \times C \times (H \times O)^{0.1462} \\ & +2.1436 \times \left(\frac{H}{O}\right)^{-0.3846} \\ & +0.1076 \times C \times H^{-0.3846} + 0.1098 \times N \times S \\ & -11.2794 \times \left(\frac{H}{C}\right) \end{aligned} \quad (3)$$

where C , H , N , O , and S represent carbon, hydrogen, nitrogen, oxygen, and sulfur contents, respectively.

2.4 Thermogravimetric analysis of *G. pectorale* biomass

TGA analysis was conducted using the SDT Q600 TG-DTA thermogravimetric analyzer to explore the non-isothermal pyrolysis of microalgae remnants. Approximately 5–6 mg of each dried sample were placed in an alumina crucible, which was then inserted into the analyzer chamber. Nitrogen was continuously supplied with a constant flow of 100 ml/min as a purging gas to prevent undesirable oxidation reactions and remove any trapping gases. At first, the temperature for each run was equilibrated at 30°C. The sample was then heated from 30 to 800°C, with a heating rate of 5°C per minute. Additionally, two more heating rates at 10 and 20°C per minute were employed using the same procedure.

2.5 Kinetic analysis

The kinetics of chemical reactions can easily be determined from DSC or TGA measurements (Vyazovkin, 2020). The basic rate equation for this kinetic analysis is given by Eq. 4.

$$\frac{d\alpha}{dt} = k(T) \cdot f(\alpha) \quad (4)$$

where $k(T)$ is the rate constant, $f(\alpha)$ is the kinetic model, and α is the degree of conversion, which is calculated by Eq. 5

$$\alpha = \frac{w_0 - w}{w_0 - w_f} \quad (5)$$

In which w_0 , w , and w_f are the initial, instantaneous, and the remaining mass of the sample, respectively.

With Arrhenius equation

$$k(T) = A \exp\left(\frac{-E_a}{RT}\right) \quad (6)$$

where A , E_a , R , and T are the pre-exponential factor, activation energy, gas constant, and temperature.

The term $k(T)$ in Eq. 4 is combinable with Eq. 6 and gives the equation below

$$\frac{d\alpha}{dt} = A \exp\left(\frac{-E_a}{RT}\right) \cdot f(\alpha) \quad (7)$$

Incorporating the temperature dependence of the reaction from the Arrhenius law and subsequently modifying it for isochronal heating, the equation becomes the following.

$$\frac{d\alpha}{dT} = \frac{A}{\beta} \cdot \exp\left(\frac{-E_a}{RT}\right) \cdot f(\alpha) \quad (8)$$

In which β is the applied heating rate ($\frac{dT}{dt}$)

After integration, Eq. 8 becomes:

$$g(\alpha) = \int_0^\alpha \frac{d\alpha}{f(\alpha)} = \int_{T_0}^T \frac{A}{\beta} \cdot \exp\left(\frac{-E_a}{RT}\right) \cdot dT \quad (9)$$

where $g(\alpha)$ is the integral form of $f(\alpha)$ and T_0 is the initial temperature.

A model-free technique will be adopted to estimate the activation energy.

2.5.1 Model-free kinetics

Model-free kinetics assumes that the activation energy changes during the reaction. Furthermore, this approach also assumes that the activation energy at a particular conversion point is independent of temperature ("isoconversion principle"). Various model-free kinetic approaches are reported. The model-free approach allows one to determine the activation energy of a reaction without assuming a kinetic model. Various model-free kinetics approaches are reported. Friedman is a differential isoconversional method, whereas Ozawa-Flynn-Wall (OFW) and Kissinger-Akahira-Sunose (KAS) are integral isoconversional methods. In all methods, the measurements are analyzed for multiple conversion levels. These methods are suitable for multistep reactions and give an average activation energy value (Naqvi et al., 2018). Friedman requires at least two measurements.

Friedman (Friedman, 2007):

$$\ln\left(\beta \frac{d\alpha}{dT}\right) = \ln\left(\frac{d\alpha}{dT}\right) = \ln[A \cdot f(\alpha)] - \frac{E_a}{RT} \quad (10)$$

E_a is determined from the slope of $\ln\left(\frac{d\alpha}{dT}\right)$ versus $\frac{1}{T}$ plot at constant α .

OFW (Maia and de Morais, 2016):

$$\ln \beta = \text{constant} - 1.052 \frac{E_a}{RT_\alpha} \quad (11)$$

KAS (Naqvi et al., 2018):

$$\ln \frac{\beta}{T_\alpha^2} = \text{constant} - \frac{E_a}{RT_\alpha} \quad (12)$$

Popescu (Kokalj et al., 2017):

$$\ln\left(\frac{\beta}{T_\alpha - T_{\alpha-\Delta\alpha}}\right) = \text{constant} - \frac{2E_a}{R(T_\alpha + T_{\alpha-\Delta\alpha})} \quad (13)$$

where $\Delta\alpha$ is the conversion interval, $T_{(\alpha-\Delta\alpha)}$ is the absolute temperature at $\alpha-\Delta\alpha$, and T_α is the temperature corresponding to α .

2.5.2 Model-fitting kinetics

The model function in the rate equation can be attained by the linear regression of the equation below, which is known as the combined kinetics method (Pérez-Maqueda et al., 2006).

$$\ln\left(\frac{d\alpha}{dT}\right) - \ln[(1-\alpha)^n \alpha^m] = \ln(cA) - \frac{E_a}{RT_\alpha} \quad (14)$$

where c , n , and m are the parameters of the model function, $f(\alpha) = c(1-\alpha)^n \alpha^m$

2.5.3 Thermodynamic analysis

Thermodynamic parameters such as changes in the Gibbs free energy of activation, the enthalpy of activation, and the entropy of activation are obtained from the kinetic parameters by the equations below.

$$\Delta H = E_a - RT \quad (15)$$

$$\Delta G = E_a + RT_p \ln\left(\frac{K_B T_p}{hA}\right) \quad (16)$$

$$\Delta S = \frac{\Delta H - \Delta G}{T_p} \quad (17)$$

where K_B is the Boltzmann constant (1.381×10^{-23} J/K), h is the Planck constant (6.626×10^{-34} J s), and T_p is the temperature corresponding to the maximum DTG in Kelvin.

2.6 Artificial neural network

In this study, artificial neural network (ANN) models were developed to predict activation energy. ANN use the input/target data to map the patterns between the variables. Statistica 13.5 was used to develop the network architecture using MLP regression to model the target values. Temperature (K), heating rate ($^{\circ}\text{C}/\text{min}$), conversion ($-$) and conversion rate (s^{-1}) were used as input neurons in the input layer, while the activation energy was used as output neuron in the output layer. Three subsets were obtained randomly from the original data set as training (70%), testing (15%) and validation (15%). The Broyden-Fletcher-Goldfarb-Shanno (BFGS) algorithms were used to develop MLP based ANN regression models. The hidden and output layers use different built-in activation functions such as logistic, exponential, tangent hyperbolic, SoftMax, sine and gaussian. Each neuron is connected through its nodes to all nodes in the other layers with some network parameters (weights and biases). Neural networks are trained

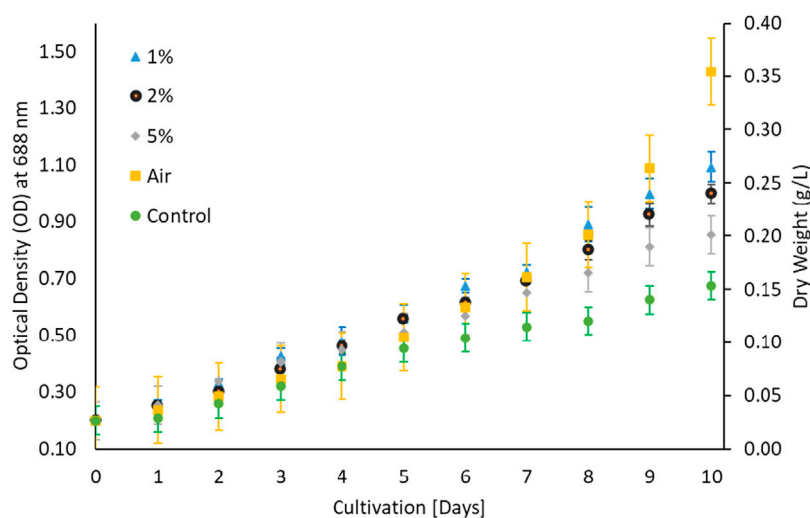


FIGURE 1
Different CO₂ concentrations in 3NBBM.

through supervised learning by minimizing the sum of squared errors. Trained networks were evaluated and verified using testing and validation data sets. Five best-performing models are retained, out of which one best is chosen using external validation and predictions.

3 Results and discussion

3.1 *G. pectorale* growth

Microalga *G. pectorale* was cultivated under standard room conditions in a modified Bold 3N medium with initial pH of 6.8 at different CO₂ concentrations; 1, 2 and 5%. A maximum of 5% CO₂ concentration was investigated, as some studies suggest that exceeding this concentration can harm algal cells and hinder their growth (Farooq, 2022; Farooq et al., 2022). Furthermore, *N. oculata* and *Chlorella* sp. strains have shown optimal growth at a concentration of 2% CO₂ (Farooq et al., 2022). A light intensity of 100 $\mu\text{mol m}^{-2} \text{s}^{-1}$ using cool white florescent light was used for the growth analysis. The effect of CO₂ concentration on *G. pectorale* microalgal growth was found to be inversely proportional (Figure 1). Preference of microalgae for carbon source either inorganic as CO₂ and organic carbon depends on algal species (Khan et al., 2022). There is no published study on this strain, that makes comparative analysis more difficult. However, when comparing its biomass concentration after 10 days of cultivation with *N. oculata*, around 0.35 g/L was achieved, while the latter achieved a higher value, which is approximately 1.20 g/L.

Furthermore, less biomass concentration was achieved without feeding CO₂ to our cultivation process and a higher value was achieved when the ambient air was fed instead of CO₂.

The growth of microalgae for 10 days period (Ale et al., 2014) is shown in Figure 1 which implied that microalgae prefer low CO₂ contents and do not prefer higher CO₂ for its growth despite controlling pH. To investigate the possibility of microalgae preference for organic carbon, microalgae were cultivated in Triacetate Phosphate medium containing organic carbon (acetic acid and glucose) and without the organic carbon. Figure 2 showed that microalgae growth was affected by the presence of the organic carbon source in the form of acetic acid. A difference in growth is evident during growth without acetic acid. Purging the growth media with air in the presence of acetic acid further improved growth, which could be due to mixotrophic behavior and exposure of cells to lighter cells due to mixing (Gao et al., 2019; Patel et al., 2020). The use of organic waste and wastewater loaded with organic carbon will be a good cultivation medium for the growth of microalga, *G. pectorale*, because of its mixotrophic mode of growth.

The growth of microalgae was further investigated at various glucose concentrations as a carbon source. The results in Figure 3 showed that growth improved with low glucose supplementation. Biomass increased from 0.4 g/L under control to 0.7 g/L under 0.2% glucose supplementation. The *G. pectorale* microalga was shown to be capable of consuming different types of organic carbon. TAP medium was preferred for glucose supplementation, unlike Modified Bold 3N medium. When the cultivation

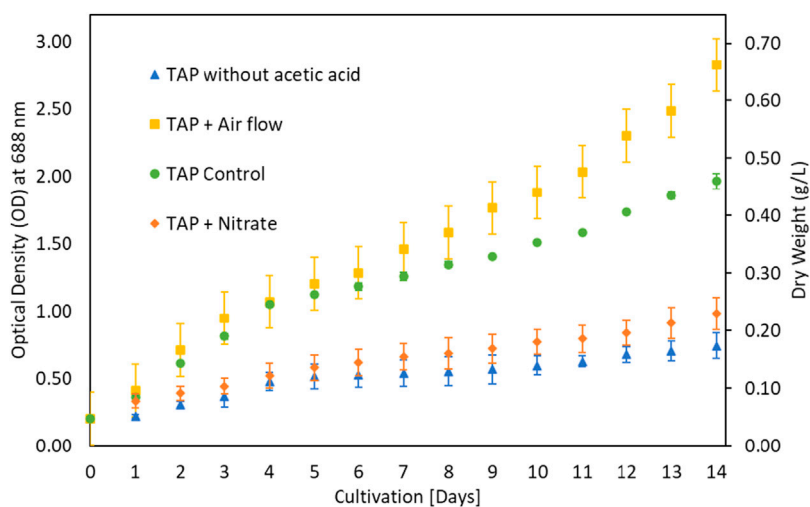


FIGURE 2
Supplementation variation in TAP medium.

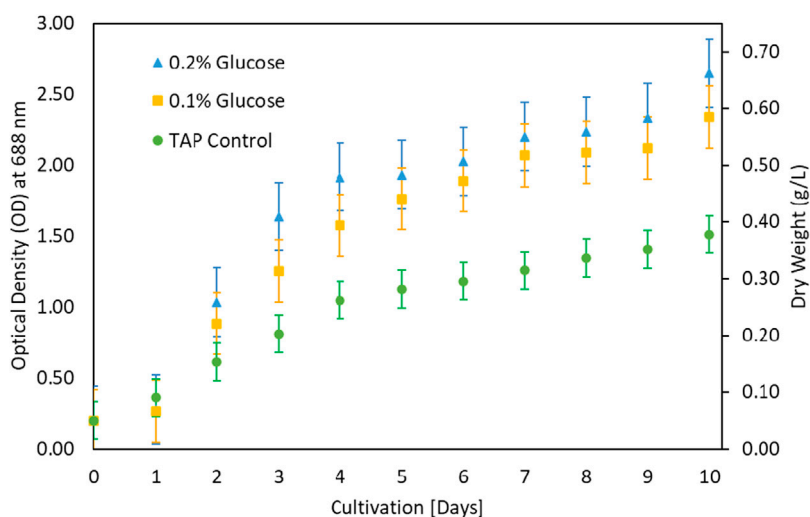


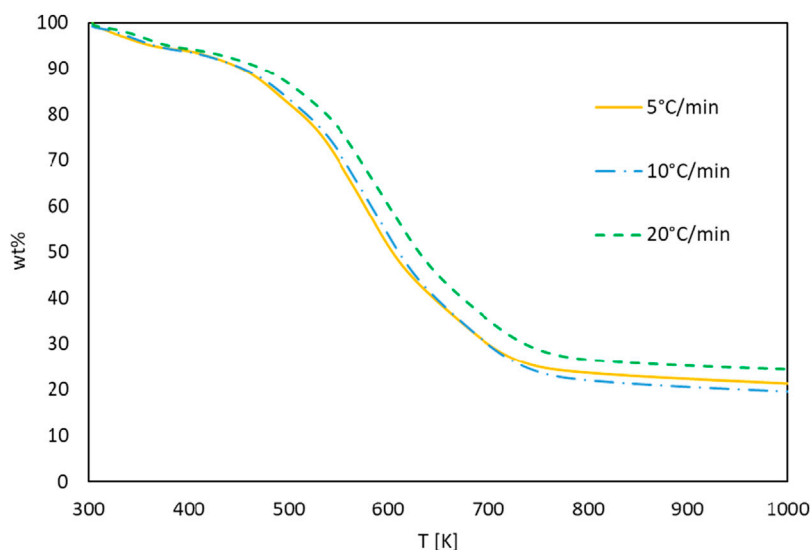
FIGURE 3
Growth comparison after glucose addition in TAP medium.

process was conducted in a modified Bold 3N medium with the addition of glucose, the culture growth failed. However, adding a higher glucose concentration (0.5%) to the TAP medium also resulted in growth failure. The biomass concentrations achieved in [g/L] are 1.01 ± 0.05 , 1.10 ± 0.07 , and 0.98 ± 0.08 for control, 0.1 and 0.2% glucose, respectively. For the same supplementation concentration and conditions, Karpagam et al. (2015) found the biomass concentration in [g/L] to be 0.77 ± 0.04 , 0.81 ± 0.01 , and $0.85 \pm$

0.03 for control, 0.1 and 0.2% glucose, respectively, for *Chlamydomonas reinhardtii*, strain CC1010 (Karpagam et al., 2015). In Figure 3, although 0.2% glucose supplementation improved *G. pectorale* growth, it does not make a noticeable difference compared to control growth using acetic acid as a source of organic carbon. Consumption of organic and inorganic form of carbon is supported by optimal light intensity, types and its duration (Mondal et al., 2017).

TABLE 1 Ultimate analysis and higher heating value of *G. pectorale* at different TAP media conditions.

	Ultimate analysis [wt%]					HHV [MJ/kg]	P [mg/L/Day]	R _{CO} [g/L/Day]
	C	H	N	S	O			
TAP + air	50.78	7.70	8.83	0.48	32.69	23.69	118.8	—
TAP + nitrate	48.43	7.72	8.78	0.57	35.07	22.67	84.7	—
TAP without acetic acid	43.17	6.55	7.0	0.96	43.28	18.42	68.3	—
TAP + 0.1% glucose	54.55	7.09	9.72	0	28.64	22.14	98.1	—
TAP + 0.2% glucose	45.99	6.53	8.30	0	39.18	18.08	110	—
TAP control	49.00	8.67	8.54	0.42	29.34	20.69	101	—
3NBBM control	47.19	7.49	7.75	0	37.57	19.01	65.4	—
3NBBM + air	47.18	6.49	8.16	0.05	38.17	18.62	72.8	—
3NBBM + 1% CO ₂	44.58	8.81	6.28	0	40.33	18.24	79.4	0.130
3NBBM + 2% CO ₂	49.34	7.04	8.64	0.69	34.98	20.42	74.2	0.134
3NBBM + 5% CO ₂	45.46	5.96	8.50	0.44	40.08	18.01	77	0.128

FIGURE 4
TG curves of *G. pectorale* at different heating rates.

3.2 Ultimate analysis, CO₂ fixation rate and higher heating value

The results of the ultimate analysis for the microalgae in Table 1 are consistent with a previous study (Yang et al., 2016; Farooq et al., 2022) in which most species of algae have a carbon content ranging from 40 to 50%, while the hydrogen content is approximately 7% of the total dry weight of the algal. The sulfur content in the microalgae is small, which ranges from 0.5% to 1.5%. The nitrogen content related to the

microalgae protein content and amino acids ranges from 3.1% to 10.6%.

3.3 TG-DTG analysis of *G. pectorale* and pyrolytic kinetics

The TG and DTG curves of the *G. pectorale* at 5, 10, and 20°C/min are shown in Figures 4, 5. It is noticeable that an increase in the heating rate results in an increase in both the

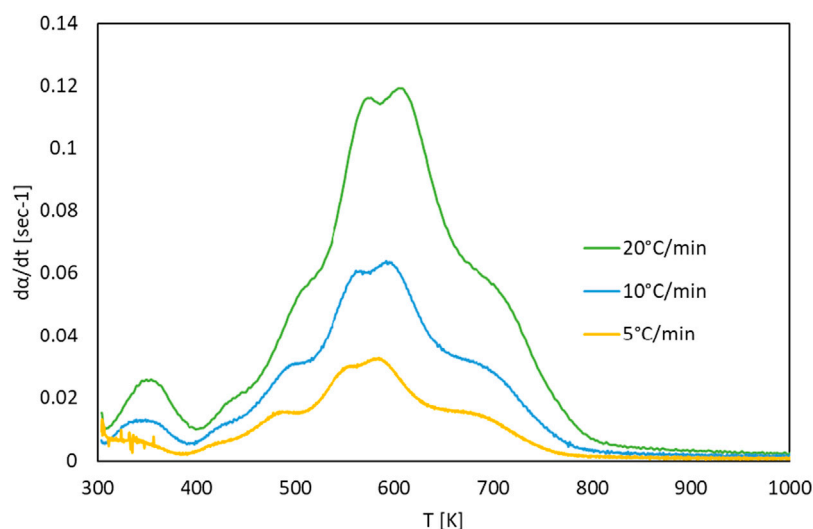


FIGURE 5
DTG curves of *G. pectorale* at different heating rates.

TABLE 2 Characteristics of DTG curves at different heating rates of *G. pectorale* pyrolysis.

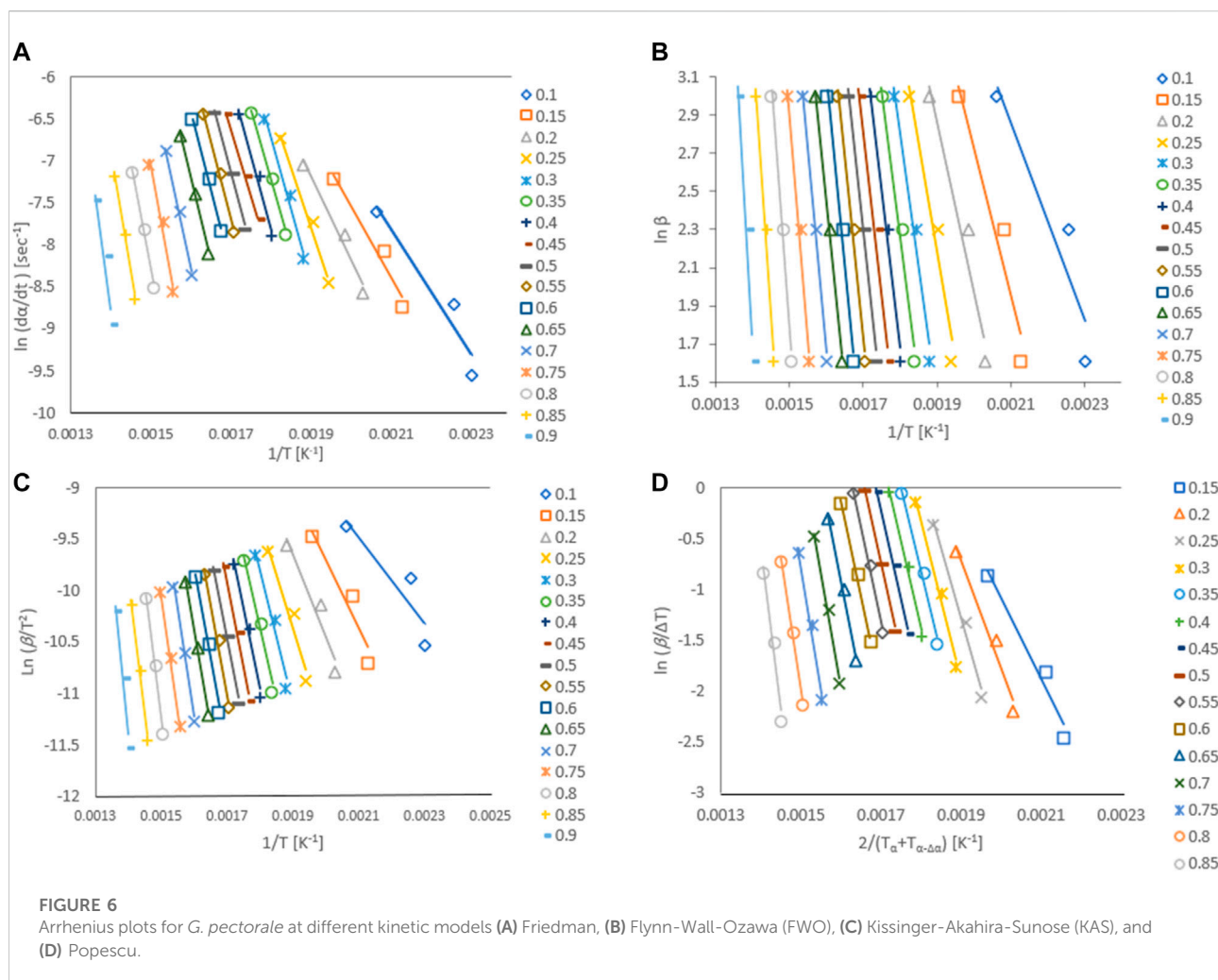
β [$^{\circ}\text{C min}^{-1}$]	T_p [K]	da/dt [sec^{-1}] $ _{T_p}$
5	592.72	0.031
10	593.62	0.063
20	606.99	0.119

degradation rate (da/dt) and the releases of volatile matter and in fewer pyrolysis residues (Subagyono et al., 2021). This is due to the limitation of mass and heat transfer that is normally attributed to high temperatures (Ceylan et al., 2014). Figure 4 shows a significant weight loss in the temperature range of 540–740 K. In addition, even the DTG peaks shifted to higher temperatures. The DTG curves at 5, 10, and 20°C/min indicated the presence of multiple peaks and pyrolysis zones, with the maximum peaks' temperatures shown in Table 2 that correspond to the devolatilization process or the main pyrolysis. These peaks are generally attributed to the decomposition of proteins and carbohydrates (Vuppaladadiyam et al., 2019). Three stages can be clearly shown on the TG-DTG curves. The first stage is at ≤ 400 K, where evaporation of moisture and low-boiling point organic compounds occurs. Furthermore, chlorophyll decomposition can occur during this stage because it is an unstable compound that generally degrades at 80°C–145°C (Chen et al., 2012). The second stage lies between 400 and 740 K, is the active pyrolysis zone where the thermal decomposition of carbohydrates, proteins and lipids occurs at 410–540 K, 470–550 K, and 560–630 K, respectively. The third stage, known as the

passive pyrolysis zone, is indicated by flat curves that are higher than 760 K, where the decomposition of the compounds occurs due to gasification and non-volatile carbon compounds that evaporate to form gaseous CO_2 and CO at high temperature (Agrawal and Chakraborty, 2013).

3.4 Model-free kinetics

Activation energy, E_a , is the minimum energy required in order to form a product. The value of activation energy can be found from Arrhenius plot. Arrhenius plot analyze the effect of reaction temperature on rate of reaction. The Arrhenius plots for *Gonium pectorale* are plotted for different kinetic models as Figure 6. The estimated values of the activation energy, which depend on the composition of the biomass, for the pyrolysis of the microalgae biomass are given in Figure 7. The obtained E_a values were calculated for the conversion range of 0.1–0.8 with a step interval of 0.05. The relative contents of lipids, carbohydrates, and protein and their classes vary between microalgae strains. A higher standard deviation at the end might be due to the presence of ash contents containing minerals. Furthermore, calculated activation energy values using FWO (40.6–260 kJ/mol), Friedman (61.7–287 kJ/mol), Popescu (66.4–255 kJ/mol) and KAS (35.0–262 kJ/mol), respectively. The estimated values of activation energies from different models at multiple heating rates of 5, 10 and 20°C/min are in close agreement with each other and agree with the reported literature. (Farooq et al., 2021). estimated activation energy for the pyrolytic conversion of *Parachlorella kessleri* HY-6 using KAS and Friedman methods as



241.91 (± 53.05) kJ/mol and 253.54 (± 58.81) kJ/mol, respectively. In another study, the authors calculated activation energy for *Spirulina* pyrolysis using KAS method in the range of 160–335 kJ/mol (Hong et al., 2020).

Activation energy values using the KAS, FWO, Popescu, and Friedman methods for conversion rates from 0.1 to 0.3 increased due to protein decomposition in this conversion temperature range (233°C–340°C). A slight decrease in the activation energy value was observed at conversion rates of 0.4–0.6, which showed cellulose decomposition in the temperature range (326°C–393°C). Pyrolytic degradation of lipid compounds required higher activation energy values conversion rates of 0.6–0.9, in a higher temperature range of 377°C–484°C (Vuppaladadiyam et al., 2019; Subagyono et al., 2021). Similar observation was reported in another study, where model compound of protein decomposed earlier at lower temperature than carbohydrates and then lipid (Hong et al., 2020).

3.5 Thermodynamics parameters estimation

Endothermic or exothermic nature of the reaction is indicated by ΔH . The value of ΔH also indicates the energy difference between the activated complex and the reactants. Small ΔH represents the formation of activated complex and a low potential energy barrier (Naqvi et al., 2018). The average ΔH was 135.82 (± 57.58) kJ/mol and the difference between E_a and ΔH is around 5 kJ mol⁻¹. ΔG refers to the increase in the energy of the system towards an equilibrium by forming activated complex. ΔG values range from (61.2–250 kJ/mol), (168–384 kJ/mol), (176–214 kJ/mol), and (121–162 kJ/mol) for the Popescu, KAS, FWO, and Friedman methods, respectively. These ΔG values indicate the increase in total energy available in *G. pectorale* pyrolysis and the formation of an activated complex. Furthermore, these values are higher compared to the values of waste red peppers (139.0 kJ/mol) (Maia and de Moraes, 2016) and rice straw (165.1 kJ/mol) (Xu and Chen, 2013). ΔS indicates the

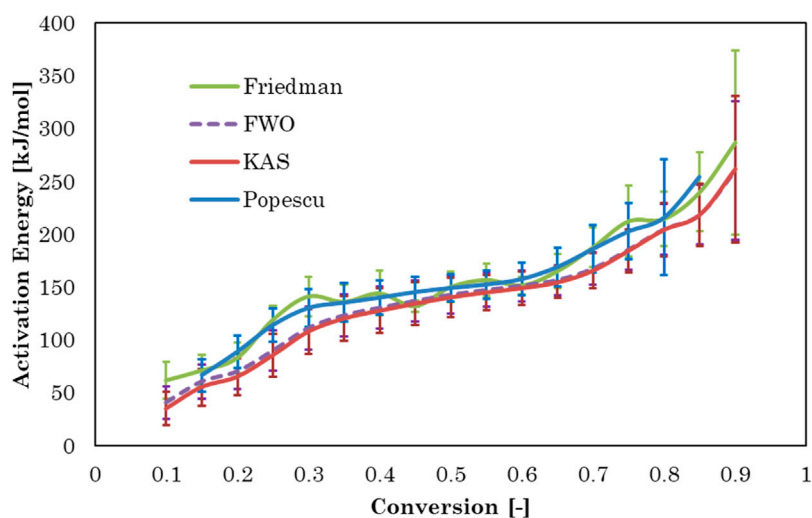


FIGURE 7

Activation energy versus conversion for four model-free methods.

TABLE 3 *G. pectorale* thermodynamic parameters by Flynn-Wall-Ozawa (FWO) method.

Conversion	E_a [kJ/mol]	R^2	A [min^{-1}]	ΔH [kJ/mol]	ΔG [kJ/mol]	ΔS [kJ/mol/K]
0.1	40.6	0.88	5.14E + 01	35.4	175.9	-0.227
0.15	60.3	0.93	5.22E + 03	55.2	171.8	-0.188
0.2	70.0	0.95	3.05E + 04	64.8	172.4	-0.173
0.25	89.6	0.96	2.06E + 06	84.5	170.3	-0.138
0.3	111.2	0.97	1.97E + 08	106.0	168.3	-0.101
0.35	123.1	0.97	1.85E + 09	118.0	168.8	-0.082
0.4	130.3	0.98	5.51E + 09	125.2	170.3	-0.073
0.45	136.9	0.98	1.37E + 10	131.7	172.2	-0.065
0.5	142.7	0.98	2.80E + 10	137.5	174.3	-0.059
0.55	147.3	0.99	4.36E + 10	142.1	176.6	-0.056
0.6	151.3	0.99	5.71E + 10	146.1	179.2	-0.053
0.65	156.6	0.99	9.12E + 10	151.5	182.2	-0.050
0.7	167.4	0.99	3.71E + 11	162.2	185.7	-0.038
0.75	185.6	0.99	5.12E + 12	180.4	190.3	-0.016
0.8	204.8	0.99	6.66E + 13	199.7	196.4	0.005
0.85	218.7	0.98	2.51E + 14	213.5	203.4	0.016
0.9	260.3	0.94	9.88E + 16	255.2	214.3	0.066

degree of proximity of the system to thermodynamic equilibrium. Lower values of ΔS indicate that material passed a process, moving to a thermodynamic equilibrium, while higher ΔS values states that the material is away from thermodynamic equilibrium. The negative value of ΔS and the positive value of ΔG indicated in Table 3 imply that the thermal decomposition of

G. pectorale is a non-spontaneous process. When R^2 is close to 1, this indicates that we have an excellent fit model to the experimental data from TG. However, a higher R^2 of fit is not always a suitable criterion to decide which methods are best because it does not determine whether the activation energies are correct (Subagyono et al., 2021).

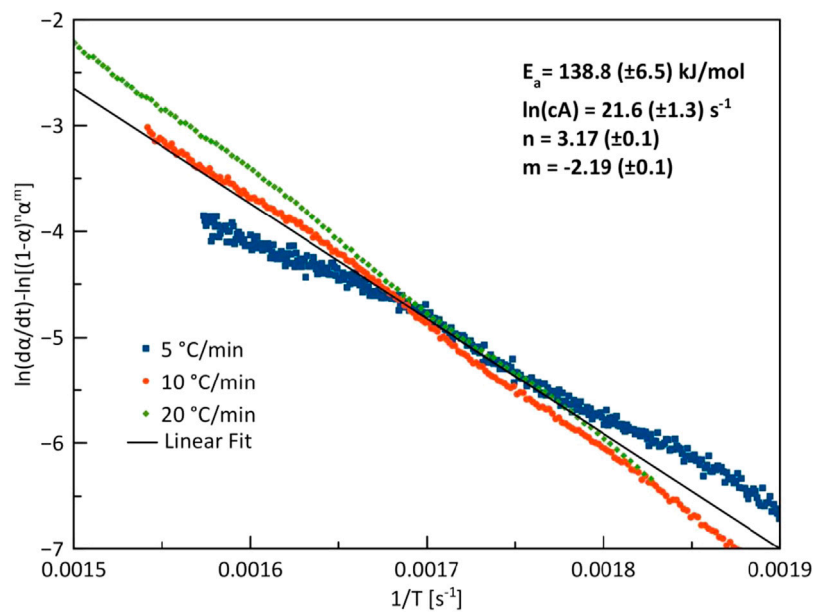


FIGURE 8
Combined kinetics plot of *G. pectorale* at heating rates of 5, 10, and 20°C/min.

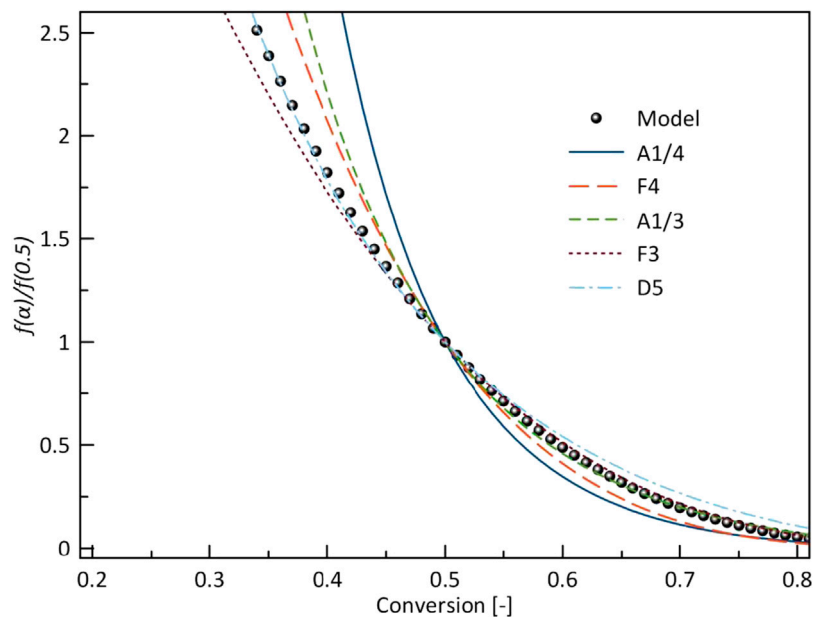


FIGURE 9
Normalized model function $f(\alpha)/f(0.5)$ with different ideal models.

3.6 Model-fitting kinetics

Figure 8 shows the kinetics plots of the conversion of *G. pectorale* under slow pyrolytic conditions with three different

heating rates. At 10 and 20°C/min, the heating rates yielded near-straight lines that fit the experimental curve. However, at 5°C/min, the line produced differs from the experimental curve.

TABLE 4 Summarizes the combined kinetics plots of *G. pectorale* at three different heating rates.

Heating rate [°C/min]	E_a [kJ/mol]	$\ln(cA)$ [1/s]	n [–]	m [–]
5	71.5 ± 2.5	9.7 ± 0.5	3.38 ± 0.04	0.4 ± 0.04
10	99.9 ± 3.3	15.6 ± 0.7	3.61 ± 0.06	-0.43 ± 0.06
20	82.6 ± 9.6	12.1 ± 1.9	3.07 ± 0.18	-0.18 ± 0.18

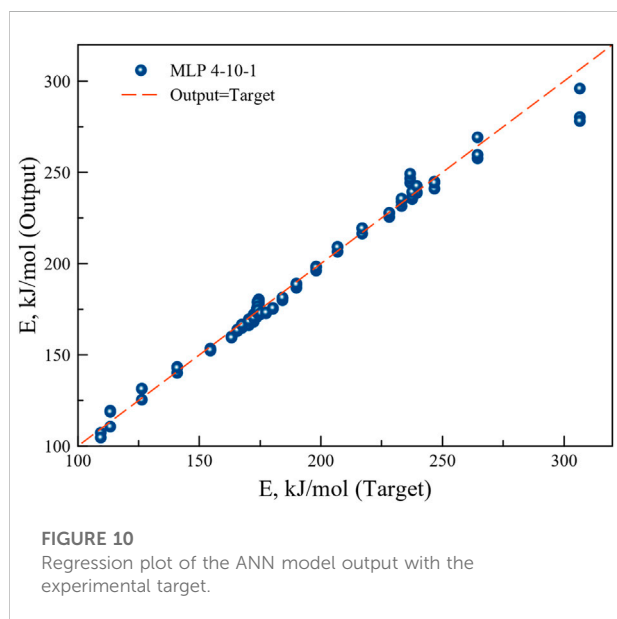
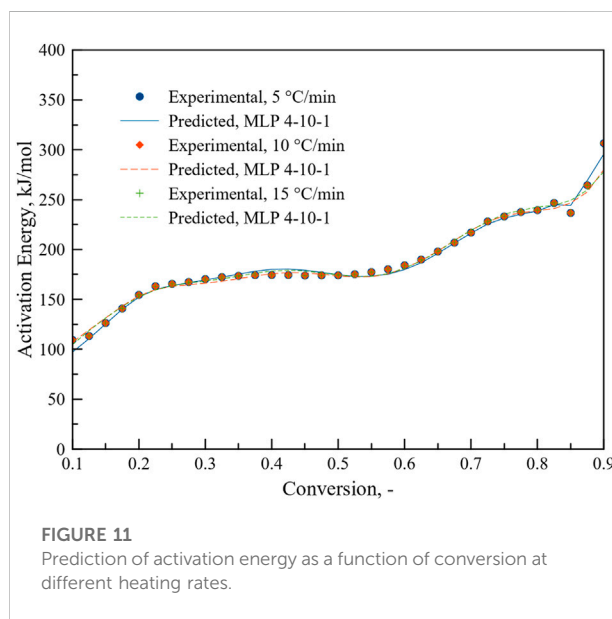


Figure 9 shows model-fitting kinetics with master plot agreement with five different models. These models are the most likely reaction mechanism for a single-step reaction. A third-order (F3) corresponded to the combined kinetic parameters obtained in this study. The obtained kinetics order at different heating rates is shown in Table 4, the order is slightly lower than reported by (Alshareef and Ali, 2020) in the pyrolysis of halophyte. By the high reaction order indicates random nucleation within the particles during pyrolysis (Xu et al., 2017).

3.7 Artificial neural network prediction

MLP based ANN regression models were trained and five better performing models were retained. The most suitable model was selected on the basis of the highest correlation coefficient and lowest sum of squared errors during training, testing and validation of the data sets. The structure of the best performing network at different heating rates was MLP 4-10-1. MLP based ANN model containing 10 hidden layers with exponential function in the hidden layers and sine function in the output layer returned excellent correlation coefficient. MLP 4-10-1 was therefore used to understand the



microalgae biomass conversion process through pyrolysis. The BFGS algorithm for the said model reached optimal outcomes after 62 cycles.

The regression graph in Figure 10 shows the correlation between the target and the model output values. The high correlation coefficient implies good agreement of the model output with the experimental target values.

To see the performance, MLP 4-10-1 was used to predict the activation energy at different heating rates. As can be seen from Figure 11, MLP based ANN regression model can predict activation energy accurately for different heating rates as a function of conversion. R^2 value reached to 0.999. MLP based ANN performed better than ANN results reported in a recent study on the thermal degradation of green river shale (You and Lee, 2022) where heat flow, heating rate and difference in conversion were chosen as inputs. There model performance was relatively poor at lower heating rate.

4 Conclusion

G. pectorale was grown to analyze its growth, CO_2 fixation capacity, thermogravimetric analysis (TG), derivative thermogravimetric analysis (DTG), and elemental analysis to

estimate its energy content. Growth was carried out under different culture conditions in two different media, reporting the highest biomass productivity, and the CO₂ fixation rate was obtained from TAP culture and 3NBBM with a concentration of 2% CO₂, respectively. The highest biomass concentration achieved after 14 days of cultivation was 1.08 g/L. As a result, TAP is considered a better medium compared to 3NBBM for the cultivation of *G. pectorale*. This shows that *G. pectorale* prefers organic carbon over inorganic carbon (CO₂). TG-DTG curves at 5, 10, and 20°C/min indicated the presence of multiple peaks and active pyrolysis zones due to the multicomponent biomass of microalgae (carbohydrates, protein, and lipids). In addition, the kinetics of *G. pectorale* was studied using model-free and model-fitting methods. The predicted activation energy values of the Friedman, FWO, KAS and Popescu models indicated excellent agreement with the experimental values ($R^2 > 0.96$). The higher values of 200 kJ/mol of *Ea* obtained suggest that algal lipids are more difficult to decompose in the N₂ atmosphere. Moreover, it was found that the most probable reaction mechanism for the pyrolysis of *G. pectorale* was the third-order function. Also, the F3 model-fitting method gave a good prediction. The study showed the effectiveness of MLP based ANN regression model for the prediction of activation energy at different heating rates. Further investigations must be conducted on the heterotrophic and mixotrophic cultivation using different organic molecules for lipids production. Detailed characterization of the strain with respect to its biomolecules is also recommended. As this microalga showed a preference for organic carbon, it is recommended to use this strain for treatment of high organic load wastewater.

Data availability statement

The original contributions presented in the study are included in the article/Supplementary Material, further inquiries can be directed to the corresponding author.

Author contributions

AA conducted all the experiment and collected raw data and wrote the first draft of manuscript. ImA analyze the data by ANN and ML methods IrA provided the support for growth of microalgae and edited the first draft. SR revised the manuscript and help in analyzing the CHNS and growth

data WF supervised the whole process from experimental design to data collection and manuscript writing, editing and submission.

Funding

The experimental work is supported by project number DF191033 by Deanship of Research Oversight and Coordination (DROC), King Fahd University of Petroleum and Minerals (KFUPM) Dhahran, Saudi Arabia.

Acknowledgments

We acknowledge the King Fahd University of Petroleum and Minerals (KFUPM), Dhahran, 31261, Saudi Arabia for providing the facilities for this work. Authors would like to acknowledge the funding provided by Deanship of Research Oversight and Coordination (DROC), King Fahd University of Petroleum and Minerals (KFUPM) Dhahran, Saudi Arabia for article processing charges (APC).

Conflict of interest

The authors declare that the research was conducted in the absence of any commercial or financial relationships that could be construed as a potential conflict of interest.

Publisher's note

All claims expressed in this article are solely those of the authors and do not necessarily represent those of their affiliated organizations, or those of the publisher, the editors and the reviewers. Any product that may be evaluated in this article, or claim that may be made by its manufacturer, is not guaranteed or endorsed by the publisher.

Supplementary material

The Supplementary Material for this article can be found online at: <https://www.frontiersin.org/articles/10.3389/fbioe.2022.925391/full#supplementary-material>

References

- Adamczyk, M., Lasek, J., and Skawińska, A. (2016). CO₂ biofixation and growth kinetics of *Chlorella vulgaris* and *nannochloropsis gaditana*. *Appl. Biochem. Biotechnol.* 179, 1248–1261. doi:10.1007/s12010-016-2062-3
- Agrawal, A., and Chakraborty, S. (2013). A kinetic study of pyrolysis and combustion of microalgae *Chlorella vulgaris* using thermo-gravimetric analysis. *Bioresour. Technol.* 128, 72–80. doi:10.1016/j.BIORTECH.2012.10.043

- Ale, M. T., Pinelo, M., and Meyer, A. S. (2014). Assessing effects and interactions among key variables affecting the growth of mixotrophic microalgae: PH, inoculum volume, and growth medium composition. *Prep. Biochem. Biotechnol.* 44, 242–256. doi:10.1080/10826068.2013.812562
- Alshareef, K. A. A., and Ali, I. (2020). Pyrolytic conversion of halophyte (*Tetraena coccinea*). *Bioresour. Technol. Rep.* 12, 100577. doi:10.1016/J.BITEB.2020.100577
- Aresta, M., Dibenedetto, A., and Barberio, G. (2005). Utilization of macro-algae for enhanced CO₂ fixation and biofuels production: Development of a computing software for an LCA study. *Fuel Process. Technol.* 86, 1679–1693. doi:10.1016/J.FUPROC.2005.01.016
- Ceylan, S., Topcu, Y., and Ceylan, Z. (2014). Thermal behaviour and kinetics of alga *Polysiphonia elongata* biomass during pyrolysis. *Bioresour. Technol.* 171, 193–198. doi:10.1016/J.BIORTECH.2014.08.064
- Chen, C., Ma, X., and He, Y. (2012). Co-pyrolysis characteristics of microalgae *Chlorella vulgaris* and coal through TGA. *Bioresour. Technol.* 117, 264–273. doi:10.1016/J.BIORTECH.2012.04.077
- Christenson, L., and Sims, R. (2011). Production and harvesting of microalgae for wastewater treatment, biofuels, and bioproducts. *Biotechnol. Adv.* 29, 686–702. doi:10.1016/J.BIOTECHADV.2011.05.015
- Daneshvar, E., Wicker, R. J., Show, P. L., and Bhatnagar, A. (2022). Biologically-mediated carbon capture and utilization by microalgae towards sustainable CO₂ biofixation and biomass valorization – a review. *Chem. Eng. J.* 427, 130884. doi:10.1016/J.CEJ.2021.130884
- Farooq, W., Ali, I., Raza Naqvi, S., Sajid, M., Abbas Khan, H., and Adamu, S. (2021). Evolved gas analysis and kinetics of catalytic and non-catalytic pyrolysis of microalgae *Chlorella* sp. biomass with Ni/θ-Al₂O₃ catalyst via thermogravimetric analysis. *Front. Energy Res.* 9, 1–13. doi:10.3389/fenrg.2021.775037
- Farooq, W. (2022). Maximizing energy content and CO₂ bio-fixation efficiency of an indigenous isolated microalga *Parachlorella kessleri* HY-6 through nutrient optimization and water recycling during cultivation. *Front. Bioeng. Biotechnol.* 9, 804608–804612. doi:10.3389/fbioe.2021.804608
- Farooq, W., Naqvi, S. R., Sajid, M., Shrivastav, A., and Kumar, K. (2022). Monitoring lipids profile, CO₂ fixation, and water recyclability for the economic viability of microalgae *Chlorella vulgaris* cultivation at different initial nitrogen. *J. Biotechnol.* 345, 30–39. doi:10.1016/J.JBIOTEC.2021.12.014
- Friedman, H. L. (2007). Kinetics of thermal degradation of char-forming plastics from thermogravimetry. Application to a phenolic plastic. *J. Polym. Sci. C. Polym. Symp.* 6, 183–195. doi:10.1002/polc.5070060121
- Gao, F., Yang, H. L., Li, C., Peng, Y. Y., Lu, M. M., Jin, W. H., et al. (2019). Effect of organic carbon to nitrogen ratio in wastewater on growth, nutrient uptake and lipid accumulation of a mixotrophic microalgae *Chlorella* sp. *Bioresour. Technol.* 282, 118–124. doi:10.1016/J.BIORTECH.2019.03.011
- Guerriero, G., Sergeant, K., Legay, S., Hausman, J.-F., Cauchie, H.-M., Ahmad, I., et al. (2018). Novel insights from comparative in silico analysis of green microalgal cellulases. *Int. J. Mol. Sci.* 19, 1782. doi:10.3390/ijms19061782
- Hanschen, E. R., Marriage, T. N., Ferris, P. J., Hamaji, T., Toyoda, A., Fujiyama, A., et al. (2016). The *Gonium pectorale* genome demonstrates co-option of cell cycle regulation during the evolution of multicellularity. *Nat. Commun.* 7, 11370–11410. doi:10.1038/ncomms11370
- Hong, Y., Xie, C., Chen, W., Luo, X., Shi, K., and Wu, T. (2020). Kinetic study of the pyrolysis of microalgae under nitrogen and CO₂ atmosphere. *Renew. Energy* 145, 2159–2168. doi:10.1016/j.renene.2019.07.135
- Karpagam, R., Preeti, R., Ashokkumar, B., and Varalakshmi, P. (2015). Enhancement of lipid production and fatty acid profiling in *Chlamydomonas reinhardtii*, CC1010 for biodiesel production. *Ecotoxicol. Environ. Saf.* 121, 253–257. doi:10.1016/J.ECOENV.2015.03.015
- Khan, M. J., Singh, N., Mishra, S., Ahirawar, A., Bast, F., Varjani, S., et al. (2022). Impact of light on microalgal photosynthetic microbial fuel cells and removal of pollutants by nanoabsorbent biopolymers: Updates, challenges and innovations. *Chemosphere* 288 (2), 132589. doi:10.1016/j.chemosphere.2021.132589
- Kokalj, F., Arbiter, B., and Samec, N. (2017). Sewage sludge gasification as an alternative energy storage model. *Energy Convers. Manag.* 149, 738–747. doi:10.1016/J.ENCONMAN.2017.02.076
- Lerche, K., and Hallmann, A. (2009). Stable nuclear transformation of *Gonium pectorale*. *BMC Biotechnol.* 9, 64. doi:10.1186/1472-6750-9-64
- Liu, C., Duan, X., Chen, Q., Chao, C., Lu, Z., Lai, Q., et al. (2019). Investigations on pyrolysis of microalgae *diplospira* sp. MM1 by TG-FTIR and py-GC/MS: Products and kinetics. *Bioresour. Technol.* 294, 122126. doi:10.1016/J.BIORTECH.2019.122126
- Maia, A. A. D., and de Moraes, L. C. (2016). Kinetic parameters of red pepper waste as biomass to solid biofuel. *Bioresour. Technol.* 204, 157–163. doi:10.1016/J.BIORTECH.2015.12.055
- Mondal, M., Goswami, S., Ghosh, A., Oinam, G., Tiwari, O. N., Das, P., et al. (2017). Production of biodiesel from microalgae through biological carbon capture: a review. *3 Biotech.* 7, 99. doi:10.1007/s13205-017-0727-4
- Naqvi, S. R., Tariq, R., Hameed, Z., Ali, I., Taqvi, S. A., Naqvi, M., et al. (2018). Pyrolysis of high-ash sewage sludge: Thermo-kinetic study using TGA and artificial neural networks. *Fuel* 233, 529–538. doi:10.1016/J.FUEL.2018.06.089
- Noushabadi, A. S., Dashti, A., Ahmadijokani, F., Hu, J., and Mohammadi, A. H. (2021). Estimation of higher heating values (HHVs) of biomass fuels based on ultimate analysis using machine learning techniques and improved equation. *Renew. Energy* 179, 550–562. doi:10.1016/J.RENENE.2021.07.003
- Patel, A. K., Choi, Y. Y., and Sim, S. J. (2020). Emerging prospects of mixotrophic microalgae: Way forward to sustainable bioprocess for environmental remediation and cost-effective biofuels. *Bioresour. Technol.* 300, 122741. doi:10.1016/J.BIORTECH.2020.122741
- Pérez-Maqueda, A., Criado, L., and Sánchez-Jiménez, E. (2006). Combined kinetic analysis of solid-state reactions: A powerful tool for the simultaneous determination of kinetic parameters and the kinetic model without previous assumptions on the reaction mechanism. *J. Phys. Chem. A* 110, 12456–12462. doi:10.1021/jp064792g
- Subagyono, R. R. D. J. N., Masdalifa, W., Aminah, S., Nugroho, R. A., Mollah, M., Londong Allo, V., et al. (2021). Kinetic study of copyrolysis of the green microalgae *botryococcus braunii* and victorian Brown coal by thermogravimetric analysis. *ACS Omega* 6, 32032–32042. doi:10.1021/acsomega.1c04818
- Vuppalladiyam, A. K., Zhao, M., Memon, M. Z., and Soomro, A. F. (2019). Microalgae as a renewable fuel resource: A comparative study on the thermogravimetric and kinetic behavior of four microalgae. *Sustain. Energy Fuels* 3, 1283–1296. doi:10.1039/C9SE00114J
- Vyazovkin, S. (2020). Kissinger method in kinetics of materials: Things to beware and Be aware of. *Molecules* 25 (12), 2813. doi:10.3390/molecules25122813
- Xu, L., Jiang, Y., and Wang, L. (2017). Thermal decomposition of rape straw: Pyrolysis modeling and kinetic study via particle swarm optimization. *Energy Convers. Manag.* 146, 124–133. doi:10.1016/J.ENCONMAN.2017.05.020
- Xu, Y., and Chen, B. (2013). Investigation of thermodynamic parameters in the pyrolysis conversion of biomass and manure to biochars using thermogravimetric analysis. *Bioresour. Technol.* 146, 485–493. doi:10.1016/J.BIORTECH.2013.07.086
- Yang, C., Li, R., Cui, C., Liu, S., Qiu, Q., Ding, Y., et al. (2016). Catalytic hydroprocessing of microalgae-derived biofuels: A review. *Green Chem.* 18, 3684–3699. doi:10.1039/C6GC01239F
- Yang, C., Li, R., Zhang, B., Qiu, Q., Wang, B., Yang, H., et al. (2019). Pyrolysis of microalgae: A critical review. *Fuel Process. Technol.* 186, 53–72. doi:10.1016/J.FUPROC.2018.12.012
- Yang, X., Wang, X., Zhao, B., and Li, Y. (2014). Simulation model of pyrolysis biofuel yield based on algal components and pyrolysis kinetics. *Bioenergy Res.* 7, 1293–1304. doi:10.1007/S12155-014-9467-Z
- You, J., and Lee, K. J. (2022). The experimental investigation and data-driven modeling for thermal decomposition kinetics of Green River Shale. *Fuel* 320, 123899. doi:10.1016/j.fuel.2022.123899

Advantages of publishing in Frontiers



OPEN ACCESS

Articles are free to read
for greatest visibility
and readership



FAST PUBLICATION

Around 90 days
from submission
to decision



HIGH QUALITY PEER-REVIEW

Rigorous, collaborative,
and constructive
peer-review



TRANSPARENT PEER-REVIEW

Editors and reviewers
acknowledged by name
on published articles

Frontiers

Avenue du Tribunal-Fédéral 34
1005 Lausanne | Switzerland

Visit us: www.frontiersin.org

Contact us: frontiersin.org/about/contact



REPRODUCIBILITY OF RESEARCH

Support open data
and methods to enhance
research reproducibility



DIGITAL PUBLISHING

Articles designed
for optimal readership
across devices



FOLLOW US

@frontiersin



IMPACT METRICS

Advanced article metrics
track visibility across
digital media



EXTENSIVE PROMOTION

Marketing
and promotion
of impactful research



LOOP RESEARCH NETWORK

Our network
increases your
article's readership